

UNIVERSITY OF BIRMINGHAM

B CELL CHARACTERISATION IN ADULT AND PAEDIATRIC LIVER DISEASES

by

ARZOO PATEL BSc MSc

A thesis submitted to the University of Birmingham for the degree of
DOCTOR OF PHILOSOPHY

Institute of Immunology and Immunotherapy
College of Medical and Dental Sciences Graduate School
The University of Birmingham
Edgbaston
Birmingham
B15 2TT

August 2023

UNIVERSITY OF
BIRMINGHAM

University of Birmingham Research Archive

e-theses repository

This unpublished thesis/dissertation is copyright of the author and/or third parties. The intellectual property rights of the author or third parties in respect of this work are as defined by The Copyright Designs and Patents Act 1988 or as modified by any successor legislation.

Any use made of information contained in this thesis/dissertation must be in accordance with that legislation and must be properly acknowledged. Further distribution or reproduction in any format is prohibited without the permission of the copyright holder.

Publications, Presentations and Posters

Publications

- **Patel, A.M.**, Liu, Y.S., Davies, S.P., Brown, R.M., Kelly, D.A., Scheel-Toellner, D., Reynolds, G.M. & Stamataki, Z. 2021. The Role of B Cells in Adult and Paediatric Liver Injury. *Frontiers in Immunology,* 12.
- Wiggins, B.G., Pallett, L.J., Li, X., Davies, S.P., Amin, O.E., Gill, U.S., Kucykowicz, S., **Patel, A.M.**, Aliazis, K., Liu, Y.S., Reynolds, G.M., Davidson, B.R., Gander, A., Luong, T.V., Hirschfield, G.M., Kennedy, P.T.F., Huang, Y., Maini, M.K. & Stamataki, Z. 2021. The human liver microenvironment shapes the homing and function of CD4(+) T-cell populations. *Gut*.
- Hargreaves, C.E., Salatino, S., Sasson, S.C., Charlesworth, J.E.G., Bateman, E., **Patel, A.M.**, Anzilotti, C., Broxholme, J., Knight, J.C. & Patel, S.Y. 2021. Decreased ATM Function Causes Delayed DNA Repair and Apoptosis in Common Variable Immunodeficiency Disorders. *J Clin Immunol*, 41, 1315-1330

Oral Presentations

- **Arzoo M Patel**, Maiar Elghobashy, Maxim Harris, Carla Lloyd, Rachel M Brown, Deirdre A Kelly, Gary M Reynolds, Zania Stamataki. 28th November 2022. B cell characterisation in adult and paediatric liver diseases. Institute of Immunology and Immunotherapy away day in Birmingham, UK.
- **Arzoo M Patel**, Maiar Elghobashy, Maxim Harris, Carla Lloyd, Rachel M Brown, Deirdre A Kelly, Gary M Reynolds, Zania Stamataki. 17th June 2022. B cell subsets in

Biliary Atresia. Biliary Atresia and Related Diseases (BARD) Conference in Bruges, Belgium

- **Arzoo M Patel**, Gary M Reynolds, Zania Stamataki. 27th February 2020. B cell subsets in chronic liver disease. Institute of Immunology and Immunotherapy PGR Research Gala.

Poster presentations

- **Arzoo M Patel**, Maiar Elghobashy, Maxim Harris, Carla Lloyd, Rachel M Brown, Deirdre Kelly, Gary Reynolds, Zania Stamataki. 13-14 May 2021. B cell distribution in biliary atresia. Liver unit 30 year meeting, virtual conference, UK. – BEST POSTER AWARD
- **A. Patel**, S. Purswani, K. Aliazis, R. Rahman, E. Liaskou, G. Hirschfield, G. Reynolds, Z. Stamataki. 2-5 December 2019. Pro-inflammatory CD24- B cells were enriched in the liver in end-stage diseases: implications for primary biliary cholangitis (PBC). BSI Congress, Liverpool, UK.
- **A. Patel**, S. Purswani, K. Aliazis, R. Rahman, E. Liaskou, G. Hirschfield, G. Reynolds, Z. Stamataki. 4th October 2019. Pro-inflammatory CD24- B cells were enriched in the liver in end-stage diseases: implications for primary biliary cholangitis (PBC). MIDAS Conference, Birmingham, UK.

Abstract

B cells contribute to the pathology in many diseases such as autoimmune diseases and in many lymphomas. However, there is little literature on liver B cells in health and in disease for paediatric and adult liver diseases. Our aim was to characterise B cell subsets in adult and paediatric livers. We used multiparametric flow cytometry to identify B cell subsets in adult non-cirrhotic and cirrhotic livers, with cholestatic or metabolic disorders. We used immunohistochemistry and immunofluorescence to map the distribution of B cell subsets within liver tissue obtained from biliary atresia (BA) patients at the time of Kasai portoenterostomy (KPE, hilum tissue and wedge tissue from liver periphery) or during orthotopic liver transplantation (explant). We then carried out inflammation-focused transcriptomic analyses to identify differences between non-syndromic and syndromic BA patients and during disease progression. We found that CD24- B cells and age-associated B cells were detected across all adult end-stage liver diseases. We found that paediatric BA hilum samples had increased immune cell infiltration and the presence of B cell and lymphoid aggregates in both non-syndromic and syndromic cases. B cell and lymphoid aggregates mainly consisted of CD20+ CD24- B cells, and CD138+ antibody-secreting cells were rare. CD20+ CD24- B cells in B cell and lymphoid aggregates often expressed IL-6. Nanostring nCounter transcriptomics showed that the hilum was the site of active inflammation during KPE surgery, with pro-inflammatory cytokines being highly expressed. No remarkable differences in genetic profiles were observed between non-syndromic and syndromic BA patients, indicating that liver injury may be similar between the two groups. Our work showed that B cells may contribute to pathology in paediatric and adult liver diseases through the production of inflammatory mediators such as IL-6 and potentially

through interactions with T cells. Lymphoid aggregates may also contribute to inflammation observed in the hilum. The hilum region is poorly studies in both adult and paediatric liver diseases and warrants further investigations.

Dedication

Dedicated with love to my number one supporters, my family and friends.

Acknowledgements

I would like to thank both of my supervisors, Dr Zania Stamataki and Dr Gary Reynolds for your mentorship, guidance, and support throughout my PhD. Your excitement over my data analysis and enthusiasm was much appreciated. I'd like to also thank Dr Gary Reynolds for continuing to help me with my PhD despite retiring.

A huge thank you to Professor Deirdre Kelly for your constant support and advice. Thank you for being available to help me despite your retirement. Thank you to Carla Lloyd and Rachel Brown for your help with the paediatric samples.

This work was funded by the Birmingham Childrens Hospital Research Foundation for which I am very thankful for. I'd like to thank all the patients, paediatric and adult, who have contributed to this work.

Thank you to everyone in the liver labs for all your help. You've all made this PhD an enjoyable experience. A special thanks goes to Dr Scott Davies for your constant support, encouragement, and mentorship throughout my PhD. Thank you for being my soundboard and for all our coffee chats about science. You have been a great motivator throughout my PhD, and I really appreciate it. Thank you for everything that you have done for me.

Thank you to all my friends for their constant support and endless encouragement throughout this PhD. To Rajeelan, thank you for always being available with your motivational speeches and for listening to me whenever I felt overwhelmed. To Raaji, thank you for keeping me company whilst I analysed my data and for always being by my side, cheering for me.

A huge thank you goes out to my parents, Shilpa and Mohinish for your continued faith and support. To my brother Dr. Mo, thank you for constantly pushing me to be better. To my mother-in-law and father-in-law, Gita and Kishor, and to Raj and Jayna, thank you for listening to me whenever I needed to talk. To my beautiful niece Sienna, a huge thank you goes to you for brightening up my days with your cheeky smiles, big cuddles and for making me dance with you. Lastly, but by no means the least, thank you to my other half, Sunil, for your constant motivation, encouragement, and support throughout my PhD. Thank you for always listening to me whenever I needed to talk and for making the most difficult days easier to handle.

Contents listing

Table of Contents

Publications, Presentations and Posters i
Publications i
Oral Presentations i
Poster presentations ii
Abstract iii
Dedication v
Acknowledgements vi
Contents listing viii
Table of Contents viii
List of illustrations xii
List of tables xv
List of abbreviations xvi
CHAPTER 1 – GENERAL INTRODUCTION 1
1.1 B cell development 2
1.2 Liver 10
1.2.1 Alcohol related liver disease 13
1.2.2 Non-alcoholic steatohepatitis 18
1.2.3 Viral hepatitis 21
1.2.4 Autoimmune hepatitis 25
1.2.5 Primary sclerosing cholangitis 28
1.2.6 Primary biliary cholangitis 30
1.3 Paediatric acute liver failure 33
1.3.1 Biliary atresia 33
1.3.2 Sudden onset acute hepatitis 38
1.3.3 Paediatric viral hepatitis 42
1.3.3.1 Paediatric hepatitis B viral infection 42
1.3.3.2 Paediatric hepatitis C viral infection 43
1.4 Hypothesis and aims 48
CHAPTER 2 – B CELL CHARACTERISATION IN ADULT END-STAGE LIVER DISEASES 50
2.1 Introduction 51

2.1.1 Age-associated B cells....51
2.1.2 Aims and objectives....55
2.2 Methodology....57
2.2.1 Human liver tissue....59
2.2.2 Haemochromatosis blood....59
2.2.3 Liver infiltrating mononuclear cell isolation....60
2.2.4 Peripheral blood mononuclear cell isolation....61
2.2.5 Flow cytometry staining....61
2.2.5.1 Optimisation....61
2.2.5.2 Cell staining....67
2.2.6 Fortessa spectral flow cytometer....69
2.2.7 Statistical analysis....70
2.3 Results....71
2.3.1 B cell frequencies in liver health and in different end-stage diseases....71
2.3.2 CD24- B cells and ABCs were phenotypically consistent in different liver diseases 76
2.3.3 Investigation of APC markers in liver B cell subsets in liver explants....81
2.3.4 Expression of TLR7 and TLR9 in liver B cell subsets....91
2.3.5 B cell populations express low levels of class-switched immunoglobulins....94
2.3.6 CD138 expression in liver B cell subsets in different end-stage liver diseases....101
2.3.7 CD5 and FcRL5 expression in liver B cell subsets....105
2.3.8 Comparison of ABC subsets in liver diseases....109
2.4 Discussion....114
2.4.1 B cell composition from infancy to adulthood....115
2.4.2 ABCs as antigen presenters....116
2.4.3 Activation of ABCs....118
2.4.4 ABCs in healthy and disease....119
2.4.5 ABCs play a role in antiviral responses....124
2.4.6 Limitations....125
2.5 Conclusion....125
CHAPTER 3 – B CELL LOCALISATION IN PAEDIATRIC LIVERS....127
3.1 Introduction....128
3.3.1 Distribution of B cells in liver health and disease....128

3.1.2 IL-6 in disease 132
3.1.3 Aims and objectives 132
3.2 Methodology 134
3.2.1 Human paediatric liver tissue 134
3.2.2 Human adult liver tissue 134
3.2.3 Immunohistochemistry 134
3.2.3.1 Optimisation 134
3.2.3.2 ImageJ 140
3.2.4 Immunofluorescence 143
3.2.4.1 Optimisation 143
3.2.5 Statistical analysis 151
3.3 Results 152
3.3.1 B cells were found in the liver around bile ducts and in fibrotic tracts 152
3.3.2 Lymphoid aggregates were found in the hilum region of BA liver samples 154
3.3.3 Lymphoid aggregates mostly contained CD20+ CD24- B cells and CD3+ T cells 158
3.3.4 Mixed immune infiltrate was observed surrounding bile ducts 165
3.3.5 Lymphoid aggregates and mixed immune infiltrates were observed in adult livers 166
3.3.6 CellProfiler was used to quantify B cell subsets present in the liver 169
3.4 Discussion 181
3.4.1 Characterisation of lymphoid aggregates 182
3.4.2 Lymphoid aggregates in disease 182
3.4.3 Mixed immune infiltrates observed in livers 184
3.5 Conclusions 185
CHAPTER 4 – DIFFERENTIAL GENE EXPRESSION IN BILIARY ATRESIA 187
4.1 Introduction 188
4.1.1 Transcriptomic studies in BA 188
4.1.2 Nanostring nCounter panels 190
4.1.3 Aims and objectives 191
4.2 Methodology 192
4.2.1 Paediatric liver samples 192
4.2.2 RNA isolation 192

4.2.2.1 PureLink FFPE Total RNA Isolation Kit 192
4.2.2.2 High Pure FFPET RNA Isolation Kit 196
4.2.2.3 Quality check for isolated total RNA 199
4.2.3 Nanostring nCounter Human Organ Transplant v2 panel 199
4.2.4 Statistical analysis 200
4.3 Results 201
4.3.1 BCR signalling genes were differentially expressed between the hilum and the periphery 201
4.3.2 Cytokine signalling genes were differentially expressed between the hilum and the periphery 204
4.3.3 The hilum had higher expression of oxidative stress-related genes compared to the periphery 209
4.3.4 Activation markers were differentially expressed in hilum samples 211
4.3.5 Chemokine signalling genes were highly expressed in the hilum of BA patients 214
4.4 Discussion 220
4.4.1 The hilum was different compared to the periphery 220
4.4.2 Inflammatory gene expression was higher in the hilum compared to the periphery 222
4.4.3 Oxidative stress-related genes were highly expressed in the hilum 225
4.4.4 TLR signalling gene expression was higher in the hilum compared to the periphery 226
4.4.5 Non-syndromic and syndromic BA had similar genetic profiles 229
4.5 Conclusions 230
CHAPTER 5 – GENERAL DISCUSSION 232
5.1 Age-associated B cells in adult chronic liver diseases 234
5.2 The role of B cell and lymphoid aggregates in chronic liver diseases 236
5.3 Differences in TLR signalling in liver B cells between diseases 238
5.4 Germinal centres; are they found in the liver? 239
5.5 Pathogenesis and treatment of biliary atresia 240
5.6 General conclusions 241
BIBLIOGRAPHY 244
APPENDICES 264

List of illustrations

Figure 1.1 B cell developmental stages 3
Figure 1.2 The liver lobule is the functional unit of the liver 11
Figure 1.3 The progression of liver disease 12
Figure 1.4 Alcohol related liver disease pathogenesis 17
Figure 1.5 Non-alcoholic fatty liver disease pathogenesis 21
Figure 1.6 Proposed pathogenesis of biliary atresia 38
Figure 2.1 Antibody titration to find the optimal working dilution 64
Figure 2.2 FMOs were carried out on antibodies that would be used together and had spectral overlap 65
Figure 2.3 DNase treated cells had better yields compared to cells treated without DNase 66
Figure 2.4 Samples were checked for normal distribution using the Shapiro-Wilk test on GraphPad prism 70
Figure 2.5 B cell characterisation using flow cytometry 72
Figure 2.6 Naïve and memory B cells were detected in similar proportions across adult liver diseases 73
Figure 2.7 B cell populations were detected in similar proportions across different liver diseases 76
Figure 2.8 Gating strategy for CD21-/lo ABCs and CD11c+ T-bet+ ABCs 77
Figure 2.9 Phenotyping of CD24- B cells and ABC populations based on naïve and memory B cells in liver diseases 80
Figure 2.10 Phenotyping of CD24- B cells and ABCs based on APC markers in liver diseases 86
Figure 2.11 CD11c+ T-bet+ ABCs expressed higher amounts of co-stimulatory markers CD80 and CD86 compared to B cell subsets 90
Figure 2.12 CD11c+ T-bet+ ABCs had significantly higher expression of T-bet+ TLR9+ cells across all adult livers 93
Figure 2.13 CD24- B cells and ABCs express low levels of class-switched immunoglobulins 98
Figure 2.14 Class-switched immunoglobulins were present in all livers and amongst CD24- B cell populations and ABC subsets 100
Figure 2.15 CD11c+ T-bet+ ABCs have high CD138 expression compared to CD24+ CD38-, CD24- B cells and CD21-/lo ABCs 103
Figure 2.16 Inhibitory molecules expression is low in both CD24- B cell populations and CD21-/lo ABCs 108
Figure 2.17 CD21-/lo ABCs positively correlated with the age of the livers 111
Figure 2.18 TLR9 correlation analyses comparing CD21-/lo ABCs and CD11c+ T-bet+ ABCs 113
Figure 3.1 Titration of antibodies for immunohistochemistry 140
Figure 3.2 ImageJ analysis pipeline for CD20+ immunohistochemistry images 142

Figure 3.3 Spectral viewer of the fluorophores used in immunofluorescence panels 146
Figure 3.4 FMO for AF555 147
Figure 3.5 Comparison of AxioObserver Z1 Apotome.2 and LSM 880 Airyscan on an adult PBC liver section 148
Figure 3.6 Separation of AF594 and AF555 was clear 150
Figure 3.7 CD20+ B cells were found around bile ducts, fibrotic tracts, triads and in ductular reactions 153
Figure 3.8 BA samples were collected from different locations in the liver 154
Figure 3.9 CD20+ B cells were found at varying frequencies across a range of paediatric liver diseases 155
Figure 3.10 BA samples do not have an enrichment of B cells 157
Figure 3.11 Immunofluorescence positive controls using BA lymph nodes 159
Figure 3.12 Immunofluorescence negative controls using IMC on BA lymph nodes 160
Figure 3.13 CD20+ B cells are found around bile ducts and in fibrotic tracts in BA tissue . 161
Figure 3.14 CD20+ CD24- B cells made up most of the aggregates and were IL-6+ 164
Figure 3.15 B cell express IL-6 in BA aggregates 165
Figure 3.16 Mixed immune infiltrate is detected around bile ducts 166
Figure 3.17 Aggregates were also found in adult cholestatic livers 167
Figure 3.18 Mixed immune infiltrate was also detected in adult cholestatic livers 168
Figure 3.19 CD20+ IL-6+ B cells can be found in adult cholestatic livers but are not present in all 169
Figure 3.20 CellProfiler pipeline used to quantify B cell subsets 172
Figure 3.21 CD20+ CD24- B cells make up majority of the B cells in this lymphoid aggregate 174
Figure 3.22 Lymphocyte subsets present at early and late stage in BA 177
Figure 3.23 No differences were observed in subset expression amongst adult and paediatric livers 179
Figure 4.1 RNA optimisation using different numbers of scrolls and different incubation times to get the best RNA yield 196
Figure 4.2 RNA yield using the high pure FFPET RNA isolation kit 198
Figure 4.3 Differential gene expression between the hilum and the periphery for BCR signalling genes 203
Figure 4.4 Syndromic and non-syndromic were similar in BCR related signalling genes 204
Figure 4.5 Cytokine signalling genes were differentially expressed between hilum and periphery in non-syndromic and syndromic BA patients 206
Figure 4.6 Minimal differences between syndromic and non-syndromic patients were observed in cytokine signalling genes 208
Figure 4.7 Differential oxidative stress-related genes were detected between the hilum and the peripheral BA samples 210
Figure 4.8 Non-syndromic and syndromic BA patients had similar expression of oxidative stress genes 211

Figure 4.9 Differential TLR related gene signalling was detected between hilum samples and the periphery 213
Figure 4.10 Differences were observed for TLR signalling genes between syndromic and non-syndromic BA patients 214
Figure 4.11 Chemokine signalling genes were differentially expressed between the hilum and the periphery 216
Figure 4.12 Chemokine signalling genes were differentially expressed between non-syndromic and syndromic BA patients 218
Figure 4.13 Venn diagram showing the number of genes upregulated in the hilum, wedge, and explant BA samples 219

List of tables

Table 2.1 B cell markers and their function in B cell development and differentiation 57
Table 2.2 Antibodies used for flow cytometry. 62
Table 2.3 Isotype matched controls used for flow cytometry 63
Table 2.4 Surface staining panels 68
Table 2.5 Intracellular staining panel 69
Table 2.6 Calibration and compensation reagents used for each experiment 69
Table 3.1 IHC antibody working dilutions 136
Table 3.2 Isotype matched controls for immunohistochemistry and immunofluorescence 137
Table 3.3 Immunofluorescence primary antibody panels with working dilutions 145
Table 3.4 Immunofluorescence secondary antibodies 146
Table 3.5 The p-values for the comparisons shown in Figure 3.22 are shown in this table 177
Table 4.1 RNA quantity and quality results 193
Table 4.2 High Pure FFPET RNA isolation kit results 198

List of abbreviations

ABCs – Age-associated B cells
ADCC – Antibody-dependent cellular cytotoxicity
AID – Activation-induced cytidine deaminase
AIH – Autoimmune hepatitis
ALP – Alkaline phosphatase
ALT – Alanine transaminase
AMA – anti-mitochondrial antibodies
ANA – Anti-nuclear antibodies
ANCA – Anti-neutrophil cytoplasmic antibodies
Anti-SLA/LP – Anti-soluble liver antigen/ liver pancreas
APCs – Antigen-presenting cells
ArLD – Alcoholic related liver disease
ASCs – Antibody-secreting cells
ASGPR – Asialoglycoprotein receptor
BA – Biliary atresia
BAFF – B cell activating factor
BAFFR – B cell activating factor receptor
BASM – BA with splenic malformation
BCMA – B cell maturation antigen
BCR – B cell receptor
BECs – Biliary epithelial cells
BM – Bone marrow
B-regs – Regulatory B cells
CCL_4 – Carbon tetrachloride
CD – Crohn's disease
CHI3L1 – Chitinase 3 like 1
CLD – Chronic liver diseases
CLP – Common lymphoid progenitors
CMV – Cytomegalovirus
CSR – Class-switch recombination
cTFH – Circulating follicular T helper cells
D – Diversity
DAMPs – Damage-associated molecular patterns
DLL-4 – Delta-like 4
DN – Double negative memory B cells (CD27- IgD-)
DZ – Dark zone
EAT – Epididymal adipose tissue
EBF1 – Early B cell factor 1
ELP – Early lymphoid progenitors
FcRL4 – Fc receptor-like protein 4
FcRL5 – Fc receptor-like protein 5
FDCs – Follicular dendritic cells

FFA – Free fatty acids
FMO – Fluorescence minus one
FO – Follicular
FTCD - Formimidoyltransferase cyclodeaminase
GALT – Gut-associated lymphoid tissue
GC – Germinal centre
GFP – Green fluorescent protein
GGT - Gamma glutamyl transpeptidase
H. Pylori – Helicobacter pylori
HBcAg – Hepatitis B core antigen
HBeAg – Hepatitis B e antigen
HBsAg – Hepatitis B surface antigen
HBV – Hepatitis B virus
HCV – Hepatitis C virus
HFD – High fat diet
HFe – Hemochromatosis
HOT – Human organ transplant
HSCs – Haematopoietic stem cells
IBD – Inflammatory bowel disease
Ig – Immunoglobulin
IgG4RD – IgG4-related disease
IL – Interleukin
IMC – Isotype matched controls
J – Joining
KPE – Kasai portoenterostomy
LBP – Lipopolysaccharide binding protein
LC1 – Liver cytosol type 1
LCMV – Lymphocytic choriomeningitis virus
LIMCs – Liver infiltrating mononuclear cells
LKM1 – liver kidney microsome type 1
LPS – Lipopolysaccharide
LZ – Light zone
MAT – Mesenteric adipose tissue
MC – Mixed cryoglobulinemia
MDS – Myelodysplastic syndromes
MFI – Median fluorescence intensity
MS – Multiple sclerosis
MZ – Marginal zone
N – Naïve B cells (CD27- IgD+)
NAFLD – Non-alcoholic fatty liver disease
NASH – Non-alcoholic steatohepatitis
NKT – Natural killer T cells
NOSA – Non-organ-specific autoantibodies

OPN – Osteopontin
OSE – Oxidative stress-derived epitopes
pALF – Paediatric acute liver failure
PAMPs – pathogen-associated molecular patterns
pANCA – perinuclear anti-neutrophil cytoplasmic antibodies
PBC – Primary biliary cholangitis
PBMCs – Peripheral blood mononuclear cells
PBS – Phosphate buffered saline
PBs – Plasmablasts
PCs – Plasma cells
PDC-E2 – pyruvate dehydrogenase complex E2 subunit
Pre-BCR – Pre-B cell receptor
PRRs – pathogen recognising receptors
PSC – Primary sclerosing cholangitis
RA – Rheumatoid arthritis
RAG – Recombination activating gene
ROS – Reactive oxygen species
RRV – Rhesus rotavirus
SFTPD – Surfactant protein D
sIg – Soluble immunoglobulin
SLE – Systemic lupus erythematosus
SLOs – Secondary lymphoid organs
SM – Switched memory B cells (CD27+ IgD-)
SMA – Smooth muscle antibodies
SMH – Somatic hypermutation
SOAH – Sudden onset acute hepatitis
SS - Sjogren's syndrome
TBS – Tris buffered saline
TFH – Follicular T helper cells
TGF-β – Transforming growth factor β
TLRs – Toll-like receptors
TLS – Tertiary lymphoid structures
TNFR – Tumour necrosis factor receptor
TRIF – Toll/IL-1R-domain-containing adapter-inducing interferon-β
UC – Ulcerative colitis
UDCA – Ursodeoxycholic acid
USM – Unswitched memory B cells (CD27+ IgD+)
V – Variable
VAT – Visceral adipose tissue
WT – Wild-type

CHAPTER 1 – GENERAL INTRODUCTION

In this chapter I will introduce basic concepts in B cell biology and discuss B cell subsets in health and disease. I will then give an overview of the role of B cells in multiple adult and paediatric liver injuries, which will set the scene for the biological questions investigated in this thesis. A large portion of this introduction had been published in a review by Patel et al., (Patel et al., 2021)

1.1 B cell development

B cells play an important role in humoral immune protection against pathogens. B cells express clonally diverse surface immunoglobulin (Ig) receptors that enable them to detect specific antigenic epitopes (LeBien and Tedder, 2008) and differentiate into antibody-secreting cells, secrete cytokines, act as antigen-presenting cells and provide co-stimulatory signals to T cells (Fischer et al., 2020). B cells produce high affinity antibodies against specific bacterial and viral epitopes (Nakashima et al., 2012) and contribute to immune regulation and maintenance of self-tolerance (Almeida et al., 2015). The size of the B cell peripheral compartment is regulated by several factors during B cell development: self-reactivity, unsuccessful VDJ rearrangement and competition for survival signals (Shahaf et al., 2016).

Early studies by Owen et al., in the 70's identified that B cell production, initiated in the foetus, occurs in sites in the liver and bone marrow (BM) (Owen et al., 1974, Owen et al., 1976). B cells develop in the BM from haematopoietic stem cells (HSCs) (Zhang et al., 2021) and undergo various stages of development **(figure 1.1)**.

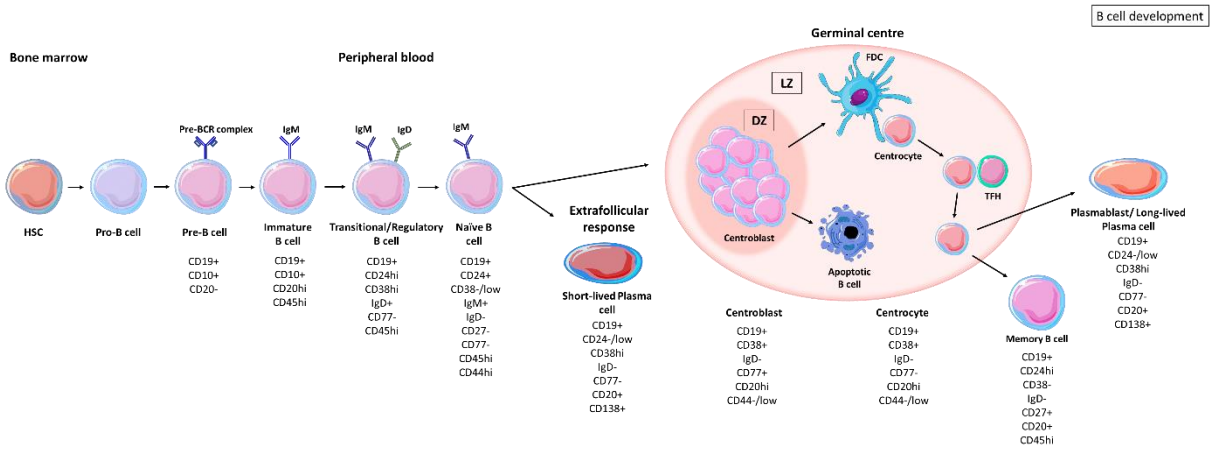


Figure 1.1 B cell developmental stages. *B cells develop in the bone marrow (BM) from haematopoietic stem cells (HSCs). Their development progresses from pro-B cells to pre-B cell stages prior to exiting the BM into the periphery. Recently migrated B cells in the periphery are termed transitional B cells and they mature further into naïve B cells. B cells become activated upon recognition of a cognate antigen. These activated B cells enter germinal centra (GC) reactions where they undergo somatic hypermutation (SMH) and class-switch recombination (CSR) to increase BCR affinity. B cells with disadvantageous mutations die by apoptosis. B cells with improved BCR affinities interact with follicular dendritic cells (FDCs) and follicular T helper cells (TFH) for survival signals. These B cells then differentiate into memory B cells and plasmablasts (PB)/ plasma cells (PCs). Image modified from (Patel et al., 2021).*

The BM stroma is composed of mesenchymal cells, osteoblasts and endothelial cells that provide a special niche for HSCs and B cell precursors (Eibel et al., 2014). Growth factors and cytokines secreted by the BM stroma correctly position B cell precursors ensuring their survival and differentiation (Eibel et al., 2014). The main stages of B cell development in the BM are pro-B, pre-B and immature B cells. HSCs lose their self-renewal ability, differentiate into early lymphoid progenitors (ELP) and then give rise to common lymphoid progenitor (CLP) cells which can differentiate into all lymphocytes (Ghaedi et al., 2016, Fischer et al., 2020, Montecino-Rodriguez and Dorshkind, 2012). E2A (E12/E47) and early B cell factor 1 (EBF1) initiates commitment to B cell lineage in CLPs as mice deficient in either of these transcription factors resulted in the failure of precursors reaching the pro-B cell stage of

development (Eibel et al., 2014). This is because both these factors induce the expression of B cell lineage genes; *CD79a*, *CD79b*, *CD179a*, *CD179b*, *Pax5* and *Foxo1* (Eibel et al., 2014). *CD79a* and *CD79b* encode the Igα and Igβ subunits required for signal transduction at the B cell receptor (BCR) (Eibel et al., 2014). *CD179a* and *CD179b* encode surrogate light chain molecules V-preB and lambda 5, respectively (Eibel et al., 2014). PAX5 initiates the transcription of *CD19* and *BLNK*, and represses the transcription of *Notch1* and MCSF-R genes, required for T cell and myeloid development, fixing the precursor to the B cell fate (Eibel et al., 2014). *Foxo1* activates recombination activating gene (Rag) 1 and Rag 2 (Eibel et al., 2014). Rag 2 is vital for the rearrangement of the heavy and light chains (Eibel et al., 2014). Upregulation of CD45R on precursors plays a role in CLP transition into pre-pro-B cells (Montecino-Rodriguez and Dorshkind, 2012).

Pro-B cells express CD45 and recombination of the variable (V), diversity (D) and joining (J) regions is induced (Wang and Clark, 2003, LeBien and Tedder, 2008, Pieper et al., 2013) where RAG sequentially recombines segments encoding VDJ of the heavy chain (Aslam et al., 2020). Successful rearrangement of the heavy chain generates a pool of B cells termed (precursor) pre-B cells which can progress to the next stage of development, however unsuccessful rearrangement results in developmental arrest and apoptosis of pro-B cells (Aslam et al., 2020). Pax5 is essential for the progression of B cell development from the pro-B stage to pre-B stage (Fischer et al., 2020).

CD19 co-receptor is expressed on pre-B cells but does not contribute to B cell development until the mature B cell stages (Montecino-Rodriguez and Dorshkind, 2012). After the successful rearrangement of the heavy chain, the pre-B cell receptor (pre-BCR) is expressed on the cell surface and is composed of the surrogate light chain molecules (V-preB (CD179A)

and lambda 5 (CD179B)) and signal transducing subunits Igα (CD79A) and Igβ (CD79B) (Eibel et al., 2014, Aslam et al., 2020, LeBien and Tedder, 2008, Gauld et al., 2002). Both signal transducing subunits contain conserved sites for tyrosine phosphorylation and docking for Src family of kinases that are vital for BCR signalling and B cell activation (LeBien and Tedder, 2008). A suitable pre-BCR signalling results in the inhibition of further rearrangement on the heavy chain locus in a process called allelic exclusion, which can only occur upon the presence of a competent BCR (Aslam et al., 2020, Wang and Clark, 2003). Successful pre-BCR signalling induces B cells to proliferate and become small pre-B cells that begin light chain rearrangement at the kappa (Igκ) locus followed by the lambda (Igλ) locus (Wang and Clark, 2003). The successful rearrangement of the VJ regions of the light chain (Eibel et al., 2014) creates a diverse repertoire of B cells expressing a functional membrane-bound IgM (Aslam et al., 2020).

Immature B cells express surface IgM and undergo receptor-mediated negative selection where BCRs that are highly self-reactive will undergo clonal deletion and BCRs with low-avidity will enter a state of anergy and become unresponsive to further antigenic stimulation (Wang and Clark, 2003). Negative selection of B cells with high-avidity to self-proteins can also result in receptor editing (Kuppers, 2021); the light chain undergoes secondary rearrangement to replace the autoreactive BCR (Eibel et al., 2014, Wang and Clark, 2003). B cells that pass this checkpoint migrate to the periphery; to the spleen (Eibel et al., 2014) and secondary lymphoid organs (SLOs), where they will undergo further maturation. An important protein required for the transition of immature B cells to transitional B cells is B cell activating factor receptor (BAFFR), which is upregulated after the expression of a functional BCR (Smulski and Eibel, 2018). B cell activating factor (BAFF) ligation to BAFFR

induces survival signals that are essential for the transition of immature B cells into transitional and mature B cells (Eibel et al., 2014, Smulski and Eibel, 2018) as BAFFR deficiency prevents B cells from transitioning from the immature B cell stages (Warnatz et al., 2009, Eibel et al., 2014). Humans with BAFFR deficiency suffer from hypogammaglobulinemia and are unable to mount responses against T-independent antigens (Warnatz et al., 2009). On the other hand, excessive BAFF increases the development of autoreactive B cells (Smulski and Eibel, 2018) highlighting that fine-tuned interactions between BAFF and BAFFR are crucial for the maturation and survival of B cells in the periphery.

Transitional B cells are defined as CD19+ CD24hi CD38hi CD77- IgM+ IgD+ (van Zelm et al., 2007). All transitional B cells have low avidity to self-antigens (Smulski and Eibel, 2018) and circulating transitional B cells are able to rapidly internalise their BCRs upon recognition of self-antigens and are unable to home to lymph nodes as they do not express homing molecule L-selectin (CD62L) (Eibel et al., 2014). CD19+ CD24hi CD38hi B cell populations also contain regulatory B cells (B-regs) that modulate immune responses through the production of interleukin (IL)-10 and transforming growth factor β (TGF-β) (Liu et al., 2016, Rosser and Mauri, 2015).

Transitional B cells mature into naïve B cells, defined as CD19+ CD24+ CD38-/low CD27- IgM+ IgD+, that wait to encounter cognate antigen (Patel et al., 2021). BAFF binds to B cell maturation antigen (BCMA), a member of the tumour necrosis factor receptor (TNFR) family, supporting the survival of naïve B cells (Kuppers, 2021) and naïve B cells that do not encounter antigen re-circulate back into the periphery and die within several days (Perez-

Andres et al., 2010). This shows that a basal level of BCR signalling is necessary to ensure the survival of mature B cells (Wang and Clark, 2003).

B cell maturation is complete when they develop into either follicular (FO) B cells or marginal zone (MZ) B cells. MZ B cells recognise blood-borne antigens and provide a rapid response to pathogens (Eibel et al., 2014) as these cells maintain a partially active phenotype (Wang and Clark, 2003). MZ B cells express toll-like receptors (TLRs), pathogen recognising receptors (PRRs) that recognise pathogen-associated molecular patterns (PAMPs) (Eibel et al., 2014). Upon recognition of PAMPs by TLRs, MZ B cells rapidly differentiate into short-lived IgM secreting plasma cells (PCs) (Eibel et al., 2014) as part of the extrafollicular response (Elsner and Shlomchik, 2020) however, MZ cells do not differentiate into memory cells (Wang and Clark, 2003). Naïve B cells that have encountered antigen can also enter SLOs where they receive signals from T cells and enter the germinal centre (GC) to further differentiate (Patel et al., 2021).

Majority of B cells encounter and respond to T-dependent antigens within lymphoid follicles (LeBien and Tedder, 2008). Subcapsular macrophages present antigen as immune complexes to non-cognate B cells that transport the antigen to B cell follicles where they are recognised by cognate antigen-specific B cells (Eibel et al., 2014). The BCR co-receptor CD19 lowers the threshold for BCR signalling (Gauld et al., 2002) and BCR interaction with cognate antigen results in the formation of an immunological synapse (McHeyzer-Williams and McHeyzer-Williams, 2005) and activates downstream signalling via Igα and Igβ. Igβ can act as an enhancer of Igα phosphorylation that results in the lowering the threshold for BCR activation (Wang and Clark, 2003). Activated B cells form stable interactions with antigen-specific follicular T helper (TFH) cells by migrating to the outer region of B cell follicles (Okada et al.,

2005) which is regulated by GPR184 (Eibel et al., 2014). CCR7 promotes the migration to T cell zones where B cells receive CD40/CD40L interactions and co-stimulating cytokines signals IL-4 and IL-21 from CD4+ T helper cells (Eibel et al., 2014, Basso and Dalla-Favera, 2015). Both B and T cells move together towards CXCL13-expressing follicular dendritic cells (FDCs) in a CXCR5-dependent manner, where they aggregate together to form a nascent GC in the centre of the follicle (Eibel et al., 2014, Basso and Dalla-Favera, 2015).

The GC structure consists of a light zone (LZ) and a dark zone (DZ) that is surrounded by GC stromal cells (Basso and Dalla-Favera, 2015). Activated B cells undergo clonal expansion, rapidly proliferating (Kuppers, 2021) in the DZ and express high levels of CXCR4 which interacts with CXCL12 positive stromal cells. These B cells are termed centroblasts and they undergo somatic hypermutation (SMH); a process that introduces point mutations into the variable region genes (Patel et al., 2021) to generate BCR variants with different affinities to cognate antigen and, class-swich recombination (CSR) of the heavy chain to produce antibodies of different isotype classes (IgG, IgA and IgE) (Kuppers, 2021) . Activation-induced cytidine deaminase (AID) is expressed on centroblasts and patients lacking AID do not develop memory B cells or PCs and suffer from hyper-IgM syndrome (Revy et al., 2000). This shows that AID expression on B cells is crucial for the development of memory B cells and long-lived PCs. Centroblasts downregulate CXCR4 and move to the LZ where they interact with antigen complexes on FDCs and those BCRs with the highest affinity result in the highest number of peptide-MHC II complexes being presented to TFH cells (Batista et al., 2001) that provide pro-survival signals to B cells (Eibel et al., 2014). B cells with low affinity BCRs undergo apoptosis as they do not receive survival signals from TFH cells (Eibel et al., 2014).

B cells are selected for higher antigen-specific affinity BCRs in a process called affinity maturation (Kuppers, 2021, Patel et al., 2021). These B cells either re-enter the DZ for further rounds of mutation and selection (Basso and Dalla-Favera, 2015, McHeyzer-Williams and McHeyzer-Williams, 2005) and BCRs with the highest antigen-specific affinities leave the GC as memory B cells and long-lived PCs that secrete class-switched Ig (IgG, IgE and IgA) (Eibel et al., 2014, Kuppers, 2021). The transcription factor XBP-1 has an important role in preparing antibody-secreting cells for the high endoplasmic reticulum stress that arises due to extensive Ig synthesis (Eibel et al., 2014).

Memory B cells can be separated into subpopulations using the surface expression of IgD and CD27; unswitched memory B cells are defined as IgD+ CD27+, classical switched memory B cells are defined as IgD- CD27+, naïve B cells are characterised by IgD+ CD27- and IgD- CD27- B cells are referred to as double negative (DN) (Fecteau et al., 2006, Wei et al., 2007, Berkowska et al., 2011, Wu et al., 2011, Buffa et al., 2013). DN B cells are highly expressed in inflammation caused by autoimmunity (Wei et al., 2007) or infection (Bernard, 2018). Memory B cells rapidly proliferate upon re-encounter with a cognate antigen and mount a robust immune response (Bernasconi et al., 2003).

CD19+ CD24-/low CD38hi IgD- CD77- plasmablasts (PBs) are capable of differentiating into terminally differentiated PCs (van Zelm et al., 2007). GC B cells with the highest affinity BCRs become PBs and downregulate BCL-6 expression prior to exiting the GC (Basso and Dalla-Favera, 2015). PBs circulate in the blood to the BM or to target organs where they further differentiate into long lived PCs (Caraux et al., 2010, Zhang et al., 2014, Bernasconi et al., 2003, Arpin et al., 1995). Once in their niche, PCs receive survival signals (Caraux et al., 2010, Zhang et al., 2014, Bernasconi et al., 2003, Arpin et al., 1995) through BCMA ensuring

lifelong persistence (McHeyzer-Williams and McHeyzer-Williams, 2005, LeBien and Tedder, 2008).The PC pool is replenished from the memory B cell population as memory B cells can differentiate into PCs upon re-challenge with an antigen (LeBien and Tedder, 2008).

1.2 Liver

The liver plays a role in many physiological processes such as digestion, metabolism, vitamin storage, detoxification and immunity (Kalra et al., 2024). The majority of the liver is composed of hepatocytes with cholangiocytes being the second most abundant cell type within the liver (Trefts et al., 2017). Quiescent stellate cells store vitamin A in lipid droplets however upon liver damage, these stellate cells become activated are contribute to the deposition and organising of collagen which leads to fibrosis (Trefts et al., 2017). Kupffer cells are liver resident macrophages which recognise pathogenic stimuli introduced to the liver through the portal circulation (Trefts et al., 2017). Liver sinusoidal cells represent a permeable barrier between hepatocytes and blood cells (Poisson et al., 2017).

A liver lobule is the functional unit of the liver and each lobule is hexagonal, made up of chords of hepatocytes surrounding a central vein (Trefts et al., 2017), with a portal triad (portal vein, hepatic artery and bile duct) at each corner of the hexagon (Kalra et al., 2024) **(figure 1.2)**. Bile secreted from hepatocytes into the bile canaliculi travels from small bile ducts to the large bile ducts and eventually to the duodenum or gall bladder. Bile aids in the digestion and absorption of lipids (Kalra et al., 2024).

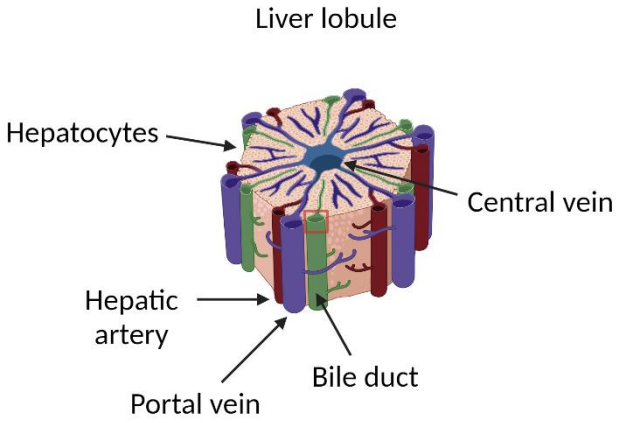


Figure 1.2 The liver lobule is the functional unit of the liver. *It consists of hepatocytes surrounding a central vein forming a hexagonal shape. Portal triads are found at each corner of the hexagon. Image created using Biorender.*

Liver cirrhosis develops due to persistent inflammation which results in the loss of healthy liver parenchyma due to the formation of fibrotic tissue and regenerative nodules (Gines et al., 2021). Liver cirrhosis is the 11th most common cause of morbidity and is responsible for approximately 3.5% of deaths globally (Asrani et al., 2019) resulting in a high demand for donor livers. The liver is the second most frequent solid organ transplant as there is currently no curative treatments for chronic liver disease (Asrani et al., 2019). Discovering alternative treatments is crucial in relieving the global demand for donor livers. Understanding how the cells of the adaptive system contribute to disease is vital in providing efficient therapies that target or manipulate the immune system (Uhl et al., 2014).

The liver is the largest organ in the human body with the hepatic artery and portal vein providing dual blood flow exposing the liver to frequent and a variety of pathogens and toxins (Bogdanos et al., 2013, Robinson et al., 2016). This requires the liver to maintain a tolerant environment but also possess strong innate immunity to tackle infections (Kubes

and Jenne, 2018, Zhang and Lu, 2018, Byun and Yi, 2017, Gao, 2016, Bogdanos et al., 2013). Acute hepatitis is able to resolve upon the elimination of the cause of injury, due to the ability of the liver to regenerate (Bogdanos et al., 2013) however failure to resolve inflammation results in dysregulation of liver homeostasis and fibrosis (Robinson et al., 2016). Persistent chronic inflammation results in damage to hepatocytes which leads to fibrosis and scarring of the liver progressing to cirrhosis, the major cause of death in chronic liver diseases (CLD) **(figure 1.3)** (Patten and Shetty, 2018, Seki and Schwabe, 2015).

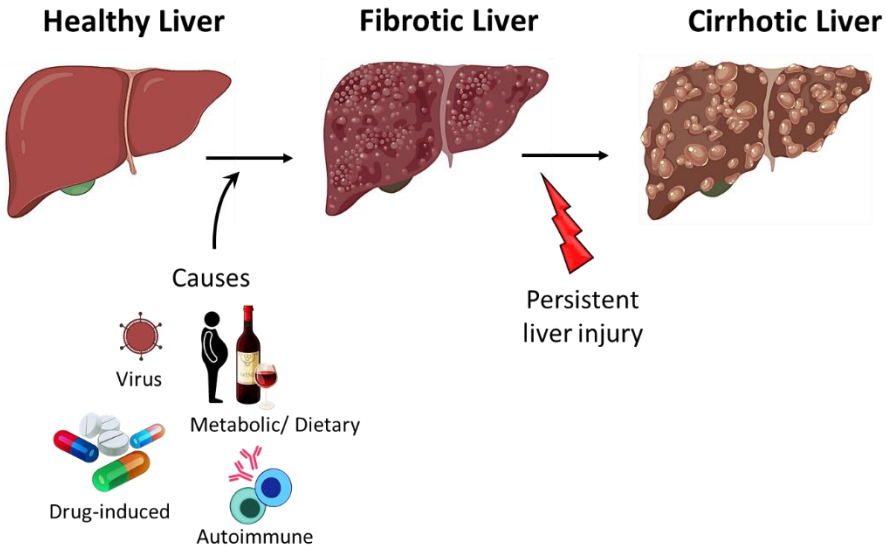


Figure 1.3 The progression of liver disease. *Upon acute liver injury, a healthy liver can regenerate once the cause of injury has been removed. Continued insult and resulting inflammation damage the liver and persistent injury to the liver results in fibrosis and eventually cirrhosis with the need for a liver transplantation. Image taken from (Patel et al., 2021).*

B cells play an important role in the immune response and are known to contribute to the pathogenesis of autoimmune disorders through the production of autoantibodies, antigen presentation and the secretion of pro-inflammatory cytokines (Hampe, 2012). The role of B cells in chronic liver diseases is less clear.

1.2.1 Alcohol related liver disease

Alcohol related liver disease (ArLD) is a metabolic disease that contributed to over three million deaths in 2018 (Subhani et al., 2022). This globally common disease results in preventable liver-related mortality (Parker et al., 2019). In the UK alcohol-related mortality in 2020 resulted in a total of 8974 deaths, an increase of 18.6% compared to 2019, the highest reported since 2001 (Office_For_National_Statistics_(ONS), 2021). There has been a 17% increase over the last decade in alcohol-related hospital admissions and alcohol-related harm costs the National Health Service (NHS) £3.5 billion per year (NHS_England, 2019).

ArLD is associated with high alcohol consumption that induces hepatocyte injury and introduces alterations in metabolism, leading to enhanced lipogenesis and fat retention known as steatosis (Nowak and Relja, 2020, Almeida et al., 2015, Seki and Schwabe, 2015). At the stage of alcoholic steatosis, cessation of alcohol intake can reverse ArLD however, excessive alcohol abuse leads to the development of alcoholic hepatitis culminating in alcoholic cirrhosis which is difficult to treat (Hollister et al., 2018, Matos et al., 2013, Zwolak et al., 2016). Cirrhosis occurs due to continued inflammatory insult and a disruption in the hepatocellular network caused by fibrotic tracts (Nowak and Relja, 2020).

Immune dysfunction arises due to excessive alcohol abuse. The B cell compartment is altered in ArLD patients with significant reductions in immature, naïve and memory B cell populations (Almeida et al., 2015, Zwolak et al., 2016). This decrease in peripheral B cells may be due to a decline in B cell egress from the spleen (Almeida et al., 2015) or a consequence of alcohol-induced B cell apoptosis (Zwolak et al., 2016). ArLD is defined as an IgA disorder due to the increased presence of IgA complexes and elevated levels of IgM, IgG

and IgA in the serum of cirrhotic ArLD patients (Massonnet et al., 2009). Increased percentages of PBs were found in ArLD patients (Almeida et al., 2015) which may account for the high levels of Igs present. In addition, levels of TGF-β, a factor involved in IgA class-switching was increased in chronic alcoholic patients (Almeida et al., 2015) suggesting abnormal IgA class-switching resulting in increased levels of serum IgA. Patients with steatohepatitis had lower levels of soluble IgM (sIgM), sIgG and sIgA positive memory B cells however, alcoholic patients who displayed no symptoms of liver disease had increased levels of IgA+ memory B cells. These patients had an expansion in CD27- sIgA+ class-switched memory B cells (Almeida et al., 2015).

A reduction in B-reg function may allow the accumulation of pro-inflammatory mediators that propagate inflammation and immune activation (Almeida et al., 2015, Massonnet et al., 2009). Almeida et al., showed that the expression of inhibitory markers CD5 and CD72 was reduced on immature B cells in ArLD patients. It can be speculated that the decline in inhibitory molecule expression promotes inflammation contributing to tissue injury and inhibition of B-reg function (Almeida et al., 2015, Massonnet et al., 2009).

B cells express a variety of TLRs on their surface. In alcoholic cirrhosis patients, TLR9 activated B cells were linked with an increase in IgA (Byun and Yi, 2017) however Massonnet et al., observed a significant decrease in the expression of TLR9 mRNA in peripheral blood mononuclear cells (PBMCs) from alcoholic cirrhosis patients (Massonnet et al., 2009). B cells isolated from alcoholic cirrhosis patients had impaired responses to TLR stimulation whereas B cells from healthy controls produced IgA in response to TLR9 stimulation with CpG (TLR9 agonist) (Almeida et al., 2015). However isolated B cells from alcoholic cirrhotic patients produced high amounts of IgA when stimulated with CpG and R848 (TLR7 agonist)

(Massonnet et al., 2009). Compared to healthy controls, unstimulated B cells from ArLD patients secreted an average of 45 times more IgA (Almeida et al., 2015). Lipopolysaccharide (LPS), a TLR4 agonist has been proposed to be a causative toxin in ArLD as patients had elevated levels of circulating LPS in the blood and LPS drives pathogenesis in rodents and humans with ArLD (Matos et al., 2013, Hollister et al., 2018).

Alcohol consumption alters intestinal permeability by downregulating the expression of tight junction proteins allowing bacterial translocation and creating a dysbiosis in gut flora. Thus contributing to inflammation via the activation of TLRs and the presence of microbial products activate immune cells (Nowak and Relja, 2020). Altered intestinal permeability and bacterial translocation observed in ArLD (Almeida et al., 2015, Zwolak et al., 2016) allows the release of LPS which binds to lipopolysaccharide binding protein (LBP), eliciting an immune response and activating lymphocytes through the ligation of TLR4 and initiating an inflammatory response (Hollister et al., 2018). Ligation of LPS to LBP may initiate the migration of peripheral B cells to gut-associated lymphoid tissues (GALT). Chronic alcoholic patients had higher numbers of GALT-derived sIgA+ B cells which was supported by a significantly higher proportion of IgA+ memory B cells and IgA+ PBs in the blood of patients (Almeida et al., 2015). Almeida et al., also showed that peripheral CD27- sIgA+ memory B cells have GC-independent responses comparable to gut lamina propria IgA producing B cells. These results indicate that gut derived PAMPs stimulate TLRs activating immune cells and contributing to ArLD pathogenesis.

Hepatocytes and leukocytes were damaged by acetaldehyde production (product of the breakdown of alcohol) which destroys the cellular membrane (Seki and Schwabe, 2015) that results in the release of damage-associated molecular patterns (DAMPs). This in turn

generates reactive oxygen species (ROS) that also contribute to hepatocellular injury. ArLD patients had B cells with a high Bcl-2 expression which was associated with the level of portal and lobular inflammation (Zwolak et al., 2016). Bcl-2 mediated B cell apoptosis and ROS-mediated hepatocellular damage results in the production of significant amounts of cellular debris and the release of DAMPs. Cellular debris, which contains self-antigens and intracellular proteins can be recognised by autoreactive B cells eliciting an inflammatory response upon antigen recognition.

ArLD patients had a breakdown in tolerance that may be due to impaired negative selection of autoreactive B cells as ArLD patients had autoantibodies against modified liver proteins (Hollister et al., 2018). A reduction in B-reg function may also contribute to the dysregulation of immunity. Anti-phospholipid, anti-nuclear, anti-dsDNA, anti-ssDNA and anti-lymphocyte autoantibodies have been detected in 25-60% of ArLD patients (Matos et al., 2013). Alcohol-induced oxidative stress activated antigen-presenting cells (APCs) which recognised toxic metabolites, haptens (Matos et al., 2013). Activated B cells secreted antibodies targeting haptens and self-proteins eliciting an inflammatory immune response and tissue damage. Excessive alcohol consumption resulted in lower numbers of TFH cells (Hollister et al., 2018) which may be a result of TFH migration to GC-like structures where they aid in B cell survival and differentiation into memory B cells and PB. The number of PBs were increased in ArLD patients (Almeida et al., 2015).

In summary, excessive alcohol consumption alters intestinal permeability allowing translocation of LPS and other gut-derived pathogens into the liver, where they activate B cells and induce the secretion of antibodies and inflammatory mediators that participate in hepatocyte injury (Zhou and Zhong, 2017). Alcohol abuse leads to an accumulation of

acetaldehyde, a metabolite that contributes to inflammation, damage to cellular membranes and the generation of ROS resulting in the exposure of cellular proteins. These activate autoreactive B cells that enter the GC reaction and differentiate into PCs that secrete vast amounts of autoantibodies which form immune complexes that further activate lymphocytes and damage hepatocytes **(figure 1.4)**. The liver becomes fibrotic because of the continued insult and progresses to cirrhosis and the need for a liver transplant.

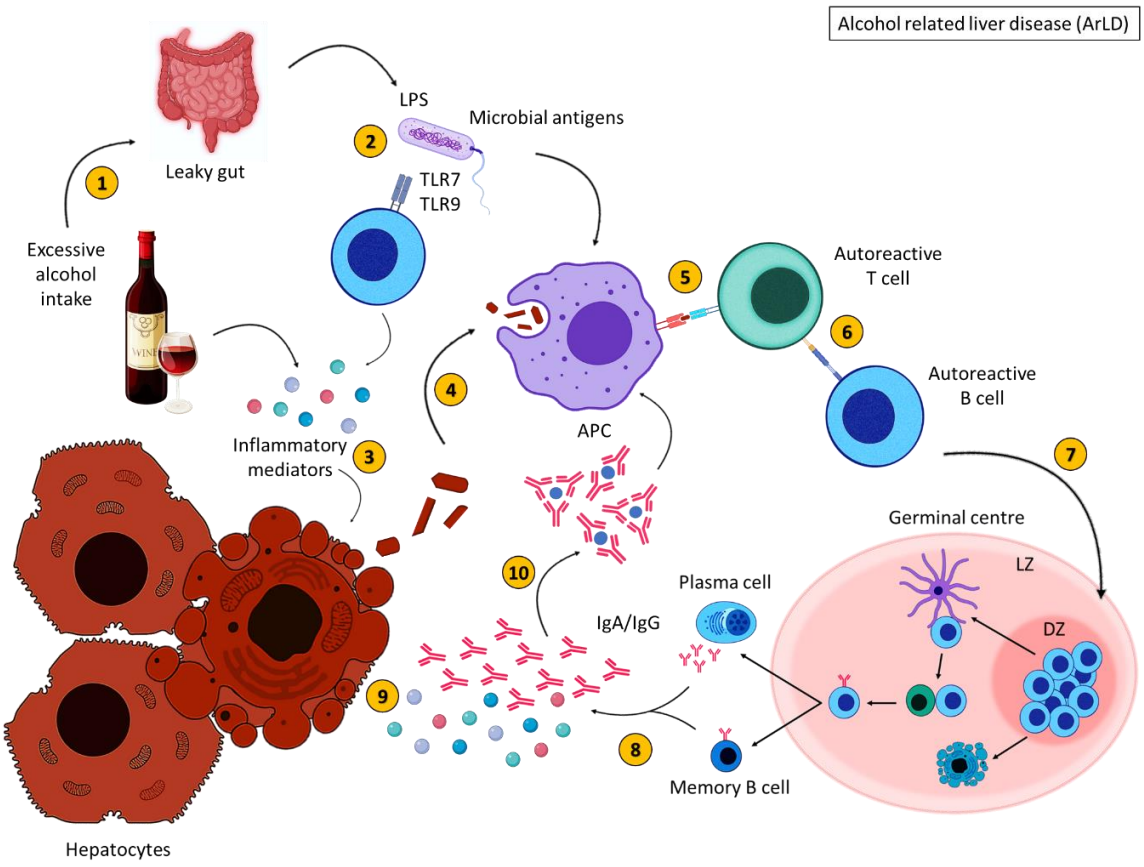


Figure 1.4 Alcohol related liver disease pathogenesis. *(1) Alcohol intake results in 'leaky gut syndrome' in which (2) translocation of gut microbial antigens activates the immune response in the liver. This results in the (3) production of inflammatory mediators which damage hepatocytes and (4) result in the expulsion of cellular debris. Self-antigens and microbial antigens are recognised by APCs which (5) activate T cells. (6) T cells recognising self-ligands are activated and in turn active autoreactive B cells which undergo the (7) GC reaction and differentiate into (8) autoreactive memory B cells and plasma cells. These cells contribute to further hepatocyte injury through the (9) production of inflammatory mediators and class-switched autoantibodies. These autoantibodies can form (10) immune complexes*

which further activate lymphocytes and contribute to hepatocyte damage. Image taken from (Patel et al., 2021).

1.2.2 Non-alcoholic steatohepatitis

The global prevalence of non-alcoholic fatty liver disease (NAFLD) in adults is approximately 25% whereas the prevalence of non-alcoholic steatohepatitis (NASH) is 6% in developed countries. 3.7 out of 100,000 NAFLD-related hospital admissions were reported in the UK in 2021 (Official_Statistics, 2022). The most common indicator for liver transplantation is NASH-related cirrhosis (Abeysekera et al., 2020).

NAFLD is a term encompassing a range of conditions caused by the accumulation of lipids in the liver (Leroux et al., 2012). NAFLD can progress from steatosis to NASH where fat retention is associated with hepatic inflammation (Bruzzi et al., 2018, Leroux et al., 2012). NASH patients have inflammatory damage to their hepatocytes that causes hepatocyte apoptosis and results in varying degrees of fibrosis (Seki and Schwabe, 2015) that can result in cirrhosis and hepatocellular carcinoma with a need for a liver transplant (Bruzzi et al., 2018, Leroux et al., 2012). Type 2 diabetes, cardiovascular diseases and osteoporosis are frequent extrahepatic manifestations observed in patients with NAFLD (Sutti and Albano, 2020, Bruzzi et al., 2018).

NAFLD pathology is thought to be a ‘two-hit’ theory; the first hit is the abnormal accumulation of lipids or an impaired liver lipid metabolism resulting in a decrease in lipid clearance. The second hit is the inflammatory response (Zeng et al., 2020) that results in an influx of activated immune cells and induces lobular and portal inflammation (Bruzzi et al., 2018). The hepatic lymphocyte compartment was altered in patients with NAFLD (Leroux et

al., 2012) with elevated numbers of B cells associated with severity of disease (Schwenger et al., 2018). 60% of NASH patients had the presence of ectopic lymphoid structures (B and T cell aggregates) that correlated in size and lobular inflammation (Sutti and Albano, 2020). Visceral adipose tissue (VAT)-isolated B cells from obese mice displayed increased production of pro-inflammatory mediators whilst the absence of B cells improved inflammation (Sutti and Albano, 2020) suggesting that B cells contribute to NAFLD progression to NASH via the production of inflammatory mediators.

Altered distribution of adipose tissue was observed obese people and obesity promoted the activation of B cells that contributed to the advancement of steatohepatitis which was observed as an early event in animal models of NASH (Bruzzi et al., 2018). Mouse models have shown that inflammatory cytokines, adipocytokines and free fatty acids (FFA), secreted by the mesenteric adipose tissue (MAT) (located between the gut and the liver), enter the liver via the portal vein affecting liver histology (Wu et al., 2019). B cells from high fat diet (HFD)-fed mice promoted inflammation of epididymal adipose tissue (EAT) and produced IgG (Wu et al., 2019).

NAFLD patients have altered intestinal permeability granting gut-derived pathogens access to the liver which activate hepatic immune cells and contribute to inflammation. LPS levels were raised in patients with NAFLD compared to healthy controls (Schwenger et al., 2018). Bacterial translocation and LPS are recognised by TLRs and B cells that become activated and contribute to lipid accumulation, liver inflammation and tissue destruction (Schwenger et al., 2018, Seki and Schwabe, 2015). Furthermore LPS-stimulated hepatic B cells promote local inflammatory responses (Byun and Yi, 2017) further contributing to the inflammatory environment observed in NAFLD.

Progression of disease from steatosis to NASH is due to cytokine release from inflamed adipose tissue and the generation of ROS due to impaired lipid metabolism (Seki and Schwabe, 2015). ROS-mediated hepatocyte apoptosis results in the release of self-epitopes into the microenvironment. These epitopes can activate autoreactive B cells and induce the release of autoantibodies. IgG antibodies targeting oxidative stress-derived epitopes (OSE) were detected in high amounts in NAFLD/NASH patients and these patients had elevated IFN-γ levels and increased incidence of fibrosis and/or cirrhosis (Bruzzi et al., 2018). MHC class II was upregulated on PBs in NASH patients (Bruzzi et al., 2018) suggesting that PBs present OSE antigens to T cells that become activated and contribute to pathogenesis. 63% of NASH liver samples had the presence of ectopic lymphoid aggregates that correlated with the severity of fibrosis and lobular inflammation. These lymphoid aggregates were associated with elevated anti-OSE IgG titres (Bruzzi et al., 2018).

In summary, the development of NASH begins with the abnormal accumulation of lipids which induces inflammation and fibrosis **(figure 1.5)**. Immune cell activation, production of inflammatory mediators and ROS-mediated hepatocyte apoptosis results in the release of OSEs which activate autoreactive B cells to generate autoantibodies. These anti-OSE autoantibodies further activate immune cells to produce cytokines resulting in tissue damage and ROS production, all of which contribute to liver damage. This vicious cycle leaves the liver unable to regenerate and causes disease progression from fibrosis to cirrhosis (Patel et al., 2021).

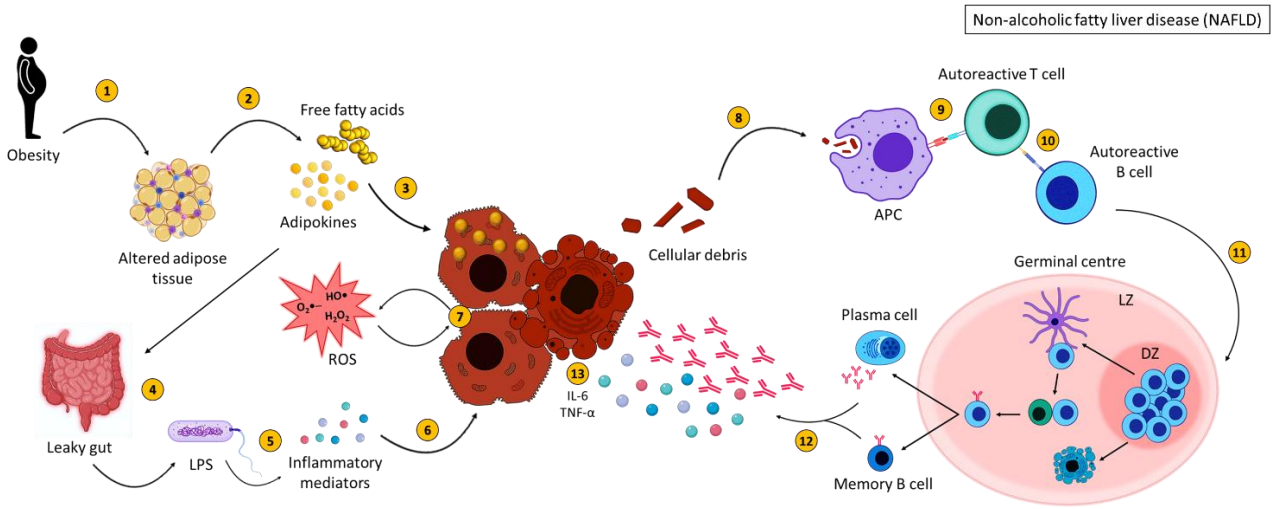


Figure 1.5 Non-alcoholic fatty liver disease pathogenesis. *(1) Altered adipose tissue occurs due to obesity. (2) These adipose tissues release adipokines and free fatty acids which (3) induce lipid accumulation in hepatocytes and (4) alter intestinal permeability enabling the (5) translocation of microbial antigens to the liver (6) where immune cells mount secrete inflammatory mediators that damage hepatocytes. (7) As a result of tissue damage, reactive oxygen species are produced which further contribute to hepatocyte damage. (8) Expulsion of cellular debris are recognised by APCs which (9) present antigens to autoreactive T cells. (10) These activated autoreactive T cells activate autoreactive B cells which then (11) undergo germinal centre reactions and (12) differentiate into memory B cells and plasmablasts/plasma cells. These differentiated B cells secrete inflammatory mediators and autoantibodies contributing to tissue destruction. Image taken from (Patel et al., 2021).*

1.2.3 Viral hepatitis

1.4 million people die from viral hepatitis related mortality each year. 90% of these deaths are due to hepatitis B virus (HBV) and hepatitis C virus (HCV) infections (Jefferies et al., 2018). In Europe, approximately 14 million and 9 million people are chronically infected with HBV and HCV, respectively (WHO, 2012). 57% of liver cirrhosis and 78% of primary liver cancer cases arise as a result of HBV or HCV infection (Perz et al., 2006), placing a heavy burden on healthcare systems due to the costs of treating chronic liver disease and liver failure (WHO, 2012).

Out of the five types of viral hepatitis, hepatitis B and hepatitis C viruses can cause chronic liver disease. These viruses are not directly cytopathic, but infection may lead to inflammation and liver injury that can last decades before progressing to end-stage liver disease requiring liver transplantation (Loggi et al., 2014, Bogdanos et al., 2013).

Infected individuals can produce antibodies against both viruses. Early HBV infection is marked by the presence of anti-core protein IgM antibodies however, as infection progresses, antibodies against the hepatitis B surface (HBsAg) and e (HBeAg) antigens were observed (Tan et al., 2015, Loggi et al., 2014). Majority of HBV infected adults can clear the viral infection (Burton et al., 2018). Activation of naïve B cells by the T-independent antigen HBsAg mounts a robust antibody response however, chronic HBV patients, circulating B cells specific for HBsAg were unable to produce effective anti-hepatitis B antibodies (Burton et al., 2018, Poonia et al., 2018). This suggests that activated naïve B cells respond by producing IgM antibodies and not class-switched antibodies. Many HCV patients are asymptomatic so it is difficult to study early humoral immune responses against HCV (Cashman et al., 2014).

Chronic HCV patients have an abundance of antibodies against the envelope glycoproteins which may appear later in HCV infection (von Hahn et al., 2007). HCV investigations in a single patient showed that HCV generated variants to evade neutralising antibodies (von Hahn et al., 2007) however antibodies can contribute to the eradication of and prevention of HCV infection *in vivo* (Laidlaw and Dustin, 2020). Whilst there is no current vaccine against HCV infection, immunisation with viral envelope glycoproteins in healthy volunteers resulted in the production of neutralising antibodies (Stamataki et al., 2011) and these antibodies were shown to be protective in a human liver chimeric mouse model (Law et al., 2008). Genetically humanised mice and non-primates immunised with insect derived soluble

envelope glycoprotein 2 generated high titres of broadly neutralising antibodies against diverse HCV envelope proteins and resulted in the activation of humoral and cellular immunity (Laidlaw and Dustin, 2020).

Severe liver damage was associated with an accumulation of circulating B cells within the liver (Ni et al., 2003). HBV and HCV patients had high numbers of activated B cells that were unable to proliferate and expressed Fc receptor-like protein 4 (FcRL4), an inhibitory marker found on exhausted memory B cells (Loggi et al., 2014). This suggests that infected livers have dysfunctional B cells that have adopted an exhausted phenotype due to chronic activation (Patel et al., 2021).

HBV evades the immune system by releasing subviral particles (empty virions consisting of mostly HBsAg) from hepatocytes (Rydell et al., 2017) that crosslink neutralising antibodies to generate immune complexes. These immune complexes continually stimulate the BCR resulting in an expansion of exhausted memory B cells, also known as atypical memory B cells (Hehle et al., 2020, Burton et al., 2018, Poonia et al., 2018). Deposits of the hepatitis B core antigen (HBcAg)-immune complexes were detected in the livers of chronic HBV patients (Vanwolleghem et al., 2020). Atypical memory B cells express PD-1 and Fc receptor-like protein 5 (FcRL5) which inhibit B cell signalling and suppress B cell activation by crosslinking to immune complexes, respectively (Ma et al., 2019, Burton et al., 2018). HBV infected patients were enriched with atypical memory B cells that had defective BCR signalling and were unable to escape apoptosis. These atypical memory B cells also had a reduced capacity to secrete antiviral cytokines and were unable to differentiate into ASCs, limiting the production of neutralising anti-HBV antibodies (Burton et al., 2018, Poonia et al., 2018, Hehle et al., 2020, Vanwolleghem et al., 2020).

HBV and HCV patients had an enrichment of a B-regs that produced IL-10 which may contribute to viral persistence (Fang et al., 2020, Loggi et al., 2014, Burton et al., 2018, Wang et al., 2018, Eiza et al., 2018). A subset of IL-10 producing B-regs highly expressed surface markers; CD5, CD1d and IgD (Fang et al., 2020, Eiza et al., 2018). Upon stimulation, CD5+ B-regs produced IL-10 and correlated with inadequate virus elimination (Eiza et al., 2018).

B cells may play a role in HCV infection. B cells can act as vehicles for HCV transmission to hepatocytes (Stamataki et al., 2009). Activated B cells bind HCV viral particles and internalise them into compartments that prevent viral degradation. The intact viral particles are then recycled to the B cell surface within hours. B cell transmitted virus was more infectious compared to cell-free virus (Stamataki et al., 2009) highlighting a role for B cells in HCV pathogenesis. HCV RNA was found in 110/132 (83%) of HCV patients (Arai et al., 2020) with HCV RNA being frequently detected in B cells compared to CD4+ and CD8+ T cells (Inokuchi et al., 2009).

Mixed cryoglobulinemia (MC) is the most frequent B cell lymphoproliferative disease associated with HCV (Dammacco et al., 2000, Agnello et al., 1992) however, rare cases of cryoglobulinemia have been reported in HBV patients (Alfraji et al., 2020). Cryoglobulins, abnormally precipitated immunoglobulins that can be coupled with rheumatoid factor (Charles et al., 2013), are characteristic of MC and 40-60% of HCV infected patients had cryoglobulins present in their circulation (Boleto et al., 2021, Tucci and Kuppers, 2014). Unregulated B cell proliferation and antibody production contribute to the formation of cryoglobulins (Boleto et al., 2021) which can form immune complexes that can cause vasculitis by accumulating in small or medium blood vessels (Alfraji et al., 2020, Saadoun et al., 2007, Agnello et al., 1992). Ectopic hepatic lymphoid aggregates may arise due to clonal

B cell proliferation in MC HCV patients (Dustin, 2017). CXCL13 can trigger B cell migration to intraportal lymphoid aggregates within the liver and form a microenvironment to support B cell aggregation (Lauletta et al., 2012).

To summarise, HBV and HCV can chronically infect individuals and alter immune responses. Both these viruses are able use evasion techniques to escape immune responses. In HBV infection, constant BCR triggering results in B cells with an exhausted phenotype. B cells may also be used as a mode of viral transmission by HCV. Both HBV and HCV infected patients have an enrichment of B-regs which may aid in viral persistence. This suggests that viral hepatitis may alter B cell biology rendering them incapable of mounting effective antibody responses.

1.2.4 Autoimmune hepatitis

Autoimmune hepatitis (AIH) is a multifactorial progressive necro-inflammatory autoimmune disease necessitating life-long immunosuppressive therapy (Dywicki et al., 2020, Jeffery et al., 2018, Taubert et al., 2014, Bogdanos et al., 2013). The global incidence rate for AIH is 0.4-3 out of 100,000 people per year (Gronbaek et al., 2020). AIH has a higher prevalence in females, but it affects all ages, races, and sexes (Moritoki et al., 2006, Bogdanos et al., 2013, Behairy et al., 2016, Than et al., 2016). Other autoimmune diseases such as coeliac disease, primary biliary cholangitis (PBC) or primary sclerosing cholangitis (PSC) can often coexist with AIH (Than et al., 2016).

The hepatic parenchyma is destroyed through immune-mediated hepatocyte destruction (Dywicki et al., 2020, Moritoki et al., 2006, Bogdanos et al., 2013, Lapierre et al., 2013, Behairy et al., 2016, Zwolak et al., 2016, Jeffery et al., 2018, Ogawa et al., 2000). Increased

immune cell infiltration and inflammation cause fibrosis which progresses to cirrhosis; identified in 40% of AIH patients at the time of diagnosis (Dywicki et al., 2020). Liver transplantation was required in 10-20% of AIH patients that progressed to end-stage liver disease, despite the use of corticosteroids and immunosuppressive (Lapierre et al., 2013).

AIH patients have several autoantibodies (Sebode et al., 2018) including; anti-nuclear antibodies (ANA), smooth muscle antibodies (SMA) and anti-liver kidney microsome type 1 (LKM1) antibodies that classify AIH into three types (Moritoki et al., 2006, Schlaak et al., 1993, Than et al., 2016, Zwolak et al., 2016). ANA and SMA antibodies are characteristic of type 1 AIH with perinuclear anti-neutrophil cytoplasmic antibodies (pANCA) being present in 65-92% of patients with type 1 AIH (Moritoki et al., 2006, Than et al., 2016). Type 2 AIH is characterised by antibodies against liver cytosol type 1 (LC1) and/or anti-LKM1 antibodies (Lapierre et al., 2013, Than et al., 2016); pANCA antibodies are not detected in this type of AIH. The antigens for anti-LKM1 and anti-LC1 are liver specific enzymes CYP2D6 and formimidoyltransferase cyclodeaminase (FTCD), respectively (Moritoki et al., 2006, Lapierre et al., 2013). Anti-LC1 IgG antibodies were detected in 30-50% of type 2 AIH patients and were associated with disease severity (Behairy et al., 2016, Moritoki et al., 2006). Type 3 AIH is classified by the presence of anti-soluble liver antigen/ liver pancreas antibodies (anti-SLA/LP) which are detected in 10-30% of patients (Moritoki et al., 2006). Antibodies against asialoglycoprotein receptor (ASGPR), a compartment of liver specific lipoproteins that is expressed on hepatocyte surfaces were detected in 50-76% of AIH patients and anti-ASGPR titres positively correlate with a poor outcome of disease (Moritoki et al., 2006).

T cells have been proposed to be the cause of hepatic destruction in AIH, however the presence of several autoantibodies suggests a role for B cells in AIH pathogenesis (Dywicki et

al., 2020). Mixed immune infiltration of CD3+ T cells, CD19+ B cells, IgG+ cells and PCs was observed in liver biopsies from AIH patients (Moritoki et al., 2006, Schlaak et al., 1993, Minaga et al., 2019, Behairy et al., 2016, Than et al., 2016) and an increased numbers of B and T cells were detected in the liver during AIH flare ups (Than et al., 2016) suggesting that B cells also contribute to AIH pathology. Self-antigens are presented to autoreactive T cells by APCs. These activated T cells activate autoreactive B cells to differentiate into PCs and produce autoantibodies (Schlaak et al., 1993). B cells from new onset AIH patients had increased CD86 expression (Ma et al., 2014) suggesting that B cells were providing co-stimulatory signals to T cells. AIH patients had elevated levels of IL-4, a cytokine produced by T cells which aids in B cell activation and differentiation (Moritoki et al., 2006, Schlaak et al., 1993).

85% of AIH patients have elevated serum IgG titres displaying ongoing inflammation (Hartl et al., 2020). Increased numbers of IgG+ and IgM+ cells were detected around bile ducts and in portal tract areas (Moritoki et al., 2006, Minaga et al., 2019, Ogawa et al., 2000, Behairy et al., 2016). IgG binds to healthy hepatocytes which becomes a target for lymphocytes resulting in inflammation and lymphocyte-mediated cellular injury (Bogdanos et al., 2013).

In summary, AIH is an autoimmune liver disease where the trigger is unknown. Mixed lymphocytic infiltrates were found in AIH livers displaying a complex role between cellular and humoral immunity. The presence of autoantibodies targeting a range of self-proteins indicates a breakdown in both B and T cell tolerance. Furthermore, these autoantibodies highlight an important role for B cells in the pathogenesis of AIH.

1.2.5 Primary sclerosing cholangitis

Primary sclerosing cholangitis (PSC) is a cholestatic autoimmune disease that is characterised by the destruction of large bile ducts due to chronic inflammation and fibrosis (Moritoki et al., 2006, Chung et al., 2018, Fischer et al., 2014, Chapman et al., 2019). The incidence of PSC is estimated to be 0.91-1.3 per 100,000 people per year based on population studies (Chapman et al., 2019). 87% of PSC patients also had ulcerative colitis (UC) and 13% had Crohn's disease (CD) (Chung et al., 2018, Ma et al., 2015, Moritoki et al., 2006). Many PSC patients will require a liver transplant due to the chronic destruction and scarring of the biliary tree that leads to cirrhosis (Fischer et al., 2014).

88% of PSC patients had the presence of anti-neutrophil cytoplasmic autoantibodies (ANCA) however these are not disease specific as they were also detected in AIH and biliary atresia (BA) patients (Moritoki et al., 2006). No PSC-specific autoantibodies have been detected thus far however, disease-relevant epitopes have been identified (Chung et al., 2017). Concentrations of anti-cardiolipin antibodies are associated with disease severity and are present in two-thirds of PSC patients (Moritoki et al., 2006).

PBMCs isolated from PSC patients showed a significant increase in total B cell numbers compared to healthy controls (Zhang et al., 2014). A significant infiltration of IgG4 PCs was observed in PSC patients and elevated serum IgG4 levels were detected in 10% of PSC patients (Fischer et al., 2014, Zen et al., 2011). PSC patient tissues had aggregates of IgG4+ PCs and deposits of IgG4 (Zen et al., 2016, Fischer et al., 2014). Fischer et al., showed that disease progression and lymphocytic infiltration correlated with the intensity of IgG4+ immunostaining (Fischer et al., 2014). Cultured B cells from PSC patients produced a variety

of autoantibodies indicating that the targets in PSC were self-antigens or were a product of cross-reactivity to foreign targets (Chung et al., 2018). Disease severity was associated with tissue infiltrating IgG4+ cells that were detected in 50% of explanted PSC livers (Fischer et al., 2014). IgG4-related disease (IgG4RD) is a chronic inflammatory disease with fibrosis and hepatic tissue damage (Al-Khalili and Erickson, 2018, Deshpande et al., 2012). This disease was associated with an increase in IgG4+ PCs and can be confused with PSC due to the presence of sclerosing cholangitis (Tanaka, 2019).

70% of PSC patients have inflammatory bowel disease (IBD; UC or CD) which was associated with a dysregulation in the intestinal barrier (O'Hara and LaRusso, 2019). This allows the translocation of gut pathogens and PSC patients had altered gut microbiota compared to healthy controls (Chung et al., 2018). The translocation of gut derived LPS, pathogens and food antigens may trigger the pro-inflammatory immune response (Chung et al., 2018, Jeffery et al., 2016). CCL25 is gut specific cytokine that recruits mucosal T cells, which are primed in the gut, migrate to the liver where they contribute to hepatic inflammation (Ma et al., 2015). LPS and other gut-derived bacterial motifs can stimulate biliary epithelial cells (BECs) to secrete cytokines that contribute to inflammatory tissue damage, propagating BEC destruction (Ma et al., 2015). PSC liver samples showed the presence of bacterial RNA (Ma et al., 2015) suggesting that altered intestinal permeability may contribute to inflammatory damage and disease progression.

In summary, PSC may be initiated due to a loss of self-tolerance which can be explained by molecular mimicry. Translocation of gut and bacterial antigens activate the immune response resulting in inflammation and the obliteration of BECs. Molecular mimicry and the expulsion of cellular debris activated autoreactive immune cells. Gut-primed T cells migrate

to the liver where they can activate B cells to differentiate into IgG4+ secreting PCs (Ma et al., 2015). These activate lymphocytes and BECs also secrete cytokines contributing to the inflammatory destruction of bile ducts and the progression of liver disease.

1.2.6 Primary biliary cholangitis

Primary biliary cholangitis (PBC) is an inflammatory autoimmune disease characterised by the destruction of intrahepatic small bile ducts (Chen et al., 2020, Moritoki et al., 2006, Kikuchi et al., 2005, Zhang et al., 2013, Zhou et al., 2017, Cichoz-Lach et al., 2018, Zwolak et al., 2016). The prevalence of PBC in the UK is estimated to affect 15,000 individuals (Hirschfield et al., 2018). The dysregulated immune response results in inflammatory damage, fibrosis and the accumulation of bile toxins that lead to cirrhosis and liver transplantation (Wang et al., 2015b, Zhou et al., 2017, Hirschfield and Gershwin, 2013).

The presence of autoantibodies in PBC indicate a loss of B cell tolerance (Zhang et al., 2013, Ma and Chen, 2019); anti-mitochondrial antibodies (AMA) directed against 2-oxoacid dehydrogenase complexes which are found on the inner mitochondrial membrane were detected in 90-95% of PBC patients (Chen et al., 2020, Moritoki et al., 2006, Kikuchi et al., 2014, Zhou et al., 2017, Cichoz-Lach et al., 2018, Zwolak et al., 2016). A key autoantigen in PBC is the E2 subunit of the pyruvate dehydrogenase complex (PDC-E2) and 50% of patients had autoantibodies directed against the nuclear pore complex members, gp210 and p62 (Moritoki et al., 2006). Disease severity was associated with ANAs targeting gp210 (Moritoki et al., 2006, Zhou et al., 2017, Ma and Chen, 2019). Frequency of PDC-E2-specific IgM, IgG and IgA PBs were significantly increased in PBC patients (Zhang et al., 2014). In addition, hyper-IgM expression was observed in the serum of many PBC patients (Kikuchi et al., 2005,

Ma and Chen, 2019). IgM agglutination activated complement and IgM augments antigen-driven IgG responses showing a crucial role for IgM agglutination in linking innate and adaptive immune responses (Kikuchi et al., 2005).

GCs are vital for the generation of class-switched immunoglobulins and long-lived PCs which arise with the help from TFH cells (Tan et al., 2016, Wang et al., 2015a, Ma and Chen, 2019, Wang et al., 2015b, Zhou et al., 2017). TFH are normally located in B cell follicles but were present in increased numbers in lymphoid-like follicles located near damaged bile ducts (Zhou et al., 2017). Hepatic TFH cells were absent in healthy control livers (Wang et al., 2015b). TFH derived from PBC patients had an enhanced ability to differentiate B cells into class-switched memory B cells and long-lived PCs (Wang et al., 2015b). PBC patients, especially those who do not respond to ursodeoxycholic acid (UDCA) treatment had an increased frequency of circulating TFH (cTFH) cells (Zhou et al., 2017). cTFH also secreted increased amounts of IL-21 inducing B cell differentiation and autoantibody secretion and cTFH positively correlated with circulating PCs (Zhou et al., 2017, Wang et al., 2015a, Wang et al., 2015b). Furthermore, serum AMA and IgM were directly correlated to levels of serum IL-21 (Wang et al., 2015a). This suggests that TFH cells contribute to PBC pathogenesis by inducing B cell proliferation and differentiation.

Intestinal permeability is impaired in PBC patients as PBC liver tissue showed the presence of multiple bacterial products (Ma et al., 2015). Hyper IgM in PBC may be a result of increased bacterial infections and PBC patients showed increased TLR signalling (Moritoki et al., 2006, Ma et al., 2015). Molecular mimicry between PDC-E2 and gut-derived bacterial proteins may be the initial cause of PBC (Zhou et al., 2017), resulting in a loss of self-tolerance, allowing the survival of autoreactive B cells (Ma and Chen, 2019). Furthermore, TLR activation results

in B cell activation and cytokine secretion that contributes to PBC pathology. B cells from PBC patients expressed high amounts of TLR9 and produced vast amounts of IgM and cytokine upon stimulation (Kikuchi et al., 2005, Ma et al., 2015). The amount of TLR9 expression positively correlated with IgM+ memory B cell numbers (Kikuchi et al., 2005, Ma et al., 2015). TLR9 expression on B cells was enhanced due to the presence of bacterial motifs and CpG stimulation of PBMCs isolated from PBC patients resulted in large amounts of AMA production compared to unstimulated controls (Moritoki et al., 2006). Cholangiocytes express TLRs on their surface and respond to stimulation by contributing to the immune response and cholangiocytes in PBC patients had high TLR4 and TLR9 expression (Bogdanos et al., 2013). BECs had increased TLR4 expression and hepatocytes in the periportal and interlobules also expressed TLR4 and were associated with advanced PBC disease (Ma et al., 2015). This shows that BECs and hepatocytes themselves contribute to inflammatory damage through TLR signalling.

Whilst BECs are the victims of the immune response, they may also have a role in the progression of PBC pathogenesis. BECs isolated from PBC livers undergo apoptosis and were engulfed by other BECs which translocated PDC-E2 into apoptotic bodies (Ma and Chen, 2019). The intact PDC-E2 antigen was presented to autoreactive immune cells initiating an inflammatory response and the production of AMA (Ma and Chen, 2019).

In summary, multiple factors contribute to PBC pathogenesis, molecular mimicry by bacterial motifs is thought to be the initial cause in the breakdown of self-tolerance and activation of the pro-inflammatory immune response. Immune-mediated destruction of BECs contributes to the inflammatory milieu and further activates autoreactive immune cells through PDC-E2

presentation in apoptotic bodies. This ongoing inflammatory damage results in the obliteration of bile ducts, fibrosis leading to cirrhosis and a liver transplant.

1.3 Paediatric acute liver failure

Paediatric acute liver failure (pALF) is a rapidly deteriorating disease that occurs in previously healthy children (Alonso et al., 2017) with no chronic liver disease (Mann et al., 2022). This life threatening disease accounts for 7.7% of all paediatric liver transplants (Mann et al., 2022) and 30% of cases have an unidentified cause of disease (Alonso et al., 2017).

Gut-derived products activate TLRs on immune cells, inducing an immune response that leads to liver damage (Patel et al., 2021, Mann et al., 2022). The microbiome plays a role in pALF as altering the microbiome alleviated disease in mice (Liu et al., 2021). Furthermore, depletion of the microbiome or induction of ALF in germ-free mice resulted in a milder disease (Mann et al., 2022), suggesting that the microbiome plays a role in ALF pathogenesis but is not the cause of disease.

1.3.1 Biliary atresia

Biliary atresia (BA) is a multifactorial paediatric liver disease (Yang et al., 2020, Wang et al., 2020, Luo et al., 2021) affecting 1 in 15,000 – 19,000 neonates (Aboughalia et al., 2021). BA is characterised by inflammatory destruction of the extrahepatic biliary tree and fibrosis (Bednarek et al., 2018, Patel et al., 2021) that result in hepatic destruction and liver failure requiring a transplant (Patel et al., 2021). There are two types of BA; acquired/non-syndromic and congenital/syndromic BA. Non-syndromic BA accounts for 80% of cases and 20% of cases are syndromic and are associated with other genetic abnormalities (Aboughalia et al., 2021, Patel et al., 2021, Mack et al., 2012).

50% of all paediatric liver transplants are due to BA (Luo et al., 2021, Aboughalia et al., 2021). Cirrhosis and end-stage liver failure resulting in death by two years of age is a consequence of untreated BA (Aboughalia et al., 2021, Yang et al., 2020). Kasai portoenterostomy (KPE) is a surgical procedure that restores bile flow from the liver to the gut by removing injured bile ducts; 95% of patients will undergo successful KPE surgery however, 80% of patients will still require a liver transplant (Taylor et al., 2019a, Patel et al., 2021, Bednarek et al., 2018). KPE timing is critical for the survival with the native liver as 49% of patients survived with their native liver if they received KPE during the first months of life. Receiving KPE after three months of life had a 23% survival rate with their native liver (Schreiber et al., 2007). Specialised centre for KPE surgery has improved survival to over 90% in the UK (Kelly and Davenport, 2007).

The pathogenesis of BA is not known however in 1974 a study suggested that the cholestatic changes observed in BA infants may be due to viral-induced liver injury (Landing, 1974). Cytomegalovirus (CMV) has been reported to infect biliary epithelia (Mack, 2007). 51 out of 85 BA liver biopsies showed the presence of human CMV (Xu et al., 2012) and another study found that BA infants who were CMV IgM positive were older at the time of KPE and had a reduced response to KPE (Zani et al., 2015). On the other hand, Jevon and Dimmick., found no CMV DNA from 12 BA patients (Jevon and Dimmick, 1999) and Yaghobi et al., detected no CMV genome in 34 BA liver tissue samples (Yaghobi et al., 2011).

Reovirus has also been implicated in BA pathogenesis. 55% of BA patients had reovirus RNA in hepatic and/or biliary tissues (Tyler et al., 1998) and Morecki et al., found that 9 out of 15 BA patients had anti-reovirus IgG antibodies (Morecki et al., 1982). A follow up study showed that anti-reovirus antibodies were detected in 62% of BA patients (Glaser et al., 1984). No

reovirus RNA was detected in the liver tissue from 14 BA patients (Steele et al., 1995) and Saito et al., also found no evidence of reovirus RNA from their cohort of BA patients (Saito et al., 2004).

Rotavirus have the ability to infect hepatocytes and bile duct epithelia (Mack, 2007). Group C rotavirus RNA was detected in 10 out of 20 BA patients (Riepenhoff-Talty et al., 1996) however, Bobo et al., found no evidence of rotavirus RNA in the biliary atresia group (Bobo et al., 1997). Despite the conflicting evidence of viral involvement in BA pathogenesis, the common animal model used for BA is the rhesus rotavirus (RRV)-induced murine model. Whilst group C rotavirus have been detected in some human BA studies, Riepenhoff-Talty et al., found that group A rotavirus-infected mice produced a hepatobiliary disease that shared characteristics with human BA, such as extrahepatic biliary obstruction, fibrosis and bile ductular proliferation (Riepenhoff-Talty et al., 1993).

Increased numbers of macrophages, CD4+ and CD8+ T cells were found in the portal tracts of BA patients (Wang et al., 2020). Intrahepatic periductular infiltrates had increased numbers of B cells at the time of diagnosis and liver transplant (Luo et al., 2021). 51% of proximal biliary remnants showed one or more reactive GCs (Luo et al., 2021) and Bednarek et al., showed that 53% of BA patients had mature GCs present in their hilar lymph nodes compared to controls (Bednarek et al., 2018) suggesting that activated B cells were differentiating into memory B cells and antibody secreting PCs. Mouse models of BA had significantly increased levels of IgG antibodies against α-enolase; an ubiquitously expressed enzyme that is found in many tissues including bile ducts and hepatocytes (Lu et al., 2010). Lu et al., also showed that IgM and IgG isolated from the sera of BA children younger than one year, reacted with cholangiocyte cytosolic proteins indicating the activation of

autoreactive B cells. IgM and IgG deposits were found along bile duct epithelial basement membranes in extrahepatic bile duct remnants in 40% of BA patients (Hadchouel et al., 1981). Luo et al., found three autoantibodies specific to highly expressed cholangiocyte proteins; anti-CHI3L1, anti-DLL-4 and anti-SFTPD IgM autoantibodies that correlated with poor outcome (Luo et al., 2021) indicating that autoimmune responses contribute to BA pathology.

Chitinase 3 like 1 (CHI3L1) is a glycoprotein highly expressed in the liver and involved in fibrogenesis; expression was increased in nodular livers correlating with fibrosis levels (Luo et al., 2021). Delta-like 4 (DLL-4) is highly expressed in cholangiocytes and has a role in the development of the biliary tree during embryogenesis. This ligand also functions to downregulate inflammation and the presence of DLL-4 autoantibodies may hinder its role in dampening down inflammation, (Luo et al., 2021) contributing to the inflammatory milieu observed in BA. Surfactant protein D (SFTPD) is found on the luminal surface membrane of intrahepatic cholangiocytes. Higher levels of portal tract C3d and fibrosis marker, desmin were detected in BA patients that were positive for all three autoantibodies (Luo et al., 2021). Increased concentrations of autoantibodies were found in the circulation of BA patients (Wang et al., 2020).

RRV-induced mouse model is commonly used to study BA as it mimics the histological and immunological abnormalities found in human BA (Bednarek et al., 2018). Ig-α deficient mice failed to develop B cells and were protected from developing BA (Luo et al., 2021) upon rotavirus infection suggesting a role for B cells in BA pathology. The absence of functional B cells was associated with a lack of T cell activation (Bednarek et al., 2018) resulting in a lack of Th1 cytokine-mediated bile duct injury (Taylor et al., 2019a). B cells contribute to biliary

obstruction by activating T cells. They can also produce significant amounts of Th1 cytokines; IFN-γ, IL-2 and TNF-α which are upregulated in both murine and human BA (Bednarek et al., 2018, Taylor et al., 2019a). A highly clonal BCR repertoire observed in BA supports a role for antigenic stimulation early on in disease (Taylor et al., 2019b).

A proposed theory of BA pathogenesis is that an initial infection with a cholangiotropic virus (Mack et al., 2012), initiates an immune response resulting in exaggerated inflammatory responses that damage bile duct epithelia (Feldman and Mack, 2012). This results in the release of altered self-antigens (Brindley et al., 2012, Mack et al., 2007) which are recognised by APCs as a foreign molecule, subsequently activating autoreactive T cells (Brindley et al., 2012). Activated autoreactive T cells stimulate autoreactive B cells, augmenting the production of inflammatory mediators and initiating the GC reaction resulting in B cell differentiation into antibody producing PCs. Despite the clearance of the virus, persistent inflammation continues obliterating bile ducts leading to fibrosis and liver failure (Lu et al., 2010).

In summary, the pathogenesis of BA is unknown. Studies suggest an original viral or autoimmune insult however, a popular theory of BA pathogenesis is that an initial perinatal viral infection either targets bile ducts or creates molecular mimicry between viral proteins and self-antigens (Lu et al., 2010) that may be followed by an autoimmune response that destroys the bile ducts (Taylor et al., 2019a) **(figure 1.6)**. The initial viral infection may be resolved from the liver however, injury to cholangiocytes continues (Lu et al., 2010), releasing neo self-antigens which activate autoreactive B cells to produce autoantibodies (Luo et al., 2021), secrete cytokines and activate T cells. RRV-induced mouse models showed

the presence of autoantibodies upon infection however, infection alone or biliary injury alone was not enough to result in autoantibody production (Lu et al., 2010).

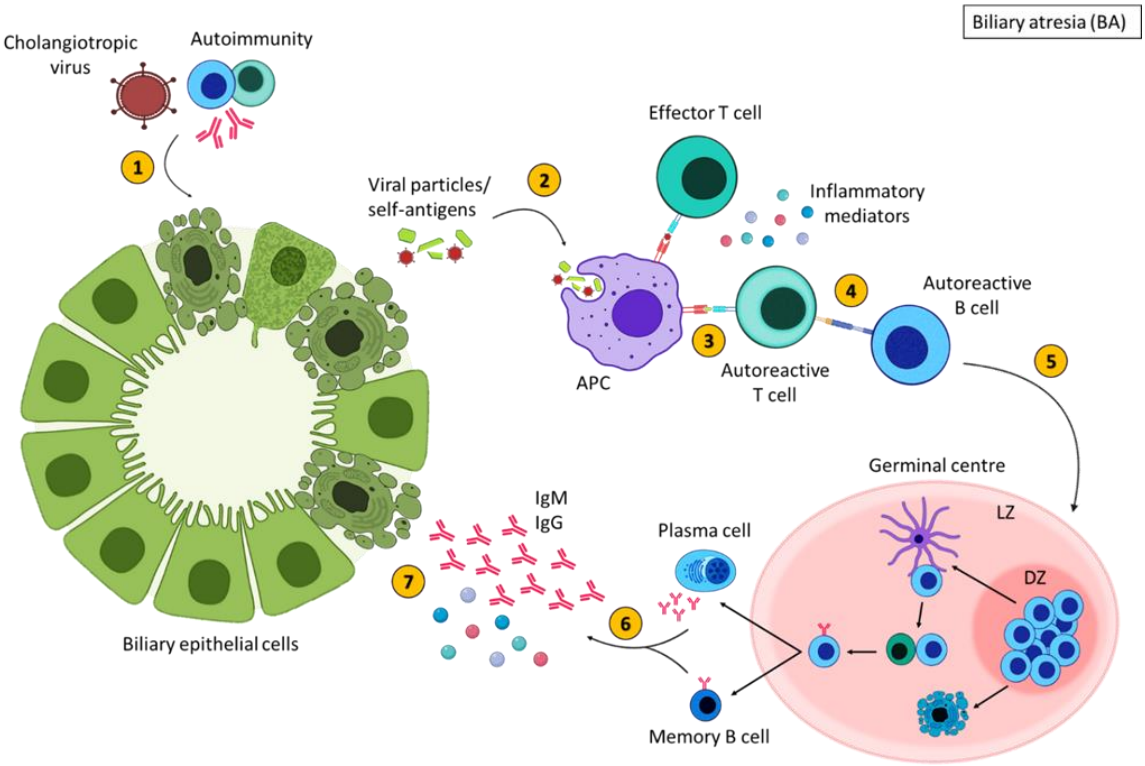


Figure 1.6 Proposed pathogenesis of biliary atresia. *The initial insult in BA is unknown. Studies have proposed that (1) an initial viral insult or autoimmunity result in destruction of biliary epithelial cells (BECs) which (2) release self-antigens and viral particles. These are (3) recognised by APCs which activate T cells. (4) Autoreactive T cells that recognise self-antigens activate autoreactive B cells which (5) undergo germinal centre reactions to differentiate into (6) memory B cells and plasma cells. (7) These differentiated B cells secrete autoantibodies and inflammatory mediators further damaging BECs. Image taken from (Patel et al., 2021).*

1.3.2 Sudden onset acute hepatitis

Sudden onset acute hepatitis (SOAH) is hepatitis of an unknown origin; the typical causes of hepatitis, Hep A-E, were ruled out (Gao et al., 2022). Cases of SOAH have trebled in 2022 raising a cause for concern and since 8th July 2022, 1010, cases have been reported in children worldwide, from over 40 countries (Mann et al., 2022, Zhang et al., 2022). The

highest incidence has been in the UK with 222 cases, then USA with 216 cases followed by the EU with 125 cases (Zhang et al., 2022). 45 children have needed liver transplants (Kelly and Stamataki, 2022) and 22 children have died due to this disease (Mann et al., 2022). No epidemiological links have been found in the Alabama cohort of patients (Baker et al., 2022) and Kajon and George., have reported that this disease is sporadic with no links between cases (Kajon and St George, 2022). All patients had elevated levels of transaminases (Baker et al., 2022, Deep et al., 2022) and majority of these patients were 5 years or younger (Kajon and St George, 2022). These patients were ineligible for the COVID vaccine (Kelly and Stamataki, 2022).

Majority of these patients presented with gastrointestinal symptoms; vomiting, diarrhoea and abdominal pain that progressed to jaundice and in some cases, acute liver failure (Brodin and Arditi, 2022, Arico and Caselli, 2022, Li et al., 2022). Adenovirus is a non-enveloped DNA virus (Mendez-Sanchez and Pal, 2022) and adenovirus type 41F has been implicated as a cause of paediatric acute gastroenteritis, which presents with gastrointestinal problems observed in SOAH cases (Baker et al., 2022, Gao et al., 2022). 72% of tested cases were positive for adenovirus type 41F (Dhawan and Vimalesvaran, 2022). SOAH patients from the UK that required liver transplants had adenoviral DNA loads that were 12 times higher compared to other children (Yao et al., 2022) suggesting a role of adenovirus in the pathogenesis.

Adenovirus is a recognised cause of hepatitis in immunocompromised children (Baker et al., 2022, Kajon and St George, 2022), however most of the children with SOAH were immunocompetent, without any chronic medical conditions (Zhang et al., 2022). This outbreak in cases occurred during the COVID-19 pandemic and coincidentally occurred

during the emergence of the highly infectious omicron variant (Chen et al., 2022b, Zhang et al., 2022).The majority of SOAH cases occurred in countries with a high incidence of omicron (Chen et al., 2022b) and unvaccinated children may have a higher infection rate with omicron (Zhang et al., 2022). There is also the possibility that a novel strain of adenovirus has emerged, that is more pathogenic and infects those that are unvaccinated against COVID-19 with a previous SARS-CoV-2 infection (Yao et al., 2022, Einberg and Fischler, 2022, Gao et al., 2022).

Co-infection with adenovirus and another virus may sensitise the liver making it more susceptible to immunopathology. Adenovirus infection sensitises the liver to subsequent infection with staphylococcal enterotoxin B which belongs to a family of superantigens (Yarovinsky et al., 2005). In the Alabama study, 7 patients were co-infected with other viral pathogens; 6 were positive for EBV however there was no detection of EBV IgM antibodies suggesting that these results were indicative of the reactivation of a previous infection sEBV, enterovirus amongst others (Kelly and Stamataki, 2022) but it is not known if any of these patients required a liver transplant.

Gao et al., has highlighted a unique relationship between adenovirus and SARS-CoV-2 (Gao et al., 2022). More than 60% of cases had seropositivity for antibodies against SARS-CoV-2 (Mann et al., 2022) and 18% of the reported cases in the UK tested positive for SARS-CoV-2 upon admission (Brodin and Arditi, 2022) with few to none of the patients being vaccinated against COVID-19 (Einberg and Fischler, 2022).

Brodin et al., has shown that SARS-CoV-2 can result in the formation of a viral reservoir (Brodin, 2022). Brodin's superantigen hypothesis states that the viral reservoir for SARS-CoV-

2 leads to persistent viral particle release in the gastrointestinal tract across the intestinal epithelium. This results in continued activation of the immune response and this constant immune activation may be mediated by a superantigen motif within the spike protein of SARS-CoV-2 (Brodin and Arditi, 2022). This superantigen mediates a skewing to Th1 cytokines, particularly IFN-γ which leads to IFN-γ-mediated liver injury (Brodin and Arditi, 2022, Mann et al., 2022). A similar release of Th1 cytokines was detected in mice who respond to the superantigen staphylococcal enterotoxin B (Yarovinsky et al., 2005). The portal vein brings blood into the liver, that has passed through the spleen and gut exposing the liver to constant pathogens (Patel et al., 2021). Due to this, the liver is a tolerogenic environment however, in disease the liver can mount a strong immune response. In SOAH, infection with adenovirus may sensitise the liver and contact with SARS-CoV-2 superantigen, released from the gut, may initiate an aberrant activation of the immune system.

Despite the evidence of adenoviral DNA in the blood, no viral inclusions or particles have been detected in 6 patients (Baker et al., 2022). There was no presence of adenovirus in hepatocytes (Chen et al., 2022a) but there was evidence of hepatocellular injury and necrosis (Dhawan and Vimalesvaran, 2022). However, Chen et al., has shown that the intra-sinusoidal lumen from liver samples was reactive to adenovirus (Chen et al., 2022b) suggesting that whilst adenovirus may not be directly involved in hepatocellular injury (Kajon and St George, 2022), it may still be involved in liver pathology (Dhawan and Vimalesvaran, 2022).

The hepatic immune infiltrate has not been characterised in the current outbreak of SOAH (Mann et al., 2022) but one can speculate that the release of gut associated pathogens and/or SARS-CoV-2 superantigen, into the liver may result in immune activation. A potential

mechanism of adenoviral and co-factor pathogenesis is described by Mann et al., where the authors stated that adenoviral particles are presented to naïve T cells by APCs (Mann et al., 2022). These activated T cells, alongside gut-derived microbial products will activate B cells (Patel et al., 2021). Gut associated lymphocytes can migrate to the liver and contribute to liver injury (Mann et al., 2022) through the secretion of antibodies and pro-inflammatory mediators (Patel et al., 2021). Alteration or depletion of the microbiome, in mouse models, resulted in a milder phenotype or mitigation of disease, respectively (Mann et al., 2022) suggesting that a second infection with a previous adenoviral infection leads to a severe disease phenotype.

1.3.3 Paediatric viral hepatitis

1.3.3.1 Paediatric hepatitis B viral infection

Approximately 3,000 babies in the UK are born to women infected with HBV (Public_Health_England, 2021). HBV transmitted from infected mothers to neonates is believed to take advantage of the immature immune system by inducing a tolerogenic state facilitating the persistence of HBV infection (Hong et al., 2015). Neonatal immunity can be controlled by external factors such as bacterial colonisation and live vaccinations. These help to protect the infant against unrelated pathogenic infections by initiating an efficient innate immune response. This is termed 'trained immunity' (Hong et al., 2015). A state of trained immunity may be induced by the exposure to HBV *in utero* resulting in innate immune cell maturation that have an improved ability to respond to exposures of unrelated pathogens (Hong et al., 2015).

Age plays a role in the spontaneous clearance of HBV as 95% of infected adults were able to clear the virus whereas 90% of exposed neonates and 30% of children aged 1-5 years developed chronic HBV infection due to the failure to resolve infection (Publicover et al., 2013).

Investigating the progression of HBV infection in neonates is difficult as at-risk patients receive Ig and vaccinations to prevent infection (Publicover et al., 2013). Mouse models have been key to understanding HBV pathology. IL-21 produced by TFH cells mounts an effective immune response to HBV however, IL-21 concentrations were diminished in young mice that were unable to effectively respond to HBV infection (Publicover et al., 2013). HBV-specific IL-21 expression was observed only in the liver and not in the spleen or lymph nodes of mice suggesting that immune cell priming occurred predominantly in the liver (Publicover et al., 2013). This may suggest that B cells were also activated in the liver as they have access to antigen and co-stimulatory signals, CD40/CD40L on activated T cells. Macrophages play a crucial role in the organisation of lymphoid structures in the liver and young mice infected with HBV may have reduced macrophages as lymphoid organisation was severely reduced (Publicover et al., 2013). These hepatic lymphoid structures support the differentiation and maturation of B cell responses and disorganised lymphoid structures may reduce the number of differentiated memory B cells and PCs.

1.3.3.2 Paediatric hepatitis C viral infection

The prevalence of chronic hepatitis C infection is lower and less aggressive in children compared to adults (Camarero et al., 2008, Garazzino et al., 2014). HCV-positive mothers had a 5-6% risk of transmitting HCV to their child and this risk increases with high viral load (Venkatesh et al., 2022, Lutckii et al., 2020). Mother-to-child (vertical) transmission accounts

for 5% of infections and is the predominant route of HCV infection in children (Garazzino et al., 2014, Lutckii et al., 2020). Vertical transmission of HCV was cleared in approximately 25 – 40% of children by the age of four and 6 – 12% had cleared their infection by adulthood. This spontaneous clearance may be due to the genotype of HCV; Bortolotti et al., showed that infection with HCV genotype 3 was more likely to be cleared compared to infection with HCV genotype 1a which is more persistent and leads to progression of cirrhosis (Bortolotti et al., 2008).

There are limited studies investigating the course of HCV infection in children and children infected with HCV tend to have a mild acute phase of disease (Venkatesh et al., 2022). HCV infection rarely causes death in childhood (Modin et al., 2019), most of these children will develop progressive disease in their adulthood (Camarero et al., 2008). The influence of risk factors such as alcohol consumption, drug usage and co-infection with HIV, which all increase with age, may result in a rapid progression of liver disease (Modin et al., 2019).

Studies have investigated histology of liver biopsies from cohorts of HCV-infected children. They found that 50% of patients had elevated aminotransferases (Leung et al., 2020), and 92% patients who had been infected for less than 10 years showed mild fibrosis (Schmelzer et al., 2020). Liver biopsies from children also showed mild necro-inflammatory changes (Badizadegan et al., 1998) accompanied by low levels of fibrosis (Camarero et al., 2008). 1 – 2% of children with chronic HCV infection developed cirrhosis (Jara et al., 2003, Rumbo et al., 2006, Goodman et al., 2008).

Majority of HCV-infected children showed signs of cytolysis however none developed acute hepatitis and extrahepatic manifestations were rare (Garazzino et al., 2014). This absence of

clinical signs and slow progression of disease may be due to a weakened immune response in infants. Children who had higher alanine transaminase (ALT) levels in the first 2 years of life achieved sustained viral clearance suggesting that a stronger cytolytic effect could predict a vigorous immune response that resolves infection (Garazzino et al., 2014).

The presence of non-organ-specific autoantibodies (NOSA) in 19 – 34% of HCV-infected infants (Camarero et al., 2008, Muratori et al., 2003) suggested that activated autoreactive B cells contributed to disease severity. NOSA levels were significantly higher in HCV-infected children compared to age-matched controls (Garazzino et al., 2014). 11% of infected children had the presence of anti-LKM1 antibodies (Muratori et al., 2003) that were also observed in young, AIH patients (Patel et al., 2021) and tends to mainly affect children (Camarero et al., 2008). The presence of NOSA were detectable even after sustained viral clearance and loss of viremia (Garazzino et al., 2014). Garazzino et al., found that HCV genotype 3 or 4 may induce NOSA production as two-thirds of infants infected with these genotypes were NOSA-positive (Garazzino et al., 2014). Anti-HCV IgG secreting B cells were present in children with vertical HCV-infection (Lutckii et al., 2020) suggesting that B cells had been activated and had undergone GC reactions to secrete HCV-specific IgG antibodies. Prenatal or perinatal exposure to HCV initiated early maturation of the neonatal B cell compartment (Lutckii et al., 2020).

A Japanese study consisting of a cohort of 109 children with chronic hepatitis C found that the presence of lymphoid aggregates was similar to those detected in adult HCV infection (Kage et al., 1997). In another study, 48% of HCV-infected children had the existence of portal lymphoid aggregates and/or follicles and only minimal hepatocellular damage was

observed (Badizadegan et al., 1998) suggesting that these ectopic aggregates do not cause hepatocyte injury.

Autoimmune and extrahepatic manifestations are associated with HCV infection. HCV can be associated with diabetes, MC and elevated levels of non-organ-specific autoantibodies (Lutckii et al., 2020, Garazzino et al., 2014). MC is the most common B cell lymphoproliferative disease (Meola et al., 2000) associated with HCV in adults (Patel et al., 2021). Cryoglobulins were more frequent in children infected with HCV genotype 1 (Garazzino et al., 2014). B cells contribute to the development of cryoglobulins through ectopic autoantibody production and B cell proliferation (Patel et al., 2021, Boleto et al., 2021).

B cells can contribute to HCV pathogenesis through the generation of autoantibodies, proliferation, and the formation of cryoglobulins. Autoreactive B cells may emerge due to molecular mimicry (Garazzino et al., 2014). HCV E2 protein mimics the natural ligand for CD81 (Meola et al., 2000), present on host cells, and interactions between the two may help the virus gain entry into host cells (Indolfi et al., 2012). In B cells, CD81 interacts with CD19 and CD21 lowering the threshold for BCR activation (Kuppers, 2019). Interactions between HCV E2 and CD81 activate biological B cell functions (Meola et al., 2000) and resulted in a lower threshold for BCR activation which may result in excessive B cell proliferation and the formation of cryoglobulins detected in HCV patients.

The persistence of cryoglobulins and NOSAs, even after achievement of sustained viral clearance suggested that HCV triggers an aberrant immune activation that continues to stay independently activated after it has passed an unknown ‘point of no return’ (Garazzino et

al., 2014). This may be due to the persistence of HCV RNA in liver and PBMCs of seropositive patients even after the clearance of HCV RNA from the serum and plasma (Sugden et al., 2012). This absence of viral RNA in the sera of previously infected patients has been termed 'occult' infection and the detection of HCV RNA in the liver may indicate an extra-hepatic reservoir of the virus (Sugden et al., 2012). This reservoir may be responsible for liver damage observed in adulthood of children with vertically transmitted HCV infections.

1.4 Hypothesis and aims

There is little literature on hepatic B cell subsets in health and in disease for paediatric and adult patients. B cells consist of heterogenous subsets with different activities and may contribute to the pathogenesis in various liver diseases in both adults and paediatric patients. I hypothesised that B cell subsets may differ in liver diseases of different aetiologies. In children with BA, I hypothesised that the inflammatory compartment may differ in the hilum region and liver periphery during disease progression, compared to end-stage disease.

My aim was to characterise B cell subsets in adult and paediatric livers to identify any B cell subsets that may contribute to pathology, highlighting any potential pathways and mechanisms of damage that can be targeted therapeutically.

Firstly, I wanted to use flow cytometry to characterise B cell subsets in adult livers. I set out to create a flow cytometry panel that included all the B cell markers that would detect B cell subsets throughout maturation. By characterising B cell subsets in the liver, I would be able to identify which B cell subsets are present in the liver and gain insight into their role in pathogenesis. The original aim was to compare B cell subsets in adults to children with BA, however due to the pandemic only adult tissue was available. My focus turned to establishing comprehensive panels for liver B cell subsets.

Secondly, I aimed to use immunohistochemistry and immunofluorescence to identify B cell subsets of interest in biliary atresia liver tissue. I set out to create immunofluorescence panels to detect B cells in biliary atresia livers and to visualise the distribution of these cells in the tissue. This would enable me to localise B cells in hepatic tissue and identify the

subsets that are detected close to bile ducts or in ectopic lymphoid structures, highlighting their role in paediatric liver pathology.

Finally, I aimed to phenotype transcriptomic differences between non-syndromic and syndromic biliary atresia livers and to identify any differences in gene expression between early disease and end-stage disease and between the hilum and the periphery. I set out to identify distinct inflammatory gene expression profiles between sample location and between non-syndromic and syndromic patients. By carrying out gene expression analysis, it would highlight any transcripts that were upregulated or downregulated in each sample group elucidating pathways that were active and contribute to pathology, possibly leading to the development of targeted therapies.

CHAPTER 2 – B CELL CHARACTERISATION IN ADULT END-STAGE LIVER DISEASES

2.1 Introduction

Liver B cells in chronic liver diseases are understudied. Hepatic B cells make up 50% of intrahepatic lymphocytes in mice (Novobrantseva et al., 2005, Holt et al., 2006) and 8% in human livers (Robinson et al., 2016). B cells contribute to fibrogenesis; B cell deficient mice injected with carbon tetrachloride (CCL_4) had reduced fibrosis compared to wild-type (WT) mice (Novobrantseva et al., 2005). B cells have been shown to induce the differentiation of hepatic stellate cells into myofibroblasts through IL-6 production, contributing to the deposition of collagen (Xue et al., 2000).

The liver is constantly exposed to gut microbial antigens and requires the expression of PRRs. TLRs detect PAMPs which consist of an array of microbial ligands and nucleic acid (Ortiz-Perez et al., 2020). TLRs also recognise DAMPs which are self-ligands that were exposed to the extracellular environment as a result of necrosis and inflammatory cellular damage (Feldman and Mack, 2012). Endosomal TLRs (TLR3,7,8 and 9) detect bacterial and viral RNA or DNA and use the adaptor molecules MyD88 and Toll/IL-1R-domain-containing adapter-inducing interferon-β (TRIF) for downstream signalling resulting in the production of pro-inflammatory mediators (Ortiz-Perez et al., 2020). TLRs form part of the innate immune system and function to protect the body against infection.

2.1.1 Age-associated B cells

A novel population of B cells discovered by Rubtsova et al., were found accumulated in aged mice and were termed age-associated B cells (ABCs) (Rubtsov et al., 2011, Rubtsova et al., 2015). ABCs were CD21- CD23- CD11c+ (Rubtsov et al., 2011, Rubtsova et al., 2015) and were detected in the spleen, blood and bone marrow in mice (Rubtsova et al., 2015). ABCs were

enriched in aged female mice compared to young female mice and males. This population was accumulated in young healthy autoimmune-prone mice (Rubtsov et al., 2011) and were associated with autoimmunity (Naradikian et al., 2016a).

Many studies have found populations of B cells that display similar characteristics to ABCs such as, little to no expression of CD21 and high CD11c expression. This ABC phenotype has been described in atypical memory B cells, tissue-like memory B cells, DN B cells and CD11c+ B cells (Karnell et al., 2017).

ABCs respond poorly to BCR cross-linking but proliferate robustly when stimulated with TLR7 or TLR9 agonists (Naradikian et al., 2016a). This proliferative response was enhanced when TLR agonist stimulation was combined with BCR signalling (Rubtsova et al., 2015). ABC development requires signalling via TLR7 as mice deficient in TLR7 and MyD88 (key adaptor of TLR signalling) failed to accumulate ABCs (Rubtsov et al., 2011). ABCs from the Hao et al., criteria proliferated in response to TLR9 compared to TLR7 (Hao et al., 2011) however ABCs stimulated with TLR7 agonists resulted in an amassing of ABCs that was significantly higher in female mice. High qPCR expression of TLR7 and TLR9 was observed in ABCs compared to FO B cells and MZ B cells (Hao et al., 2011). Upon TLR stimulation, ABCs from female mice produced IgM antibodies and were the best secretors of IgG compared to FO and MZ B cells (Rubtsov et al., 2011). Murine ABCs stimulated with TLR ligands rapidly switched from IgM production to IgG production (Rubtsova et al., 2015) and secreted a spectrum of cytokines including IL-4, IL-6, IL-10, IFN-γ and TNF-α (Rubtsova et al., 2015, Naradikian et al., 2016a).

A subset of ABCs requires intrinsic expression of T-bet for their development. These antigen-experienced B cells develop through the induction of T-bet transcriptional program that is

activated through BCR engagement and transport of the antigen to endosomal nuclei acid sensors (Naradikian et al., 2016a). T cells secrete IFN-γ providing a cytokine-mediated environment which induced T-bet expression upon antigen ligation of TLR7 or TLR9 (Rubtsova et al., 2015, Naradikian et al., 2016a). T-bet acts as the master regulator of the ABC phenotype; overexpression of T-bet resulted in an accumulation of ABCs (Rubtsova et al., 2015). Mice infected with gamma herpesvirus 68, lymphocytic choriomeningitis virus (LCMV) and vaccinia had high levels of CD11c+ T-bet+ B cells that appeared during the humoral response (Naradikian et al., 2016a). Re-stimulation with these viruses resulted in the production of virus-specific IgG, demonstrating that antigen-experienced B cells were recruited to the ABC pool (Rubtsova et al., 2015). ABCs were vital for successful humoral responses to certain classes of viral infections (Naradikian et al., 2016a) as T-bet deficient mice had no ABC differentiation therefore had low levels of IgG2a/c resulting in inefficient viral clearance and a higher viral load (Rubtsova et al., 2015).

CD138 transcript was upregulated in ABCs along with intermediate levels of Prdm1, Irf4 and Xbp1, PC transcription factors, suggesting that ABCs may be precursors of PCs, awaiting the correct signals to differentiate into PCs (Rubtsov et al., 2011). When ABCs were activated, they quickly differentiated into PCs and secreted IgG2a/c regardless of their expression of IgM and IgD (Naradikian et al., 2016a).

A similar population has been described in humans that were CD21-/lo, CD23-, CD5hi, CD80hi, CD86hi, MHC-IIhi, Fashi, CD27hi and isotype switched (Rubtsov et al., 2011, Rubtsova et al., 2015). This CD21- CD11c+ B cell population was detected at higher frequencies in peripheral blood obtained from elderly autoimmune female patients and less frequently in healthy women (Rubtsov et al., 2011). ABC-like cells expressing CD21lo CD11chi

FcRL4+ and CXCR3+ have also been described and may represent a subpopulation of ABCs (Rubtsova et al., 2015). Naïve B cells may take an alternative differentiation pathway to become ABCs which may be influenced by antigens that engage both the BCR and TLR7 or TLR9 in a pro-inflammatory cytokine milieu containing IFN-γ (Rubtsova et al., 2015).

The ABC population seems to be a heterogenous population of naïve and memory B cells (Rubtsova et al., 2015). Whilst majority of ABCs were unswitched memory cells (Naradikian et al., 2016a), a proportion of ABCs expressed class-switched IgG or IgA (Ehrhardt et al., 2005) indicative of antigen experience. Furthermore, this subpopulation of ABC expressed markers associated with antigen experience such as CD69, CD80, CD84 and CD86 (Karnell et al., 2017).

ABCs from autoimmune or aged mice were more efficient at presenting antigen compared to other B cells (Rubtsova et al., 2015) suggesting that ABCs are efficient antigen presenters. ABCs expressed MHC-II and co-stimulatory molecules CD80 and CD86 enabling them to present antigens to T cells and mount a response to infections (Rubtsov et al., 2011, Naradikian et al., 2016a).

ABCs may be involved in the development or progression of autoimmunity as they appear earlier in autoimmune-prone mice and in humans with autoimmunity (Rubtsov et al., 2011). In autoimmune mice, ABCs produced IgG2a/c autoantibodies and in infection, ABCs produced anti-viral IgG (Rubtsova et al., 2015). Furthermore, IgG produced by ABCs displayed anti-chromatin reactivity and anti-smith autoantibodies were found in the serum of mice. Depleting ABCs resulted in a reduction of autoantibodies, suggesting that ABCs contribute to autoimmunity (Rubtsov et al., 2011) through the production of autoantibodies

such as anti-dsDNA, anti-nuclear and other autoantibodies which were detected in both humans and mice (Naradikian et al., 2016a). Rubstov et al., observed an accumulation of ABCs that correlated with serum autoantibody levels (Rubtsov et al., 2011). Furthermore, ABCs may form a pool of memory B cells that generate autoantibody secreting cells (Naradikian et al., 2016a) implying that a subset of ABCs may be precursors to PCs.

2.1.2 Aims and objectives

We set out to characterise the B cell compartment in human chronic liver diseases. We initially intended to use multiparametric flow cytometry using the Aurora spectral flow cytometer in collaboration with the University of Oxford however, due to the pandemic restrictions we designed flow cytometry panels to encompass markers of B cell biology **(table 2.1)** using the Fortessa flow cytometer based at the University of Birmingham. These markers of B cell biology are important to identify B cell subsets prominent in liver tissue in various liver diseases.

Objectives

During this chapter, I set out to:

1. Determine B cell frequencies in liver health and in different end-stage diseases
2. Establish if CD24- B cells and ABCs were phenotypically consistent in different liver diseases
3. Investigate the presence of APC markers in liver B cell subsets in liver explants
4. Establish the expression of TLR7 and TLR9 in liver B cell subsets
5. Characterise class-switched immunoglobulin expression in liver B cell subsets
6. Detect CD138 expression in liver B cell subsets in different end-stage diseases

7. Investigate the expression of CD5 and FcRL5 in liver B cell subsets

8. Compare ABC subsets in liver diseases

2.2 Methodology

The aims of these experiments were to characterise the B cell compartment in different adult chronic liver diseases to identify any differences between them, **Table 2.1** is a list of B cell markers that have roles in B cell function, and these were used to differentiate B cells into subsets.

Table 2.1 B cell markers and their function in B cell development and differentiation *(Patel et al., 2021).*

Marker	Function	Reference
CD5	• Negative regulator of BCR signalling • Protects B cells from apoptosis after BCR stimulation • Supports B cell survival via IL-10 production	(Gary-Gouy et al., 2002)
CD10	• Role in pre-B cell maturation and differentiation	(Mishra et al., 2016)
CD11b	• Forms part of the complement receptor 3 present on the surface of B cells	(Vorup-Jensen and Jensen, 2018)
CD11c	• Adhesion molecule found on activated B cells, complement receptor 2	(Vorup-Jensen and Jensen, 2018)
	• Expressed on age-associated B cells	(Karnell et al., 2017)
CD1d	• May enable B cells to present antigens to invariant NKT cells • Expressed on all B cell subsets	(Chaudhry and Karadimitris, 2014)
CD19	• Co-receptor required for BCR signal transduction	(Wang et al., 2012)
	• Cooperates with CD21 for BCR-independent signalling	(Otero et al., 2003)
CD20	• Pan-B cell surface marker for mature B cells • Lost during terminal B cell differentiation	(Lee et al., 2011)
	• Regulator of calcium flux triggered by BCR • Required for optimal B cell responses to T-independent antigens	(Pavlasova and Mraz, 2020)
CD21	• B cell co-receptor required to enhance BCR signalling, complement receptor	(Cherukuri et al., 2001)
CD24	• On activated B cells, CD24 facilitates CD4+ T cell clonal expansion via co-stimulation	(Fang et al., 2010)

	• Role in the regulation of B cell development	(Ayre et al., 2016)
CD27	• Promotes the differentiation of memory B cells into plasma cells	(Agematsu et al., 2000)
	• Marker of B cell activation	(Wu et al., 2011)
CD38	• Involved in B cell differentiation	(Costa et al., 2019)
	• Crosslinking of CD38 to the BCR reduces the threshold for B cell activation	(Glaria and Valledor, 2020)
CD44	• Involved in cellular adhesion processes • Involved in signal transduction • May play a role in antigen-dependent B cell differentiation	(Kremmidiotis and Zola, 1995)
CD45	• Central regulator of BCR signalling	(Giovannone et al., 2018)
CD77	• GC B cell entering apoptosis (CD77+)	(Mangeney et al., 1991)
	• Marker of GC B lymphocytes	(Mangeney et al., 1995)
	• Discriminator of centroblasts and centrocytes	(Hogerkorp and Borrebaeck, 2006)
CD138	• Regulates the survival of plasma cells and long-term humoral immunity	(McCarron et al., 2017)
FcRL4	• Expressed on the surface of a subset of memory B cells	(Sohn et al., 2011)
	• Expressed on the surface of atypical memory B cells	(Li et al., 2020)
FcRL5	• Expressed on the surface of atypical memory B cells	(Li et al., 2020)
	• Novel IgG receptor, inhibits BCR signalling • May have a dual signalling capacity (CD21 co-engagement may result in B cell activation)	(Franco et al., 2018)
IgA	• Binds to and neutralises pathogens at mucosal sites to prevent infection • Can contribute to inflammation at mucosal and non-mucosal sites through the formation of immune complexes	(Hansen et al., 2019)
IgD	• Activates B cell signalling	(Ubelhart et al., 2015)
	• May have a role in B cell tolerance	(Ubelhart et al., 2015, Chen and Cerutti, 2011)
IgE	• Important role in protection against parasitic worm infections	(Croote et al., 2018)

	• Role in mediating allergic reactions	(Sutton et al., 2019)
IgG	• Most abundant immunoglobulin in human serum • Responds to different types of antigens • Capable of neutralising virus particles and toxins • Can activate complement upon binding C1q	(Vidarsson et al., 2014)
IgM	• BCR expressed on naïve B cells. Associates with CD79a and CD79b for BCR signalling	(Schroeder and Cavacini, 2010)
T-bet	• Promotes the survival of memory B cells and IgG2a isotype switching	(Wang et al., 2019)

2.2.1 Human liver tissue

Liver tissue samples were obtained from explanted livers (ALD n=8, NASH n=6, AIH n=2, PBC n=6, PSC n=6 and other livers n=3), taken from patients with end-stage liver disease undergoing transplantation at the Queen Elizabeth Hospital, Birmingham. These samples were processed following patient consent and in approval with local research ethics committee guidelines (LREC; reference number 06/Q2702/61 and 18-WA-0214). Donor liver samples (n=6) were also received from patients who had passed away. These donor livers were unsuitable for transplantation and form the 'healthy control' cohort. All tissues were processed within a day of collection to isolate liver infiltrating mononuclear cells (LIMCs) and frozen at - 80°C due to COVID restrictions. Patient clinical data can be found in **Appendix table 1**.

2.2.2 Haemochromatosis blood

Blood was received from patients with haemochromatosis (HFe) (n=4), from the Queen Elizabeth Hospital, Birmingham. HFe blood was used as a control as it closely resembles healthy blood, and it was a cost effective alternate to healthy blood as the HFe patients undergo phlebotomy as their treatment. The samples were used following patient consent

and in approval with the local research ethics committee guidelines (LREC Approval 14-WA-0214, Birmingham, UK). All blood samples were processed on the same day of collection to isolate PBMCs. Patient clinical data can be found in **Appendix table 1**.

2.2.3 Liver infiltrating mononuclear cell isolation

Liver slices were stored in RPMI 1640 media in the fridge prior to the processing for mononuclear cell isolation. The liver slices were then transferred to a petri dish and weighed, prior to isolation. Using two scalpels, each tissue slice was cut into small cubes and washed with sterile phosphate buffered saline (PBS) to remove residual blood. The minced liver tissue was washed with sterile PBS until the washes ran clear. RPMI 1640 media was added to the beaker until a total volume of 300 ml was reached. This solution was transferred to a stomacher bag (Seward Limited) and the air bubbles were removed prior to sealing the stomacher bag. The stomacher bag was placed into the Stomacher 400 circulator machine (Seward Limited) for 5 minutes at 8 RCF. The mashed-up liver was filtered using a fine mesh into a beaker and washed with sterile PBS. The fine mesh was removed, and the filtrate was left to rest for 5-10 minutes to let the debris settle at the bottom of the beaker. The top of the filtrate was distributed into 50 ml falcon tubes and centrifuged at 161 RCF for 5 minutes. After each round of centrifugation, the number of falcon tubes were reduced by half by mixing the pellets of two falcon tubes together, until two tubes remained. The remaining two tubes were washed, and the pellets were resuspended in 30 ml of sterile PBS before layering the solution onto 15 ml of lympholyte-H (Cedarlane, CL5020), a density-based cell separation media. The layered sample was centrifuged at 252 RCF for 20 minutes with acceleration 9 and deceleration 3. The buffy coat was extracted using a plastic pipette and washed twice with sterile PBS. The pellet was resuspended in sterile PBS and a portion

of the sample was diluted in trypan blue before being counted using a haemocytometer. LIMCs were centrifuged before being resuspended in freezing media (90% FBS, 10% DMSO) and frozen in cryovials.

2.2.4 Peripheral blood mononuclear cell isolation

Blood obtained from HFe patients was diluted with sterile PBS. 30 ml of the diluted sample was layered onto 15 ml of lympholyte-H. The sample was centrifuged at 252 RCF for 20 minutes with acceleration 9 and deceleration 3. The buffy coat was isolated using a plastic pipette and washed twice with sterile PBS. The pellet was resuspended in sterile PBS and a portion of the sample was diluted in trypan blue before being counted using a haemocytometer. PBMCs were centrifuged before being resuspended in freezing media (90% FBS, 10% DMSO) and frozen in cryovials.

2.2.5 Flow cytometry staining

2.2.5.1 Optimisation

PBMCs were stained with serial dilutions of 1/50, 1/100 and 1/200 for each antibody used in the flow cytometry antibody and isotype matched controls (IMC) panels (**table 2.2 and table 2.3**) to identify the optimal working dilution **(figure 2.1, appendix 1)**. Compensation on the flow cytometer or in FlowJo was used to correct the spectral spillover and aided in gating strategies to avoid gating on artefactual events (Biolegend, 2023). Fluorescence minus one controls (FMOs) also aided in gating, especially if the positive and negative populations were poorly defined (Biolegend, 2023). FMOs were performed on fluorophores CD24 APC, CD27 APC-Cy7 and CD1d BUV395 **(figure 2.2A)** due to concern about spill over into other channels.

CD27 FMOs for the Miltenyi antibody did not work **(figure 2.2B)** so the Biolegend antibody was bought instead **(figure 2.2C)** and compared to the Miltenyi antibody.

Table 2.2 Antibodies used for flow cytometry. *All the antibodies were used at the same dilution for each experiment. These antibodies helped to characterise B cell subsets including transitional, naïve, memory, plasmablasts/plasma cells, CD24- CD38- and CD24- CD38int subsets along with age-associated B cell subsets.*

Marker + Fluorophore	Company	Catalogue number	Lot number	Working dilution
Zombie Red Fixable Viability kit	Biolegend	423109	B286764	1/1000
CD19 PE-Cy5	Biolegend	302210	B263542	1/200
CD24 APC	MACS Miltenyi Biotec	130-095-954	5200210106	1/100
CD38 PE-Cy7	Biolegend	356608	B281408	1/200
CD27 APC-Cy7	Biolegend	356424	B313735	1/100
IgD BV510	Biolegend	348220	B263594	1/200
CD21 BV605	BD	740395	0056011	1/200
CD11c AF488	Biolegend	301618	B209841	1/200
CD69 BUV737	BD	612817	1155414	1/200
CD1d BUV395	BD	743609	1210369	1/100
CD80 BV421	Biolegend	305221	B292880	1/200
CD86 BV785	Biolegend	305441	B312706	1/200
HLA-DR AF700	Biolegend	307626	B254393	1/200
FcRL5 BV650	BD	749604	0056043	1/100
CD5 PerCP-Cy5.5	Biolegend	300619	B267967	1/200
IgA VioBlue	MACS Miltenyi Biotec	130-113-479	5210602958	1/100
IgM BV785	Biolegend	314543	B283253	1/200
CD138 AF700	Biolegend	356511	B272486	1/100
IgE BV650	BD	744318	1210372	1/200
IgG PerCP-Cy5.5	Biolegend	366909	B323138	1/100

T-bet BV711	Biolegend	644819	B348160	1/100
TLR7 PE	R&D Systems	IC5875P	ABEV0417041	1/100
TLR9 PE	Biolegend	394803	B332742	1/200

Table 2.3 Isotype matched controls used for flow cytometry. *IMCs were used at the same dilutions as the antibodies in* ***Table 2.2****. The use of IMCs enabled me to gate on my B cell populations of interest and determine where my positive cells were.*

Marker + Fluorophore	Company	Catalogue number	Lot number	Working dilution
Mouse IgG1 PE-Cy5	Biolegend	400118	B195080	1/200
Mouse IgG1 APC	MACS Miltenyi Biotec	130-113-196	5211111426	1/100
Mouse IgG1 PE-Cy7	Biolegend	400126	B146682	1/200
Mouse IgG1 APC-Cy7	Biolegend	400128	B307562	1/100
Mouse IgG2a BV510	Biolegend	400268	B188553	1/200
Mouse IgG1 BV605	BD	562652	9101658	1/200
Mouse IgG1 AF488	Biolegend	400129	B277964	1/200
Mouse IgG1 BUV737	BD	612758	1179030	1/200
Mouse IgG1 BUV395	BD	563547	0339553	1/100
Mouse IgG1 BV421	Biolegend	400158	B285247	1/200
Mouse IgG2b BV785	Biolegend	400355	B303486	1/200
Mouse IgG2a AF700	Biolegend	400247	B257649	1/200
Mouse IgG2a BV650	BD	744532	0056024	1/100
Mouse IgG2a PerCP-Cy5.5	Biolegend	400257	B308614	1/200
Mouse IgG1 VioBlue	MACS Miltenyi Biotec	130-113-205	5210601229	1/100
Mouse IgG1 BV785	Biolegend	400169	B318355	1/200
Mouse IgG1 AF700	Biolegend	400143	B288792	1/100
Mouse IgG2a BV650	BD	563417	1200658	1/200
Rat IgG2a PerCP-Cy5.5	Biolegend	400531	B268003	1/100

Mouse IgG1 BV711	Biolegend	400167	B300768	1/100
Mouse IgG2a PE	R&D Systems	IC003P	LHC1519071	1/100
Rat IgG2a PE	Biolegend	400507	B282895	1/200

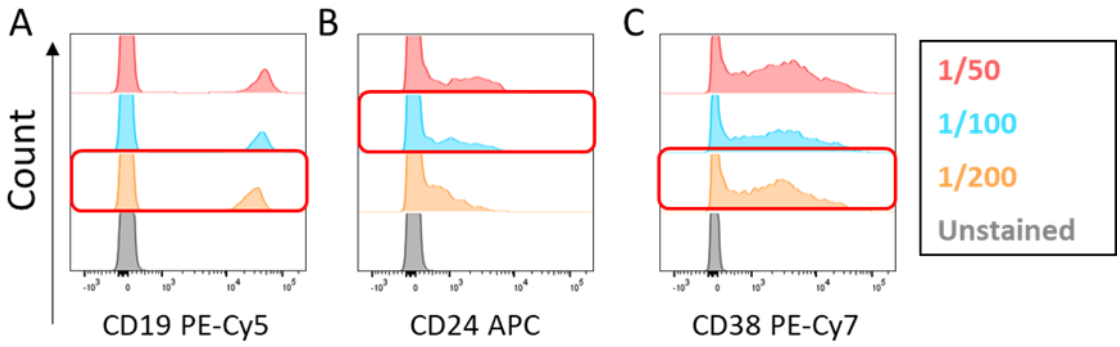


Figure 2.1 Antibody titration to find the optimal working dilution. *Total PBMCs isolated fresh from HFe blood were stained with three dilutions of each antibody used to identify which dilution offered the best separation of positive and negative staining. Dilutions used were 1/50 (red), 1/100 (blue) and 1/200 (orange). These titrations were compared to unstained PBMCs (grey). Representative plots showed titrations for (A) CD19, (B) CD24 and (C) CD38.*

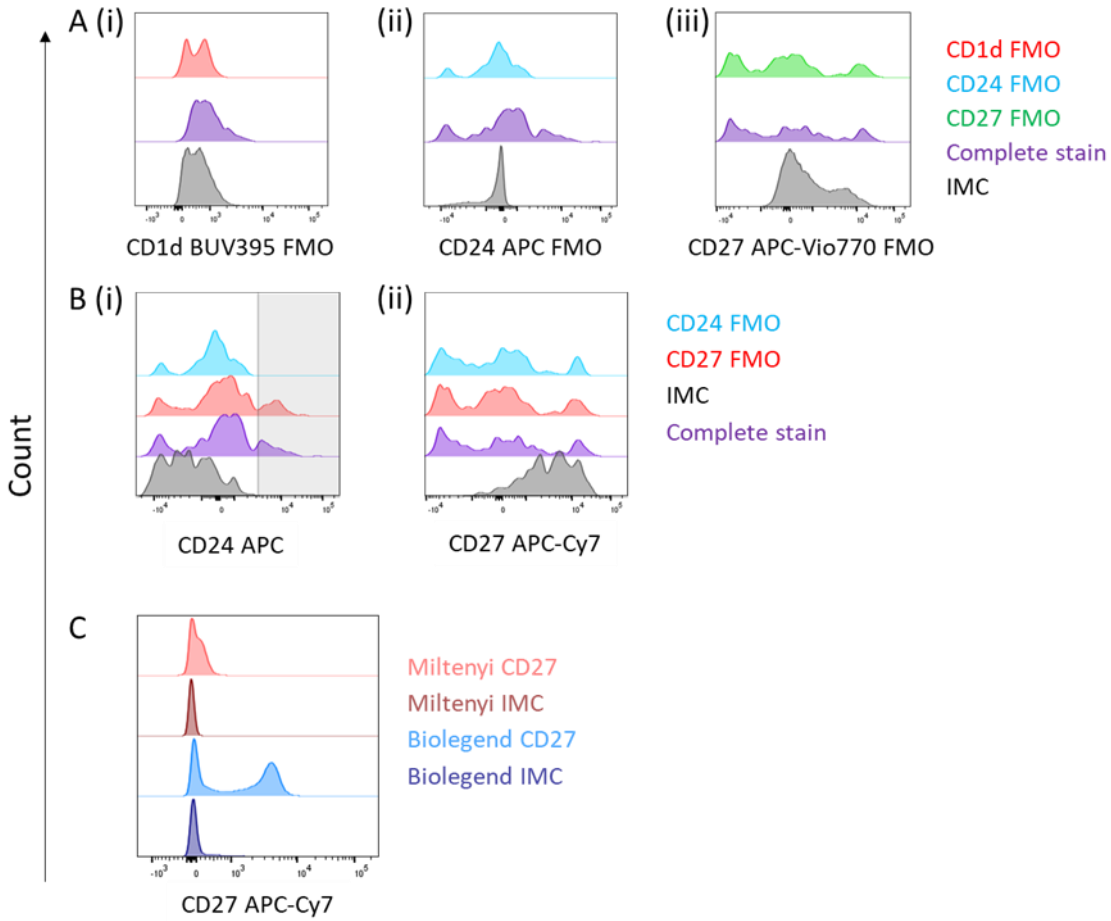


Figure 2.2 **FMOs were carried out on antibodies that would be used together and had spectral overlap.** This experiment was carried out on liver isolated mononuclear cells isolated from the livers of patients with alcoholic liver disease. FMOs ensured that positive and negative staining could be identified. In the case of CD27, it was used to help guide with gating. (A) FMOs on CD1d (red), CD24 (blue) and CD27 (green). (B) Comparison between CD24 (blue) and CD27 (red) to check if FMOs were working. (C) Comparison between two CD27 antibodies; MACS Miltenyi (red) and Biolegend (blue) to determine which antibody gave the better separation of CD27 negative and positive cells.

Upon thawing of the cells, I noticed fewer cell numbers compared to what was originally stored. Cell yield upon thawing became an issue so I used 50 µl DNase per sample (1 µg/µl, STEMCELL Technologies, 100-0762, 07900) to check if this would improve cell yield. The sample was split into two; one was treated with DNase and one without. Cells were gated on lymphocytes and total CD19+ cells were compared between the two conditions **(figure 2.3)**.

Cells treated with DNase had consistently higher yields in two replicates in the two independent experiments, so this was included for all future flow cytometry experiments.

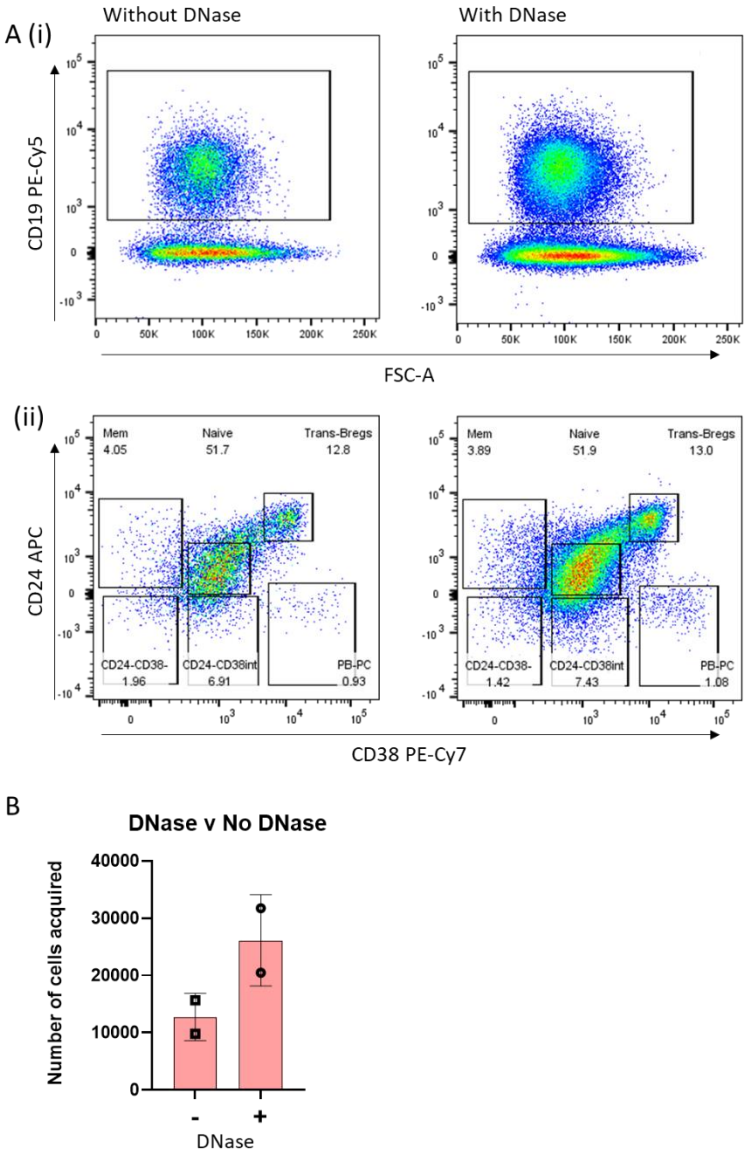


Figure 2.3 DNase treated cells had better yields compared to cells treated without DNase. *The bar chart shows the means from samples from two independent experiments from ALD livers, where total LIMCs were isolated, frozen, and thawed. Thawed cells were treated with and without 50 µl of DNase. Yields were compared between CD19+ B cells identified by flow cytometry treated with and without DNase. (A(i)) Cells gated on CD19+ cells (A(ii)) Cells displaying all six B cell subsets. Whilst the proportions of cell subsets did not differ greatly, cells treated with DNase showed a denser flow plot and were increased in cell numbers*

compared to cells treated without DNase. (B) Number of cells acquired for CD19+ B cell gate between samples treated with (open circle) and without (open square) DNase.

2.2.5.2 Cell staining

PBMCs and LIMCs were thawed in a water bath at 37°C. The cells were transferred to a 15 ml falcon tube with 9 ml of warm RPMI media. The samples were centrifuged at 161 RCF for 5 minutes (acceleration 9, deceleration 9). The supernatant was discarded, and the pellets were resuspended in warm RPMI media containing DNase (50 µl DNase/ sample) and transferred to a round bottom 96 well plate. The plate was incubated at 37°C for 10 minutes before being centrifuged at 161 RCF for 3 minutes. The cells were resuspended in 100 µl of surface stain antibody cocktails **(table 2.4)** and incubated in the dark, at room temperature for 10 minutes. 100 µl of PBS was added to each well prior to centrifugation at 287 RCF for 3 minutes. Cells were resuspended in 100 µl of fixative (FOXP3/ Transcription factor staining buffer set, eBioscience, 00-5523-00) and incubated in the dark, at 4°C for 30 minutes. 100 µl of perm buffer (FOXP3/ Transcription factor staining buffer set, eBioscience, 00-5523-00) was added to each well before the plate was centrifuged at 287 RCF for 3 minutes. The cells were washed in 200 µl of perm buffer and centrifuged at 287 RCF for 3 minutes. 100 µl of intracellular antibodies **(table 2.5)**, made up in perm buffer, was added to the relevant wells and incubated, in the dark, at room temperature for 30 minutes. Perm buffer was added to the wells and the plate was centrifuged at 287 RCF for 3 minutes. The pellets were resuspended in 200 µl PBS and transferred to fortessa tubes (5 ml polypropylene round bottom tube, 352002), ready to run on the flow cytometer.

***Table 2.4* Surface staining panels.** Catalogue and lot numbers are given in **Table 2.2** and IMC information is given in **Table 2.3**. These panels were used to identify B cell subsets in the liver and analyse the expression of co-stimulatory markers, surface immunoglobulins and activation markers.

Panel 1			**Panel 2**		
Marker	**Fluorophore**	**Working dilution**	**Marker**	**Fluorophore**	**Working dilution**
Zombie red	PE-TxRed	1/1000	Zombie red	PE-TxRed	1/1000
CD19	PE-Cy5	1/200	CD19	PE-Cy5	1/200
CD24	APC	1/100	CD24	APC	1/100
CD38	PE-Cy7	1/200	CD38	PE-Cy7	1/200
IgD	BV510	1/100	IgD	BV510	1/100
CD27	APC-Vio770	1/200	CD27	APC-Vio770	1/200
CD21	BV605	1/200	CD21	BV605	1/200
CD11c	AF488	1/200	CD11c	AF488	1/200
CD69	BUV737	1/200	CD69	BUV737	1/200
CD1d	BUV395	1/100	CD1d	BUV395	1/100
CD80	BV421	1/200	IgA	BV421	1/100
CD86	BV785	1/200	IgM	BV785	1/200
HLA-DR	AF700	1/200	CD138	AF700	1/100
FcRL5	BV650	1/100	IgE	BV650	1/200
CD5	PerCP-Cy5.5	1/200	IgG	PerCP-Cy5.5	1/100

***Table 2.5* Intracellular staining panel.** Catalogue and lot numbers are given in **Table 2.2** and IMC information is given in **Table 2.3**. Intracellular antibodies were added after the samples were surface stained and treated with perm buffer.

Panel 1			**Panel 2**		
Marker	**Fluorophore**	**Working dilution**	**Marker**	**Fluorophore**	**Working dilution**
T-bet	BV711	1/100	T-bet	BV711	1/100
TLR7	PE	1/100	TLR9	PE	1/200

2.2.6 Fortessa spectral flow cytometer

Rainbow calibration particles **(table 2.6)** were used to calibrate the machine for consistency between my experiments. The beads were run on the flow cytometer and the voltages were set so the 8th peak was always in the same position for all fluorophores **(appendix 2)**. Single colour compensation beads **(table 2.6)** were used to create positive and negative peaks, for each fluorophore so that compensation could be applied to the experiment prior to running the samples through the flow cytometer. FlowJo was used to analyse each flow experiment.

Table 2.6 Calibration and compensation reagents used for each experiment. *Calibration beads ensured the flow cytometer calibration was consistent for each experiment. Compensation beads were used to set the flow cytometer to detect positive and negative cells.*

Reagent	**Company**	**Catalogue number**
Rainbow calibration particles, 8 peaks, 3.0-3.4µm	Biolegend	122903
BD^{TM} CompBeads Anti-Mouse Ig, κ	BD	51-90-9001229
BD^{TM} CompBeads Negative Control	BD	51-90-9001291

2.2.7 Statistical analysis

GraphPad Prism 9.4.1 was used to create graphs and perform statistical analysis. The Shapiro-Wilk normality test was used to assess normal distribution of my samples **(figure 2.4)**. This test calculates the ratio between the standard deviation of the data to the computed standard deviation of the slope from the QQ plot generated for our data. Normality tests were used to determine the statistical tests carried out on our data. Dunnett's T3 multiple comparisons test was used to analyse statistical significance between unpaired, normally distributed samples. Dunn's multiple comparisons test was used to analyse unpaired samples that were not normally distributed.

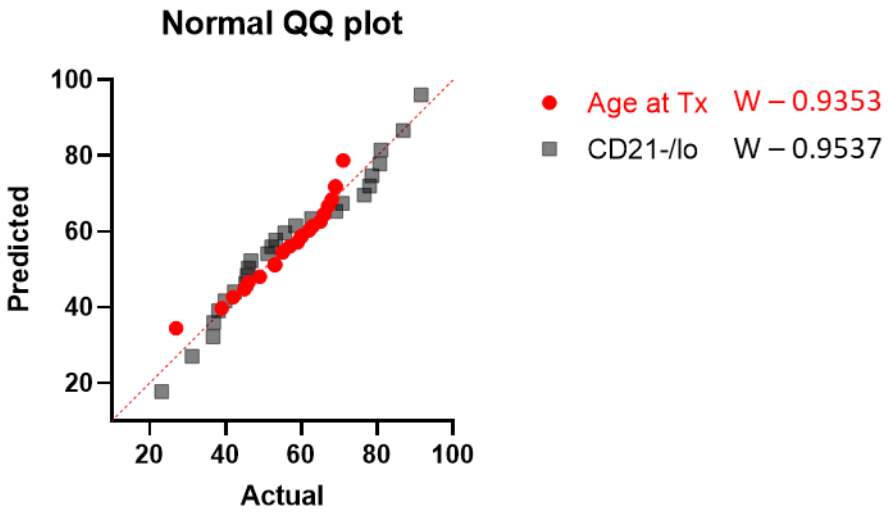


Figure 2.4 Samples were checked for normal distribution using the Shapiro-Wilk test on GraphPad prism. *The ratio (W) between the standard deviations from the data and the SD calculated from the QQ plot generated using our data was close to 1, indicating that our data was normally distributed. Two data sets were checked for normality in this plot: Age at transplant (red circles) and CD21-/lo ABC percentage positive cells (grey squares).*

2.3 Results

2.3.1 B cell frequencies in liver health and in different end-stage diseases

We first set out to measure CD19+ B cell frequencies in cells extracted from human explanted livers. Multiparametric spectral flow cytometry was used to characterise the B cell compartment across different adult liver diseases. The acquired cells were gated on lymphocytes **(figure 2.5A(i))** and then single cells **(figure 2.5A(ii))**. Single cells were then gated for live CD19+ cells **(figure 2.5A(iii))**. All downstream analysis was carried out on CD19+ cells. Total percentage of CD19+ B cells **(figure 2.5B(i))** and the median fluorescence intensity (MFI) **(figure 2.5B(ii))** were compared amongst HFe blood, donor livers and other adult chronic liver diseases. HFe blood was used as a comparison to compare the B cell compartment between the liver and blood. CD19+ B cells were present across blood and all adult livers **(figure 2.5B)**. CD19 MFI results showed that HFe blood had significantly higher CD19 MFI expression compared to adult livers (ALD p-value 0.0009; NASH p-value 0.0121; PBC p-value 0.0258; PSC p-value 0.0075; other livers p-value 0.0037) **(figure 2.5B(ii))**.

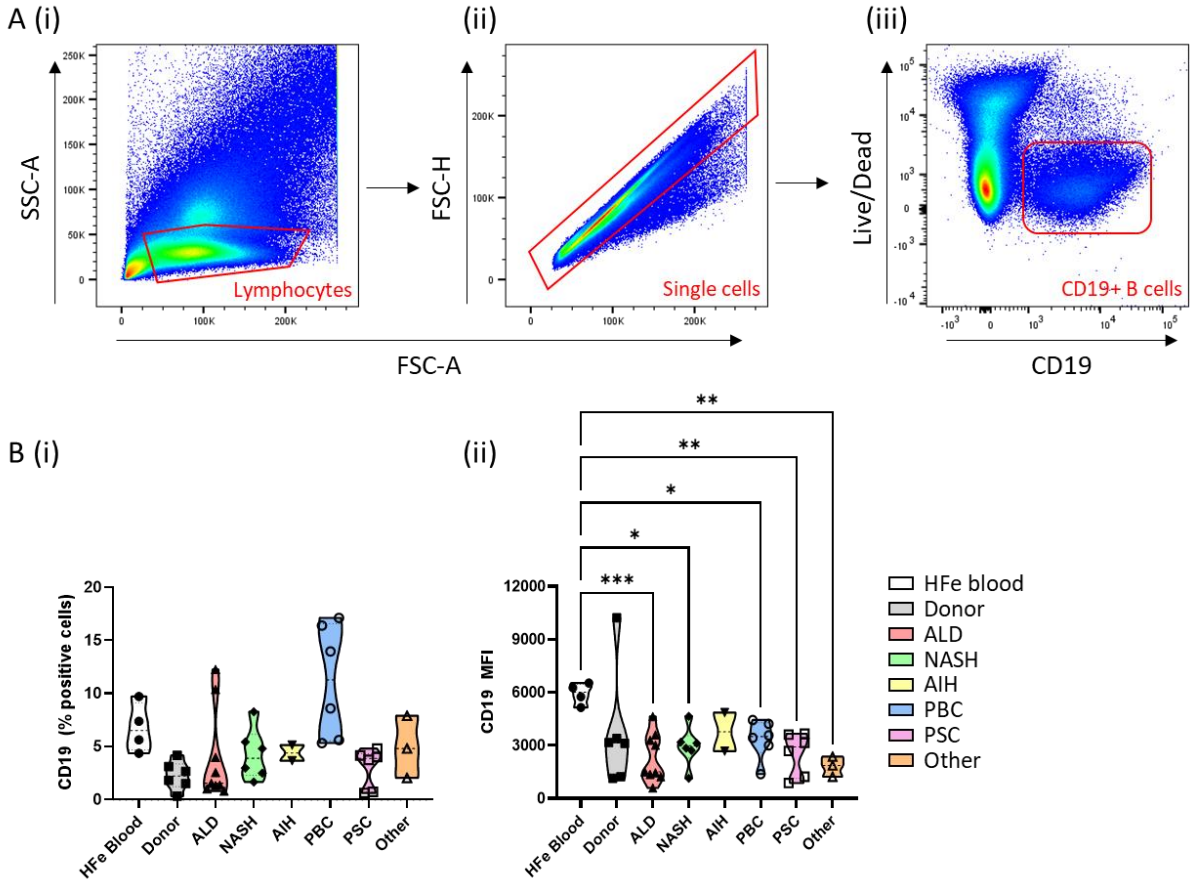


Figure 2.5 B cell characterisation using flow cytometry. *Frozen thawed liver isolated mononuclear cells (LIMCs) from adult explanted livers and peripheral blood mononuclear cells (PBMCs) from HFe blood were stained and analysed using FlowJo. (A) Total LIMCs from adult livers or PBMCs from HFe blood were gated on (A(i)) lymphocytes and then (A(ii)) single cells before gating on (A(iii)) live CD19+ cells. (B(i)) The percentage of total B cells and (B(ii)) MFI of CD19 cells were analysed in HFe blood and adult liver diseases. HFe blood (n=4), donor (n=6), ALD (n=8), NASH (n=6), AIH (n=2), PBC (n=6), PSC (n=6) and other livers (n=3). (B) Dunnett's T3 multiple comparisons test was used. p-value < 0.0332 (*), p-value < 0.0021 (**), p-value < 0.0002 (***).*

CD27 and IgD were used to further phenotype total CD19+ B cells to identify memory B cells. Using CD27 and IgD, four B cell subpopulations were identified; naïve B cells (CD27- IgD-), unswitched memory B cells (CD27+ IgD+), switched memory (CD27+ IgD-) and double negative B cells (CD27- IgD). All four subpopulations were observed across representative blood and adult livers plots **(figure 2.6A)**. Similar proportions of naïve **(figure 2.6B)**,

unswitched memory **(figure 2.6C)**, switched memory **(figure 2.6D)** and double negative **(figure 2.6E)** B cells were detected across adult liver diseases **(figure 2.6)**. Taken together, these plots showed that naïve and activated B cell subsets were detected in similar proportions in liver diseases of various aetiologies.

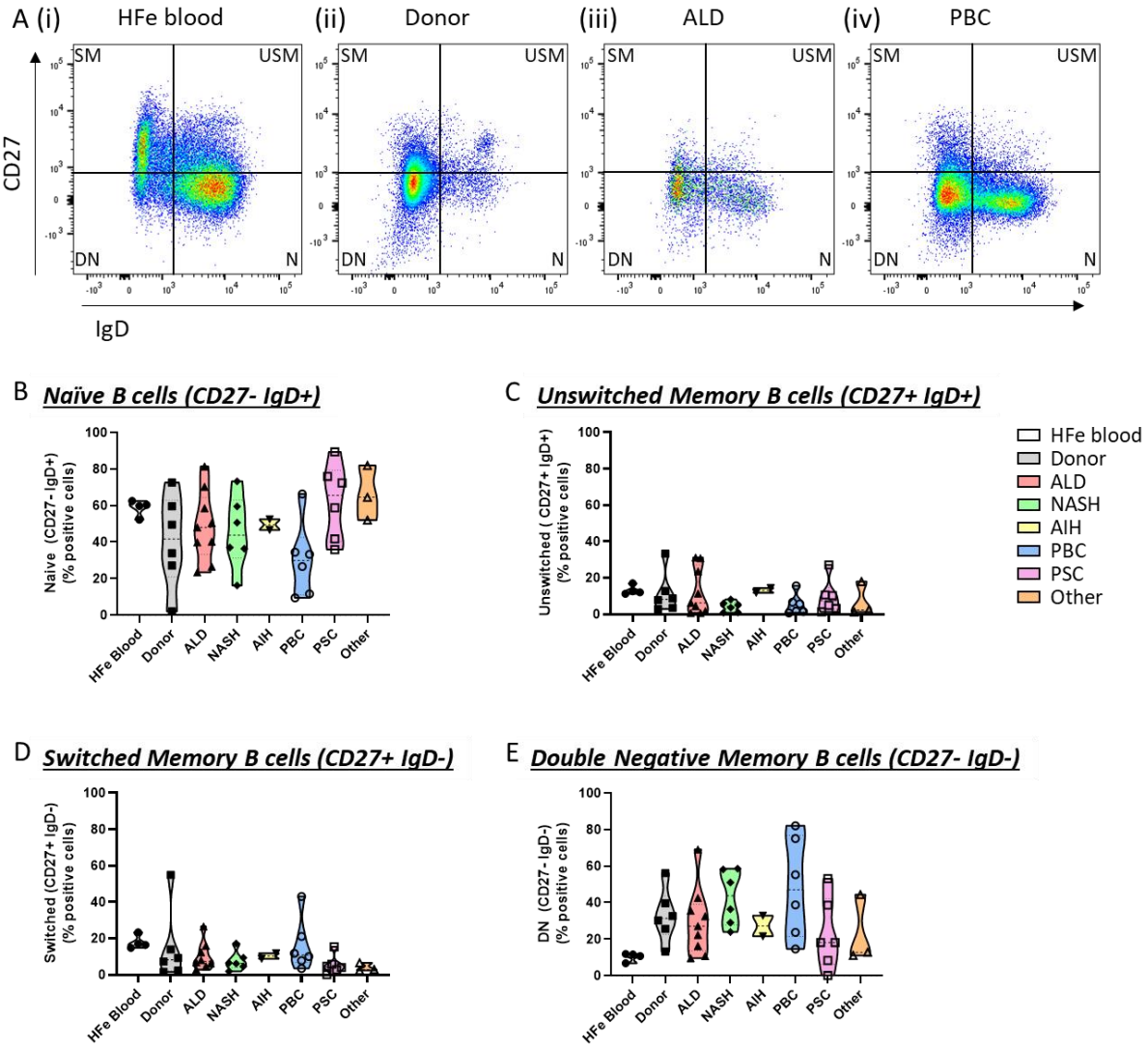


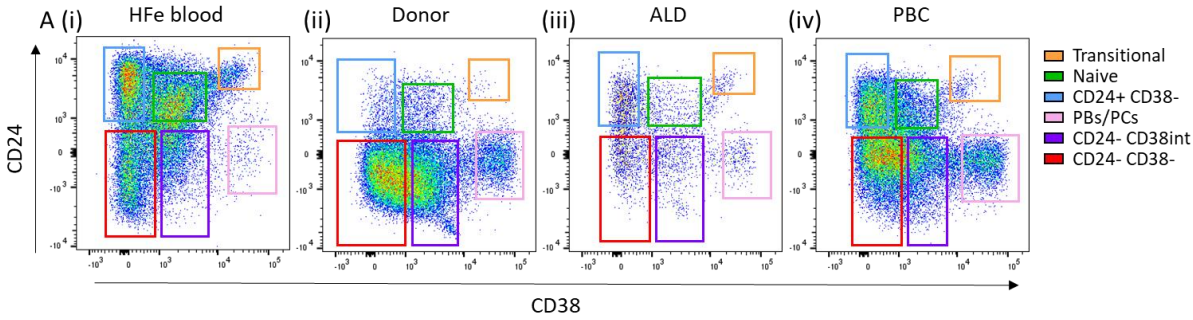
Figure 2.6 Naïve and memory B cells were detected in similar proportions across adult liver diseases. *Frozen thawed liver isolated mononuclear cells (LIMCs) from adult explanted livers and peripheral blood mononuclear cells (PBMCs) from HFe blood were stained and analysed using FlowJo. (A) Using CD27 and IgD, naïve and memory populations were detected in (A(i)) HFe blood, (A(ii)) Donor, (A(iii)) ALD and (A(iv)) PBC livers, representative plots. The proportion of (B) naïve; N, (C) unswitched memory; USM, (D) switched memory; SM and (E) double negative; DN B cells, were analysed across all liver diseases. HFe blood (n=4) (white),*

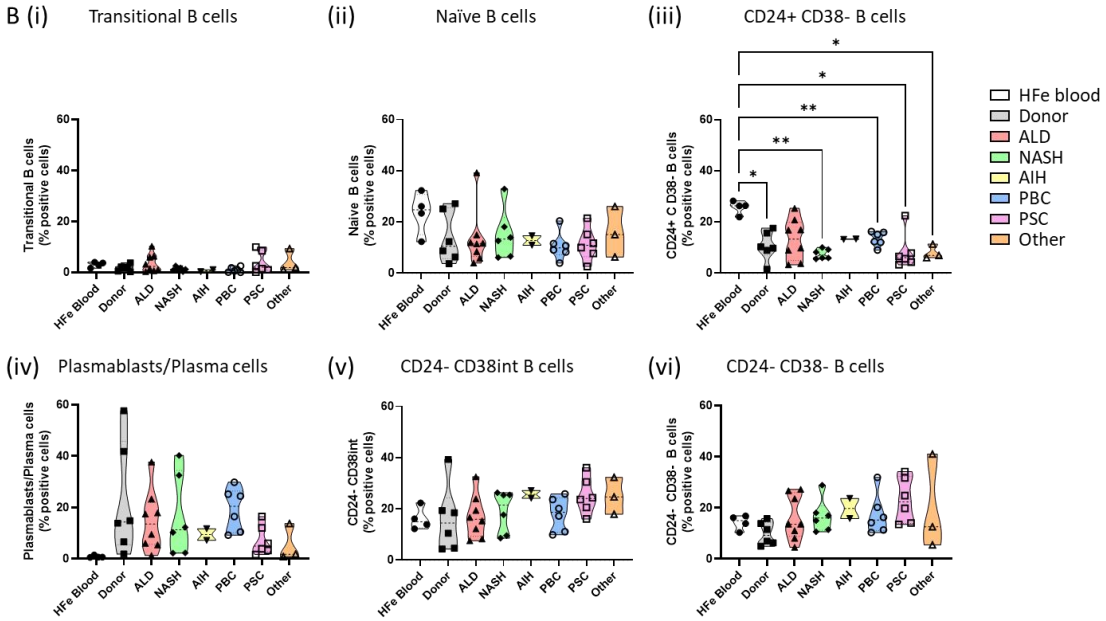
donor (n=6) (grey), ALD (n=8) (red), NASH (n=6) (green), AIH (n=2) (yellow), PBC (n=6) (blue), PSC (n=6) (pink) and other livers (n=3) (orange). (B and E) Dunnett's T3 multiple comparisons test was used. (C and D) Dunn's multiple comparisons test was used.

We wanted to observe B cells across development, starting from transitional cells all the way to differentiated PBs/PCs. Common ways of investigating B cells would be to use CD38 vs IgD (Sanz et al., 2019) or CD24 vs CD38. We focused on CD24 vs CD38 because in the liver, we previously found an increase of CD24- B cells. Representative images of CD38 vs IgD can be found in **appendix 3**. We next set out to investigate the frequencies of B cell subsets through B cell maturation more closely using CD24. CD24 and CD38 were used to identify six B cell subsets in HFe blood and adult chronic liver diseases **(figure 2.7A)**. These six subsets included transitional B cells (orange), naïve B cells (green), CD24+ CD38- B cells which contain a mixture of memory and naïve B cells (blue), PBs/PCs (pink) and two populations of CD24- B cells; CD24- CD38int B cells (purple) and CD24- CD38- B cells (red).

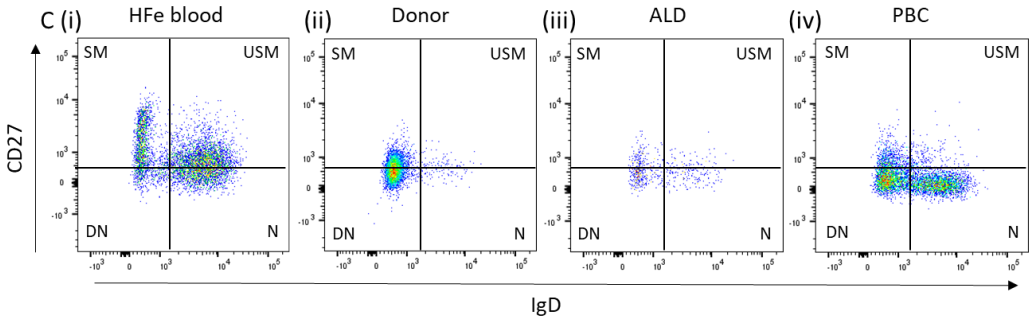
No differences were observed amongst HFe blood and adult livers analysed for the percentages of transitional B cells **(figure 2.7B(i))**, naïve B cells **(figure 2.7B(ii))**, PBs/PCs **(figure 2.7B(iv))**, CD24- CD38int B cells **(figure 2.7B(v))** and CD24- CD38- B cells **(figure 2.7B(vi))**. HFe blood had significantly higher percentages of CD24+ CD38- B cells compared to donor (p-value 0.0135), NASH (p-value 0.0011), PBC (p-value 0.0039), PSC (p-value 0.0167) and other livers (p-value 0.0124) **(figure 2.7B(iii))**.

CD24- B cell populations were detected across all adult livers and HFe blood **(figure 2.7B(v-vi))**. CD24- B cells contained a heterogeneous population of naïve and memory B cells **(figure 2.7C and 2.7D)**. Quantitative data for naïve and memory populations in two subsets across different adult liver diseases is shown in **Figure 2.8**.





CD24- CD38-



CD24- CD38int

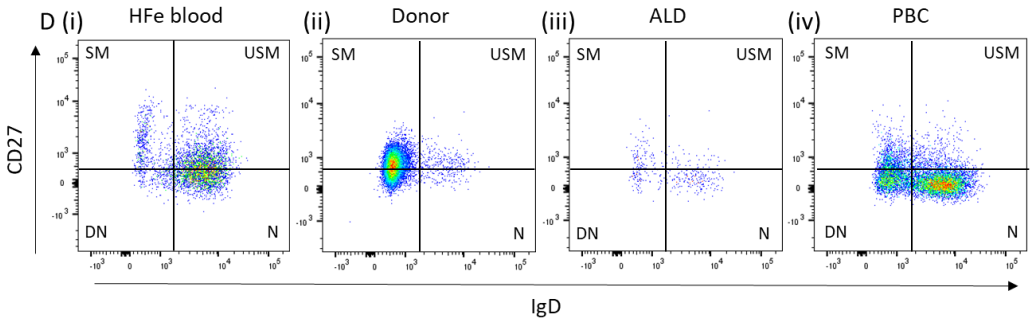


Figure 2.7 B cell populations were detected in similar proportions across different liver diseases. *Frozen thawed liver isolated mononuclear cells (LIMCs) from adult explanted livers and peripheral blood mononuclear cells (PBMCs) from HFe blood were stained and analysed using FlowJo. (A) Representative plots showing six B cell subsets were identified using CD24 and CD38. Transitional B cells (orange), naïve B cells (green), CD24+ CD38- B cells which contain a mixture of memory and naïve B cells (blue), PBs/PCs (pink), CD24- CD38int B cells (purple) and CD24- CD38- B cells (red). (B(i)) Transitional B cells, (B(ii)) naïve B cells, (B(iii)) memory B cells, (B(iv)) PBs/PCs, (B(v)) CD24- CD38int B cells and (B(vi)) CD24- CD38- B cells, were present in comparable proportions across different liver diseases. HFe blood (n=4), donor (n=6), ALD (n=8), NASH (n=6), AIH (n=2), PBC (n=6), PSC (n=6) and other livers (n=3). (C) CD24- CD38- B cells and (D) CD24- CD38int B cells contained a heterogeneous population of naïve and memory B cells in representative plots from (C(i)) HFe blood, (C(ii)) donor, (C(iii)) ALD and (C(iv)) PBC livers. SM; switched memory, USM; unswitched memory, N; naïve and DN; double negative B cells. (B(iii-vi)) Dunnett's T3 multiple comparisons test was used. (B(i and ii)) Dunn's multiple comparisons test was used. p-value < 0.0332 (*), p-value < 0.0021 (**).*

2.3.2 CD24- B cells and ABCs were phenotypically consistent in different liver diseases

ABCs were found to be accumulated in chronic infections and autoimmunity. The literature describes ABCs to be CD19+ CD21-/lo B cells and portion of these are CD19+ CD21-/lo CD11c+ T-bet+ B cells. ABCs are thought to be a heterogenous population containing naïve and memory B cells (Rubtsova et al., 2015). We therefore derived two populations of ABCs from CD19+ cells; CD21-/lo B cells **(figure 2.8A(i))** and CD11c+ T-bet+ B cells which were gated on CD19+ CD21-/lo B cells **(figure 2.8A(ii))**.

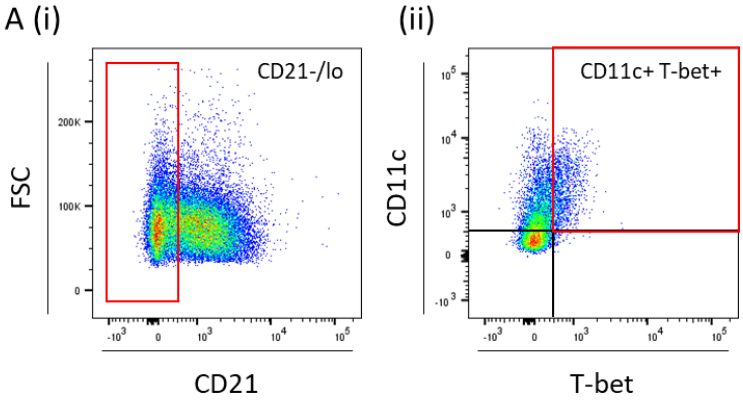
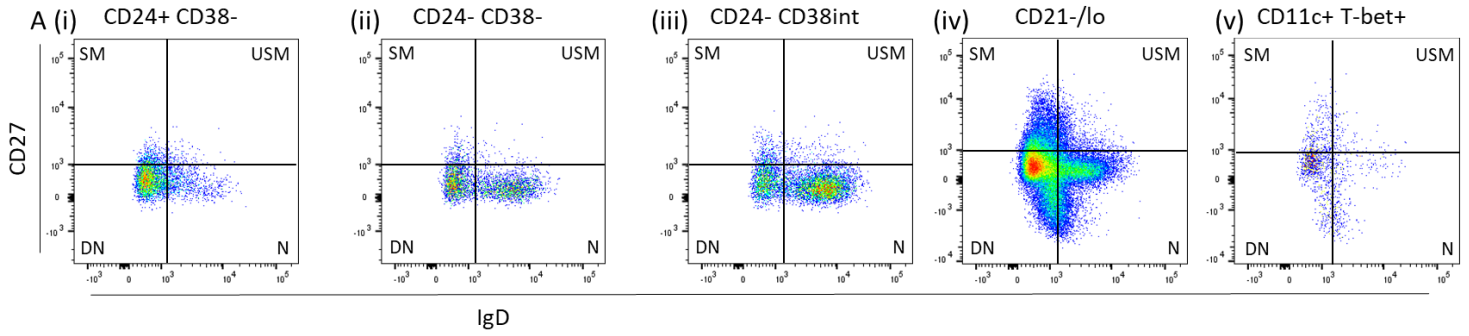


Figure 2.8 Gating strategy for CD21-/lo ABCs and CD11c+ T-bet+ ABCs. *(A) Representative plot of adult PBC liver showing gating on CD19+ cells. (A(i)) Flow cytometry gating on CD19+ CD21-/lo cells. (A(ii)) CD19+ CD21-/lo cells were gated for CD11c+ T-bet+ cells. These subsets were referred to as CD21-/lo ABCs and CD11c+ T-bet+ ABCs and were used for further analysis.*

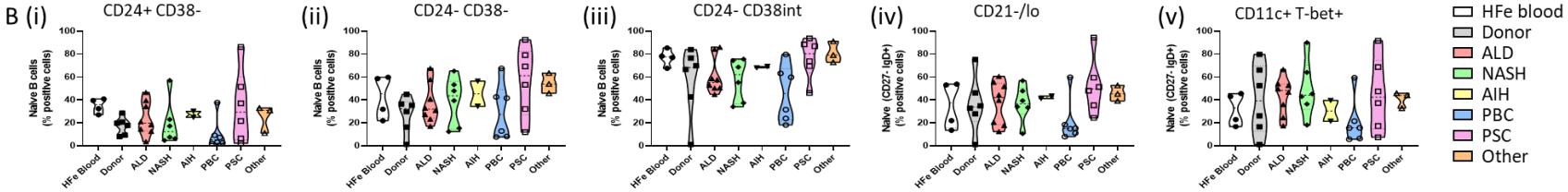
Using CD27 and IgD as markers for memory B cells, CD24+ CD38- B cells, CD24- CD38- B cells, CD24- CD38int B cells and two populations of ABCs; CD21-/lo ABCs and CD21-/lo CD11c+ T-bet+ (referred to as CD11c+ T-bet+ ABCs) were analysed. This analysis was used to determine any similarities or differences between CD24- B cell populations compared to ABCs and CD24+ CD38- B cells. Representative flow cytometry plots are shown for all five subsets **(figure 2.9A)**.

Across the different liver diseases there was no difference between B cell phenotypes. The livers analysed were of autoimmune nature and metabolic disorders. No significant differences were detected in the percentages of naïve B cells **(figure 2.9B)**. These data showed that unswitched memory B cells were present in varying percentages across different chronic liver diseases, donor livers and in HFe blood **(figure 2.9C)**. Comparable percentages of switched memory B cells were observed across CD24+ CD38- B cells, CD24- B cells and ABC populations **(figure 2.9D)**. The liver had higher percentages of DN B cells

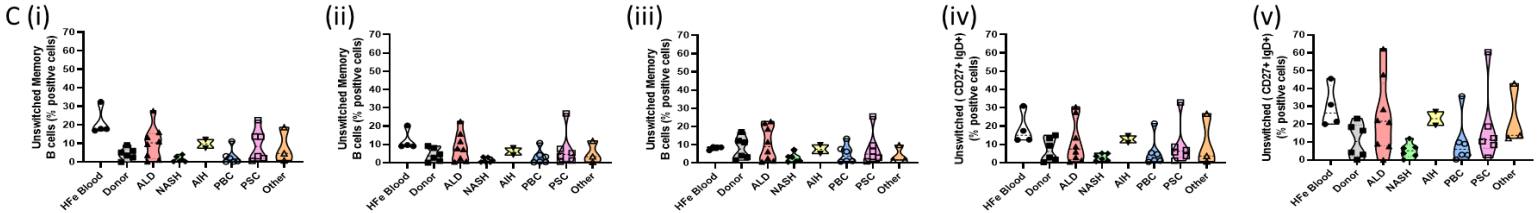
compared to HFe blood **(figure 2.9E)**, observed in CD24+ CD38- B cells for donor (p-value 0.0046) and NASH livers (p-value 0.0137) **(figure 2.9E(i))** and compared CD21-/lo B cells (p-value 0.0084) **(figure 2.9E(iv))** in NASH livers. Comparable amounts of DN B cells were detected for the remaining subsets across different liver diseases. Taken together, these data showed that CD24- and ABCs had relatively consistent phenotypes based on naïve and memory B cell markers, across different end-stage liver diseases. Furthermore, these data showed that CD24- B cells are a heterogeneous population.



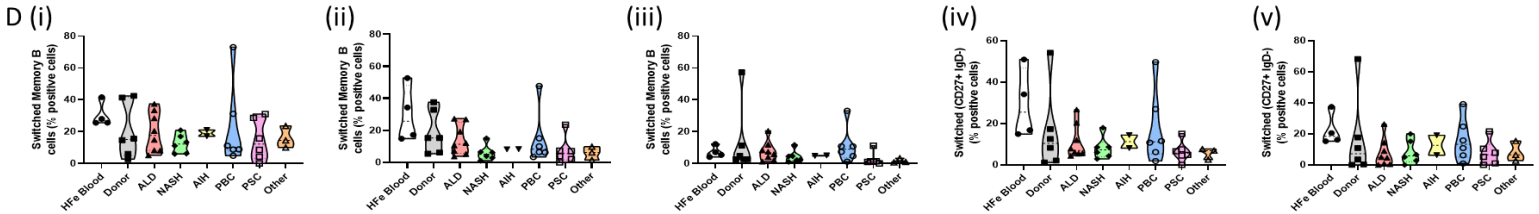
Naïve B cells (CD27- IgD+)



Unswitched Memory B cells (CD27+ IgD+)



Switched Memory B cells (CD27+ IgD-)



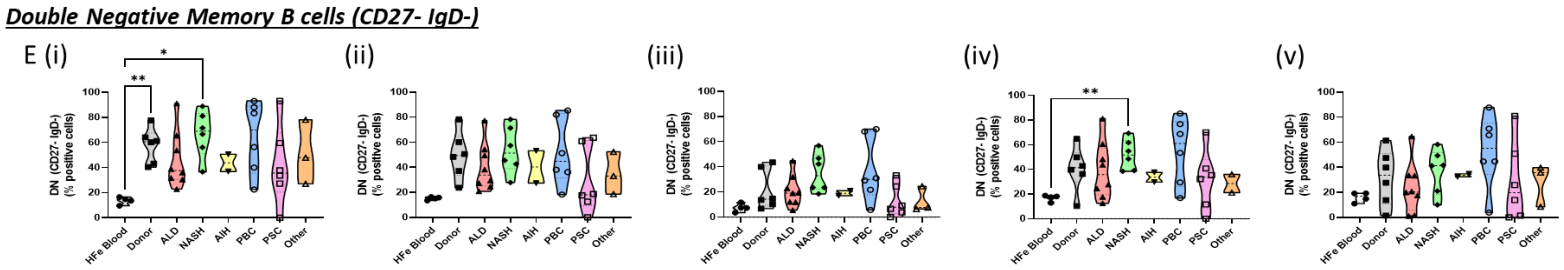


Figure 2.9 Phenotyping of CD24- B cells and ABC populations based on naïve and memory B cells in liver diseases. *Frozen thawed liver isolated mononuclear cells (LIMCs) from adult explanted livers and peripheral blood mononuclear cells (PBMCs) from HFe blood were stained and analysed using FlowJo. (A) Representative plots showing the gating strategy used to identify naïve and memory populations. (B) Naïve B cell, (C) unswitched memory B cell, (D) switched memory B cell and (E) double negative B cell percentage expression, across (C(i)) CD24+ CD38- B cells, (C(ii)) CD24- CD38- B cells, (C(iii)) CD24- CD38int B cells, (C(iv)) CD21-/lo B cells and (C(v)) CD11c+ T-bet+ B cells was analysed across HFe blood, donor liver, and adult chronic liver diseases. Naïve; N, switched memory; SM, unswitched memory; USM and double negative; DN B cells. HFe blood (n=4), donor (n=6), ALD (n=8), NASH (n=6), AIH (n=2), PBC (n=6), PSC (n=6) and other livers (n=3). (B, C(ii), D(v) and E(i, iv and v)) Dunnett's T3 multiple comparisons test was used. (C(i, iii-v), D(i-v) and E(ii and iii)) Dunn's multiple comparisons test was used. p-value < 0.0332 (*), p-value < 0.0021 (**).*

2.3.3 Investigation of APC markers in liver B cell subsets in liver explants

ABCs were efficient antigen presenters (Rubtsova et al., 2015) and expressed high levels of CD80 and CD86 (Rubtsov et al., 2011). We therefore wanted to establish their phenotype in B cells from liver explants in comparison to CD24+ CD38- and CD24- B cell subsets. All five subsets were analysed for CD80 and CD86 percentage positive cells and MFI alongside the activation markers CD69 and HLA-DR using flow cytometry. Similar phenotypes of CD80 percentage positive cells and MFI were detected across all liver diseases for CD24+ CD38- B cells **(figure 2.10A(i))**, CD24- B cells **(figure 2.10A(ii-iii))** and CD21-/lo ABCs **(figure 2.10A(iv-v))**. Low percentages of CD86 positive cells were observed amongst adult liver diseases for CD24+ CD38- B cells **(figure 2.10B(i))** and CD24- B cells **(figure 2.10B(ii-iii))**. This observation was reflected in MFI data for CD86 **(figure 2.10(vi-viii)**. CD11c+ T-bet+ ABCs had higher CD86 expression in donor livers compared to HFe blood (p-value 0.0449) **(figure 2.10(v))**. CD11c+ T-bet+ B cell subset showed no difference in CD86 MFI expression between HFe blood and across all liver diseases **(figure 2.10B(x))**. These data showed that proportions of CD24+ B cells, CD24- B cells and ABCs did not differ amongst adult liver diseases for co-stimulatory markers CD80 and CD86.

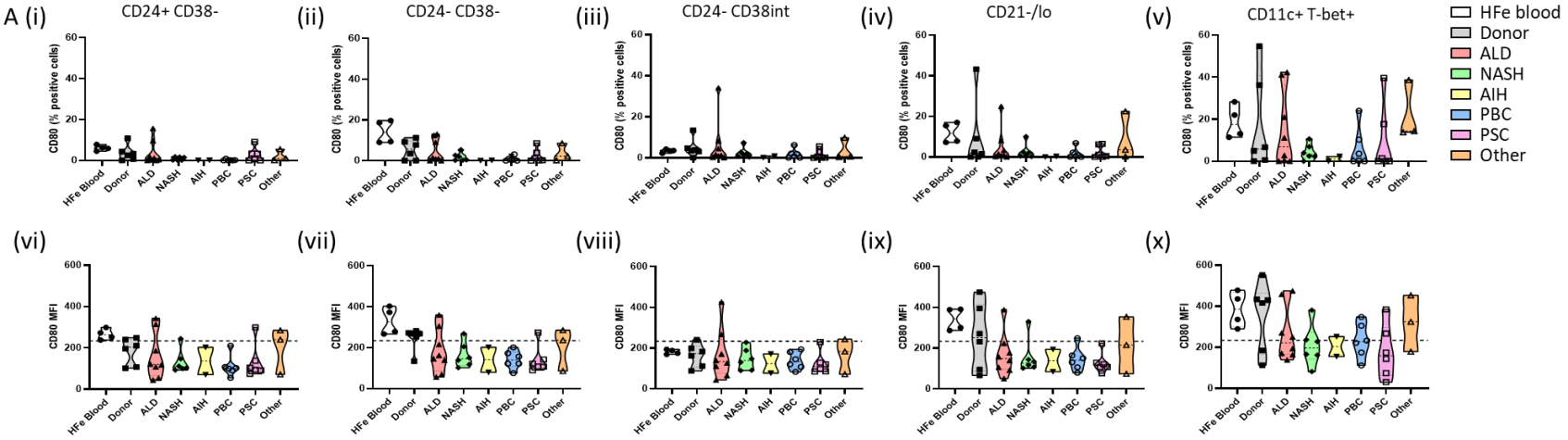
B cells are activated in chronic disease and express activation markers. CD69 and HLA-DR were used to determine B cell activation or tissue residence in the liver. PBC livers had significantly higher percentage of CD69 positive B cells in CD24+ CD38- B cells (HFe blood p-value 0.0002; donor p-value <0.0001, ALD p-value 0.0003; NASH p-value <0.0001 and other livers p-value 0.0003) **(figure 2.10C(i))**, in CD24- CD38- B cells between PBC livers and HFe blood (p-value 0.0016) **(figure 2.10C(ii))**, in CD24- CD38int B cells (HFe blood p-value 0.0039; donor p-value 0.0271, ALD p-value 0.0062; NASH p-value 0.0060; PSC p-value 0.0492 and

other livers p-value 0.0035) **(figure 2.10C(iii))** and in CD21-/lo B cells (HFe blood p-value 0.0004 and donor p-value 0.0319) **(figure 2.10C(iv))**. No difference was detected between HFe blood and adult chronic liver diseases in CD11c+ T-bet+ ABCs **(figure 2.10C(v))**. CD24+ CD38- B cells had a significant difference in CD69 MFI expression between HFe blood and PBC (p-value 0.0003) and PSC livers (p-value 0.0497) **(figure 2.10C(vi))**. PBC livers had significantly higher CD69 MFI expression compared to HFe blood in CD24- CD38- B cells (p-value 0.0010) **(figure 2.10C(vii))** and CD24- CD38int B cells (p-value 0.0007) **(figure 2.10C(viii))**. CD21-/lo ABCs showed that PBC livers had higher CD69 expression compared to HFe blood (p-value 0.0023) and donor livers (p-value 0.0269) **(figure 2.10C(ix))**. No difference was observed between HFe blood and adult chronic liver diseases in CD11c+ T-bet+ ABC subset **(figure 2.10C(x))**. These data showed that PBC livers had higher CD69 expression compared to HFe blood and adult liver diseases across all subsets analysed, except in the case of CD11c+ T-bet+ ABCs.

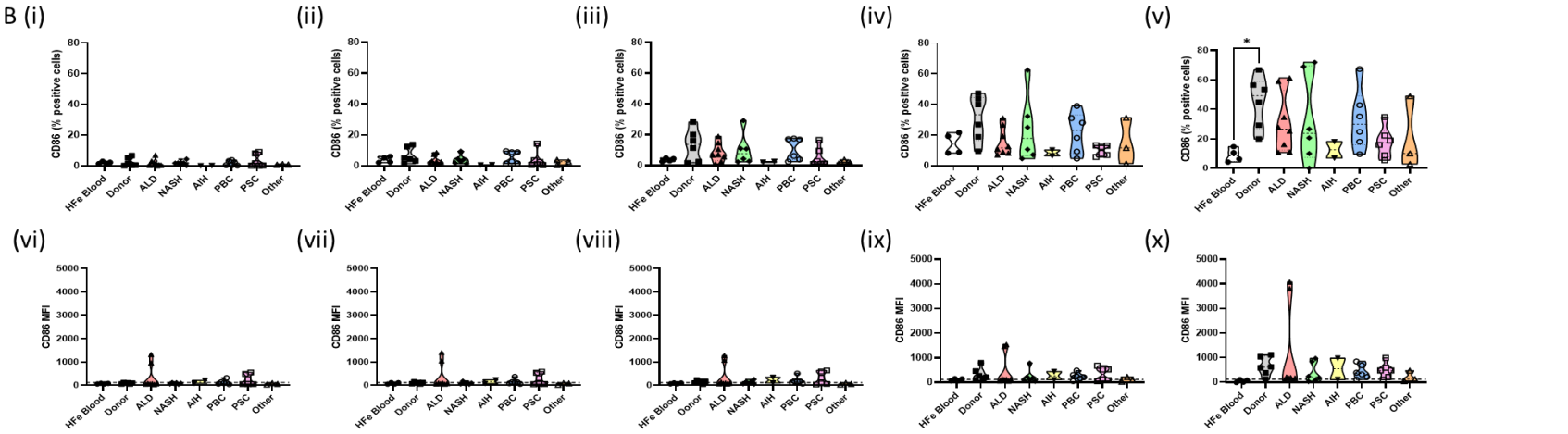
Significantly high HLA-DR percentage positive cells were expressed in HFe blood compared to PBC livers in CD24+ CD38- B cells (p-value 0.0162) **(figure 2.10D(i))**, CD24- CD38- B cells (p-value 0.0381) **(figure 2.10D(ii))** and in CD21-/lo ABCs (p-value 0.0134) **(figure 2.10D(iv))**. In CD24+ CD38- B cells, HFe blood had increased HLA-DR-expressing cells compared to PSC livers (p-value 0.0319) **(figure 2.10(i))**. Furthermore, HFe blood from CD21-/lo ABCs expressed significantly higher HLA-DR+ cells compared to ALD livers (p-value 0.0499) **(figure 2.10D(iv))**. HLA-DR MFI expression in CD24+ CD38- B cell subset showed significant differences between HFe blood compared to chronic adult liver diseases (ALD p-value 0.0014, NASH p-value 0.0246, PBC p-value 0.0103 and PSC livers p-value 0.0017) **(figure**

2.10D(vi)). No significant differences in HLA-DR expression were observed amongst CD24- B cells and ABCs across all liver diseases **(figure 2.10D(vii-x))**.

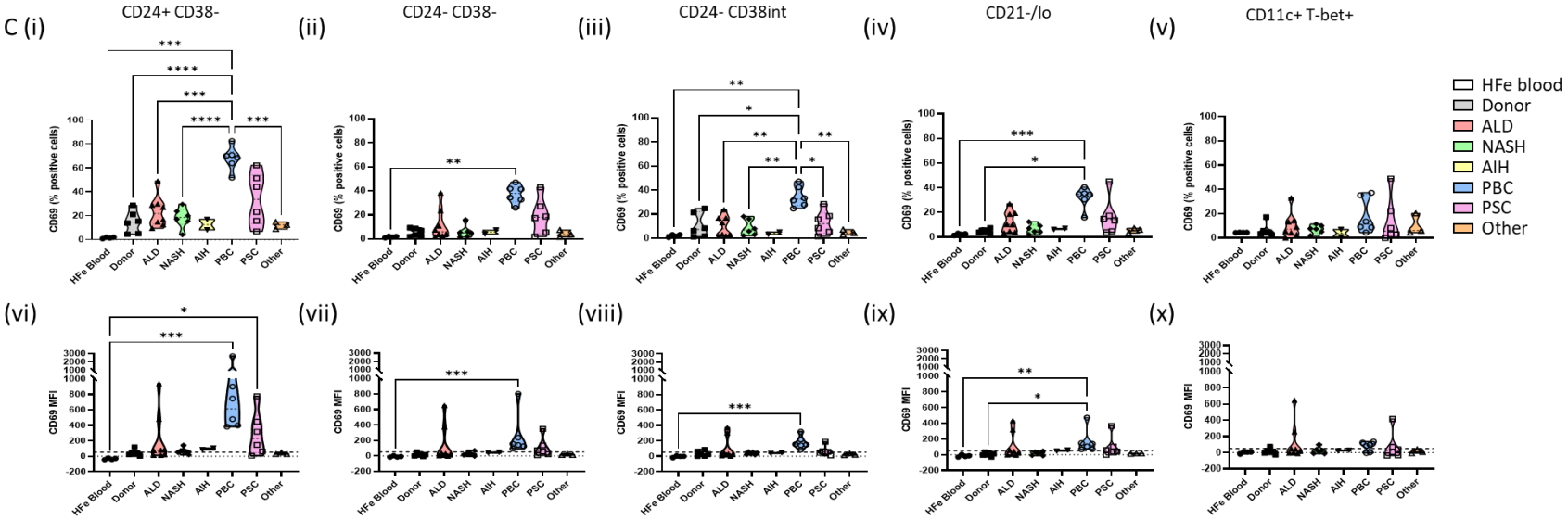
CD80


A (i)
CD24+ CD38-
(ii)
CD24- CD38-
(iii)
CD24- CD38int
(iv)
CD21-/lo
(v)
CD11c+ T-bet+
CD80 (% positive cells)
(vi)
(vii)
(viii)
(ix)
(x)
CD80 MFI
HFe Blood
Donor
ALD
NASH
AIH
PBC
PSC
Other
HFe blood
Donor
ALD
NASH
AIH
PBC
PSC
Other

CD86


B (i)
(ii)
(iii)
(iv)
(v)
CD86 (% positive cells)
*
(vi)
(vii)
(viii)
(ix)
(x)
CD86 MFI
HFe Blood
Donor
ALD
NASH
AIH
PBC
PSC
Other

CD69


C (i)
CD24+ CD38-
(ii)
CD24- CD38-
(iii)
CD24- CD38int
(iv)
CD21-/lo
(v)
CD11c+ T-bet+
CD69 (% positive cells)
(vi)
(vii)
(viii)
(ix)
(x)
CD69 MFI
HFe Blood
Donor
ALD
NASH
AIH
PBC
PSC
Other
HFe blood
Donor
ALD
NASH
AIH
PBC
PSC
Other

HLA-DR

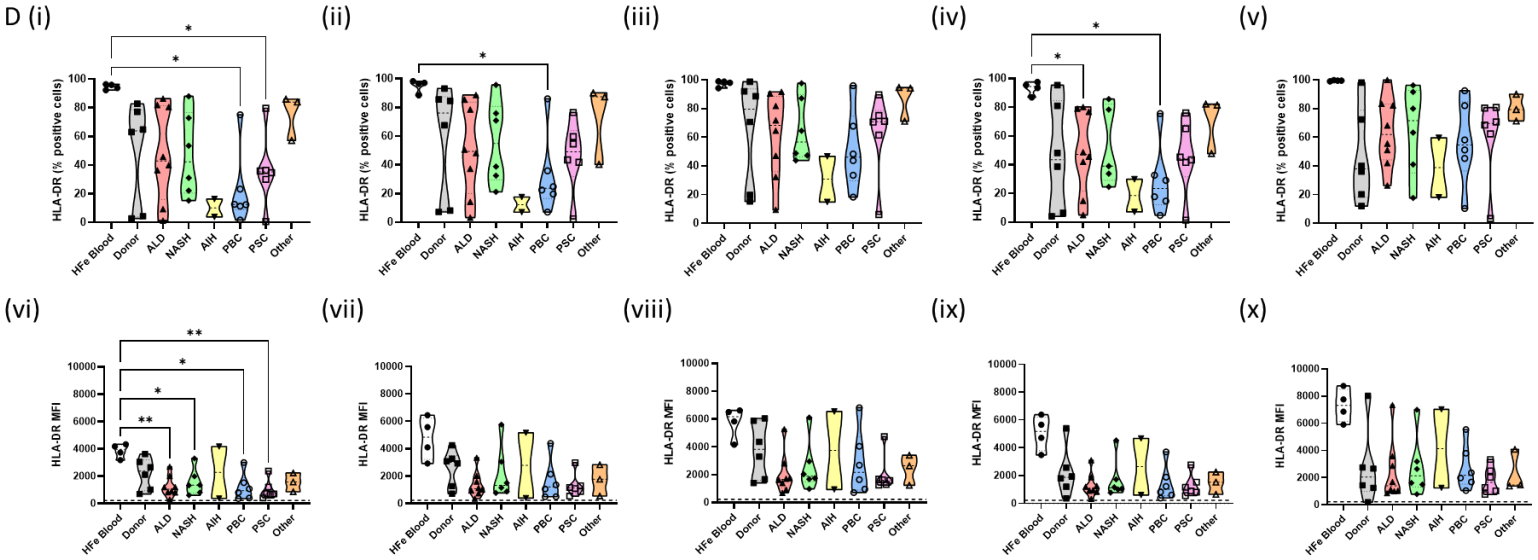

D (i)
(ii)
(iii)
(iv)
(v)
HLA-DR (% positive cells)
(vi)
(vii)
(viii)
(ix)
(x)
HLA-DR MFI
HFe Blood
Donor
ALD
NASH
AIH
PBC
PSC
Other

Figure 2.10 Phenotyping of CD24- B cells and ABCs based on APC markers in liver diseases. *Frozen thawed liver isolated mononuclear cells (LIMCs) from adult explanted livers and peripheral blood mononuclear cells (PBMCs) from HFe blood were stained and analysed using FlowJo. (A) CD80, (B) CD86, (C) CD69 and (D) HLA-DR percentage positive cells and MFI data was analysed between (i, vi) CD24+ CD38- B cells, (ii, vii) CD24- CD38- B cells, (iii, viii) CD24- CD38int B cells, (iv, ix) CD21-/lo ABCs and (v, x) CD11c+ T-bet+ ABCs across HFe blood and adult liver samples. The dashed line represents the IMC MFI line, anything above this line is positive. HFe blood (n=4), donor (n=6), ALD (n=8), NASH (n=6), AIH (n=2), PBC (n=6), PSC (n=6) and other livers (n=3). (A(ii, vi, vii, ix and x), B(iii-v), C(I and iii) and D(i-vii and ix)) Dunnett's T3 multiple comparisons test was used. (A(i, iii-v and viii), B(i, ii, vi-x), C(ii, iv-x) and D(viii and x)) Dunn's multiple comparisons test was used. p-value < 0.0332 (*), p-value < 0.0021 (**), p-value < 0.0002 (***), p-value < 0.0001 (****).*

Comparison of B cell subsets across individual liver diseases showed that CD11c+ T-bet+ ABCs expressed significantly higher percentages of CD80+ cells in ALD livers (p-value 0.0443) **(figure 2.11A(iii))**. CD21-/lo ABCs from donor liver samples had significantly higher CD86 percentage positive cells compared to CD24+ CD38- B cells (p-value 0.0265) and CD24- CD38- B cells (p-value 0.0427) **(figure 2.11B(ii))**. Donor livers also had significantly higher CD86+ cells in CD11c+ T-bet ABCs compared to CD24+ CD38- B cells (p-value 0.0117) and CD24- CD38- B cells (p-value 0.0163) **(figure 2.11B(ii))**. ALD livers had higher CD86+ cells in CD21-/lo ABCs compared to CD24+ CD38- B cells (p-value 0.0111) and CD24- CD38- B cells (p-value 0.0246) and in CD11c+ T-bet+ ABCs compared to CD24+ CD38- B cells (p-value 0.0188), CD24- CD38- B cells (p-value 0.0272), CD24- CD38int B cells (p-value 0.0440) and CD21-/lo B cells (p-value 0.0484) **(figure 2.11B(iii))**. NASH livers had significantly higher CD86+ cells in CD21-/lo ABCS (p-value 0.0191) and CD11c+ T-bet ABCs (p-value 0.0191) compared to CD24+ CD38- B cells **(figure 2.11B(iv))**.

CD69+ cells were significantly higher in CD21-/lo ABCs compared to CD24+ CD38- B cells (p-value 0.0449) and in CD11c+ T-bet+ ABCs compared to CD24+ CD38- B cells (p-value 0.0115) and CD24- CD38- B cells (p-value 0.0142) in HFe blood **(figure 2.11C(i))**. However, CD24+ CD38- B cells had significantly higher CD69+ cells compared to CD24- CD38- B cells (p-value 0.0266), CD24- CD38int B cells (p-value 0.0050) and CD11c+ T-bet+ ABCs (p-value 0.0157) in ALD livers **(figure 2.11C(iii))**. CD24+ CD38- B cells had significantly higher CD69+ cells compared to CD24- CD38- B cells (p-value 0.0148), CD24- CD38int B cells (p-value 0.0359) and CD21-/lo ABCs (p-value 0.0334) in NASH livers **(figure 2.11C(iv))**. CD24+ CD38- B cells had significantly higher CD69+ cells compared to CD24- CD38- B cells (p-value 0.0003), CD24- CD38int B cells (p-value 0.0106), CD21-/lo ABCs (p-value <0.0001) and CD11c+ T-bet+ ABCs

(p-value 0.0070) in PBC livers **(figure 2.11C(v))**. Taken together, these data showed that ABCs expressed co-stimulatory markers CD80 and CD86, higher than other B cell subsets in adult liver diseases. Furthermore, these populations were similar to CD24- B cells in terms of CD69 expression across liver diseases with different aetiologies.

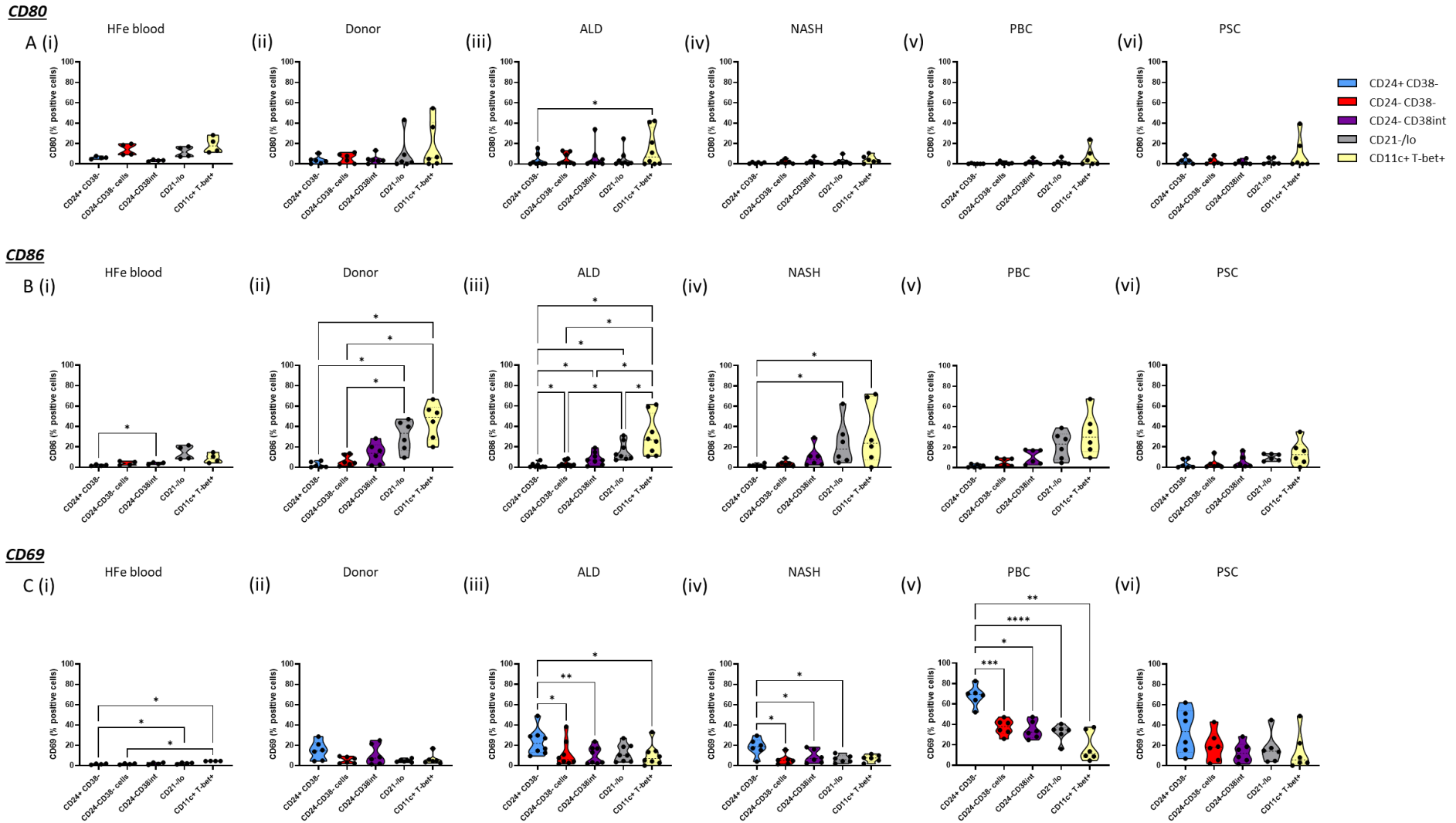
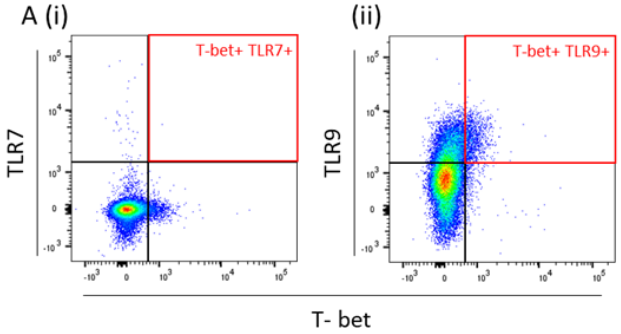

CD80
A (i)
HFe blood
(ii)
Donor
(iii)
ALD
(iv)
NASH
(v)
PBC
(vi)
PSC
CD80 (% positive cells)
CD24+ CD38-
CD24- CD38-
CD24- CD38int
CD21-/lo
CD11c+ T-bet+
CD86
B (i)
HFe blood
(ii)
Donor
(iii)
ALD
(iv)
NASH
(v)
PBC
(vi)
PSC
CD86 (% positive cells)
CD69
C (i)
HFe blood
(ii)
Donor
(iii)
ALD
(iv)
NASH
(v)
PBC
(vi)
PSC
CD69 (% positive cells)

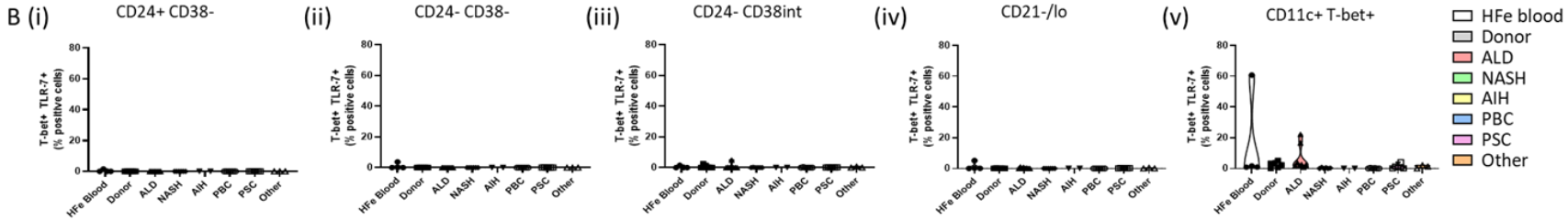
Figure 2.11 CD11c+ T-bet+ ABCs expressed higher amounts of co-stimulatory markers CD80 and CD86 compared to B cell subsets. *Frozen thawed liver isolated mononuclear cells (LIMCs) from adult explanted livers and peripheral blood mononuclear cells (PBMCs) from HFe blood were stained and analysed using FlowJo. B cell subsets were compared for each disease type for (A) CD80 positive cells (B) CD86 positive cells and (C) CD69 positive cells. CD24+ CD38- B cells (blue), CD24- CD38- B cells (red), CD24- CD38int B cells (purple), CD21-/lo ABCs (grey) and CD11c+ T-bet+ ABCs (yellow). HFe blood (n=4), donor (n=6), ALD (n=8), NASH (n=6), AIH (n=2), PBC (n=6), PSC (n=6) and other livers (n=3). (A(i), B(i-iii and v) and C(i, ii, iv-vi)) Tukey's multiple comparisons test was used. (A(ii-vi), B(iv and vi) and C(iii)) Dunn's multiple comparisons test was used. p-value < 0.0332 (*), p-value < 0.0021 (**), p-value < 0.0002 (***), p-value < 0.0001 (****).*

2.3.4 Expression of TLR7 and TLR9 in liver B cell subsets

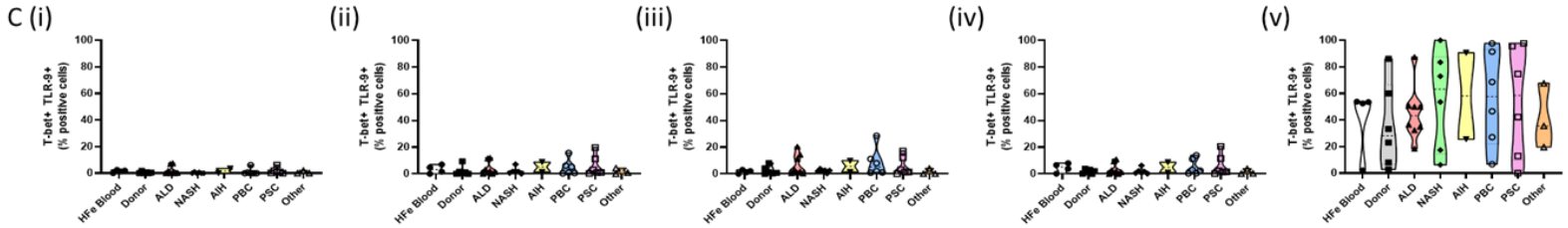
ABCs are stimulated by TLR7 and TLR9 and this induces T-bet expression (Rubtsova et al., 2017). We therefore set out to measure TLR7 and TLR9 expression in liver ABCs, CD24+ CD38- and CD24- B cells using flow cytometry. Subsets were gated on T-bet+ TLR7+ B cells **(figure 2.12A(i))** or T-bet+ TLR9+ B cells **(figure 2.12A(ii))**. Little to no T-bet+ TLR7+ cells were detected in adult livers across all five subsets **(figure 2.12B)**. TLR7 expression was also low across all subsets analysed **(appendix 4A and 4B)**. TLR9 was highly expressed across all five subsets analysed **(appendix 4C and 4D)** however, co-expression of T-bet and TLR9 was low across all subsets except CD11c+ T-bet+ ABCs **(figure 2.12C)**. CD11c+ T-bet+ ABCs highly expressed T-bet+ TLR9+ cells compared to CD24+ CD38- B cells in donor (p-value 0.0008) **(figure 2.12D(ii))**, ALD (p-value 0.0125) **(figure 2.12D(iii))**, NASH (p-value 0.0091) **(figure 2.12D(iv))**, PBC (p-value 0.0036) **(figure 2.12D(v))** and PSC livers (p-value 0.0410) **(figure 2.12D(vi))**. CD11c+ T-bet+ ABCs in ALD livers showed significantly higher percentage of T-bet+ TLR9+ cells compared to CD24- CD38- B cell (p-value 0.0208), CD24- CD38int B cells (p-value 0.0447) and in CD21-/lo ABCs (p-value 0.0169) **(figure 2.12D(iii))**. These data suggests that CD24+ CD38- B cells and CD24- B cell populations shared similarities with CD21-/lo ABCs. CD11c+ T-bet+ ABCs highly expressed TLR9 across all livers.



T-bet+ TLR7+



T-bet+ TLR9+



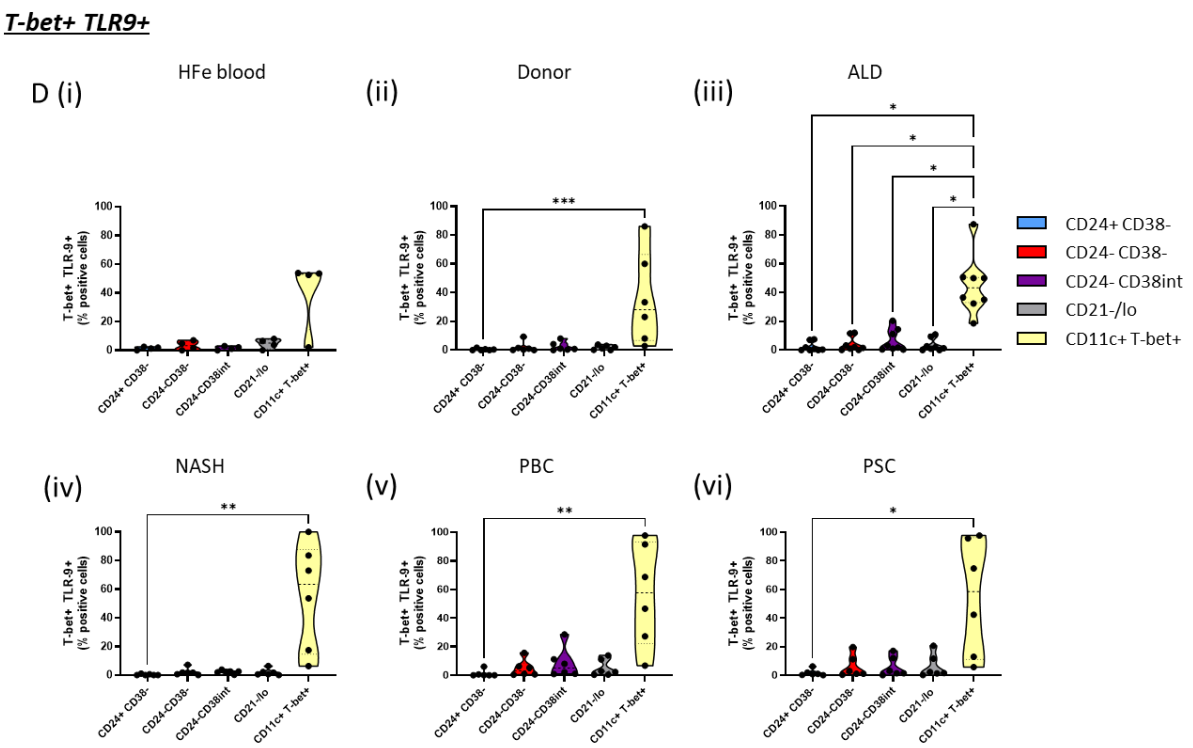


Figure 2.12 CD11c+ T-bet+ ABCs had significantly higher expression of T-bet+ TLR9+ cells across all adult livers. *Frozen thawed liver isolated mononuclear cells (LIMCs) from adult explanted livers and peripheral blood mononuclear cells (PBMCs) from HFe blood were stained and analysed using FlowJo. (A) Representative flow cytometry plots for (i) T-bet+ TLR7+ and (ii) T-bet+ TLR9+ cells. (B) The percentage of T-bet+ TLR7+ cells and (C) T-bet+ TLR9+ cells were analysed across HFe blood (n=4), donor livers (n=6) and adult chronic liver diseases; ALD (n=8), NASH (n=6), AIH (n=2), PBC (n=6), PSC (n=6) and other livers (n=3). (D) CD11c+ T-bet+ ABCs expressed high amounts of T-bet+ TLR9+ cells compared to B cell subsets in adult livers. (C(iv)) Dunnett's T3 multiple comparisons test was used. (D(iii)) Tukey's multiple comparisons test was used. (B, C(i-iii and v) and D(i, ii, iv-vi)) Dunn's multiple comparisons test was used. p-value < 0.0332 (*), p-value < 0.0021 (**), p-value < 0.0002 (***).*

2.3.5 B cell populations express low levels of class-switched immunoglobulins

ABCs are thought to be PC precursors as they were class-switched, and secreted antibodies upon stimulation (Rubtsov et al., 2011). We therefore wanted to investigate liver ABC surface Ig expression and compare it to CD24+ CD38- and CD24- B cell subsets in liver explants. Ig expression was determined across the B cell subsets using flow cytometry. All five subsets expressed moderate percentages of IgD+ IgM+ cells **(figure 11A)**. CD24+ CD38- B cells from HFe blood expressed more IgD+ IgM+ cells compared to donor (p-value 0.0154), ALD (p-value 0.0496) and PBC livers (p-value 0.0037) **(figure 2.13A(i))**. CD24- CD38int B cells from HFe blood expressed more IgD+ IgM+ cells compared to ALD livers (p-value 0.0394) **(figure 2.13A(iii))**. IgD+ IgM+ cells were similar across all livers for CD24- CD38- B cells **(figure 2.13A(ii))**, CD21-/lo ABCs **(figure 2.13A(iv))** and CD11c+ T-bet+ ABCs **(figure 2.13A(v))**. No significant differences were detected for IgD MFI between liver diseases analysed for all five subsets **(figure 2.13A(vi- x))**.

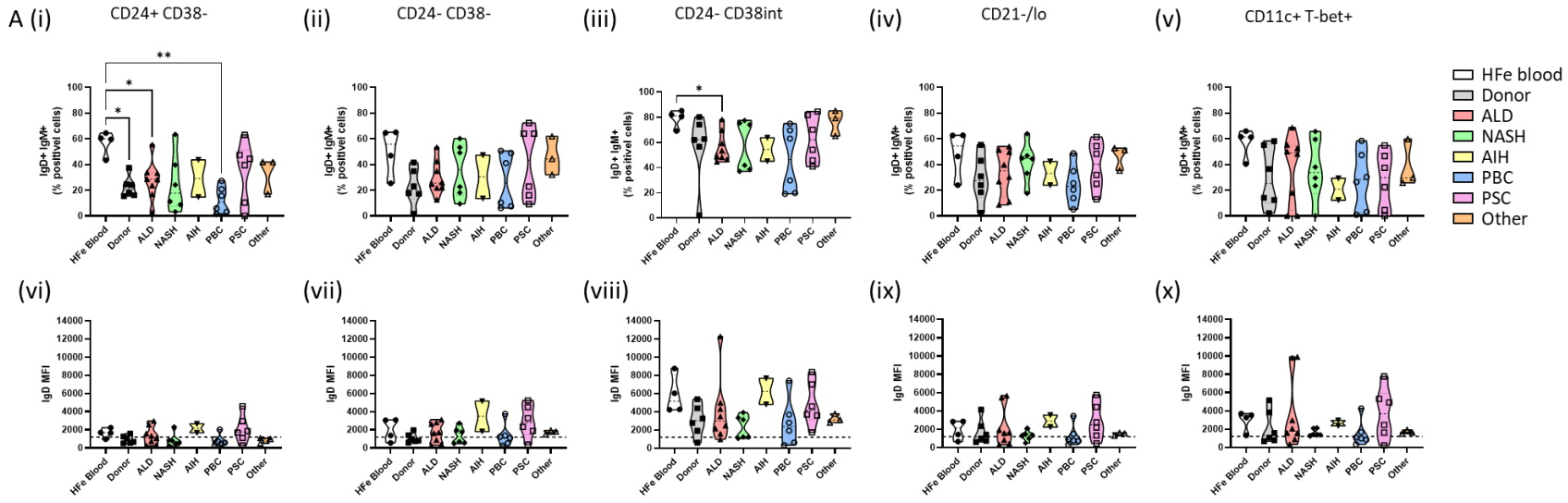
IgM+ IgD- cells were detected in low numbers across adult livers of different aetiologies for CD24+ CD38- B cells, CD24- B cells and ABCs **(figure 2.13B(i-v))**. This was mirrored for IgM MFI data with low IgM expression across the different adult livers for all five subsets **(figure 2.13B(vi-x))**.

The percentage of IgG+ B cells were low across all five subsets for both percentage positive and MFI data **(figure 2.13C(i-x))**. Whilst there were significant differences between HFe blood and adult livers, the IgG expression was still below the IMC threshold indicating that these cells were not IgG positive.

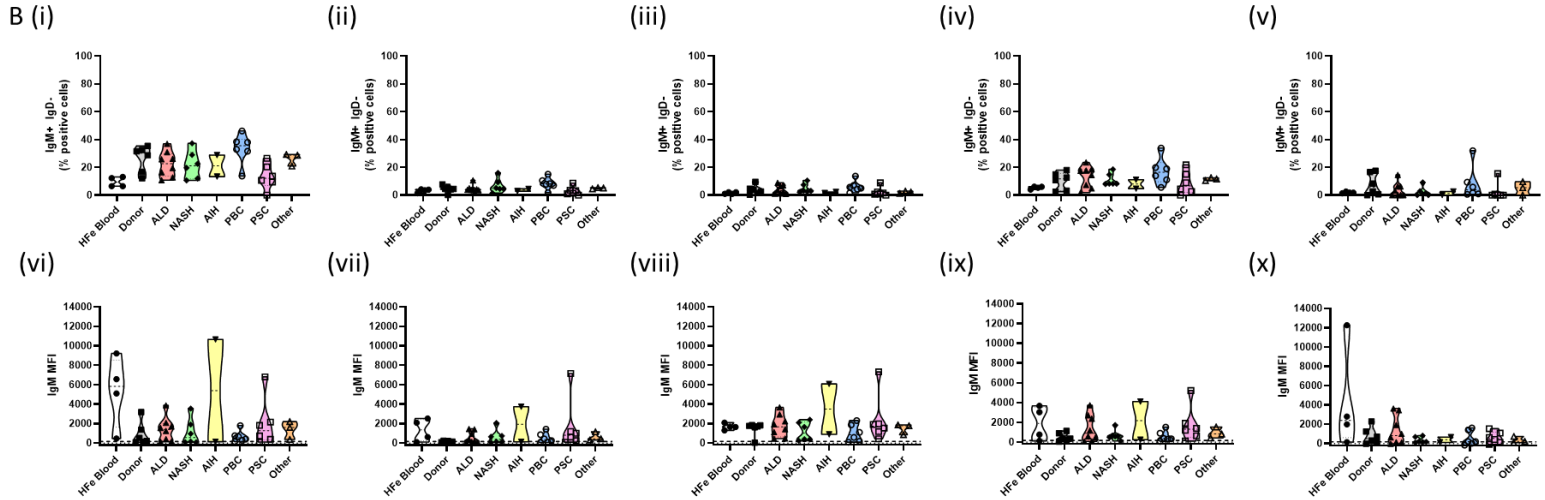
IgA percentage positive cells were comparable between different adult chronic liver diseases for all five subsets analysed **(figure 2.13D(i-v))**. IgA MFI expression was below the IMC threshold for positivity for CD24+ CD38- B cells **(figure 2.13D(vi))**, CD24- CD38- B cells **(figure 2.13D(vii))** and CD24- CD38int B cells **(figure 2.13D(viii))**. Both ABC populations **(figure 2.13D(iv-v))** contained a mixture of positive and negative IgA expressing cells across the different liver diseases analysed.

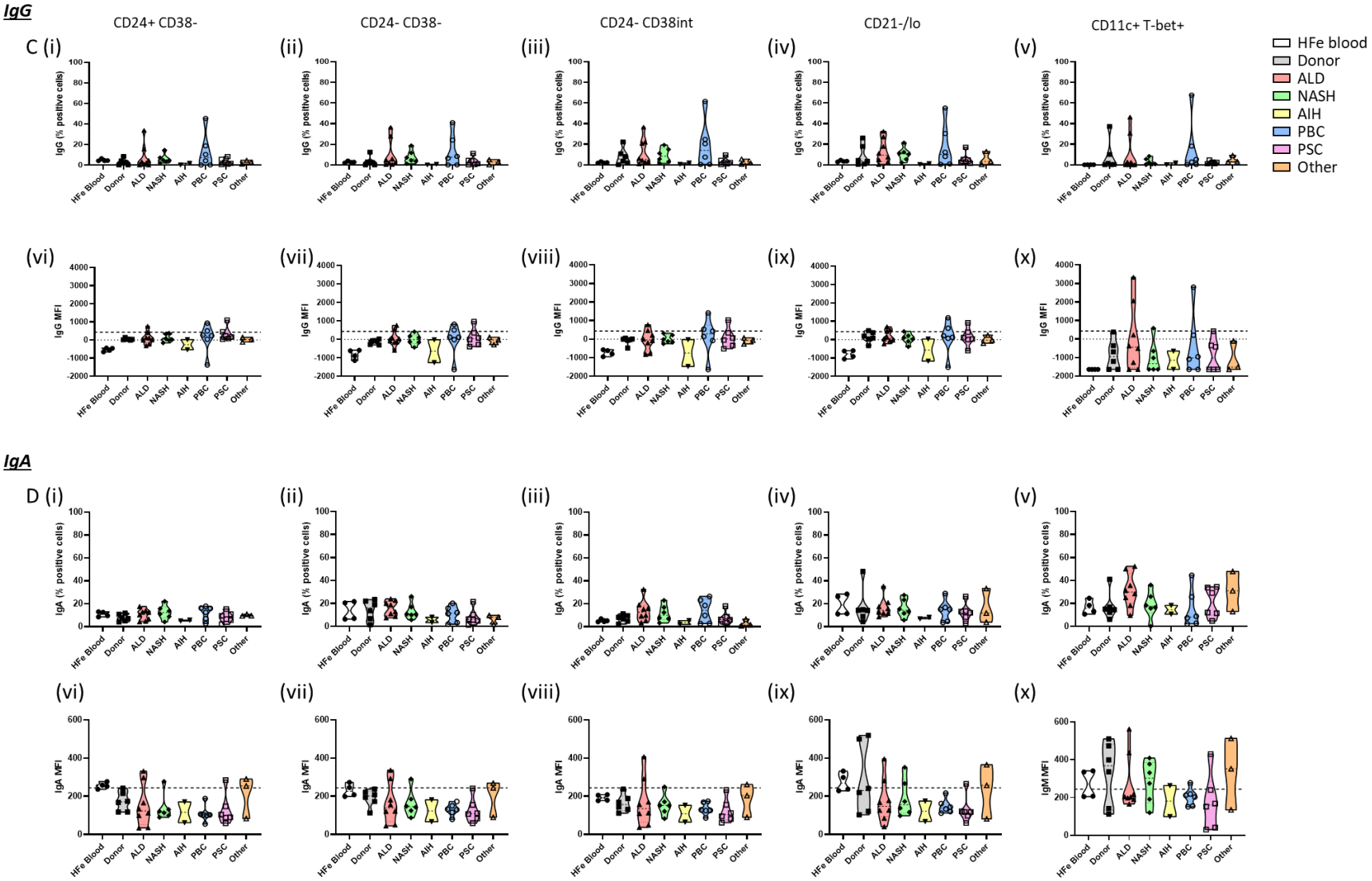
CD24+ CD38- B cells from HFe blood had higher IgE+ cells compared PSC livers (p-value 0.0223) **(figure 2.13E(i))**. No significant differences were detected in CD24- B cells and ABCs amongst HFe blood and adult livers **(figure 2.13E(ii-v))**. IgE+ cell compartment may have had some artefacts in the HFe blood group as the percentages of total Ig exceeded 100 however, this was a low error which was not detected in any of the other liver disease groups. Low IgE expression was detected for all liver samples analysed for all five subsets **(figure 2.13E(vi-x))**. CD24+ CD38- B cells isolated from HFe blood had significantly higher IgE MFI expression compared to cells isolated from donor (p-value 0.0126), ALD (p-value 0.0270), NASH (p-value 0.0058) and PSC livers (p-value 0.0177) **(figure 2.13E(vi))**. CD24- CD38- B cells isolated from HFe blood had significantly higher IgE MFI expression compared to cells isolated from NASH (p-value 0.0473) **(figure 2.13E(vii))**. CD24- CD38int B cells isolated from HFe blood had significantly higher IgE MFI expression compared to cells isolated from NASH (p-value 0.0425) **(figure 2.13E(viii))**.

IgD+ IgM+



IgM+ IgD-




IgG
CD24+ CD38-
CD24- CD38-
CD24- CD38int
CD21-/lo
CD11c+ T-bet+
C (i)
(ii)
(iii)
(iv)
(v)
(vi)
(vii)
(viii)
(ix)
(x)
IgG (% positive cells)
IgG MFI
HFe Blood
Donor
ALD
NASH
AIH
PBC
PSC
Other
HFe blood
IgA
D (i)
IgA (% positive cells)
IgA MFI
IgM MFI

IgE

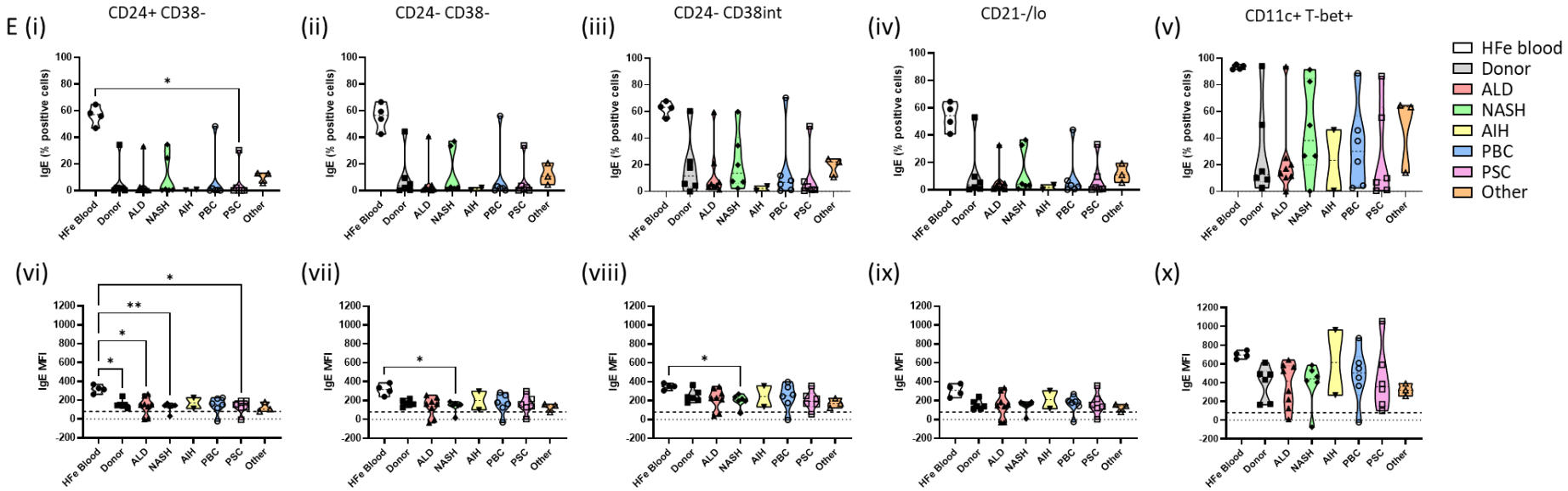


Figure 2.13 CD24- B cells and ABCs express low levels of class-switched immunoglobulins. *Frozen thawed liver isolated mononuclear cells (LIMCs) from adult explanted livers and peripheral blood mononuclear cells (PBMCs) from HFe blood were stained and analysed using FlowJo. Immunoglobulin expression was analysed amongst HFe blood (n=4), donor livers (n=6) and adult chronic liver diseases; ALD (n=8), NASH (n=6), AIH (n=2), PBC (n=6), PSC (n=6) and other livers (n=3). (A(i-v)) Co-expression of the percentage of IgD+ and IgM+ cells and (A(vi-x)) IgD MFI were analysed for each subset across different diseases. (B) IgM only B cell expression, (C) IgG expression, (D) IgA expression and (E) IgE expression were analysed across all five subsets comparing different expression in adult liver diseases. The dashed line represents the IMC, anything above this line is positive. (A(i-viii and x), B(i, iii, iv, viii and ix), C(i, iv, vi-ix), D(i, ii, iv, v, vii-x) and E(vi-x)) Dunnett's T3 multiple comparisons test was used. (A(ix), B(ii, v-vii and x), C(ii, iii, v and x), D(iii and vi) and E(i-v)) Dunn's multiple comparisons test was used. p-value < 0.0332 (*), p-value < 0.0021 (**).*

Comparing expression of class-switched Igs across different B cells was carried out in total CD19+ B cells **(figure 2.14A)**. HFe blood had significantly higher IgE+ cells compared to PSC livers (p-value 0.0235) in total CD19+ cells **(figure 2.14A(iii))**. HFe blood had significantly higher IgE expressing cells in CD24- CD38int B cells (p-value 0.0213) and CD11c+ T-bet+ ABC compartment (p-value 0.0010) compared to IgG **(figure 2.14B)**. Class-switched Ig expression was similar between adult livers in total CD19+ B cells **(figure 2.14A)**. Comparable expression of class-switched Igs was observed across all five subsets in donor livers **(figure 2.14C)**, ALD livers **(figure 2.14D)**, NASH livers **(figure 2.14E)**, PBC livers **(figure 2.14F)** and PSC livers **(figure 2.14G)**. CD11c+ T-bet+ ABCs isolated from ALD livers showed significant differences in IgA expression compared to IgG (p-value 0.0135) **(figure 2.14D)**. Taken together, these data showed that all five subsets co-expressed high amounts of IgD and IgM and had low expression of class-switched Igs in adult livers. HFe blood B cells had high expression of IgE compared to adult livers, which is worth further investigation. Furthermore, similar expression of Igs was observed between CD24+ CD38- B cells, CD24- B cells and ABCs.

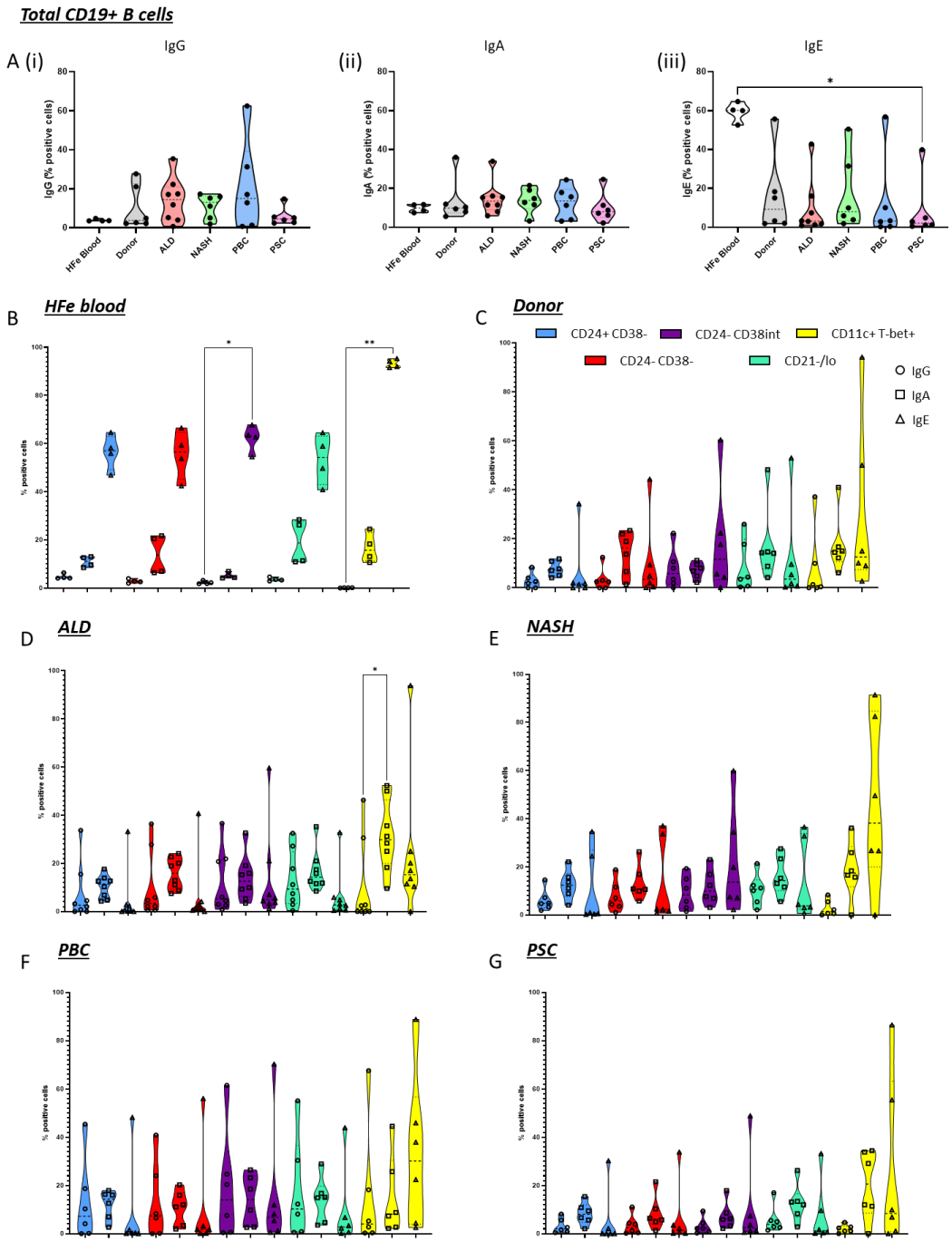


Figure 2.14 Class-switched immunoglobulins were present in all livers and amongst CD24- B cell populations and ABC subsets. *Frozen thawed liver isolated mononuclear cells (LIMCs) from adult explanted livers and peripheral blood mononuclear cells (PBMCs) from HFe blood were stained and analysed using FlowJo. (A) Total CD19 B cells were analysed for (A(i)) IgG, (A(ii)) IgA and (A(iii)) IgE across the different livers. Subset analysis of IgG, IgA and IgE were analysed in each disease; (B) HFe blood (n-4), (C) Donor (n=6), (D) ALD (n=8), (E) NASH (n=6), (F) PBC (n=6) and (G) PSC (n=6). (A(i and ii) and E) Dunnett's T3 multiple comparisons test*

was used. (A(iii), B-D, F and G) Dunn's multiple comparisons test was used. p-value < 0.0332 (*), p-value < 0.0021 (**).

2.3.6 CD138 expression in liver B cell subsets in different end-stage liver diseases

Studies have suggested that ABCs may be precursors to PCs. Expression of PC marker CD138 (syndecan-1) was analysed on CD19+ B cells across five subsets. No significant differences were detected amongst chronic liver diseases for CD138+ cells **(figure 2.15A(i-v))**. CD24- CD38- B cells isolated from HFe blood had significantly higher CD138 MFI expression compared to NASH (p-value 0.0317), PSC (p-value 0.0092) and other livers (p-value 0.0143) **(figure 2.15A(vii))**. CD24- CD38int B cells isolated from HFe blood had significantly higher CD138 MFI expression compared to NASH (p-value 0.0257), PSC (p-value 0.0022) and other livers (p-value 0.0206) **(figure 2.15A(viii))**. CD21-/lo ABCs isolated from HFe blood had significantly higher CD138 MFI expression compared to PSC (p-value 0.0162) **(figure 2.15A(ix))**. CD11c+ T-bet+ ABCs isolated from HFe blood had significantly higher CD138 MFI expression compared to PSC (p-value 0.0479) **(figure 2.15A(x))**. In HFe blood, CD21-/lo ABCs had significantly higher CD138 percentage positive cells compared to CD24+ CD38- B cells (p-value 0.0006) and CD24- CD38int B cells (p-value 0.0188) **(figure 2.15B(i))**. HFe blood also showed significant differences for CD138 percentage positive cells in CD11c+ T-bet+ ABCs compared to CD24+ CD38- B cells (p-value 0.0098), CD24- CD38- B cells (p-value 0.0278), CD24- CD38int B cells (p-value 0.0176) and CD21-/lo ABCs (p-value 0.0175) **(figure 2.15B(i))**. CD11c+ T-bet+ ABCs had significantly higher CD138+ cells compared to CD24+ CD38- B cells (p-value 0.0102) in NASH livers **(figure 2.15B(iv))**. These data suggests that a small portion of B cells in CD21-/lo B cells, possess the ability to produce surface Igs. Furthermore, CD11c+ T-bet+ B cells expressed high levels of CD138 suggesting that they could have differentiated

into ASCs. CD138 positive cells mainly reside in CD11c+ T-bet+ ABC populations which may consist of effector ABCs.

CD138

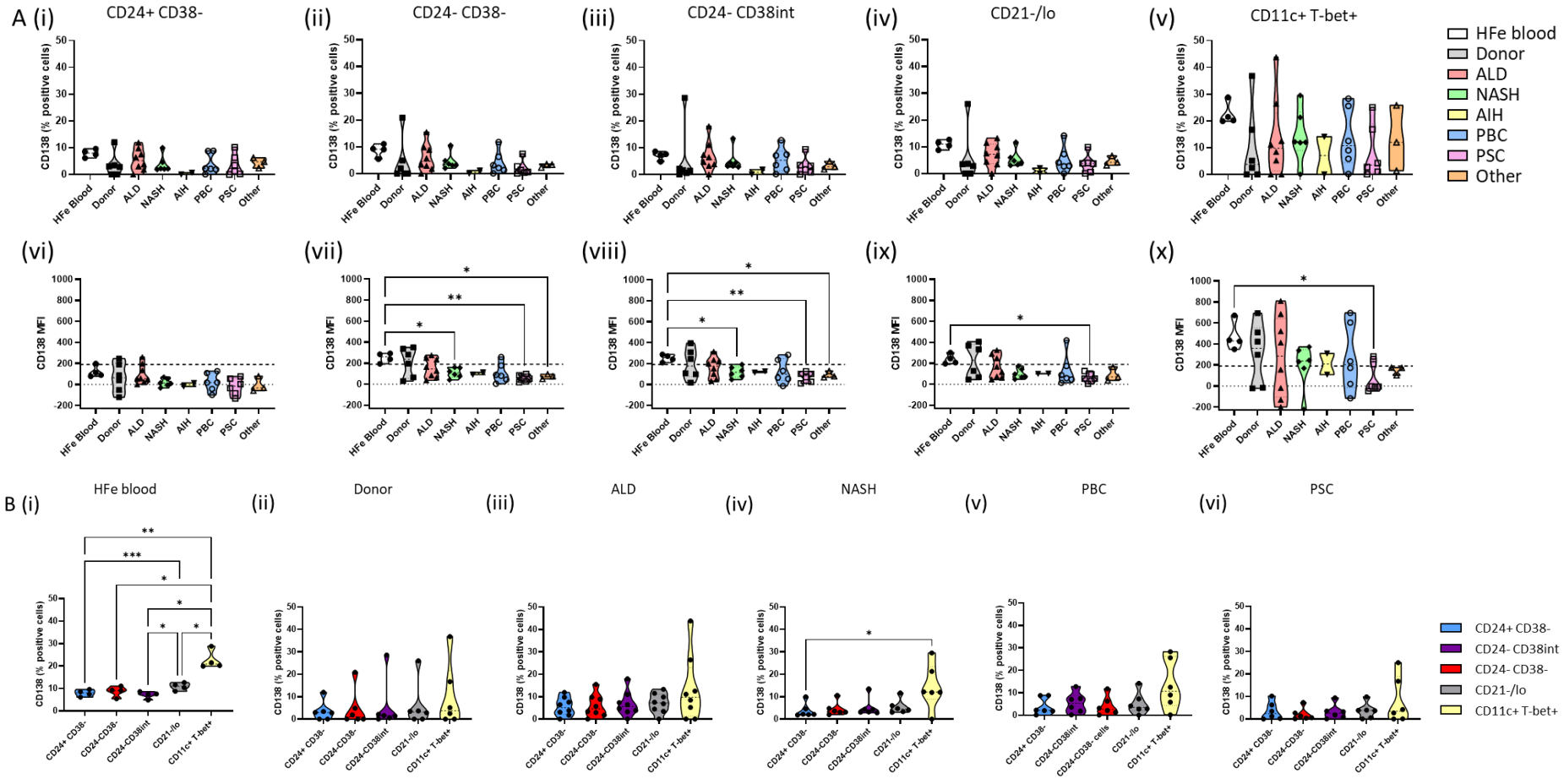


Figure 2.15 CD11c+ T-bet+ ABCs have high CD138 expression compared to CD24+ CD38-, CD24- B cells and CD21-/lo ABCs. *Frozen thawed liver isolated mononuclear cells (LIMCs) from adult explanted livers and peripheral blood mononuclear cells (PBMCs) from HFe blood were stained*

and analysed using FlowJo. (A) CD138 positive cells were analysed for each subset amongst HFe blood and adult livers. (B) The five different subsets analysed were compared in each disease to identify any differences in CD138 expression. The dashed line represents the IMC MFI line, anything above this line is positive. HFe blood (n=4), donor livers (n=6) and adult chronic liver diseases; ALD (n=8), NASH (n=6), AIH (n=2), PBC (n=6), PSC (n=6) and other livers (n=3). (A(i, iv, vi-x)) Dunnett's T3 multiple comparisons test was used. (B(i, iii, v and vi)) Tukey's multiple comparisons test was used. (A(ii, iii and v) and B(ii and iv)) Dunn's multiple comparisons test was used. p-value < 0.0332 (*), p-value < 0.0021 (**), p-value < 0.0002 (***).

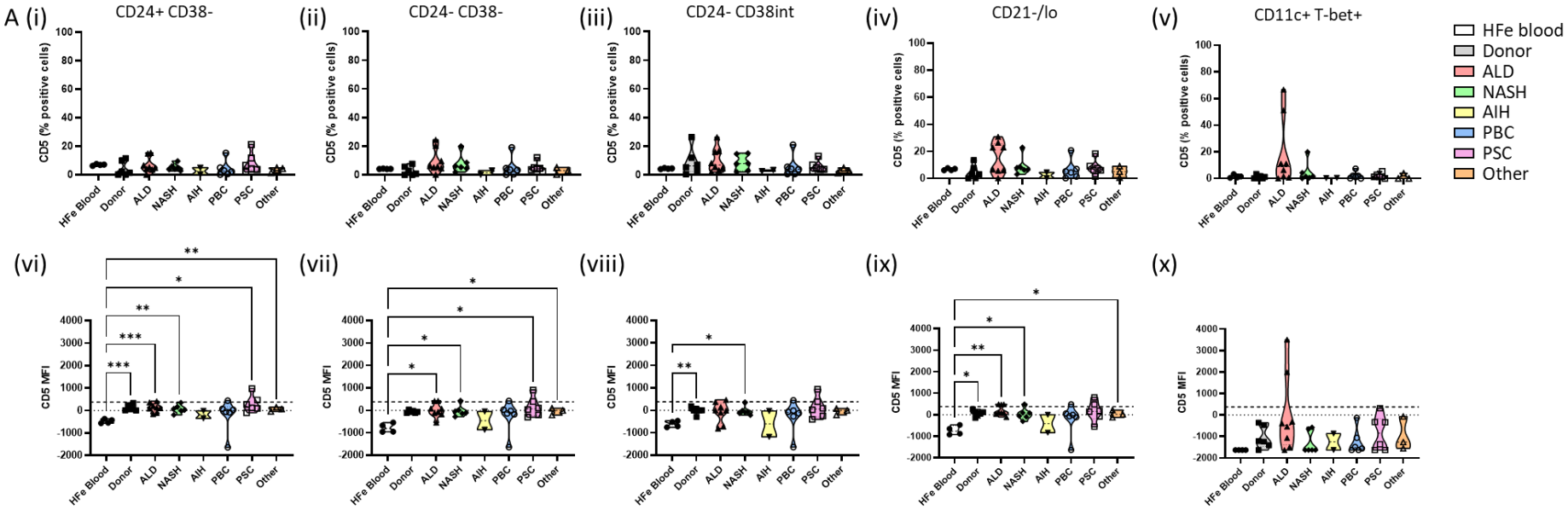
2.3.7 CD5 and FcRL5 expression in liver B cell subsets

ABCs from autoimmune patients express CD5 (Sachinidis et al., 2020). We therefore analysed CD5 expression in adult chronic liver diseases of various aetiologies across five B cell subsets. All five subsets analysed showed low expression of CD5+ cells **(figure 2.16A(i-v))**. Whilst majority of the cells analysed remained below the IMC threshold of positivity, there were significant differences in CD5 expression between HFe blood and donor (p-value 0.0008), ALD (p-value 0.0007), NASH (p-value 0.0054), PSC (p-value 0.0441) and other livers (p-value 0.0094) in CD24+ CD38- B cells **(figure 2.16A(i))**. CD24- CD38- B cells isolated from HFe blood also showed significant differences in CD5 MFI expression between HFe blood and ALD (p-value 0.0117), NASH (p-value 0.0198), PSC (p-value 0.0466) and other livers (p-value 0.0376) **(figure 2.16A(vii))**. CD5 expression was significantly different in CD24- CD38int B cells between HFe blood and donor (p-value 0.0070) and NASH livers (p-value 0.0120) **(figure 2.16A(viii))**. There were significant differences in CD5 expression between HFe blood and donor (p-value 0.0142), ALD (p-value 0.0039), NASH (p-value 0.0190), and other livers (p-value 0.0413) in CD21-/lo ABCs **(figure 2.16A(ix))**. No significant difference was observed between adult liver diseases in CD11c+ T-bet+ ABC subset **(figure 2.16A(x))**.

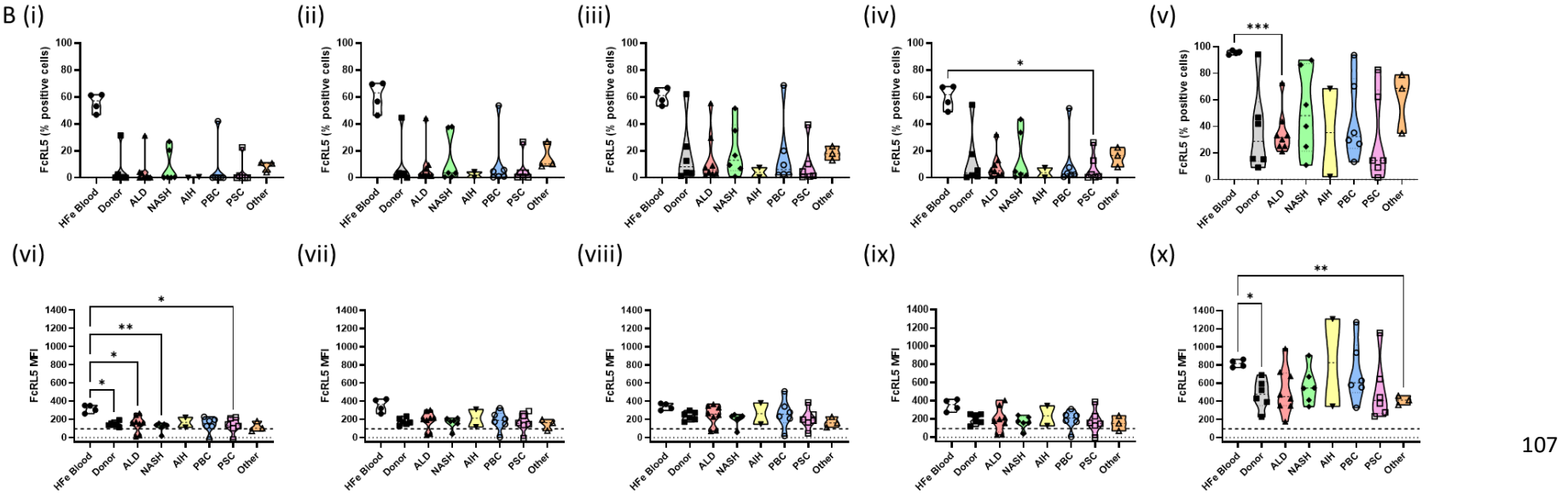
ABCs also express FcRL5 (Gao and Cockburn, 2022) therefore we analysed FcRL5 expression in all five B cell subsets. HFe blood had significantly higher percentage of FcRL5 positive cells compared to PSC livers in CD24+ CD38- B cells (p-value 0.0120) **(figure 2.16B(i))**, compared to PSC in CD21-/lo ABCs (p-value 0.0429) **(figure 2.16B(iv))**, and compared to ALD livers (p-value 0.0004) in CD11c+ T-bet+ ABCs **(figure 2.16B(v))**. CD24+ CD38- B cells had significantly higher FcRL5 expression in HFe blood compared to donor (p-value 0.0120), ALD (p-value 0.0321), NASH (p-value 0.0054) and PSC livers (p-value 0.0397) **(figure 2.16B(vi))**. No

significant differences were found between liver samples in CD24- B cell subsets and CD21-/lo ABCs **(figure 2.16B(vii-ix))**. CD11c+ T-bet+ ABCs isolated from HFe blood had significantly higher expression of FcRL5 compared to donor (p-value 0.0408) and other livers (p-value 0.0040) **(figure 2.16B(x))**. CD24- CD38int B cells had significantly higher FcRL5 expression compared to CD24+ CD38- B cells in HFe blood (p-value 0.0277) **(figure 2.16C(i))**, ALD (p-value 0.0050) **(figure 2.16C(iii))**, NASH (p-value 0.0349) **(figure 2.16C(iv))**, PBC (p-value 0.0191) **(figure 2.16C(v))** and PSC livers (p-value 0.0140) **(figure 2.16C(vi))**. CD11c+ T-bet+ ABCs had significantly elevated FcRL5 expression compared to CD24+ CD38- B cells observed in HFe blood (p-value 0.0041) **(figure 2.16C(i))**, donor (p-value 0.0013) **(figure 2.16C(ii))**, ALD (p-value <0.0001) **(figure 2.16C(iii))**, NASH (p-value 0.0001) **(figure 2.16C(iv))**, PBC (p-value 0.0001) **(figure 2.16C(v))** and PSC livers (p-value 0.0026) **(figure 2.16C(vi))**. CD11c+ T-bet+ ABCs also showed a significant difference in FcLR5 expression compared to CD24- CD38- B cells in donor (p-value 0.0349) **(figure 2.16C(ii))** and ALD (p-value 0.0090) **(figure 2.16C(iii))**. Furthermore, in HFe blood, CD11c+ T-bet+ ABCs had significantly higher FcRL5 expression compared to CD24- CD38- B cells (p-value 0.0263), CD24- CD38int B cells (p-value 0.0042) and CD21-/lo ABCs (p-value 0.0127) **(figure 2.16C(i))**. Taken together, these data showed that CD11c+ T-bet+ ABCs had phenotypically higher FcRL5 expression in HFe blood and across all adult liver diseases analysed.

CD5


A (i)
CD24+ CD38-
(ii)
CD24- CD38-
(iii)
CD24- CD38int
(iv)
CD21-/lo
(v)
CD11c+ T-bet+
CD5 (% positive cells)
(vi)
(vii)
(viii)
(ix)
(x)
CD5 MFI
HFe Blood
Donor
ALD
NASH
AIH
PBC
PSC
Other
HFe blood
Donor
ALD
NASH
AIH
PBC
PSC
Other

FcRL5


B (i)
(ii)
(iii)
(iv)
(v)
FcRL5 (% positive cells)
(vi)
(vii)
(viii)
(ix)
(x)
FcRL5 MFI
HFe Blood
Donor
ALD
NASH
AIH
PBC
PSC
Other

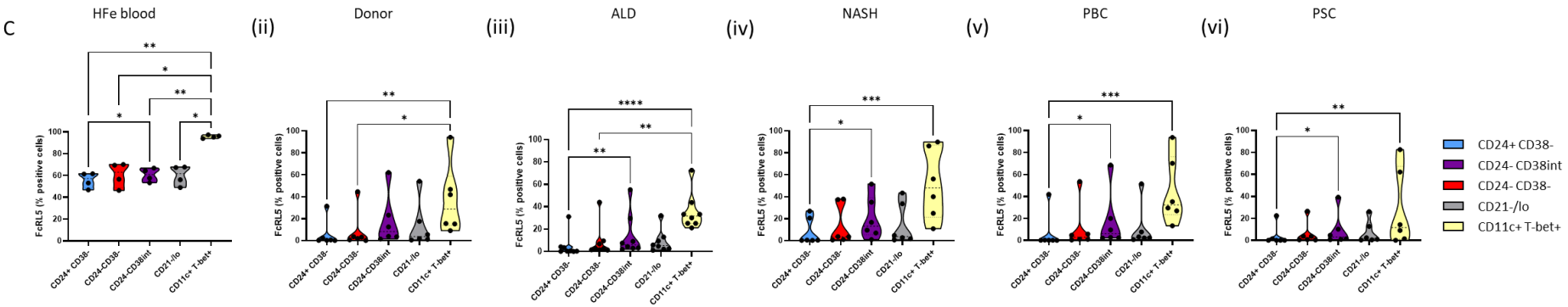
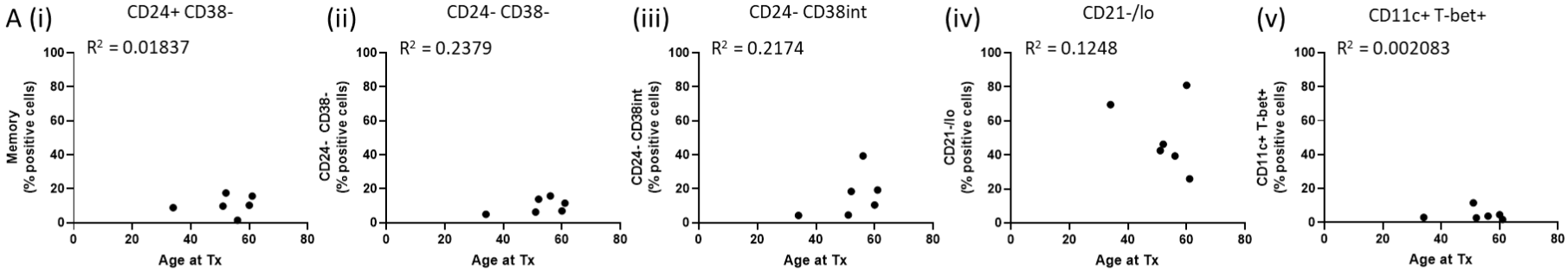


Figure 2.16 Inhibitory molecules expression is low in both CD24- B cell populations and CD21-/lo ABCs. *CD11c+ T-bet+ ABCs expressed high amounts of FcRL5. Frozen thawed liver isolated mononuclear cells (LIMCs) from adult explanted livers and peripheral blood mononuclear cells (PBMCs) from HFe blood were stained and analysed using FlowJo. (A) CD5 and (B) FcRL5 expression was analysed across the five different subsets. (C) Subsets were compared in each adult disease. The dashed line represents the IMC MFI line, anything above this line is positive. HFe blood (n=4), donor livers (n=6) and adult chronic liver diseases; ALD (n=8), NASH (n=6), AIH (n=2), PBC (n=6), PSC (n=6) and other livers (n=3). (A(i, iv, vi-ix) and B(v-x)) Dunnett's T3 multiple comparisons test was used. (C(i)) Tukey's multiple comparisons test was used. (A(ii, iii, v and x), B(i-iv) and C(ii-vi)) Dunn's multiple comparisons test was used. p-value < 0.0332 (*), p-value < 0.0021 (**), p-value < 0.0002 (***), p-value < 0.0001 (****).*

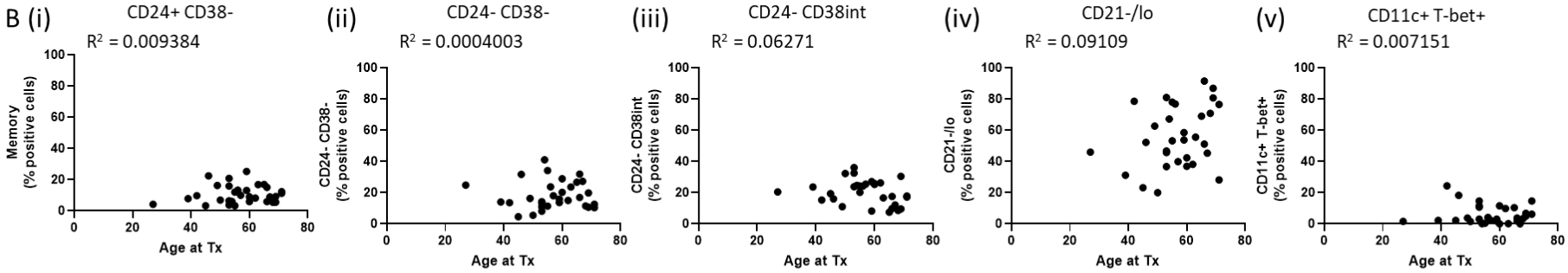
2.3.8 Comparison of ABC subsets in liver diseases

Pearson's correlation analysis was carried out to determine if the percentages of B cell subsets correlated with the age of the livers at transplant in each subset **(figure 2.17)**. No correlation was detected between B cell subsets and age at liver transplant in donor livers **(figure 2.17A(i-v))** and adult chronic liver diseases **(figure 2.17B(i-v))**. No difference was observed between non-cirrhotic livers **(figure 2.17A(i-v))** and cirrhotic livers **(figure 2.17B(i-v))**. No correlation was detected between males, females and both ABC subsets **(figure 2.17C)**.

Donor



All livers



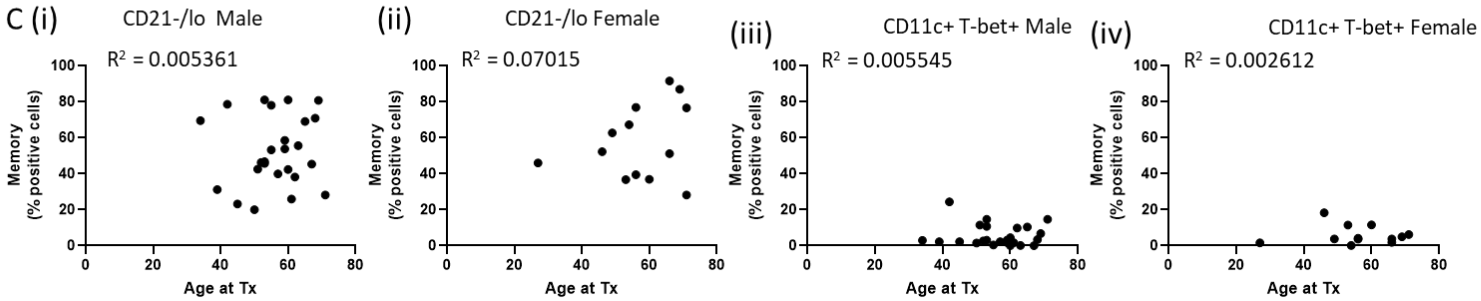


Figure 2.17 CD21-/lo ABCs positively correlated with the age of the livers. *Pearson's correlation analysis was conducted on adult explanted livers. (A) Donor livers (n=6) and (B) all adult livers (n=31) were analysed for correlation between (i) CD24+ CD38- B cells, (ii) CD24- CD38- B cells, (iii) CD24- CD38int B cells, (iv) CD21-/lo B cells and (v) CD11c+ T-bet+ B cells. (C) Pearson's correlation was carried out between CD21-/lo (C(i)) males and (C(ii)) females and CD11c+ T-bet+ (C(iii)) males and (C(iv)) females.*

T-bet+ TLR9+ cells were increased in CD11c+ T-bet+ ABCs and not in CD21-/lo ABCs. We wanted to investigate the correlation between TLR9 percentage positive cells and age, PC marker CD138, IgD, activation marker CD69 and co-stimulatory marker CD86. No correlation was observed between TLR9 and age in either ABC populations **(figure 2.18A(i))**. Moderate degree of correlation was observed between TLR9 and CD138 (r^2 0.3431) in CD21-/lo ABCs whereas low degree of correlation (r^2 0.1716) was observed in CD11c+ T-bet+ ABCs **(figure 2.18A(ii))**. No correlation was detected between TLR9 and IgD **(figure 2.18A(iii))** and low degree of correlation was observed between TLR9 and CD69 for CD21-/lo ABCs (r^2 0.1073)

(figure 2.18A(iv)). A moderate degree of correlation between TLR9 and CD86 was observed in CD11c+ T-bet+ ABCS (r^2 0.3808) compared to CD21-/lo ABCs (r^2 0.1499) **(figure 2.18A(v))**.

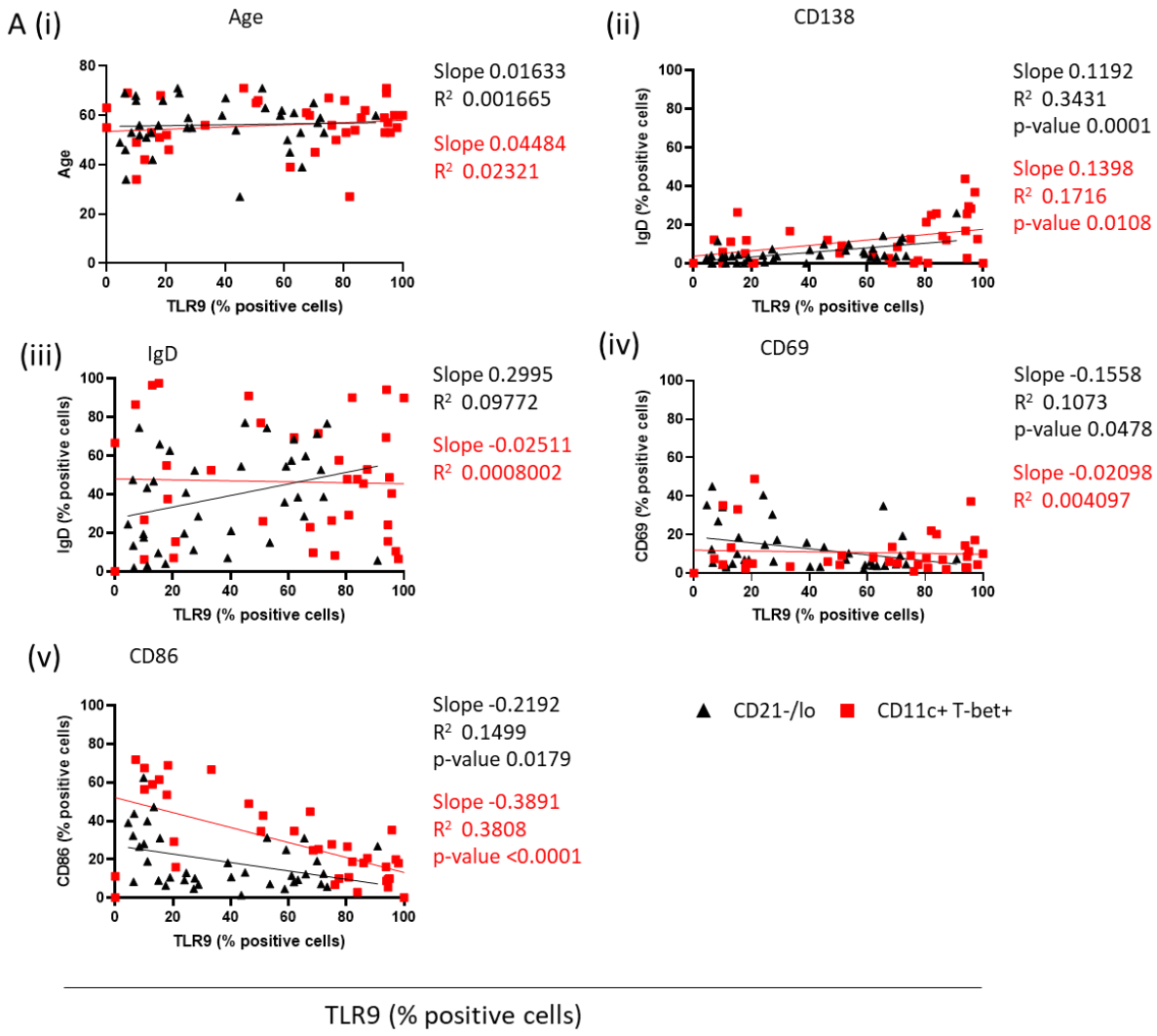


Figure 2.18 TLR9 correlation analyses comparing CD21-/lo ABCs and CD11c+ T-bet+ ABCs. *Pearson's correlation analysis and simple linear regression analysis was conducted to compare TLR9 percentage positive cells with (A(i)) age, (A(ii)) CD138 (A(iii)) IgD, (A(iv)) CD69 and (A(v)) CD86 percentage positive cells between CD21-/lo ABCs (black triangles) and CD11c+ T-bet+ ABCs (red squares) across all adult livers (n=37); donor (n=6), ALD (n=8), NASH (n=6), AIH (n=2), PBC (n=6), PSC (n=6) and other livers (n=3).*

2.4 Discussion

Initially this spectral flow cytometry-based investigation was going to be carried out using the Aurora spectral flow cytometer in collaboration with Oxford University. The Aurora enables the detection of 24 markers (Cytek_Biosciences). This cytometer was originally going to be used as it did not require the sample to be distributed in many tubes as precious biliary atresia explant tissue availability was limited. However, due to the COVID-19 pandemic, using the Aurora was not possible and new flow cytometry panels were created to analyse the B cell compartment using the Fortessa spectral flow cytometer, which was available, in house. Access to fresh paediatric liver explants was delayed due to the pandemic. Unfortunately, by the time the protocol to collect paediatric liver explants was in place, the ethical approvals had expired. The ethical approvals were not renewed due to the retirement of senior staff members at the Birmingham Women and Childrens hospital. The phenotyping of the B cell compartment was carried out in adult chronic liver disease explants instead.

B cells play a crucial role in the adaptive immune response to pathogens. B cells present antigens to T cells resulting in T cell activation. B cells secrete pro-inflammatory mediators and produce antibodies targeting pathogens for clearance by antibody-dependent cellular cytotoxicity (ADCC) (Temming et al., 2019). Liver diseases were analysed separately instead of grouping them into autoimmune and metabolic diseases to identify any discrepancies in B cells phenotype amongst individual liver diseases. CD19+ B cells were present across all end-stage livers analysed **(figure 2.5B)**.

2.4.1 B cell composition from infancy to adulthood

Age influences B cell composition and differences in the B cell compartment can be observed between infancy and adulthood. Morbach et al., used flow cytometry to analyse peripheral blood samples from infants through to adulthood to determine the changes in the frequencies of B cell populations with age (Morbach et al., 2010). Total CD19+ B cells were reduced in frequency with increasing age and the B cell compartment underwent age-related changes (Morbach et al., 2010). Infants had increased frequencies of transitional and naïve B cells (Morbach et al., 2010) which represent their inexperienced immune system. As the infant is exposed to infections and appropriate stimuli, antigen-specific memory B cells will increase in numbers in peripheral blood. The memory B cell pool contained several memory B cell populations with increasing age (Morbach et al., 2010). PBs/PCs were rarely detected in peripheral blood (Morbach et al., 2010) as they were found more commonly in secondary lymphoid organs or in the BM. Determining age related changes regarding PBs/PCs is difficult using peripheral blood samples for this reason. Morbach et al., found that CD21lo CD38lo B cells were present in infancy and the population slightly increased with age (Morbach et al., 2010). This population may be ABCs which accumulate with age.

Total B cells contained a mixture of naïve and memory B cells **(figure 2.6A)** which was also observed in CD24- CD38- B cells **(figure 2.7C)** and CD24- CD38int B cells **(figure 2.7D)**. Both CD24- B cell populations were detected in adult livers and in HFe blood **(figure 2.7C and 2.7D)** suggesting that these populations were not disease specific. ABCs were originally thought to accumulate with age in mice (Rubtsov et al., 2011), however many studies identified high frequencies of ABCs in disease (Mouat et al., 2022) and infection (Mouat and Horwitz, 2022) suggesting that ABCs may have a role in immunity. ABCs were present in

higher frequencies in disease, and we speculated that CD24- B cells may share characteristics with ABCs as all subsets contained a heterogenous population of naïve and memory B cells **(figure 2.9)**. Naïve B cells made up majority of the cells in CD24+ CD38- B cells, CD24- B cells and the ABC compartments analysed **(figure 2.9B)**. These populations also contained low numbers of switched memory B cells **(figure 2.9D)** and unswitched memory B cells (**figure 2.9C)** suggesting that these B cells had been exposed to cognate antigens. Exposures to appropriate stimuli have a role in determining the rate of ABC accumulation in individuals (Naradikian et al., 2016a). Furthermore, these data corroborated findings by Sanz et al., who used flow cytometry to gate B cell subsets using CD24 and CD38 and suggested that CD24- CD38- B cell populations consisted of naïve and activated memory B cells (Sanz et al., 2019) which was also the case for ABCs B cells (Swain et al., 2017).

2.4.2 ABCs as antigen presenters

A subset of activated ABCs can contribute to the humoral response by acting as APCs. These cells express MHC-II and co-stimulatory markers CD80 and CD86 (Rubtsov et al., 2011, Rubtsova et al., 2015, Swain et al., 2017). Expression of CD80, CD86 and HLA-DR showed no difference between liver diseases **(figure 2.10)** however a difference in CD86 expression was observed between CD21-/lo ABCs and CD11c+ T-bet+ ABCs **(figure 2.11)**. CD11c+ T-bet+ ABCs had higher CD80 expression compared to CD24+ CD38- B cells in ALD livers **(figure 2.11A(iii))**. CD11c+ T-bet+ ABCs had significantly higher CD86 expression compared to the other B cell subsets **(figure 2.11B)**. This suggests that within the ABC population there are two phenotypes; CD11c+ T-bet+ ABCs may form an effector arm of the ABC population and contribute to antigen presentation. High percentages of HLA-DR+ cells were observed across all livers for all subsets analysed **(figure 2.10D)**. HLA-DR expression was detected on ABCs by

the Marrack group (Rubtsov et al., 2011, Rubtsova et al., 2015, Swain et al., 2017). Majority of CD21-/lo ABCs did not express co-stimulatory molecule CD80, similar to CD24- B cells **(figure 2.11A)**. CD24- B cells expressed HLA-DR across adult chronic liver diseases **(figure 2.10D)** suggesting that there may be a role for them in antigen presentation. CD11c+ T-bet+ green fluorescent protein (GFP)-labelled ABCs were isolated from old mice and injected into naïve mice to determine the localisation of ABCs. ABCs were found in the T cell zone in the spleen (Rubtsova et al., 2015, Naradikian et al., 2016a) suggesting that ABCs present antigens to T cells here. Rubtsov et al., also showed that CD11c+ T-bet+ B cells from aged or autoimmune female mice were better at presenting antigens than FO B cells (Rubtsova et al., 2015).

CD69 was used to investigate activation or tissue residence status of ABCs as it has been used to delineate tissue-resident T cells. Wiggins et al., used flow cytometry and co-culture assays on human liver tissues to characterise the hepatic CD4 T cell compartment. They found that hepatic CD4+ T cells that expressed high levels of CD69 were tissue-resident T cells that were excluded from circulation (Wiggins et al., 2021). We saw that CD69 expression was low amongst CD24- B cells in all adult livers analysed **(figure 2.11C)** suggesting that these populations were not tissue-resident memory cells as they were also found in HFe blood. Furthermore, many studies investigating ABCs were conducted on peripheral blood (Rubtsov et al., 2011, Buffa et al., 2013, Thorarinsdottir et al., 2016) and not on liver samples.

PBC livers had significantly higher CD69 expression compared to HFe blood and other adult liver diseases **(figure 2.10C)**. PBC livers also had lower HLA-DR+ cells compared to HFe blood **(figure 2.10D)**. Low amounts of CD5+ cells were detected across all samples analysed **(figure**

2.16A). CD5 is a negative regulator of BCR signalling and CD5 expression was upregulated following BCR stimulation (Gary-Gouy et al., 2002). Furthermore, CD5 expression activates downstream signalling pathways that result in IL-10 production (Garaud et al., 2018) suggesting that CD5 may have a role in B cell tolerance. Low expression of CD5 suggested that B cells were not activated and combined with low HLA-DR expression, it could be speculated that PBC livers may contain tissue-resident CD69+ cells. Whilst CD5 expression was high in ABCs, our data showed that ABCs had low expression of CD5. CD5 B cells contribute to the modulation of the inflammatory response by producing IL-10 which is an anti-inflammatory cytokine that aids in the resolution of inflammation (Gary-Gouy et al., 2002). Chronic inflammation may impair IL-10 production from CD5-expressing B cells reducing the anti-inflammatory effects of IL-10 in liver diseases. Chronic inflammation may be the cause of low CD5 expressing B cells observed in our cohort.

2.4.3 Activation of ABCs

ABCs require three signals for their activation and development; the first signal is provided by cross-linking of the BCR, the second signal is provided upon PAMP/DAMP ligation to TLR7 or TLR9 and the third signal is provided by IFN-γ which is secreted by TFH cells (Rubtsova et al., 2015, Naradikian et al., 2016a). ABCs rapidly proliferate in response to TLR7 and TLR9 stimulation (Naradikian et al., 2016a) and Rubtsov et al., found that culturing splenic murine B cells with TLR7 agonist induced T-bet expression which was elevated upon combining BCR cross-linking with TLR7 stimulation (Rubtsov et al., 2013). Stimulation of mouse splenocytes with CpG, a TLR9 agonist, rapidly upregulated T-bet transcription which was diminished in TLR9 deficient mice (Liu et al., 2003). No TLR7+ cells or T-bet+ TLR7+ were detected in any of the subsets analysed across all samples **(figure 2.12B and appendix 4A and 4B)** suggesting

that these ABCs do not rely on TLR7 for activation. TLR9 was highly expressed amongst all subsets however only CD11c+ T-bet+ ABCs co-expressed T-bet and TLR9 compared to the other B cell subsets across all livers and HFe blood **(figure 2.12D and appendix 4C and 4D)**. This suggests that ABCs may have different TLR activation requirement and hepatic ABCs may respond poorly to TLR7. TLR9 activated ABCs may downregulate CD86 expression and therefore reduce their antigen presenting abilities as there was a negative correlation between TLR9 and CD86 in both ABC subsets analysed (**figure 2.18(v)**). ABCs may be PC precursors and produce Ig upon stimulation (Sathe and Cusick, 2023) and therefore they may reduce CD86 expression to allow them to carry out their effector functions.

2.4.4 ABCs in healthy and disease

ABCs contribute to protection against pathogens by producing antibodies. Upon TLR stimulation, mice produced IgM and IgG antibodies (Rubtsov et al., 2011). ABCs can also produce antigen-specific antibodies as mice re-stimulated with viral infections produced viral-specific antibodies (Rubtsova et al., 2015). CD24+ CD38- B cells, CD24- B cells and ABCs expressed Igs across all adult chronic liver diseases (**figure 2.13)** suggesting that these populations were not disease specific. Majority of the cells in each subset consisted of naïve IgD+ IgM+ B cells **(figure 2.13A)**. Swain et al., showed that majority of ABCs in mice were naïve (Swain et al., 2017) which fits nicely with our data. IgM and IgD are expressed on naive B cells and upon antigenic stimulation, IgD expression is downregulated (Chen and Cerutti, 2011). Low IgM+ IgD- B cells were observed amongst analysed B cell subsets **(figure 2.13B)** suggesting that only a small proportion of cells are IgM-only memory B cells that protect against broad spectrum pathogens (Weill and Reynaud, 2020). Low IgM expression was detected amongst the different B cell subsets across all livers analysed **(figure 2.13B(vi-x))**.

IgM expression may be related to antigenic stimulation and subsequent exposure to the stimuli results in class-switching to IgG, IgA or IgE (Sathe and Cusick, 2023). ABCs produced IgG1 in humans (IgG2a/c in mice) in response to viral infections (Mouat and Horwitz, 2022). Low expression class-switched Igs, IgG **(figure 2.13C)**, IgA **(figure 2.13D)** and moderate IgE expression **(figure 2.13E)** was detected amongst B cells suggesting that antigenic exposure in the form of viral antigens or self-ligands may have occurred in small numbers in these subsets. Ehrhardt et al., stimulated cells with different agonists and collected the supernatant to put through ELISA assays. This study showed that a proportion of FcRL4 atypical memory B cells expressed IgG and to a lesser extent IgA (Ehrhardt et al., 2005). In chronic adult liver diseases, it could be possible that chronic inflammation sensitises the body to allergens generating IgE-expressing ABCs. Cardoso et al., showed that mice sensitised to peanuts had a sensitive gut that responded to food antigens by producing IgG and IgE (Cardoso et al., 2008). Taken together, these data showed that ABCs expressed a variety of Igs at a range of levels. Furthermore, these data indicated that a small proportion of these subsets were antigen-experienced and had undergone class-switching.

CD138 expression was comparable between the different liver diseases in all five subsets **(figure 2.15A)** however CD138 MFI data showed that HFe blood had significantly higher expression compared to adult livers **(figure 2.15A(vi-x))**. CD11c+ T-bet+ ABCs had significantly high CD138 expression compared to CD24+ CD38- B cells in HFe blood **(figure 2.15B(i))** and NASH livers **(figure2.15B(iv))**. Transcripts of CD138 and PC transcription factors, Prdm1 Irf4 and Xbp1 were upregulated in ABCs derived from mice (Rubtsov et al., 2011) suggesting that they possess antibody-secreting capabilities. Rubtsov et al., showed that ABCs cultured in media alone did not produce Igs indicating that ABCs were not fully

differentiated into PCs and required appropriate stimuli to produce antibodies in vitro (Rubtsov et al., 2011). CD21-/lo ABCs may represent precursors to CD11c+ T-bet+ ABCs which can differentiate in ASCs.

Michael Cancro's group originally described ABCs as a resting population (Naradikian et al., 2016b, Hao et al., 2011) whilst Philippa Marrack's group described ABCs as activated/memory B cells that expressed CD11c and T-bet (Rubtsov et al., 2011, Rubtsov et al., 2013). Furthermore, the Marrack group stated that these activated ABCs were associated with autoimmunity (Rubtsova et al., 2015). Maybe both groups were describing ABCs at different stages of differentiation and resting ABCs possess the ability to differentiate into activated/effector ABCs upon appropriate stimulation. We have shown that CD11c+ T-bet+ ABCs highly expressed CD86, HLA-DR, CD138 and co-expressed T-bet and TLR9. This subset also had low expression of class-switched Igs and contained a high proportion of memory B cells suggesting that this population may be activated memory ABCs that protect the host from infection or may be involved in autoimmunity where they are pathogenic. ABCs in unimmunised mice were mostly naive, however upon infection with influenza A virus, these naïve ABCs differentiated into activated/effector ABCs (Swain et al., 2017). The expression of adhesion molecule CD11c indicates that CD11c+ T-bet+ ABCs migrate to sites of inflammation (Swain et al., 2017) which also explains why this population was detected in HFe blood.

FcRL5+ atypical memory B cells share characteristics with ABCs such as reduced CD21 and CD27 expression and the expression of inhibitory receptors (Kim et al., 2019). Furthermore this population was expanded in chronic infections (Charles et al., 2011, Portugal et al., 2015, Portugal et al., 2017) and autoimmunity (Jacobi et al., 2008). Our data showed significantly

high expression of FcLR5 in CD11c+ T-bet+ ABCs **(figure 2.16C)**. FcRL5 contains an activating and inhibiting signalling motif and may have immunomodulatory roles on B cells (Haga et al., 2007). This suggests that FcRL5 may play inhibitory roles but may have an activating role in CD11c+ T-bet+ ABCs. BCR stimulation of naïve B cells resulted in the upregulation of FcRL5 which was further elevated by IL-21 (Li et al., 2020). A proportion of naïve B cells may become ABCs which express FcRL5. Furthermore, IL-21 has been shown to regulate T-bet expression (Myles et al., 2017) which suggests that CD11c+ T-bet+ ABCs could be receiving activating signals through FcRL5 resulting in differentiation into an effector phenotype. These cells could also differentiate into ASCs as IL-21 promoted the differentiation of PCs (Li et al., 2020). FcRL4 is expressed on ABCs and FcRL4+ B cells have been shown to infiltrate the damaged biliary epithelium in PBC livers (Liu et al., Submitted). A similar case could be made for FcRL5+ cells.

ABCs are termed “age-associated” and accumulate with age however we observed no correlation between non-cirrhotic livers **(figure 2.17A)**, cirrhotic livers **(figure 2.17B)** and age suggesting that chronic inflammation in liver disease may have induced ABC differentiation. No correlation was observed amongst the other B cell subsets and age either **(figure 2.17B)**. Whilst the literature originally found ABCs to accumulate with age in healthy elderly individuals, ABCs are prematurely expanded in autoimmune diseases such as rheumatoid arthritis (RA), systemic lupus erythematosus (SLE), Sjogren’s syndrome (SS), CD, and multiple sclerosis (MS). Furthermore ABCs also accumulate in viral infections such as HIV, Malaria, HCV, COVID (Sachinidis et al., 2020).

ABCs have been reported to be enriched in female humans and mice (Rubtsov et al., 2011) however we saw no correlation between age and sex in either of the ABC populations

analysed **(figure 2.17C)** which may be due to lack of TLR7 expression. TLR7 is an X-linked gene associated with the accumulation of ABCs in females (Sachinidis et al., 2020). Females have two gene copies of *TLR7* compared to males (Rubtsov et al., 2013). Rubtsov et al., showed that mice lacking *TLR7* gene copies failed to accumulate ABCs compared to mice with one or two *TLR7* gene copies (Rubtsov et al., 2013). Furthermore, this group showed that the number of *TLR7* gene copies correlated with the percentage of ABCs in these mice (Rubtsov et al., 2013). TLR7 stimulation also resulted in a robust production of IgM and IgG antibodies from female mice (Rubtsov et al., 2011) suggesting that female bias in ABC accumulation may be driven by TLR7.

ABCs were present across all adult livers in cirrhotic and non-cirrhotic livers indicating that ABCs are not disease specific and arise in many different types of disease. CD24- B cells shared many characteristics mainly with CD21-/lo ABCs and a few with CD11c+ T-bet+ ABCs. Buffa et al., showed that CD24- CD38- B cells accumulated with age in the blood of the elderly (Buffa et al., 2013) suggesting that CD24- B cells may contribute to the ABC pool. These populations of CD24- B cells and ABCs may form different stages of ABC differentiation which would explain why they had varying expression of markers. This suggests that CD24- B cells and CD21-/lo ABCs may form an activated naïve pool of cells awaiting the appropriate stimuli for their development into effector ABCs and antibody-producing ABCs which is what the CD11c+ T-bet+ ABC compartment has been hypothesised to be (Swain et al., 2017, Rubtsov et al., 2011, Rubtsova et al., 2015). We have shown that CD24- B cells and CD21-/lo ABC compartment mainly consisted of naïve B cells which indicates that they have not received signals to differentiate into effectors. CD11c+ T-bet+ ABCs most likely represent effector ABCs or ASCs as they expressed class-switched Igs and

had high expression of CD138 further supporting their role as ASCs. More work needs to be conducted to determine the function of these CD24- B cells in health and ABCs in health and disease and to determine if the ABC pool contains ABCs with different phenotypes.

2.4.5 ABCs play a role in antiviral responses

ABCs provide the host with anti-viral responses against viral infections (Mouat and Horwitz, 2022) such as the production of antibodies. In the context of autoimmunity, ABCs contributed to the production of autoantibodies such as anti-chromatin, anti-smith antibodies (Rubtsov et al., 2011), anti-dsDNA and anti-nuclear antibodies (Naradikian et al., 2016a). Depletion of ABCs in animal models of autoimmunity resulted in a reduction of autoantibody production (Rubtsov et al., 2011). The literature suggests that ABCs play a protective role in infection and a pathogenic role in autoimmunity, and this may depend on TLR stimulation (Naradikian et al., 2016a). Autoimmune mouse models showed that activation via TLR7 or TLR9 may ameliorate or exacerbate disease, respectively. TLR7 deficient mice had improved autoimmune disease whereas TLR9 deficient mice displayed exacerbated autoimmune disease (Naradikian et al., 2016a). Furthermore, mouse models with an extra TLR7 gene resulted in a disease that resembled SLE (Naradikian et al., 2016a). Whilst TLR9 had a protective role in SLE mouse models, other models of autoimmunity did not have the same results (Naradikian et al., 2016a). This suggests that TLR9 may provide a regulatory role in certain diseases and contribute to pathogenesis of other diseases. Our data showed that TLR9+ **(appendix 4C and 4D)** and T-bet+ TLR9+ cells were found expressed in all adult chronic liver disease **(figure 2.12D)**. This may indicate that ABCs have different outcomes dependent on whether they recognise RNA or DNA moieties and activate TLR7 or TLR9 (Naradikian et al., 2016a). This suggests that ABCs have a dichotomous role in disease

and more work needs to be undertaken to determine whether activation of TLR7 or TLR9 result in protection or pathogenesis.

2.4.6 Limitations

Whilst HFe blood and donor liver were used as controls, they do not represent true healthy controls. HFe blood is a good comparison to detect differences in B cell phenotype between the blood and liver however, it is not a true representation of healthy blood. This is due to the patients suffering from haemochromatosis which is a disease where iron accumulates in the blood and needs to be removed frequently. Comparisons made between the liver and HFe blood need to take this into account. Donor livers are livers that do not meet the criteria for liver transplantation and thus have been rejected. This may explain why similar numbers of CD24- B cells and ABCs were observed between chronic adult liver diseases and donor livers.

2.5 Conclusion

ABCs have not been previously been characterised in the liver (Mouat et al., 2022) which suggests our data may elucidate characteristics of hepatic ABCs. We have identified two subsets of ABCs which differ in the expression of CD86, T-bet+ TLR9+ cells, CD138 and FcRL5 positive cells which may highlight two distinct populations. An increased cohort of samples would be necessary to elucidate any further differentiations between CD21-/lo and CD11c+ T-bet+ ABCs. Further experiments such as stimulation assays need to be conducted to investigate the range of Igs and cytokines produced by ABCs and if this is liver specific. The liver is an immunologically privileged site that is constantly exposed to pathogens and maintains tolerance, which explains why hepatic ABCs and CD24- B cells can produce a range

of antibodies. In addition, future multiparametric experiments may help elucidate the roles of ABCs in chronic liver diseases. Gene expression analysis would help highlight the immune pathways activated in these ABCs and help identify if ABCs subsets contain a heterogenous population of cells that are at different developmental stages or if they are poised to become PCs or effectors.

CHAPTER 3 – B CELL LOCALISATION IN PAEDIATRIC LIVERS

3.1 Introduction

To study the impact of B cells in liver inflammation, it would be important to study B cells at earlier stages of liver injury, however this is difficult due to the lack of access to liver tissue. In BA, tissue samples are obtained at the time of KPE, during early disease and there are also tissue samples obtained at end-stage disease during liver transplantation. These samples enable us to study disease progression from early and late disease and we can identify B cell subsets and observe any changes in the B cell compartment from early disease to end-stage disease. Our adult liver samples were obtained during liver transplantation, at end-stage disease, so with these samples we were only able to study the B cell compartment and inflammation during end-stage disease.

3.3.1 Distribution of B cells in liver health and disease

Limited knowledge about the localisation of B cells in the liver is documented. B cells make up approximately 8% of the total hepatic lymphocyte population (Robinson et al., 2016). B cells were found near portal tracts within hepatic sinusoids and ASCs were found in connective tissue surrounding the portal tracts (Moro-Sibilot et al., 2016, Cheng et al., 2021).

Primary lymphoid follicles are precursors of SLOs which have GCs that are mainly composed of naïve B cells and FDCs (Beyer and Meyer-Hermann, 2008). Primary follicles filter antigens and bring B cells into contact with FDC-presented antigens in order to form GCs (Beyer and Meyer-Hermann, 2008).

Tertiary lymphoid structures (TLS) form in response to chronic inflammation (Bery et al., 2022), autoimmune responses, localised infections and in areas surrounding tumours (Pipi et al., 2018). TLS share similarities with SLOs as both consist of B and T cell zones (Pipi et al.,

2018) however, they differ from SLOs as they can form in non-lymphoid tissues (Bery et al., 2022).

TLS can contribute to the immune response at sites of chronic inflammation and injury however this is dependent on the tissue microenvironment where they form (Bery et al., 2022). In autoimmunity, TLS could contribute to disease by developing into GCs and through the production of autoantibodies (Bery et al., 2022). TLS from patients with SS were associated with elevated autoantibody levels and high production of cytokines which resulted in worsened clinical symptoms (Bery et al., 2022). On the other hand TLS can contribute to protective antigen-specific immune responses at sites of chronic inflammation (Sato et al., 2023).

TLS can be organised into compartments with a GC (Bery et al., 2022) however lymphoid aggregates, that are like primary lymphoid follicles have been detected in different diseases however their role in disease pathology is not well understood. 8.1% of patients who underwent BM biopsies had the presence of lymphoid aggregates (Dominis et al., 2005). In addition, lymphoid aggregates have also been found in BM biopsies from myelodysplastic syndrome (MDS) patients (Book et al., 2022). 24.3% of MDS patients were positive for lymphoid aggregates and these aggregates had a trend to appear in younger patients.

Lymphoid aggregates have been found in gastric biopsies from patients suffering from Helicobacter pylori (H.Pylori) gastritis. Patients who were H.Pylori negative had an average of three aggregates whereas patients positive for H.Pylori had an average of six aggregates (Chakhachiro et al., 2020) suggesting an association between H.Pylori and the number of aggregates. Lymphoid aggregates were found in 65/68 patients and lymphoid aggregates in

30 patients had GCs however, 35 (51%) of patients had aggregates lacking GC (Chakhachiro et al., 2020) indicating that majority of lymphoid aggregates may represent primary lymphoid follicles.

In HCV liver biopsies, 59% of patients had focal lymphoid aggregates within the portal tract with the average number of lymphoid aggregates ranging between two to seven in each sample (Freni et al., 1995). Wong et al., also found that lymphoid aggregates were present in the portal tracts in 60% of patients with chronic HCV (Wong et al., 1996). Lymphoid aggregates were detected in HBV livers (24%) however these aggregates were significantly lower compared to HCV patients (60%) but they had similar composition of cells (Akyol et al., 2001). Chronic HCV patients had higher lymphoid aggregate numbers in 49% of patients compared to chronic AIH patients, out of which only 10% had lymphoid aggregates however in both diseases, lymphoid aggregates were found in the portal tracts (Bach et al., 1992).

Lymphoid aggregates were found in higher frequencies in patients with colorectal cancer and diverticular disease compared to IBD (Nascimbeni et al., 2005). In this cohort, patients with IBD and colorectal cancer had larger lymphoid aggregates which were made up of a central B cell area surrounded by T cells (Nascimbeni et al., 2005). In HCV liver biopsies, lymphoid aggregates were composed of B cells mixed with CD4+ T cells surrounded by an outer ring of CD8+ cytotoxic T cells (Freni et al., 1995). Portal lymphoid aggregates in chronic HCV patients showed the presence of a mixture of B and T cells with few PCs (Dhingra et al., 2016). Lymphoid aggregates from MDS BM biopsies were positive for B (CD20) and T (CD3) cells (Book et al., 2022).

A study in MS suggested that the presence of meningeal lymphoid aggregates contributed to chronic inflammation and tissue destruction (Ransohoff, 2023). Furthermore, this group stated that the formation of chronic active lesions in MS was driven by meningeal lymphoid aggregates. These aggregates have been found in majority of postmortem MS tissues and they were present prior to the onset of MS contributing to early disease pathology (Ransohoff, 2023). In addition, meningeal lymphoid aggregates were associated with cortical demyelination (Ransohoff, 2023) suggesting a pathogenic role for these aggregates. Clonally expanded B cells made up majority of meningeal lymphoid aggregates (Ransohoff, 2023) suggesting that they play a pathogenic role in MS progression.

Lymphoid aggregates may contribute to pathology and liver injury in chronic HCV patients through immune mediated mechanisms (Freni et al., 1995). Lymphoid aggregates in chronic HCV liver biopsies strongly correlated with portal tract inflammation and were associated with damage to bile ducts (Wong et al., 1996). These studies show a possible role for lymphoid aggregates in the progression of disease.

Lymphoid aggregates in paediatric cholestatic liver disease have not been widely analysed in the literature. The literature provides information about lymphoid aggregates in paediatric patients with gastrointestinal problems. Lymphoid aggregates were detected in young children with gastrointestinal symptoms and were not associated with clinical symptoms however, these lymphoid aggregates were increased in number and in size of the follicles (Mansueto et al., 2012). Another study stated that out of 80 paediatric biopsies with gastritis, 34 patients had the presence of lymphoid aggregates (Carpentieri et al., 2000). Lymphoid aggregates were also observed in 65/525 patients who did not develop gastritis (Carpentieri et al., 2000). Furthermore, lymphoid aggregates were larger in children with

gastric mucosal pathology (Jaskiewicz and Kobierska, 2000). Kara et al., also showed the presence of lymphoid aggregates in paediatric patients with gastritis and found that patients with H.Pylori had a prevalence of lymphoid aggregates (Kara et al., 2014).

3.1.2 IL-6 in disease

IL-6 is a pro-inflammatory cytokine that plays a pathogenic role in many chronic inflammatory diseases such as RA, SLE, cancer and asthma (Widjaja et al., 2020). IL-6 also contributes to pathogenesis by increasing the production of autoantibodies, inducing B cell proliferation, and enabling the survival of pathogenic PCs (Maeda et al., 2010). Significantly high levels of IL-6 were produced by B cells in murine BA (Bednarek et al., 2018) suggesting a role for B cells and IL-6 in bile duct injury. Whilst IL-6 may contribute to pathology in many diseases, it also plays a role in promoting liver regeneration (Widjaja et al., 2020). Liver regeneration was accelerated in mice with hyper IL-6 compared to mice without IL-6 which showed impaired regeneration (Widjaja et al., 2020). During liver injury, cholangiocytes respond by secreting cytokines such as IL-6 which can aid in damage repair or result in the development of cholangiopathies (Pinto et al., 2018).

3.1.3 Aims and objectives

B cells have not been extensively studied in BA and their location within the liver tissue is not well understood. We set out to map the location of B cells in BA livers. Access to early and end-stage samples allowed us to study the B cell compartment during disease progression.

Objectives

In this chapter, I set out to:

1. Map the location of B cells in the liver around bile ducts and in fibrotic tracts

2. Identify B cell and lymphoid aggregates in BA liver samples
3. Characterise immune subsets present in B cell and lymphoid aggregates
4. Detect the location of mixed immune infiltrates in BA livers
5. Map the location of lymphoid aggregates and mixed immune infiltrates in adult livers
6. Use CellProfiler software to quantify immune subsets present in paediatric and adult livers

3.2 Methodology

3.2.1 Human paediatric liver tissue

Paediatric sections (BA (n=50), SOAH (n=7), and HHV6 (n=3) were stained for CD20 using the protocol mentioned in 3.2.3. Paediatric liver tissue samples were obtained from paraffin blocks taken from patients with end-stage liver disease undergoing transplantation and at the time of KPE (BA samples) at the Birmingham Children's Hospital, Birmingham. All samples were obtained from the liver unit tissue bank registry (South West – Central Bristol Research ethics committee approval reference 17/SW/0073). Clinical data for BA patients is available in **Appendix table 2**. Clinical data for sudden onset acute hepatitis patients is available in **Appendix table 3**. Clinical data for HHV6 patients is available in **Appendix table 4**.

3.2.2 Human adult liver tissue

Liver tissue samples were obtained from explanted livers, taken from patients with end-stage liver disease undergoing transplantation at the Queen Elizabeth Hospital, Birmingham. These samples were processed following patient consent and in approval with local research ethics committee guidelines (LREC; reference number 06/Q2702/61 and 18-WA-0214). Some of the adult patients used for B cell characterisation using flow cytometry were also used in this chapter. Clinical data for these patients is available in **Appendix table 1**.

3.2.3 Immunohistochemistry

3.2.3.1 Optimisation

All antibodies to be used in either immunohistochemistry or immunofluorescence were titrated **(figure 3.1)** to find the optimal working dilutions for each antibody **(table 3.1)** and

the IMCs **(table 3.2)**. Each antibody had three different serial dilutions based around the company's recommended working dilution except for CD20 antibody **(figure 3.1A)**. This was because the manufacturers recommended dilution for CD20 was more dilute, so two dilutions were used to determine if smaller dilutions were required. 1/1000 dilution detected our B cells of interest, so no further dilutions were conducted. Adult PBC or HCV tissue sections were used for the optimisation. The tissue sections were placed into a slide rack and submerged in 3 rounds of xylene baths followed by 3 rounds of alcohol baths and 2 rounds of water baths, for 3 minutes each. A bucket with 1 L tap water and 10 ml of TrisBase antigen unmasking solution was heated in a microwave for 10 minutes. The slides were placed into the bucket and microwaved for 30 minutes and left to rest for 10 minutes. Cold tap water was added to the bucket. The slides were taken out individually, patted dry and using a wax pen, a hydrophobic ring was drawn around the tissue. The slides were placed in a humidifier box. Tris buffered saline (TBS) was pipetted onto the tissue to ensure that the reagents remained within the hydrophobic barrier, on top of the tissue. 200 µl of peroxidase block (Dako, S2023) was added to all slides and the humidifier box was placed on the rocker for 10 minutes. The slides were washed in TBS for 5 minutes on the rocker. A 2x solution of casein, made up in TBS, was added to each slide and placed on the rocker for 10 minutes. The slides were washed in TBS for 5 minutes on the rocker. 150 µl of antibody was added to the relevant slides before being placed on the rocker for 1 hour. Slides were washed in TBS for 5 minutes on the rocker. A few drops of impress universal polymer reagent (Vector laboratories, MP-7500) were added to each slide, enough to cover the tissue. The humidifier box was placed onto the rocker for 30 minutes. The slides were washed 3 times with TBS before 200 µl of ImmPACT DAB solution (Vector laboratories, SK-4105) was added to each

slide for 5 minutes. The slides were washed with tap water before the tissue was covered in haematoxylin mayers for 45 seconds. Hot tap water was used to wash the slides and transferred to a slide rack. The slide rack was submerged in 2 rounds of water baths, 3 rounds of alcohol baths and 3 rounds of xylene baths for 3 minutes each. Excess xylene was removed from each slide before a cover slip with a drop of DPX was mounted onto the tissue slides. Air bubbles were removed from the slides and the slides were left to dry before being scanned on the slide scanner.

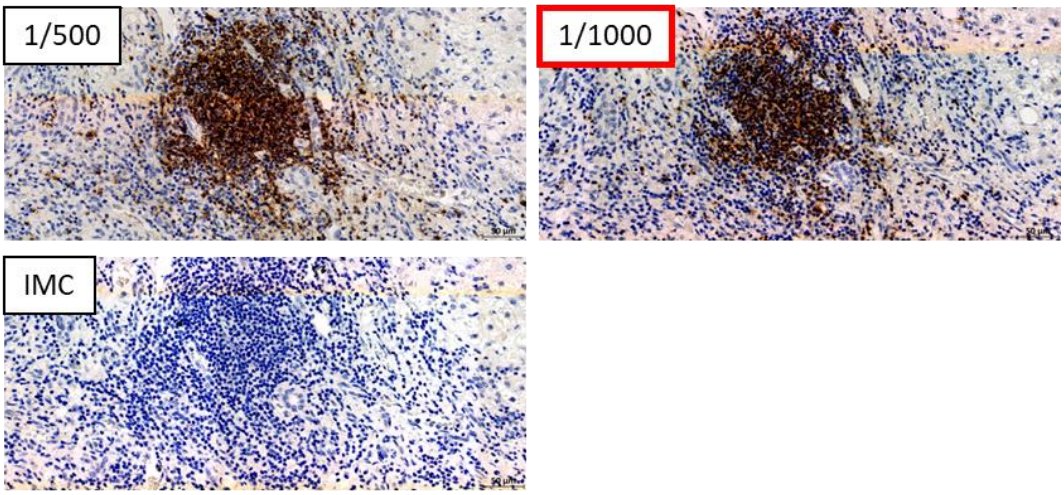
Table 3.1 IHC antibody working dilutions. *All the antibodies were used at the same dilution for each experiment. These antibodies helped to characterise B cells including CD20+ CD24+ B cells, CD20+ CD24- B cells, CD20+ CD24- IL-6+ B cells and identify CD3+ T cells in liver tissue.*

Marker (isotype)	**Company**	**Catalogue number**	**Lot number**	**Working dilution**
CD20 (mouse IgG2a)	Invitrogen	MA5-13141	UI2840511A	1:1000
CD24 (mouse IgG1)	Novus	NB100-64861	160549	1:100
CD38 (rabbit IgG)	Abcam	ab108403	GR210295-16	1:1000
CD138 (rabbit IgG)	Abcam	ab130405	GR3382382-1	1:200
CD3 (mouse IgG1)	Abcam	ab17143	GR3395244-1	1:100
IL-6 (mouse IgG2b)	Novus	NBP2-89149	H00125	1:200
Bcl2 (mouse IgG2b)	Origene	TA806591	W001	1:300

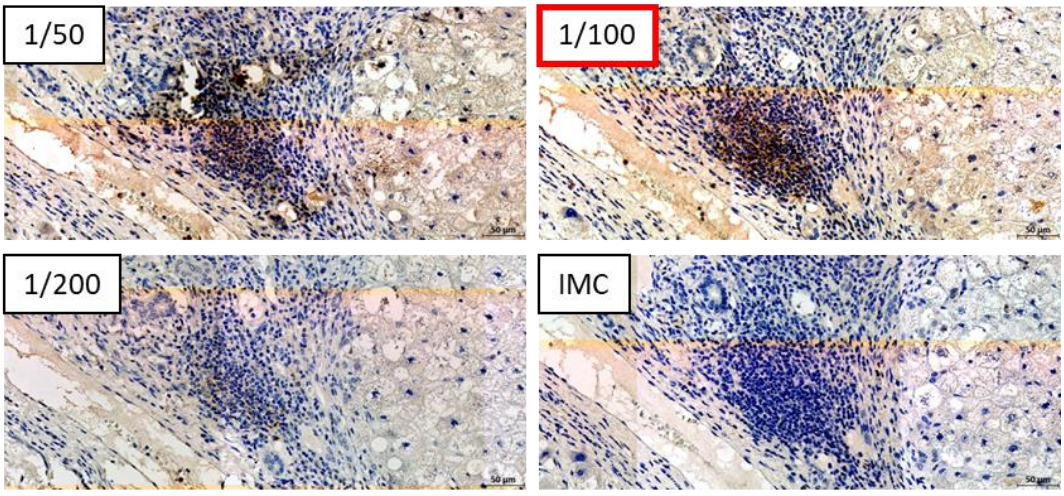
Table 3.2 Isotype matched controls for immunohistochemistry and immunofluorescence.
IMCs were used at the same dilution as the antibodies in ***Table 3.1.***

Isotype matched control	**Company**	**Catalogue number**	**Lot number**	**Working dilution**
Mouse IgG2a	Biolegend	401502	B278533	1:1000
Mouse IgG1	eBioscience	14-4714-85	4291364	1:100
Rabbit IgG	Cell Signaling Technologies	#3900S	16	1:200/1:1000
Mouse IgG2b	Biolegend	401202	B317705	1:200/1:300

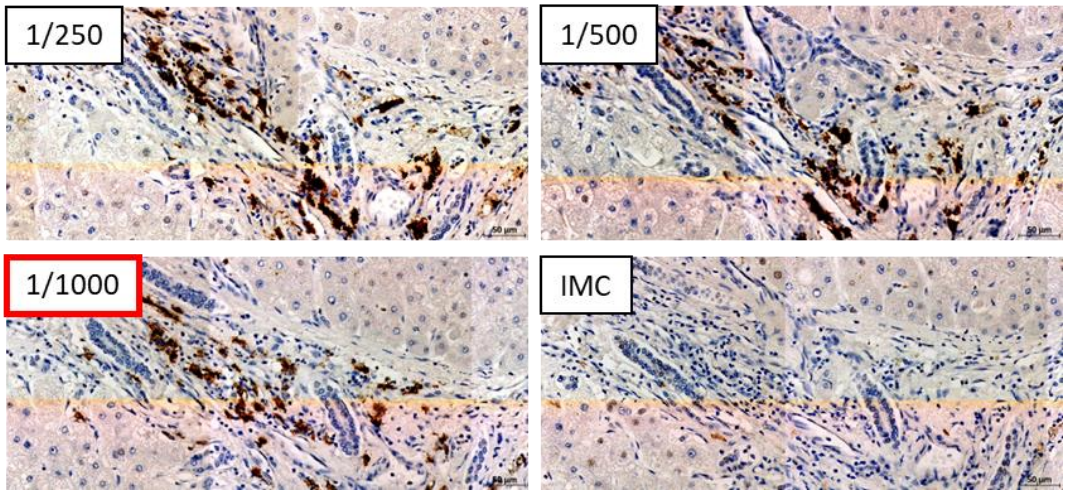
A **CD20**



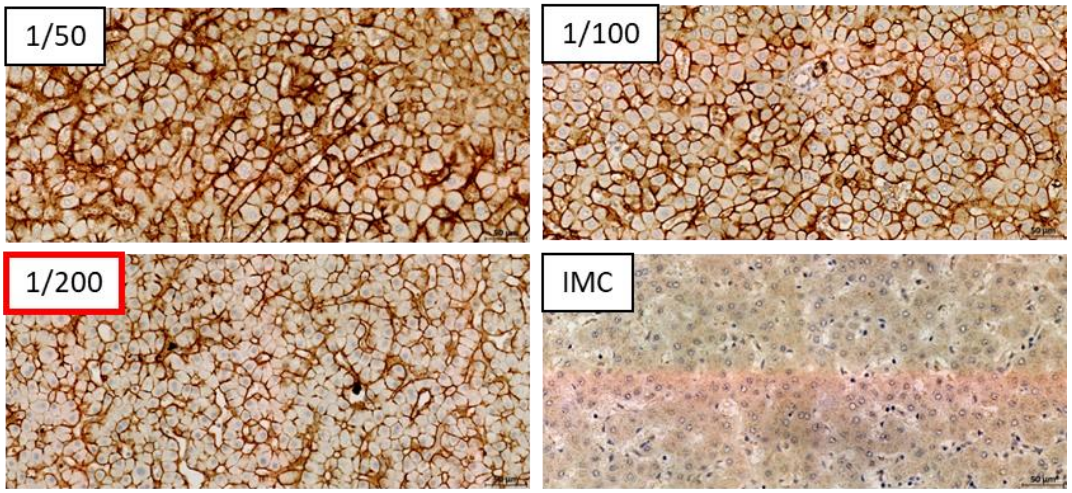
B **CD24**



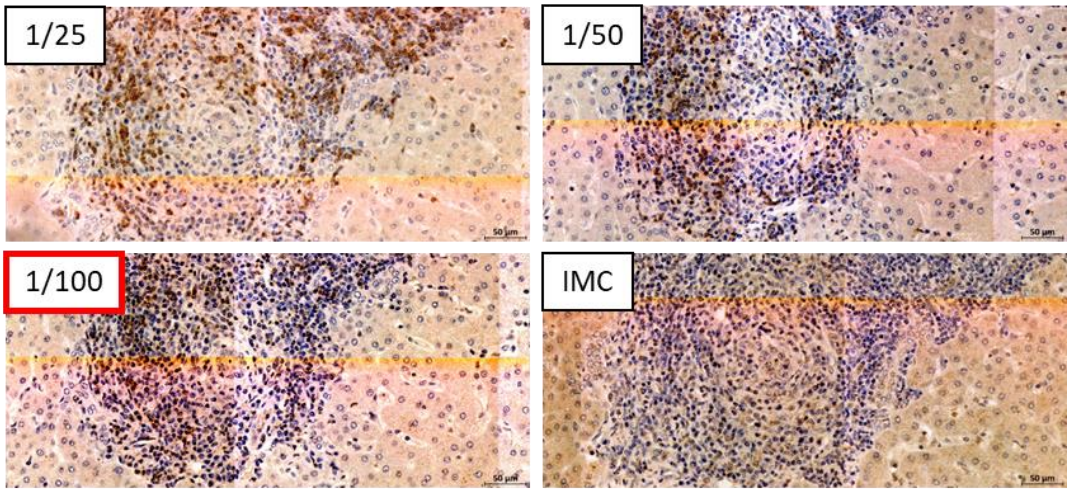
C **CD38**



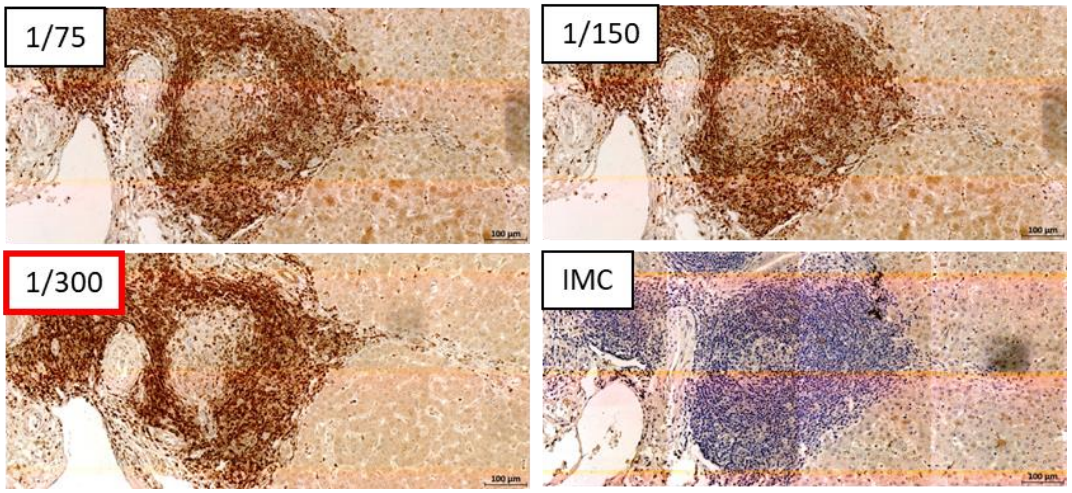
D **CD138**



E **CD3**



F **Bcl2**



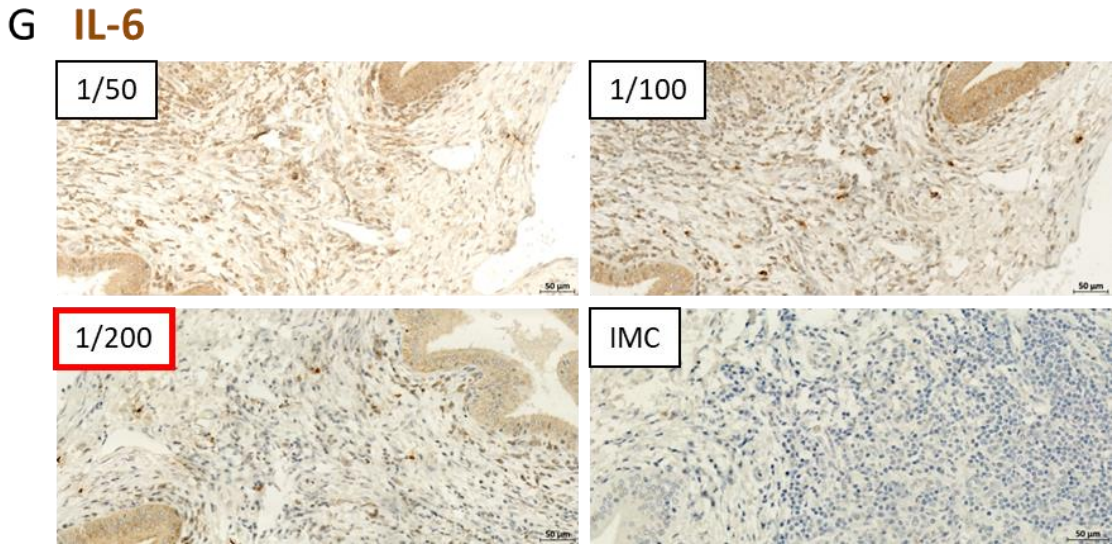


Figure 3.1 Titration of antibodies for immunohistochemistry. *Three serial dilutions were used to titrate the antibodies, based on the manufacturers recommended titration to identify the dilution with optimal staining and minimal background staining on adult PBC livers. (A) CD20, (B) CD24, (C) CD38, (D) CD138, (E) CD3, (F) Bcl2 and (G) IL-6.*

3.2.3.2 ImageJ

ImageJ software was used to quantify CD20+ B cells and total lymphocytes in our cohort of paediatric livers. Ten random images were taken on Zen 3.2 Blue edition (Carl Zeiss microscope GmbH) for each sample **(figure 3.2A)** before these images were analysed using ImageJ. The images were converted into 8-bit grayscale images **(figure 3.2B)**. A threshold was set to detect CD20+ B cells **(figure 3.2C(i))** and total lymphocytes (based on darker haematoxylin mayers staining) **(figure 3.2C(ii))**. The threshold was adjusted on ImageJ to highlight all the cells positive for the stain. Artefacts, bile ducts and other structures that were darker and not our cells of interest were removed (white squares, **figure 3.2C(ii)**) using the original immunohistochemistry image as a reference. This ensured that any positive cells being detected were the cells of interest and not any background staining. The image was then converted into a mask of all the pixels that were above the set threshold **(figure 3.2D)**.

These were my cells of interest in pixel data. From this mask, I measured the mean gray value for the total area of the tissue. The total area of the tissue in pixels was 157502. The mean gray value uses the sum of all gray value pixels and divides them by the number of pixels. The mean gray value pixel data for all ten images were averaged out for each sample, before being plotted using GraphPad Prism.

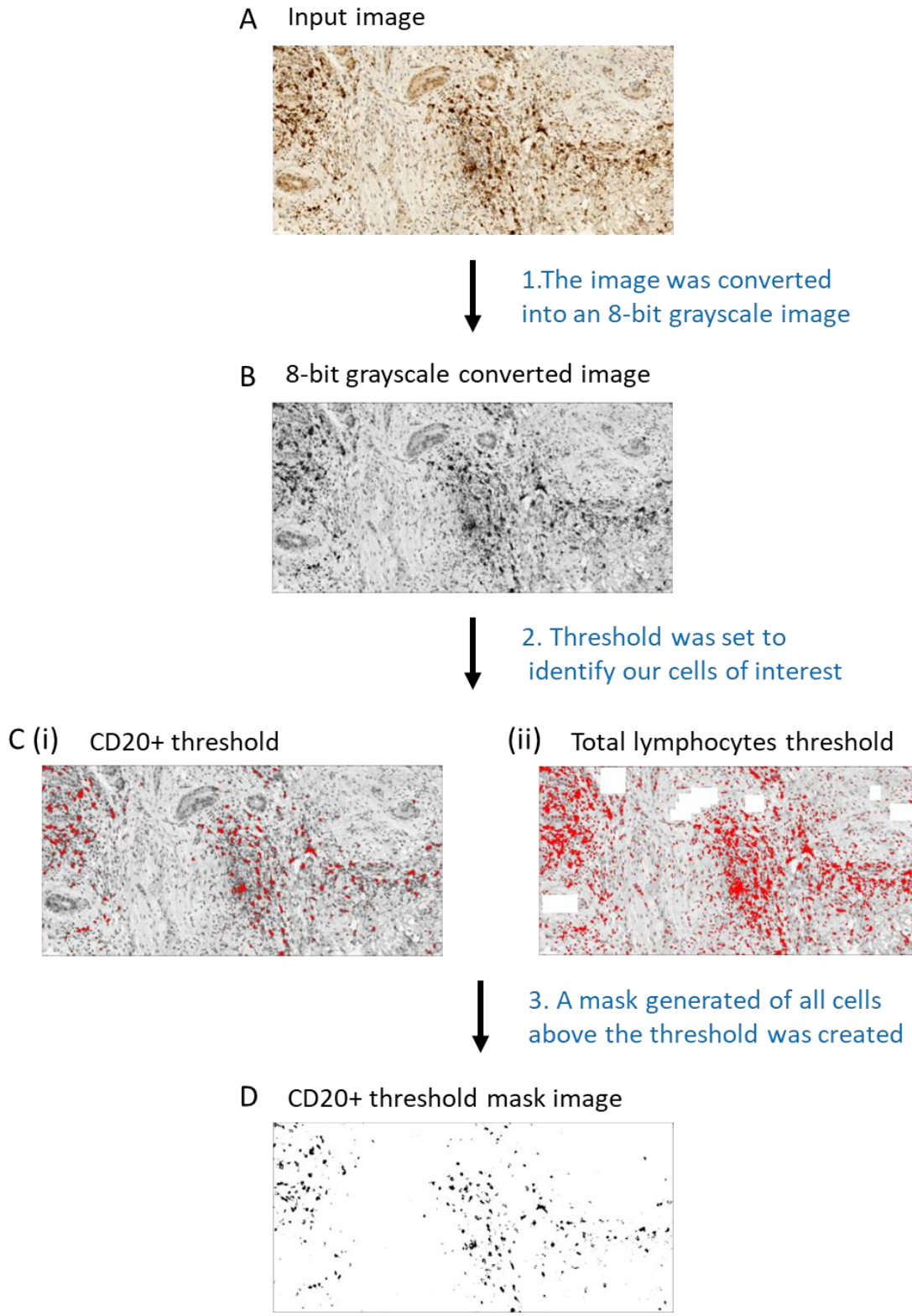


Figure 3.2 ImageJ analysis pipeline for CD20+ immunohistochemistry images. *The representative plots are from the hilum of a BA patient who was 31 days old. (A) Input image for ImageJ pipeline which was converted into (B) an 8-bit grayscale image for further*

analysis. Thresholds were set to detect (C(i)) CD20+ B cells and (C(ii)) total lymphocytes based on darker haematoxylin mayers staining. Red highlighted cells were cells that were above the set threshold. White squares were used to remove any background staining to ensure cells of interest were detected. Once the threshold had been applied, (D) a mask of the pixels that were above the threshold was created. From this, we measured the mean gray value which was averaged out between the ten images for each sample before being plotted on a graph.

3.2.4 Immunofluorescence

3.2.4.1 Optimisation

BA and adult tissue sections were stained with antibodies according to the optimal IHC titrations. The slides were submerged in three xylene baths, three alcohol baths and two water baths for 3 minutes each. 10 ml of TrisBase was heated in a microwave with 1 L of water, in a bucket, for 10 minutes. The slides were transferred to the bucket and heated in a microwave for 30 minutes with a 10 minute cooling period. After cooling down the solution with cold tap water, the slides were removed, and a wax ring was drawn around the tissue creating a hydrophobic barrier. This barrier ensured that the reagents would stay on top of the tissue. TBS was added to the slides in a foiled humidifier box, to check the integrity of the of the wax rings. All TBS washes were for 5 minutes on the rocker. 200 µl of 2x casein block was added to each slide and incubated on the rocker for 5 minutes. Antibody cocktails were made up in TBS, for each panel **(table 3.3)** and added to the relevant slides for 1 hour on the rocker. The slides were washed in TBS prior to the addition of secondary antibodies **(table 3.4)**. The humidifier box was placed on the rocker for another hour. The slides were washed three times in TBS before 150 µl of the Vector TrueView Autofluorescence Quenching kit (Vector laboratories, SP-8400) was added to each slide and incubated on the bench for 5 minutes. The slides were washed with TBS. Excess precipitate was removed with TBS before the slides were mounted on coverslips with a drop of VECTASHIELD Vibrance

antifade mounting medium with DAPI (Vector laboratories, H-1800). Air bubbles were removed from the slides and the slides were placed onto slide trays and covered with foil. Slides were stored at 4°C prior to being imaged on the LSM 880 Airyscan confocal microscope.

Table 3.3 Immunofluorescence primary antibody panels with working dilutions. *Catalogue numbers and lot numbers are given in* ***Table 3.1****. These panels were used to characterise immune cells and determine which B cell subsets were present in hepatic tissue.*

Panel 1	**Isotype matched control**	**Fluorophore**	**Working dilution**
CD20	Mouse IgG2a	Alexa Fluor 647	1:1000
CD24	Mouse IgG1	Alexa Fluor 488	1:100
CD38	Rabbit IgG	Alexa Fluor 594	1:1000
Panel 2	**Isotype matched control**	**Fluorophore**	**Working dilution**
CD20	Mouse IgG2a	Alexa Fluor 647	1:1000
CD24	Mouse IgG1	Alexa Fluor 488	1:100
CD138	Rabbit IgG	Alexa Fluor 594	1:200
IL-6	Mouse IgG2b	Alexa Fluor 555	1:200
Panel 3	**Isotype matched control**	**Fluorophore**	**Working dilution**
CD3	Mouse IgG1	Alexa Fluor 488	1:100
Bcl2	Mouse IgG2b	Alexa Fluor 555	1:300
CD138	Rabbit IgG	Alexa Fluor 594	1:200

Table 3.4 Immunofluorescence secondary antibodies. *Catalogue numbers and lot numbers are given in* ***Table 3.2****.*

Secondary antibodies	Fluorophore	Company	Catalogue number	Working dilution
Mouse IgG2a	Alexa Fluor 647	Invitrogen	A21241	1:1000
Mouse IgG1	Alexa Fluor 488	Invitrogen	A21121	1:1000
Rabbit IgG	Alexa Fluor 594	Invitrogen	A11012	1:1000
Mouse IgG2b	Alexa Fluor 555	Invitrogen	A21147	1:1000

Thermofisher fluorescence spectral viewer was used to make sure each fluorophore was compatible and had minimal spectral overlap with other fluorophores in the panel **(figure 3.3)** (ThermoFisher_Scientific).

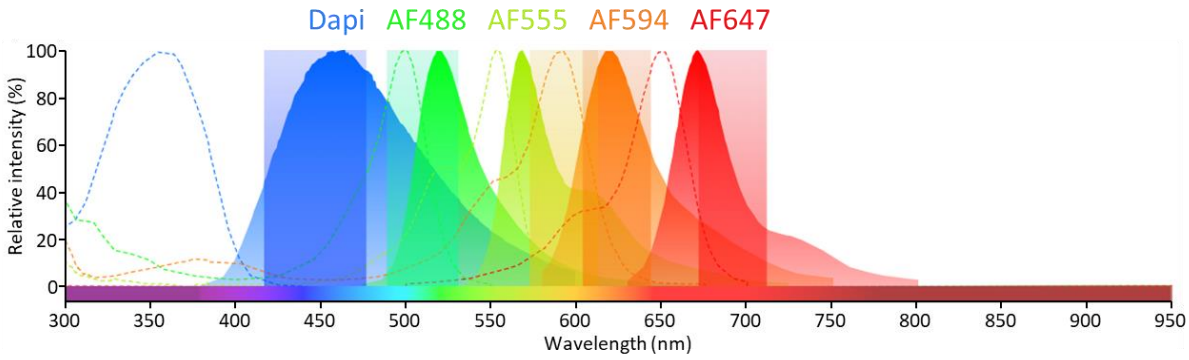


Figure 3.3 Spectral viewer of the fluorophores used in immunofluorescence panels. *This spectral viewer allowed me to visualise any problematic spectral overlap in the fluorophores I was using. This image helped determine that my fluorophores would have minimal spectral overlap into other fluorophore channels. DAPI (blue), AF488 (green), AF555 (yellow), AF594 (orange) and AF647 (red). Edited image from (ThermoFisher_Scientific).*

FMO for Alexa Fluor 555 was carried out and there was no evidence of spectral overlap in any of the other fluorophore channels **(figure 3.4)**.

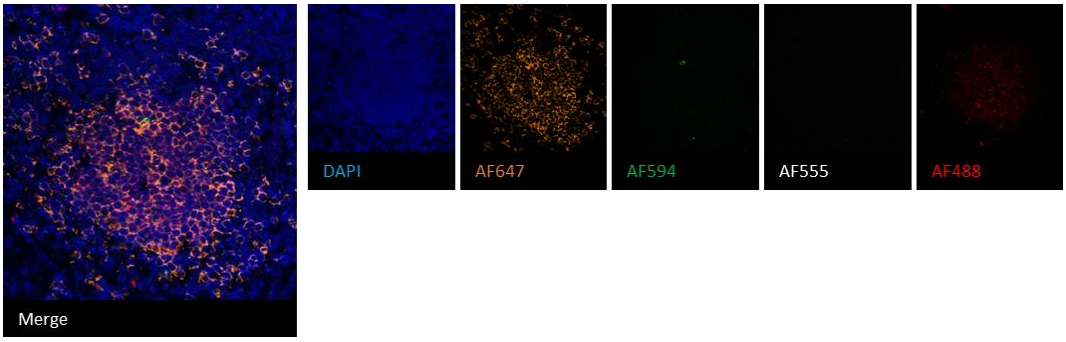


Figure 3.4 FMO for AF555. *Spectral spill-over for AF555 fluorophore was a concern however the FMO showed that there was no spectral spill-over. Adult PBC liver. DAPI (blue), AF647 (orange), AF594 (green), AF555 (white) and AF488 (red).*

Zeiss AxioObserver Z1 Apotome.2 and Zeiss LSM 880 with Airyscan Fast were compared to see which of those machines would give the best images, at a cellular level. PBC liver tissue was stained with panel 1 **(table 3.3)** and imaged on both machines **(figure 3.5)**. LSM 880 confocal machine gave the best image resolution, so this was used to image all the immunofluorescence slides.

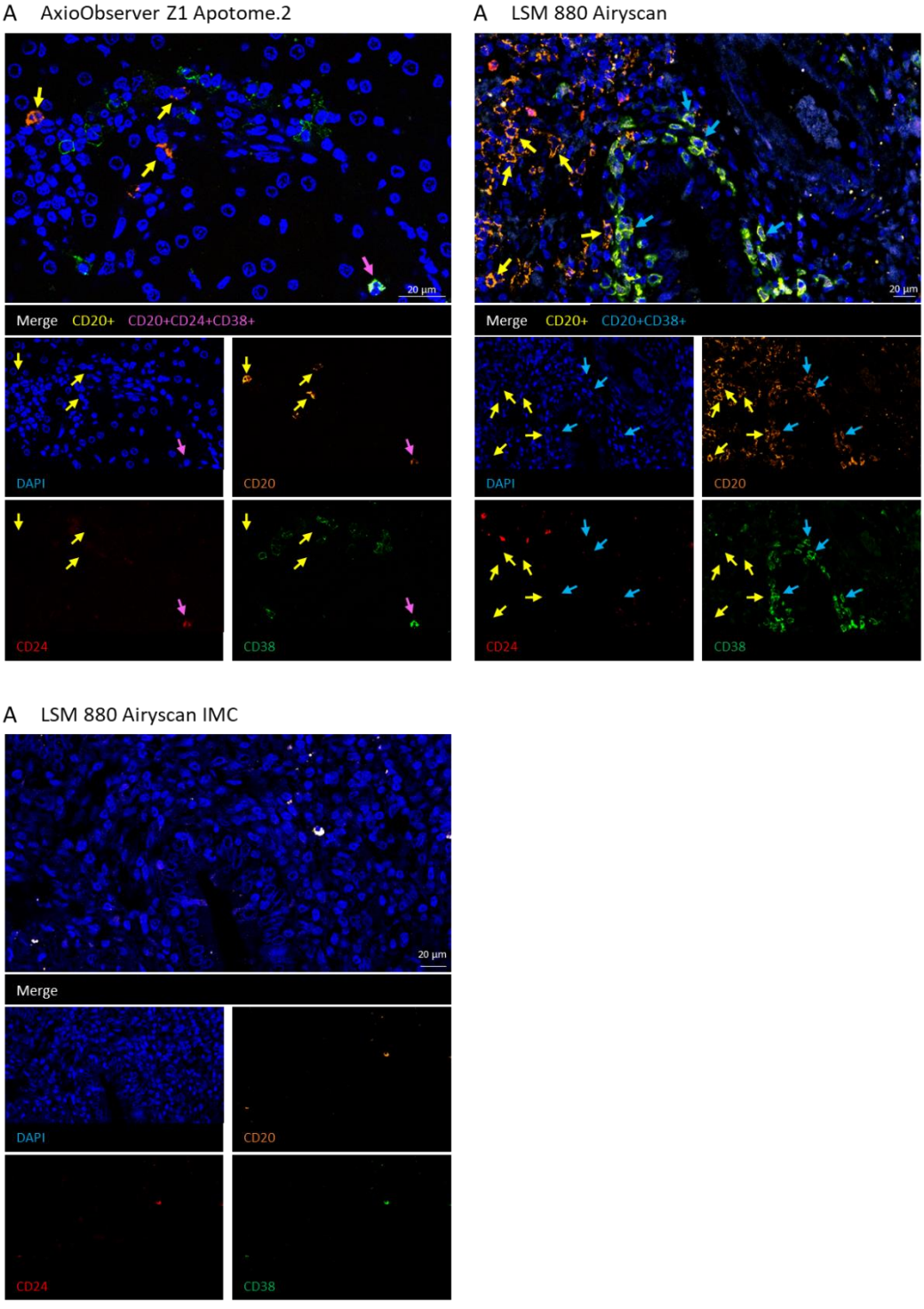


Figure 3.5 **Comparison of AxioObserver Z1 Apotome.2 and LSM 880 Airyscan on an adult PBC liver section.** The (A) AxioObserver detected fewer cells compared to the (B) LSM 880 Airyscan. (C) IMC for adult PBC liver. DAPI (blue) *AF647 (orange), AF594 (green), and AF488 (red).*

Panel 2 was tested on PBC sections to make sure all five colours worked together, especially IL-6 as this antibody was likely to crossover with Alexa Fluor 594 **(figure 3.6)**. From testing panel 2 on a PBC liver section, I concluded that the IL-6 Alexa Fluor 555 (white) does not spill over into the Alexa Fluor 594 channel (CD138; green). In addition, the IL-6 antibody worked and co-localised with CD20+ B cells, giving me confidence in my panels. **Figure 3.6** showed that my antibodies were detecting my cells of interest.

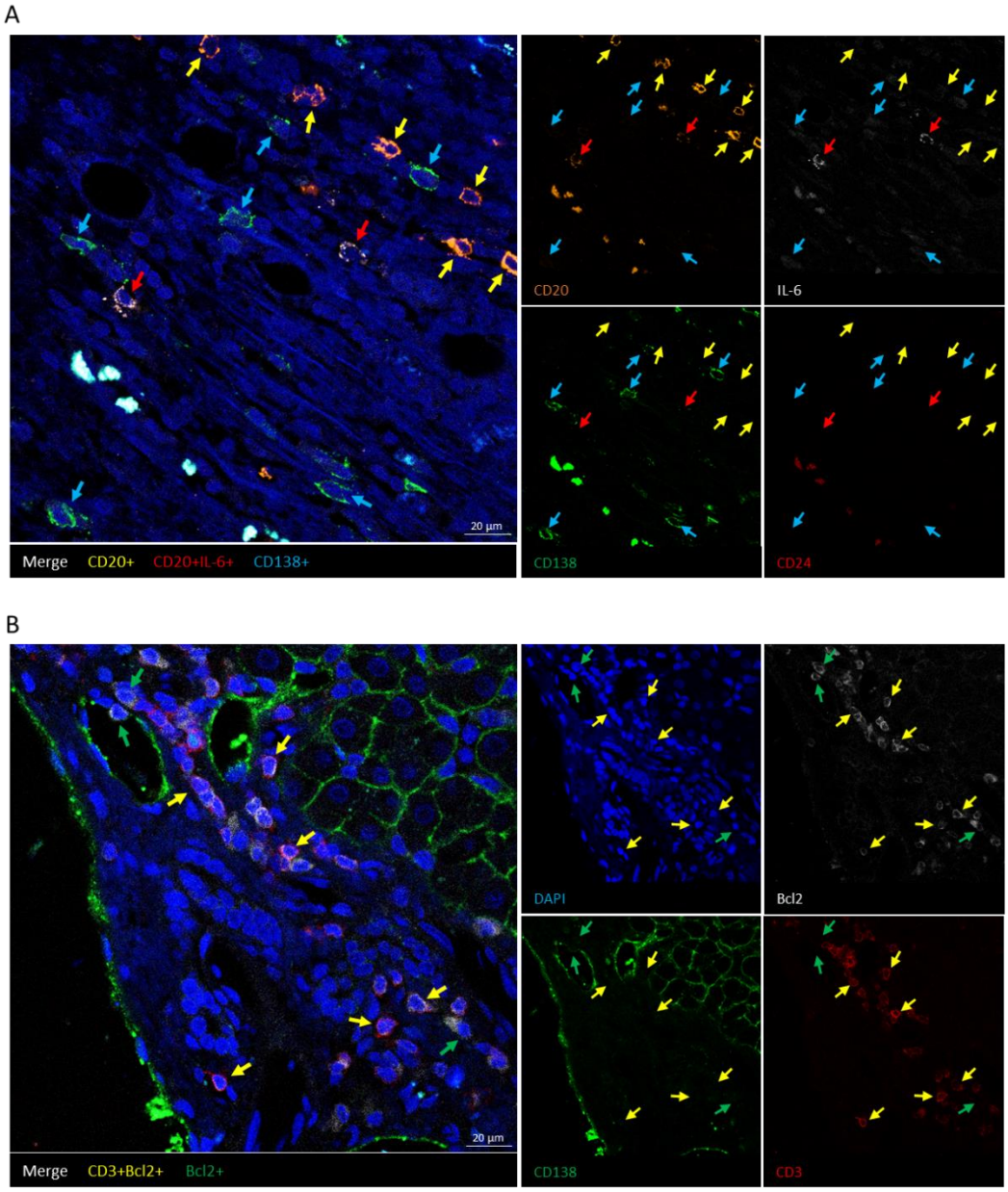


Figure 3.6 Separation of AF594 and AF555 was clear. *These antibodies worked to detect specific cells with little to no background staining. This staining was carried out on an adult PBC liver and showed that our cells of interest were easily detected in hepatic tissue with little to no autofluorescence detected. (A) This representative plot showed a good separation of IL-6 AF555; white and CD138 AF594; green. (B) This representative plot showed detection of Bcl2 AF555; white and CD3 AF488; red in liver tissue.*

I tried to image the whole immunofluorescence-stained tissue section to gain a better understanding of the localisation of my cells of interest within the entire area of tissue. I

used the slide scanner to detect immunofluorescence however the image it generated was not useable **(appendix 5)**.

These panels were then used to stain selected BA patients and adult PBC and PSC liver tissue sections. CellProfiler was used to quantify the cell types present in each image of tissue using pixel-based analysis.

3.2.5 Statistical analysis

GraphPad Prism 9.4.1 was used to create graphs and perform statistical analysis. The Shapiro-Wilk normality test was used to assess the normal distribution of my samples **(figure 2.4)**. This test calculates the ratio between the standard deviation of our data to the computed standard deviation of the slope from the QQ plot generated for our data. Normality tests were used to determine the statistical tests carried out on our data. Wilcoxon test was used to compared paired samples between two groups. Dunnett's T3 multiple comparisons test was used to analyse statistical significance between unpaired, normally distributed samples. Dunn's multiple comparisons test was used to analyse unpaired samples that were not normally distributed.

3.3 Results

3.3.1 B cells were found in the liver around bile ducts and in fibrotic tracts

The distribution of liver B cells in children with BA had not been studied previously in detail. First, immunohistochemistry was used to determine the localisation of B cells in paediatric liver tissue from explants of children with BA that underwent orthotopic liver transplantation. Representative staining is shown in **Figure 3.7**. CD20+ B cells were found around bile ducts **(figure 3.7A)**, in fibrotic tracts **(figure 3.7B)**, in small numbers in the tissue around triads **(figure 3.7C)** and present in ductular reactions **(figure 3.7D)**. Lymph nodes from BA tissues were used as positive controls for CD20 staining **(figure 3.7E)** and IMC is shown **(figure 3.7F)**.

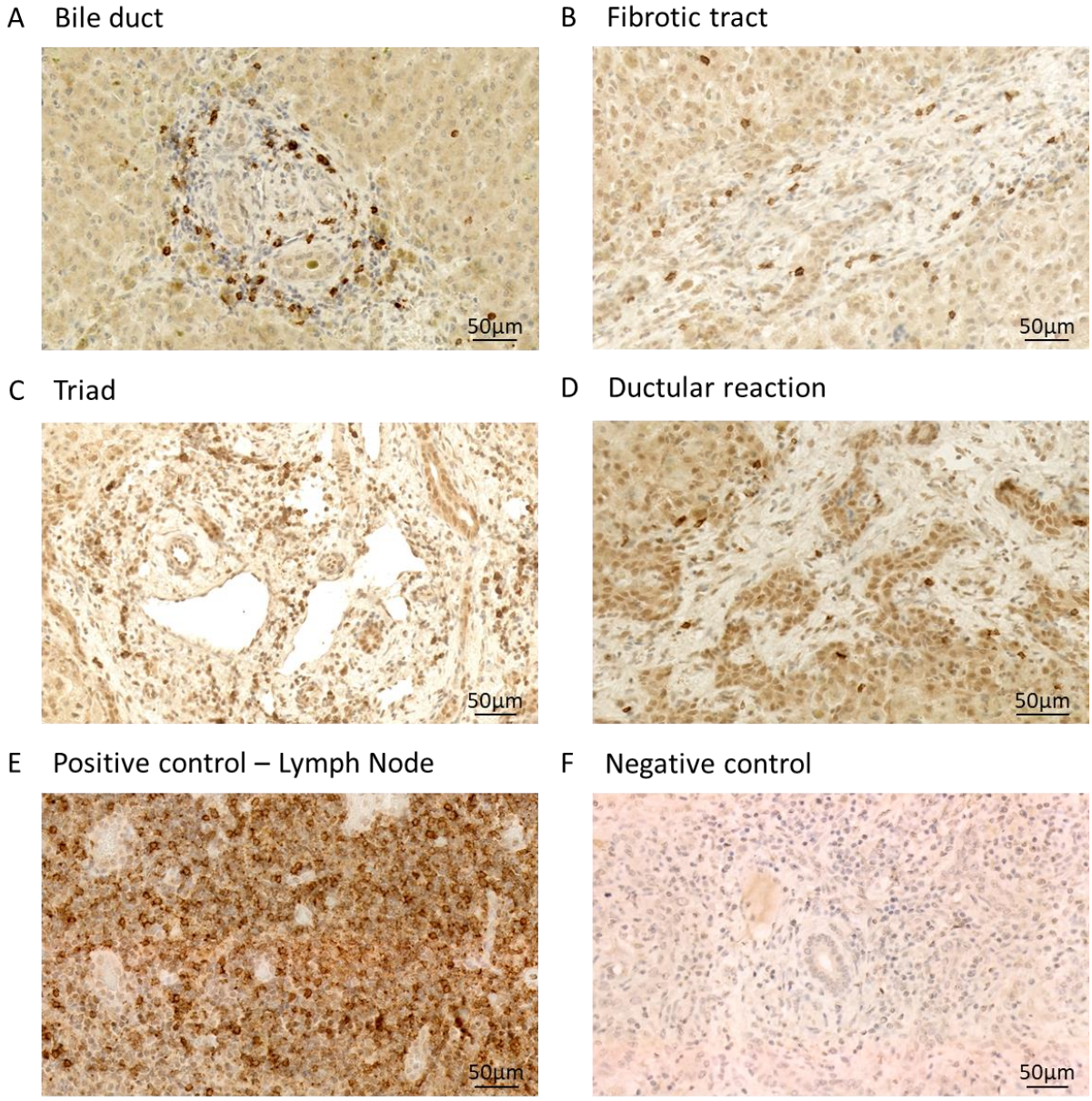


Figure 3.7 CD20+ B cells were found around bile ducts, fibrotic tracts, triads and in ductular reactions. *B cells were identified in (A) bile duct from the wedge of a BA patient who was 48 days old, (B) fibrotic tract from the wedge of a BA patient who was 31 days old, (C) portal triad taken from the wedge of a BA patient who was 36 days old and (D) ductular reaction taken from the wedge of a BA patient who was 64 days old. (E) BA lymph node was used as positive control taken from a hilum sample of a BA patient who was 52 days old and (F) IMC was used as a negative control. CD20 (brown).*

As expected, B cells were detected amongst the lymphocyte infiltrates in various liver locations, similar to adult liver diseases.

3.3.2 Lymphoid aggregates were found in the hilum region of BA liver samples

Next, we set out to detect B cells in biopsies from earlier in liver disease pathogenesis. In BA livers, samples were taken during KPE from the hilum and wedge, and during liver transplantation, from explanted livers **(figure 3.8)**.

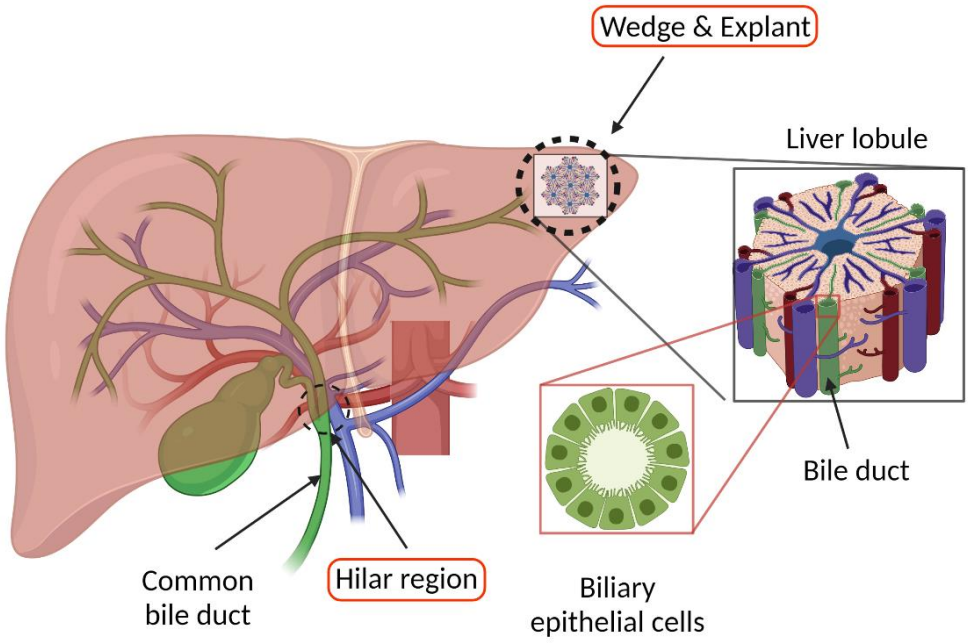


Figure 3.8 BA samples were collected from different locations in the liver. *Samples were obtained from the hilum and wedge during early disease and from the periphery of the explanted liver during late-stage disease. Image created using Biorender.*

CD20+ B cells were investigated in the following paediatric liver diseases: BA hilum **(figure 3.9A)**, BA wedge **(figure 3.9B)**, BA explant **(figure 3.9C)**, SOAH explant **(figure 3.8D)** and HHV6 explant **(figure 3.9E)**.

CD20+ B cells were present at varying frequencies in tissue locations in various paediatric liver diseases. Aggregates of CD20+ B cells were detected in BA hilum **(figure 3.9A)** and not in BA wedge samples **(figure 3.9B)**. CD20+ aggregates were also detected in some of the BA

explant tissues **(figure 3.9C(i))** however, the majority of BA explants had no B cell aggregates **(figure 3.9C(ii))**. SOAH and HHV6 explants showed clusters of B cells but no B cell or lymphoid aggregates were present **(figure 3.9D and 3.9E, respectively)**.

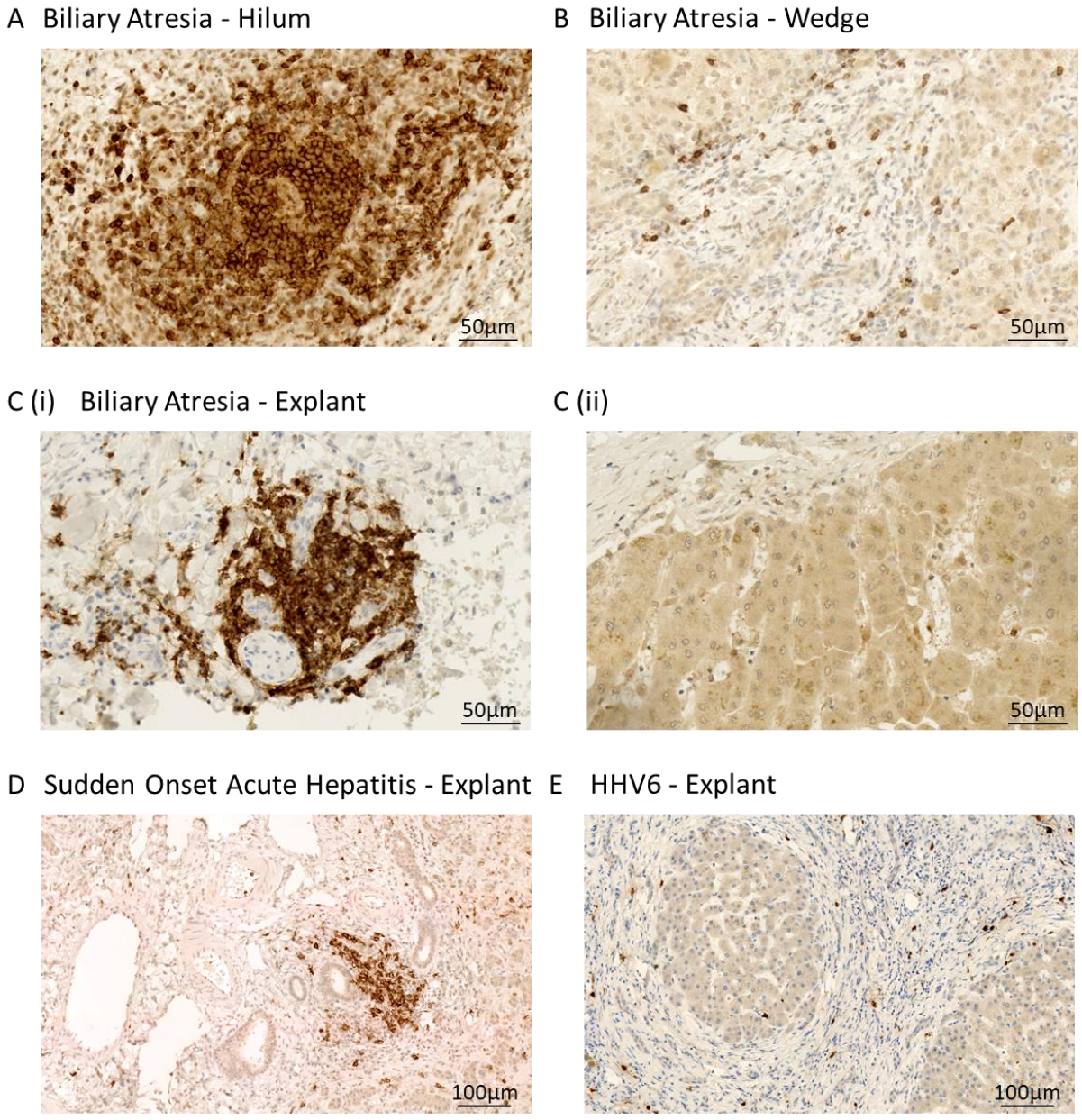


Figure 3.9 CD20+ B cells were found at varying frequencies across a range of paediatric liver diseases. *(A) BA hilum region had B cell aggregates present whereas (B) wedge samples did not. (C(i)) Few B cell aggregates were detected in BA explants whereas (C(ii)) majority of BA explants only showed CD20+ B cells. (D) Sudden onset acute hepatitis explants showed the presence of B cell clusters whereas (E) HHV6 explants showed B cell infiltration. CD20 (brown).*

ImageJ software was used to quantify CD20+ B cells and total lymphocytic infiltrate (based on haematoxylin stain) in paediatric livers. BA samples taken at KPE (hilum and wedge, n=49) showed a significant difference in CD20+ B cell infiltration between the hilum and wedge (p-value <0.0001) **(figure 3.10A)**. Hilum samples had significantly higher amounts of CD20+ B cells compared to matched wedge (p-value 0.0491) and explant samples (p-value 0.0182) (n=17) **(figure 3.10B(i))**. Total lymphocytic infiltrate was also significantly higher in the hilum compared to wedge (p-value 0.0022) and explant livers (p-value 0.0010) **(figure 3.10B(ii))**. B cell enrichment was measured by calculating the ratio between CD20+ B cells and total lymphocytes amongst BA samples. B cell enrichment was not significantly different between hilum, wedge, and explant samples **(figure 3.10C)** showing that BA patients did not have elevated levels of B cell infiltration compared to total lymphocytes. The high number of B cells observed was in proportion to the lymphocytic infiltration occurring in these patients suggesting and that the hilum was where there is active ongoing disease. Compared to other paediatric diseases, BA explant samples had lower B cell infiltration which was not significantly different **(figure 3.10D)** however this may be due to differences in age between these paediatric diseases **(Appendix table 2-5)**.

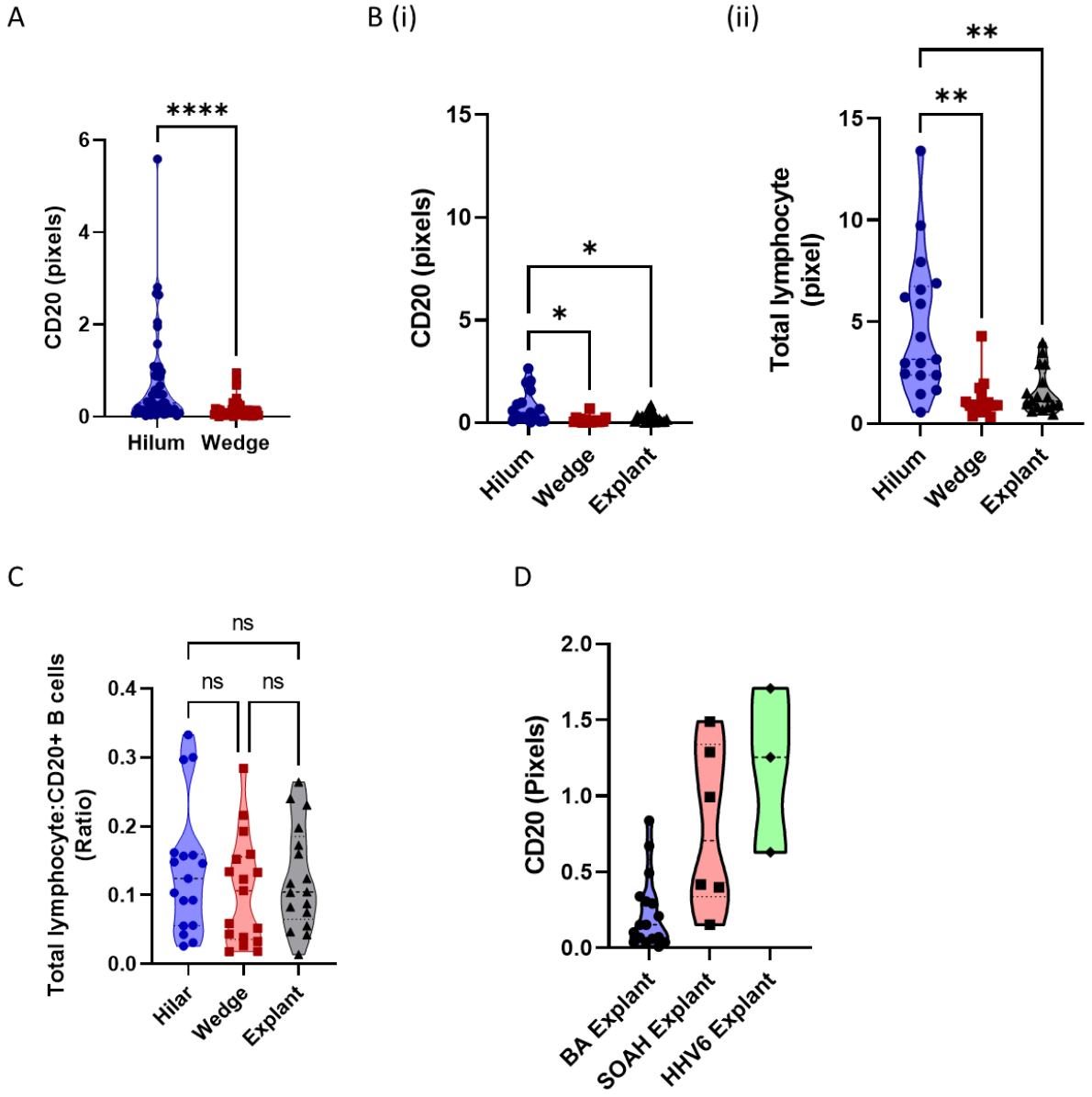


Figure 3.10 BA samples do not have an enrichment of B cells. *(A) The hilum (n=49) had increased CD20 B cells compared to the wedge (n=49). (B(i)) This was also observed when comparing hilum to wedge and explant (n=17) samples. (B(ii)) Total lymphocytes were also increased in the hilum however (C) the ratio between total lymphocytes and CD20+ B cells showed no difference between sample location; hilum (n=17) (blue), wedge (n=17) (red) and explant (n=17) (grey). (D) Comparison of CD20 amongst other paediatric diseases showed that BA had a lower B cell infiltration. BA explant (n=17) (blue), SOAH explant (n=7) (red) and HHV6 explant (n=3) (green). (A) Wilcoxon test was used. (B(i) and C) Dunn's multiple comparisons test was used. (B(ii) Tukey's multiple comparisons test was used. (D) Dunnett's multiple comparisons test was used. p-value < 0.0332 (*), p-value < 0.0021 (**), p-value < 0.0001 (****).*

3.3.3 Lymphoid aggregates mostly contained CD20+ CD24- B cells and CD3+ T cells

Immunofluorescence was used to identify B cell subsets present within BA tissue. Lymph nodes from BA patients were used as positive controls **(figure 3.11A and 3.11B)** and IMCs were used as negative controls **(figure 3.12A-C)**. We stained for CD20 to identify B cells, CD24 to determine proportions of CD24+ and CD24- B cells following on from our adult B cell liver phenotyping, CD3 to identify lymphoid aggregates with high T cell frequencies and Bcl2 to identify any potential TLS, which do not contain Bcl2+ cells. To measure IL-6-expressing cells, we co-stained with anti-IL-6. Syndecan-1+ PBs/PCs were detected with anti-CD138.

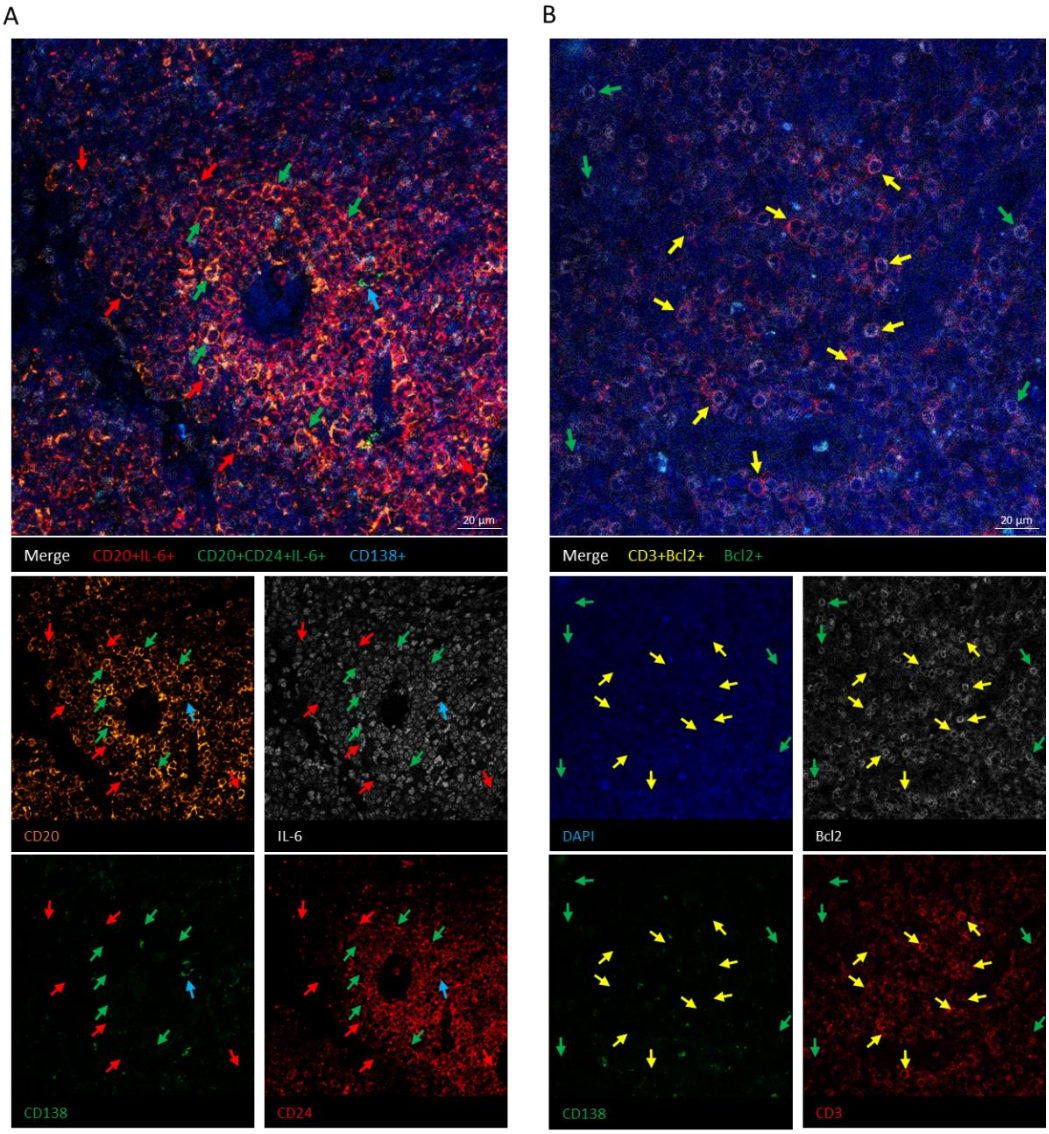


Figure 3.11 Immunofluorescence positive controls using BA lymph nodes. *BA hilum sample that contained lymph nodes was used as a positive control. Age at KPE was 52 days. (A) BA lymph node with panel 2 staining. CD20 (orange), IL-6 (white), CD138 (green) and CD24 (red). (B) Panel 3 staining on BA lymph nodes. DAPI (blue), Bcl2 (white), CD138 (green) and CD3 (red).*

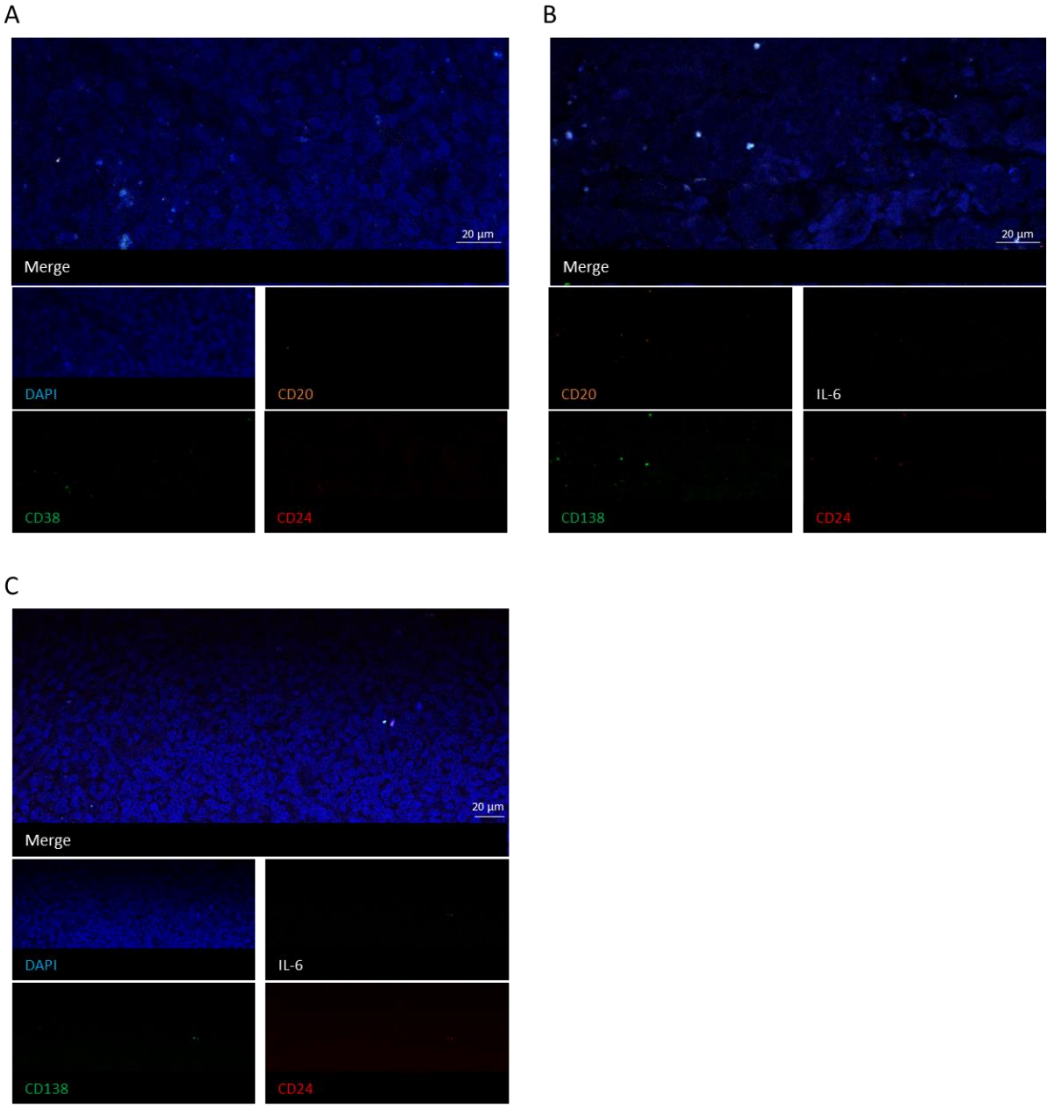


Figure 3.12 Immunofluorescence negative controls using IMC on BA lymph nodes. *BA hilum sample that contained lymph nodes was used as a negative control for IMC. Age at KPE was 48 days. (A – C) IMC was used as negative controls in BA tissue. (A) DAPI (blue), CD20 (orange), CD38 (green) and CD24 (red). (B) CD20 (orange), IL-6 (white), CD138 (green) and CD24 (red). (C) DAPI (blue), Bcl2 (white), CD138 (green) and CD3 (red).*

CD20+ B cells can be found around bile ducts **(figure 3.13A)** and within fibrotic tracts **(figure 3.13B)** as observed in IHC **(figure 3.7)**.

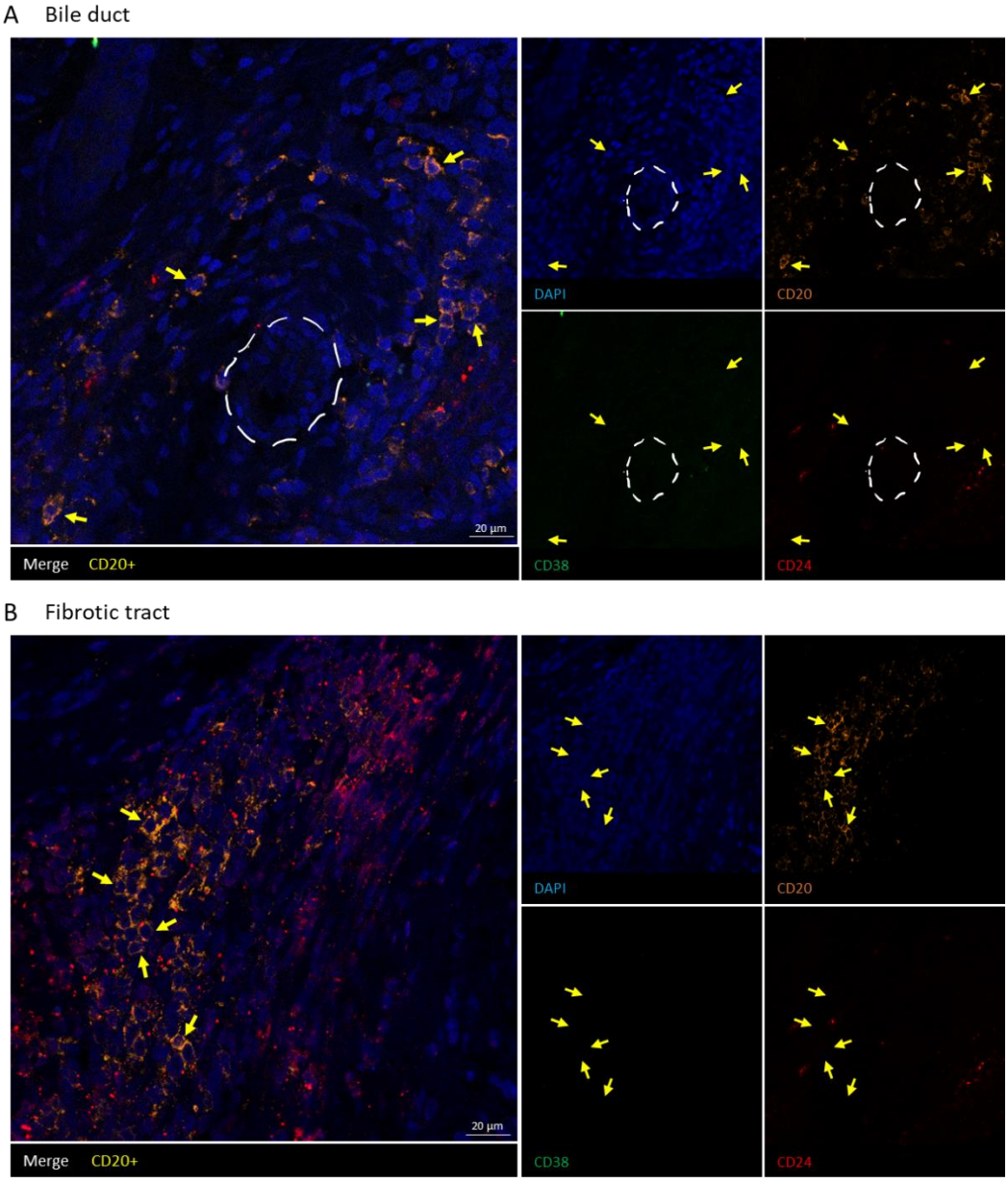


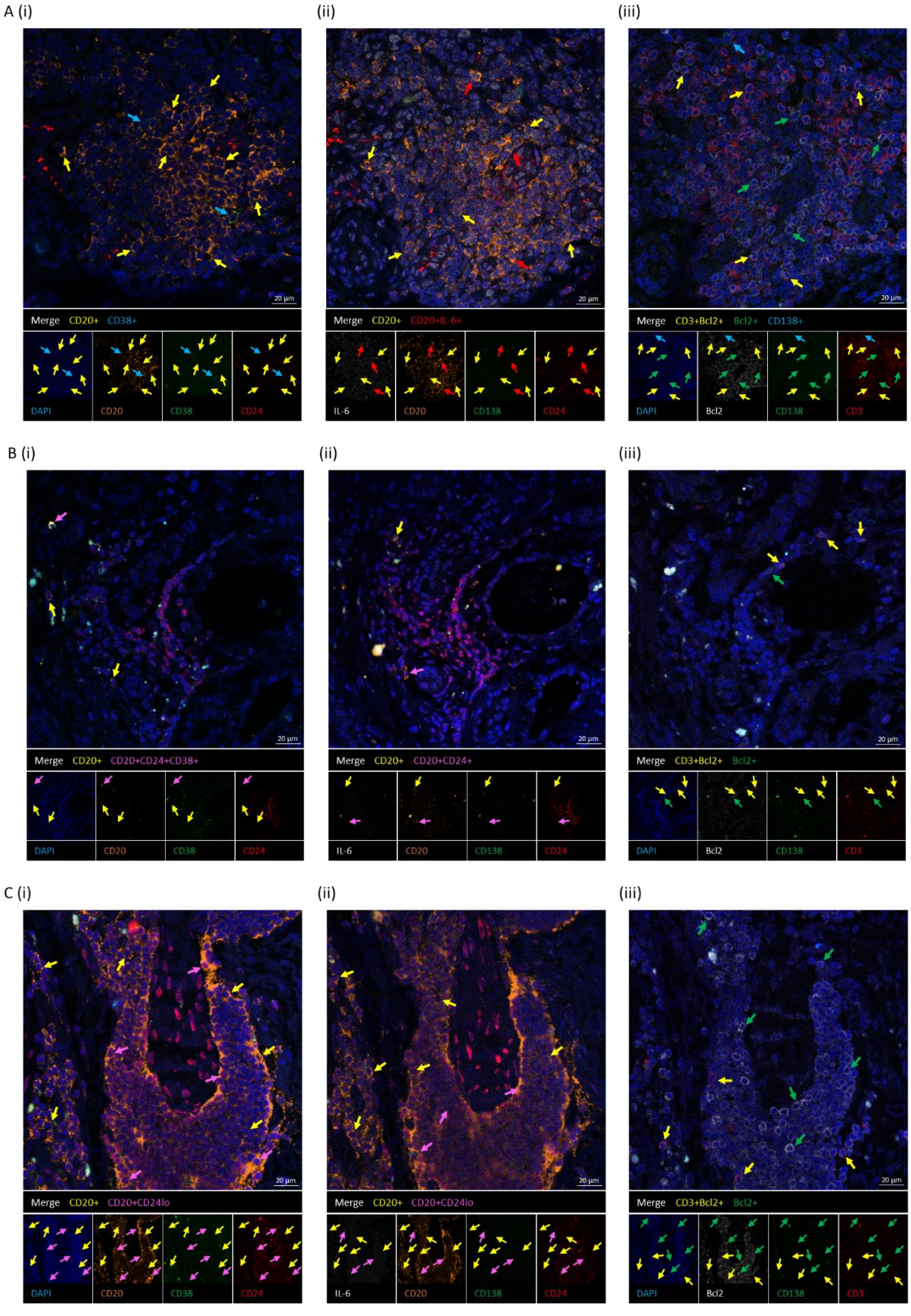
Figure 3.13 CD20+ B cells are found around bile ducts and in fibrotic tracts in BA tissue. *(A) CD20+ B cells were found around bile ducts (dashed white line). This sample was taken from BA hilum and the age of the patient at KPE was 37 days. DAPI (blue), CD20 (orange), CD38 (green) and CD24 (red). (B) B cells were also found in fibrotic tracts. This sample was taken from BA hilum and the age of the patient at KPE was 31 days. DAPI (blue), CD20 (orange), CD38 (green) and CD24 (red).*

Samples from the same patient from the hilum, wedge and explant were analysed using the three immunofluorescence panels **(table 3.3)**. CD20+ CD24- CD38- B cells made up majority

of the B cells within the aggregate in the hilum **(figure 3.14A(i))**. CD20+ CD24- B cells also expressed IL-6 **(figure 3.14A(ii))**. To differentiate between B cell aggregates and lymphoid aggregates, CD3 was used to identify T cells. In this aggregate, CD3+ T cells were dispersed within the B cells **(figure 3.14A(iii))** showing that this was a lymphoid aggregate. Bcl2 staining was used to identify GC-like structures. Bcl2+ cells were detected throughout the aggregate showing that this aggregate was not a GC-like structure **(figure 3.14A(iii))**.

In the wedge sample from the same patient, low amounts of CD20+ CD24- CD38- B cells were observed **(figure 3.14B(i))** and no IL-6+ cells were identified near the bile duct in this section of tissue **(figure 3.14B(ii))**. CD3+ T cells were also detected around the bile duct in this wedge sample **(figure 3.14B(iii))**.

Explant from this patient showed the presence of a B cell aggregate **(figure 3.14C)** and mixed immune cells surrounding a bile duct **(figure 3.14D)**. The explant tissue section containing the B cell aggregate consisted of mostly CD20+ CD24lo/- B cells **(figure 3.14C(i))** and these cells did not express IL-6 **(figure 3.14C(ii))** and were Bcl2+ **(figure 3.14C(iii))**. Furthermore, in this B cell aggregate CD3+ T cells were present around the periphery of the aggregate **(figure 3.14C(iii))**. The bile duct tissue section from the same patient explant sample showed the presence of CD20+ CD24- CD38- B cells **(figure 3.14D(i))** and majority of these CD20+ CD24- B cells were IL-6+ **(figure 3.14D(ii))**. An abundance of CD3+ T cells were also observed around the bile duct **(figure 3.14D(iii))**.


A (i)
(ii)
(iii)
Merge CD20+ CD38+
DAPI CD20 CD38 CD24
Merge CD20+ CD20+IL-6+
IL-6 CD20 CD138 CD24
Merge CD3+Bcl2+ Bcl2+ CD138+
DAPI Bcl2 CD138 CD3
B (i)
(ii)
(iii)
Merge CD20+ CD20+CD24+CD38+
DAPI CD20 CD38 CD24
Merge CD20+ CD20+CD24+
IL-6 CD20 CD138 CD24
Merge CD3+Bcl2+ Bcl2+
DAPI Bcl2 CD138 CD3
C (i)
(ii)
(iii)
Merge CD20+ CD20+CD24lo
DAPI CD20 CD38 CD24
Merge CD20+ CD20+CD24lo
IL-6 CD20 CD138 CD24
Merge CD3+Bcl2+ Bcl2+
DAPI Bcl2 CD138 CD3

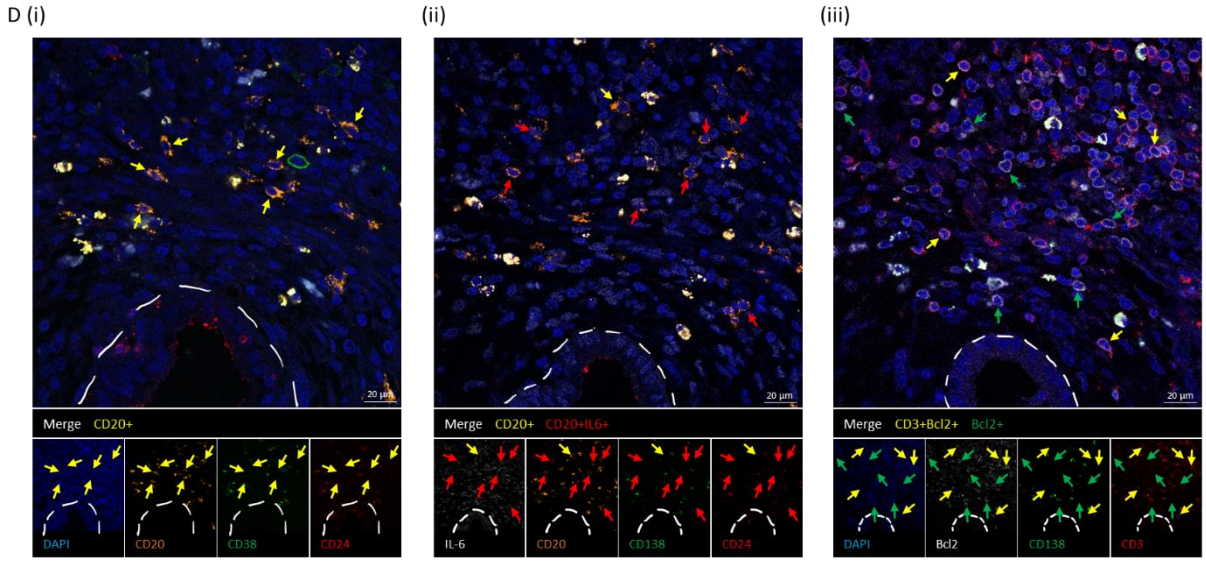


Figure 3.14 CD20+ CD24- B cells made up most of the aggregates and were IL-6+. *These images are from the hilum, wedge, and explant of one BA patient. Age at KPE was 31 days and age at transplant was 208 days. This figure showed (A) lymphoid aggregates in the hilum, (B) B cells in wedge samples, (C) B cell aggregates in explant tissue and (D) B cells in explant tissue which is what majority of BA explants look like across (i) panel 1, DAPI (blue), CD20 (orange), CD38 (green) and CD24 (red), (ii) panel 2, IL-6 (white), CD20 (orange), CD138 (green) and CD24 (red) and (iii) panel 3, DAPI (blue), Bcl2 (white), CD138 (green) and CD3 (red).*

Figure 3.14A showed that the aggregate contained a mixture of B and T cells indicating that this was a lymphoid aggregate. Analysis of a B cell aggregate from a different BA patient also showed that CD20+ CD24- B cells made up majority of the aggregate **(figure 3.15A(i))** alongside Bcl2+ cells and majority of the lymphocytes expressed IL-6, including CD20+ CD24- B cells **(figure 3.15A(ii))**. Bcl2 expression confirmed that this B cell aggregate was not a GC-like structure **(figure 3.15A(iii))**. CD3+ T cells are present surrounding the B cell aggregate **(figure 3.15A(iii))**.

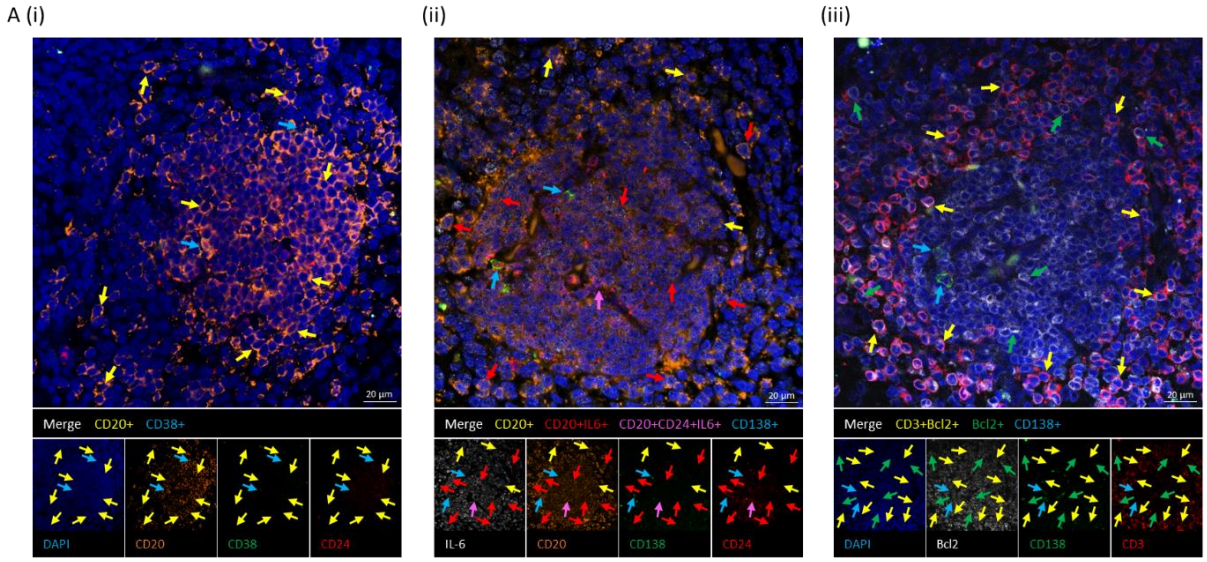


Figure 3.15 B cell express IL-6 in BA aggregates. *Another B cell aggregate from the hilum of a BA patient. Age at KPE was 57 days. This B cell aggregate was composed of a CD20+ B cell core surrounded by CD3+ T cells. The same aggregate was analysed using (i) panel 1, DAPI (blue), CD20 (orange), CD38 (green) and CD24 (red), (ii) panel 2, IL-6 (white), CD20 (orange), CD138 (green) and CD24 (red) and (iii) panel 3, DAPI (blue), Bcl2 (white), CD138 (green) and CD3 (red).*

3.3.4 Mixed immune infiltrate was observed surrounding bile ducts

The BA patient analysed in **Figure 3.14** showed mixed immune infiltrate surrounding bile ducts. B and T cells were detected around the bile duct in another BA patient sample **(figure 3.16)**. CD20+ CD24- CD38- B cells were present around the bile duct **(figure 3.16A(i))**, and majority of these infiltrates expressed IL-6 **(figure 3.16A(ii))**. High amounts of CD3+ T cells were also detected around the bile duct **(figure 3.16A(iii))**. An interesting observation showed that cholangiocytes themselves were IL-6+ **(figure 3.16A(ii))**. Cholangiocytes were identified by morphological identification of bile ducts.

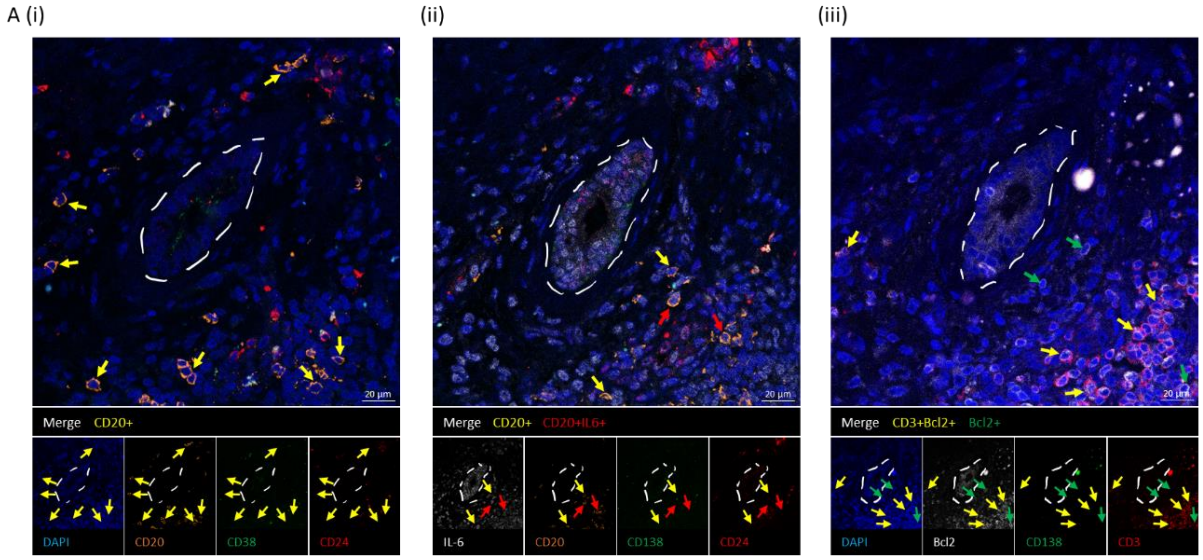


Figure 3.16 Mixed immune infiltrate is detected around bile ducts. *This sample was taken from the hilum of a BA patient. Age at KPE was 57 days. The immune cells around the bile duct (dashed white line) were analysed using (i) panel 1, DAPI (blue), CD20 (orange), CD38 (green) and CD24 (red), (ii) panel 2, IL-6 (white), CD20 (orange), CD138 (green) and CD24 (red) and (iii) panel 3, DAPI (blue), Bcl2 (white), CD138 (green) and CD3 (red). CD20+ B cells, CD20+ IL-6+ B cells and CD3+ T cells were detected around the bile ducts.*

3.3.5 Lymphoid aggregates and mixed immune infiltrates were observed in adult livers

BA is a cholestatic liver disease, as we had no access to other paediatric cholestatic livers, we made the decision to compare BA to adult cholestatic liver diseases (PBC and PSC). The presence of lymphoid aggregates was also observed in adult PBC livers **(figure 3.17)**. Most of this lymphoid aggregate consisted of CD20+ CD24- B cells **(figure 3.167(i) and 3.167(ii))** with CD3+ T cells dispersed amongst the B cells **(figure 3.17A(iii))**.

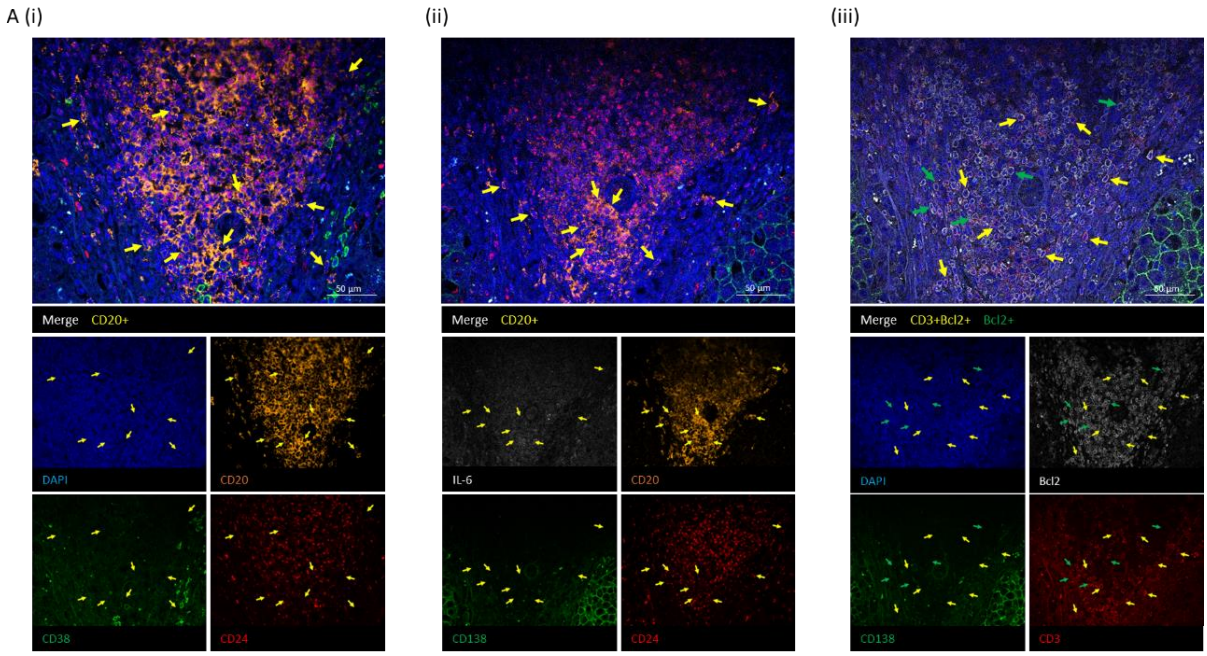


Figure 3.17 Aggregates were also found in adult cholestatic livers*. Representative images of a lymphoid aggregate in adult PBC liver tissue for (i) panel 1, DAPI (blue), CD20 (orange), CD38 (green) and CD24 (red), (ii) panel 2, IL-6 (white), CD20 (orange), CD138 (green) and CD24 (red) and (iii) panel 3, DAPI (blue), Bcl2 (white), CD138 (green) and CD3 (red).*

Mixed immune infiltrate was also located near bile ducts **(figure 3.18)**. Majority of the surrounding B cells consisted of CD20+ CD24- B cells **(figure 3.18A(i))** with CD3+ T cells mixed amongst the infiltrates **(figure 3.18A(iii))**. These lymphoid aggregates also had the presence of CD138+ PCs **(figure 3.18A(ii) and 3.18A(iii))** suggesting that these cells produced autoantibodies, as CD138 is a PC marker, and could contribute to disease pathogenesis in adult cholestatic liver diseases.

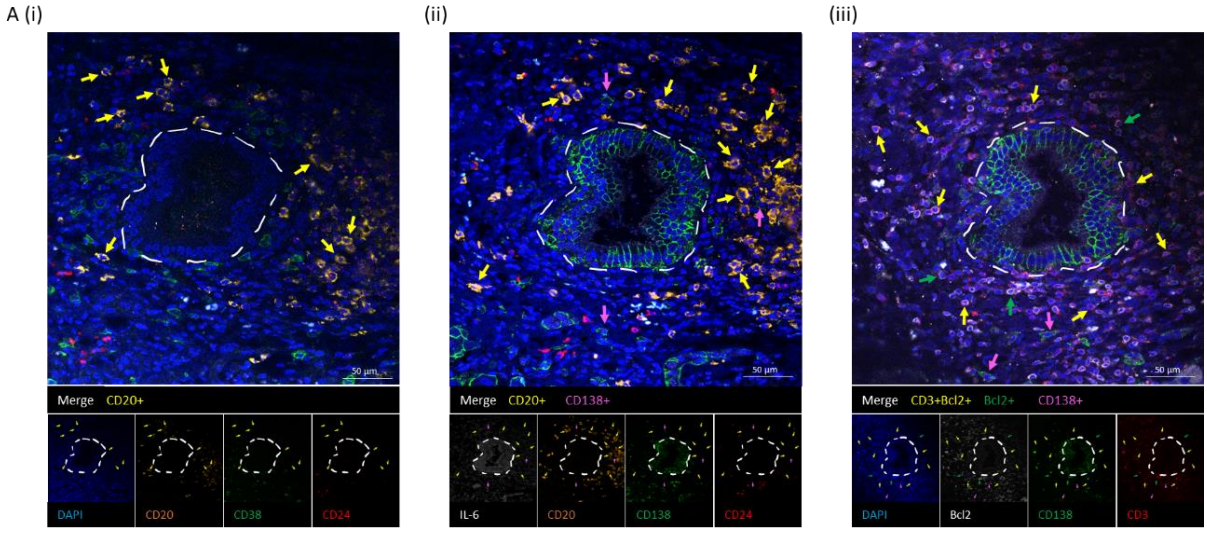


Figure 3.18 Mixed immune infiltrate was also detected in adult cholestatic livers. *Representative images showing mixed immune infiltrate was detected around the bile duct (dashed white line) in adult PBC liver tissue in (i) panel 1, DAPI (blue), CD20 (orange), CD38 (green) and CD24 (red), (ii) panel 2, IL-6 (white), CD20 (orange), CD138 (green) and CD24 (red) and (iii) panel 3, DAPI (blue), Bcl2 (white), CD138 (green) and CD3 (red).*

Adult cholestatic livers also showed the presence of IL-6 **(figure 3.19A)** however IL-6 was not present in all adult livers analysed **(figure 3.19B)**.

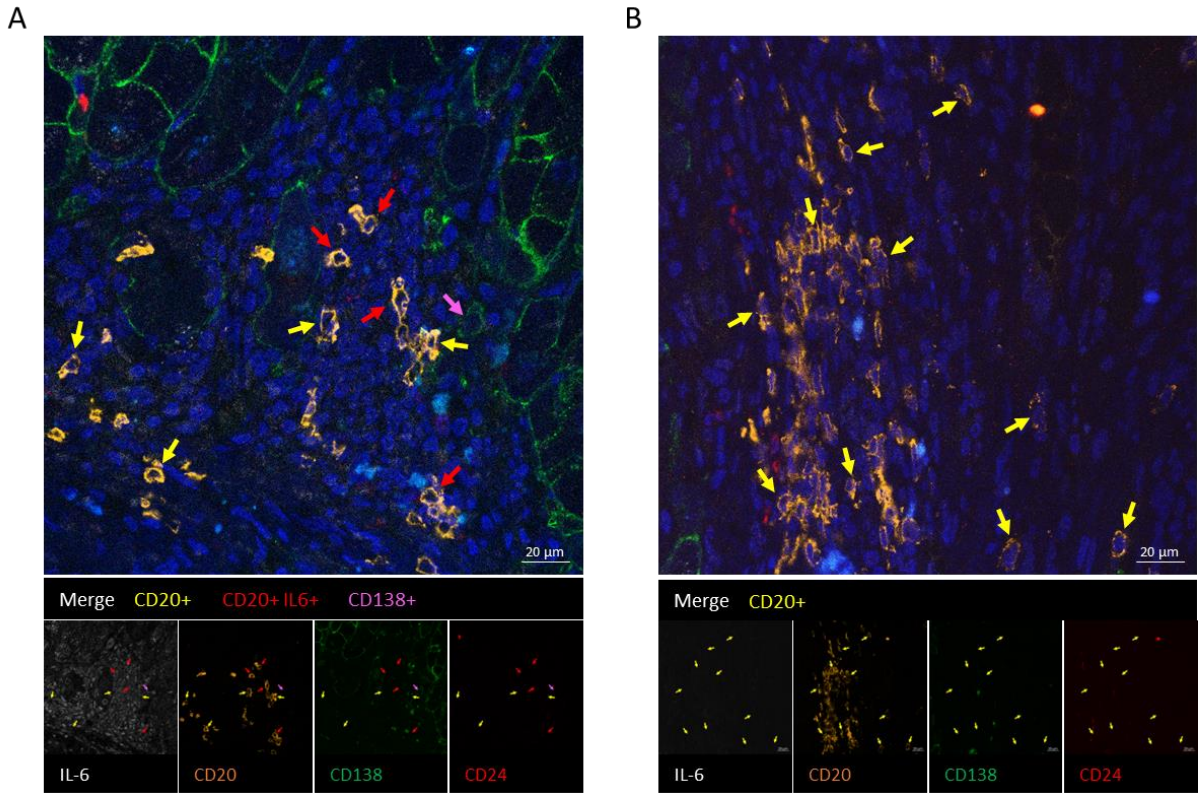
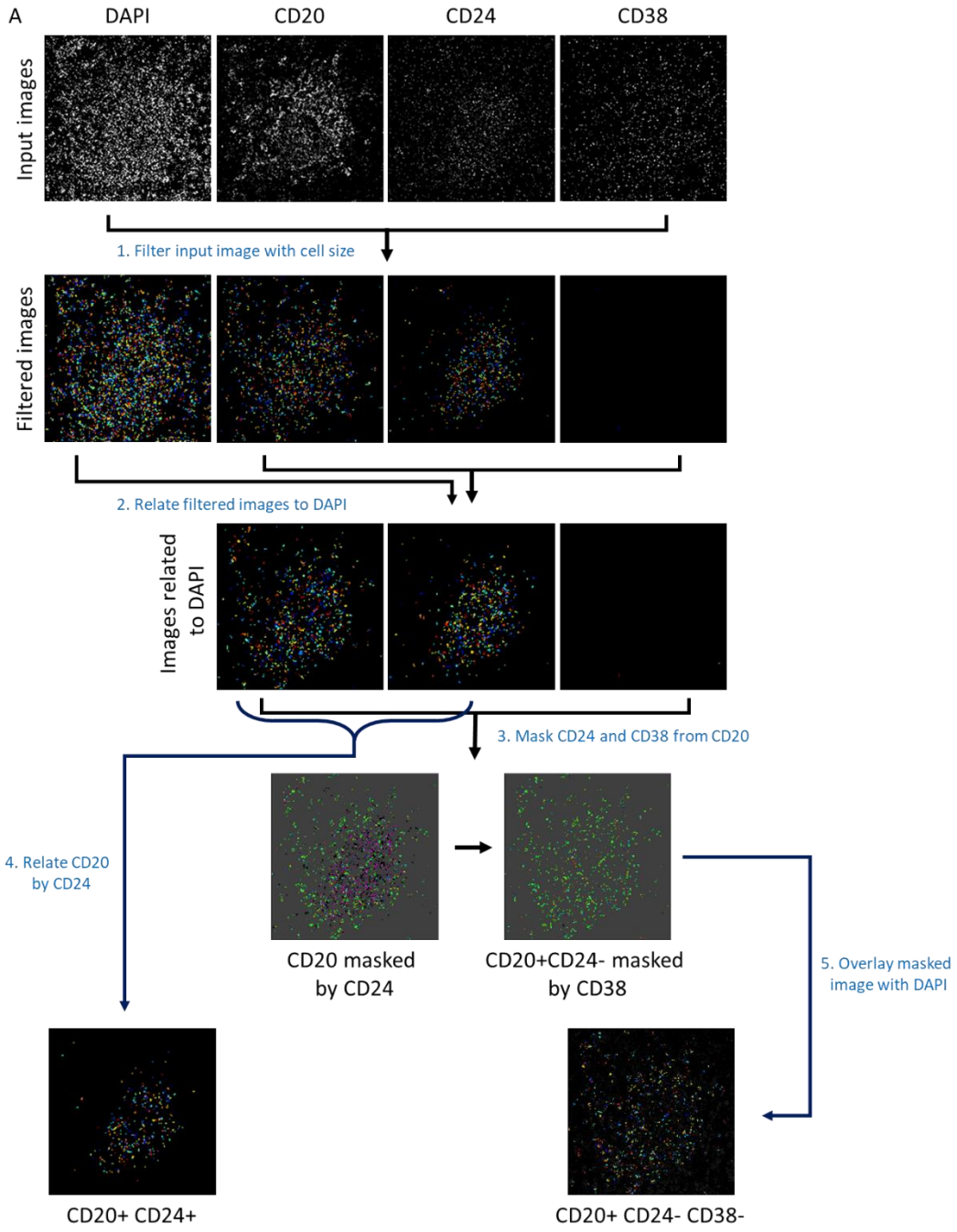


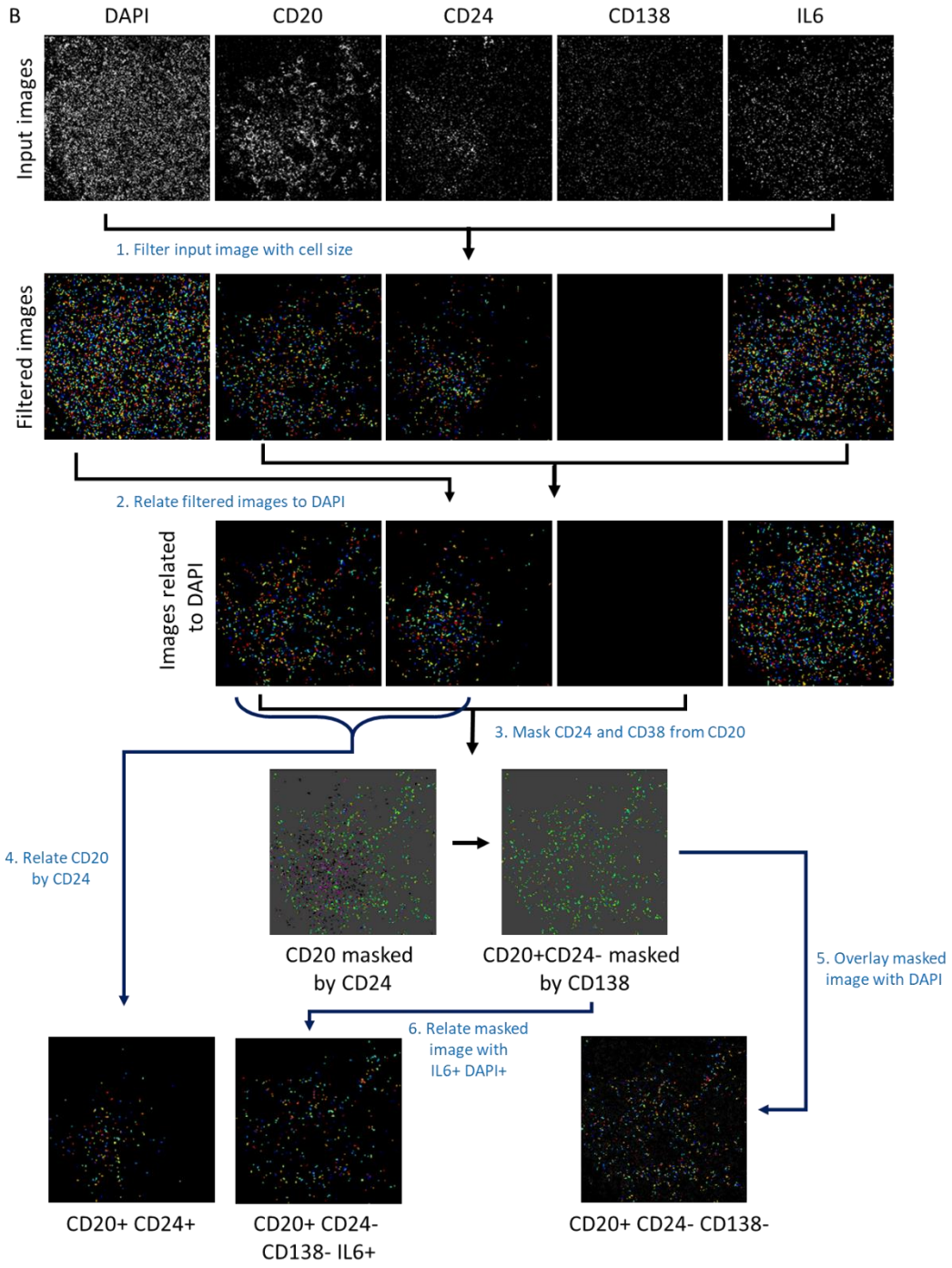
Figure 3.19 CD20+ IL-6+ B cells can be found in adult cholestatic livers but are not present in all. *Representative images showed (A) IL-6+ B cells can be found in adult PBC livers and (B) that CD20+ B cells were present in the fibrotic tract of adult PSC livers.*

3.3.6 CellProfiler was used to quantify B cell subsets present in the liver

Immunofluorescence image sections provide qualitative data on the location of B cells. CellProfiler was used to quantify counts of B cell subsets present within each immunofluorescence single stain image from all the BA samples and locations. The cell profiler pipeline for each panel is shown in **Figure 3.20**. Each marker was filtered to remove background noise and these filtered images were combined with DAPI to identify live cells that were positive for each marker. From this point CD20 images were masked with CD24+ and CD38+ cells in panel 1 **(figure 3.20A)** and CD24+ and CD138+ in panel 2 **(figure 3.20B)** to get CD20+ CD24- B cells. For panel 3, Bcl2 images were masked with CD3 and vice versa

(figure 3.20C). CellProfiler counts for CD20+ CD24+ B cells, CD20+ CD24- B cells, CD20+ CD24- IL-6+ B cells, Bcl2+ CD3- cells and CD3+ T cells were quantified.




B
DAPI
CD20
CD24
CD138
IL6
Input images
1. Filter input image with cell size
Filtered images
2. Relate filtered images to DAPI
Images related to DAPI
3. Mask CD24 and CD38 from CD20
4. Relate CD20 by CD24
CD20 masked by CD24
CD20+CD24- masked by CD138
5. Overlay masked image with DAPI
6. Relate masked image with IL6+ DAPI+
CD20+ CD24+
CD20+ CD24- CD138- IL6+
CD20+ CD24- CD138-

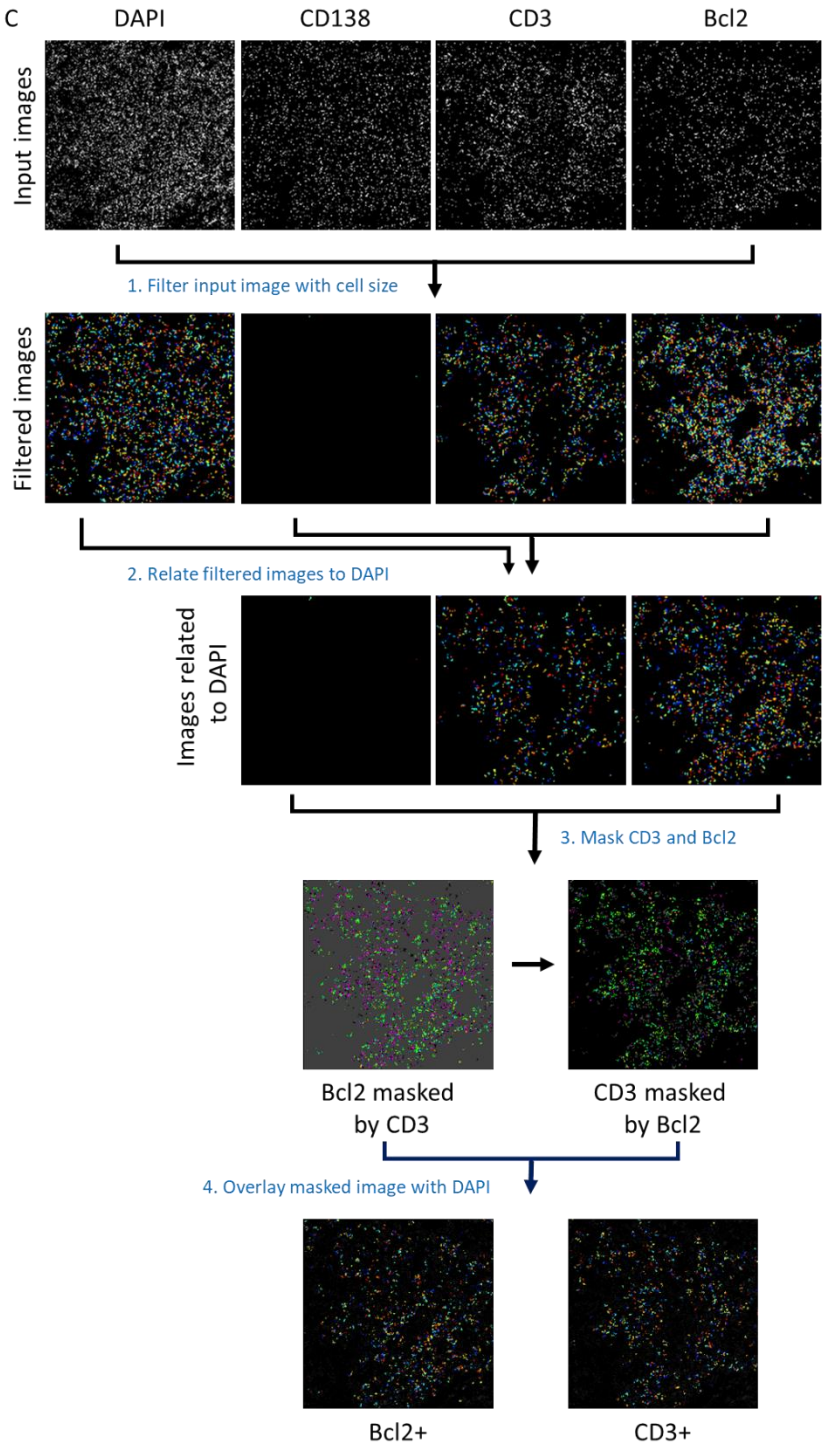


Figure 3.20 CellProfiler pipeline used to quantify B cell subsets. *CellProfiler pipeline for (A) panel 1, (B) panel 2, and (C) panel 3. Cells were identified based on single colour images and related to DAPI for live cells. Downstream analysis categorised pixel data into the different subsets analysed; CD20+ CD24+ B cells, CD20+ CD24- B cells, CD20+ CD24- IL-6+ B cells, Bcl2+ CD3- cells and CD3+ cells.*

CellProfiler created images based on the information obtained from the pipeline, showing all the different subsets, helping to clarify and focus what is observed in the raw immunofluorescence images **(figure 3.21)**. The raw images for the three panels **(figure 3.21A)** were put through the pipelines and figures were composed based on the subsets of interest **(figure 3.21B)**. The counts of each subset were normalised to DAPI and then plotted onto a stack chart to show the distribution of subsets across each image **(figure 3.21C)**. CD20+ CD24- B cells made up majority of the subsets detected in lymphoid aggregates along with Bcl2+ CD3- cells, suggesting that this aggregate was not a TLS. Whilst majority of aggregates consisted of Bcl2+ CD3- cells, these cells were not B cell specific and encompass all cells that were Bcl2+ CD3-. This lymphoid aggregate also contained CD20+ CD24- IL-6+ cells and a small portion of the cells in the aggregate were CD3+ T cells **(figure 3.21C)**.

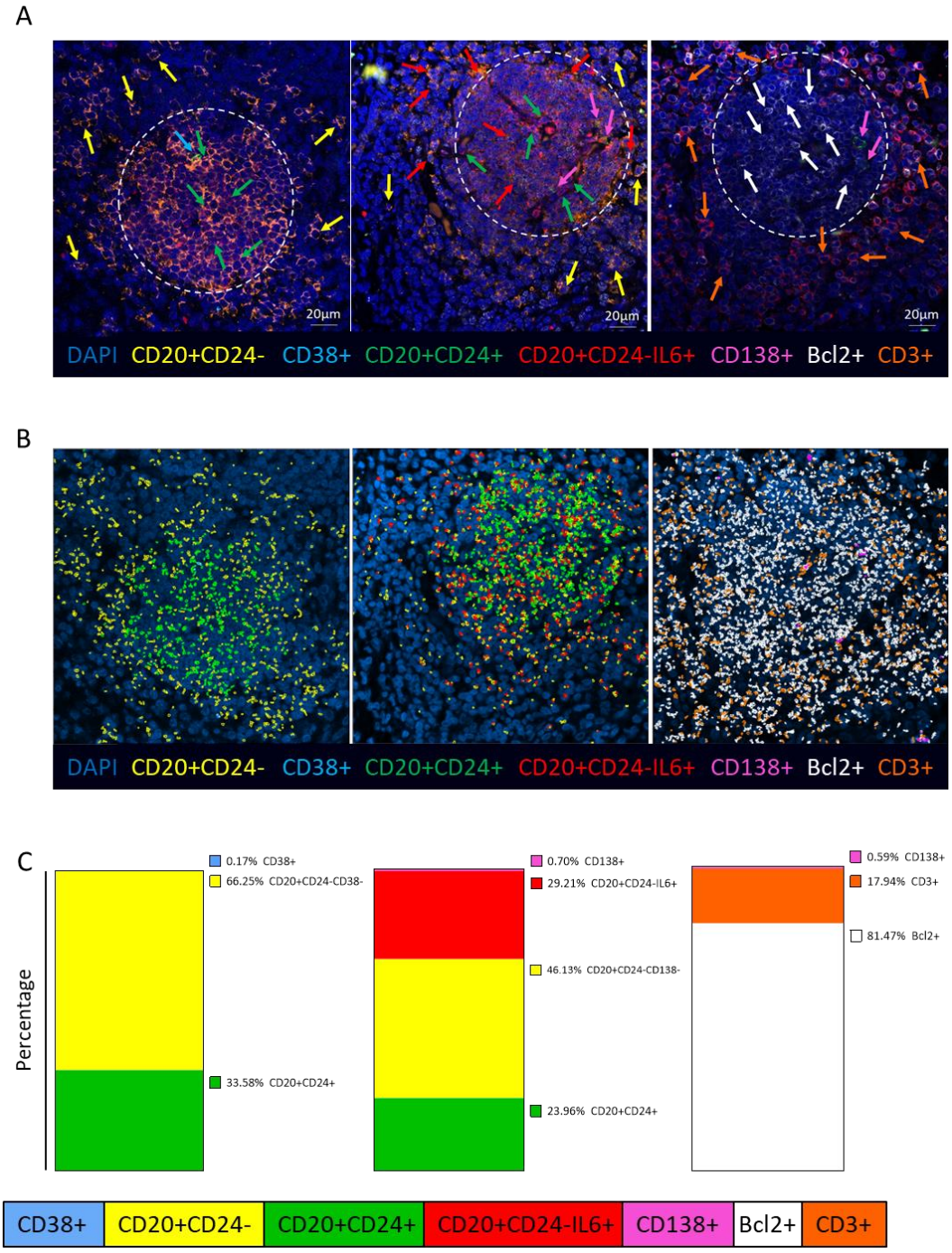


Figure 3.21 CD20+ CD24- B cells make up majority of the B cells in this lymphoid aggregate. *(A) Representative immunofluorescence panels on a lymphoid aggregate from the hilum of a BA patients who was 57 days old. (B) CellProfiler images composed to pixel subset data obtained from the pipeline for all three panels. (C) Stack charts created using normalised subset data to visualise the subsets present in each panel image analysed. The percentages for each subset are shown. DAPI (blue), CD20+ CD24- B cells (yellow), CD20+ CD24+ B cells (green), CD20+ CD24- IL-6+ B cells (red), CD138+ plasma cells (pink), Bcl2+ cells (white) and CD3+ T cells (orange).*

Subset count data was analysed in adult and BA liver tissue sections **(figure 3.22)**. Subset data as percentages of total DAPI+ cells was plotted for IMC **(figure 3.22A)**, positive control **(figure 3.22B)** and paediatric and adult livers. The distribution of subsets was significantly different in adult cholestatic liver diseases **(figure 3.22C)**, BA hilum **(figure 3.22D)**, wedge **(figure 3.22E)** and explant livers **(figure 3.22F)**. Significant differences were observed between subset expression for all liver samples analysed **(figure 3.22)**. **Table 3.5** shows the p-values for all significant comparisons.

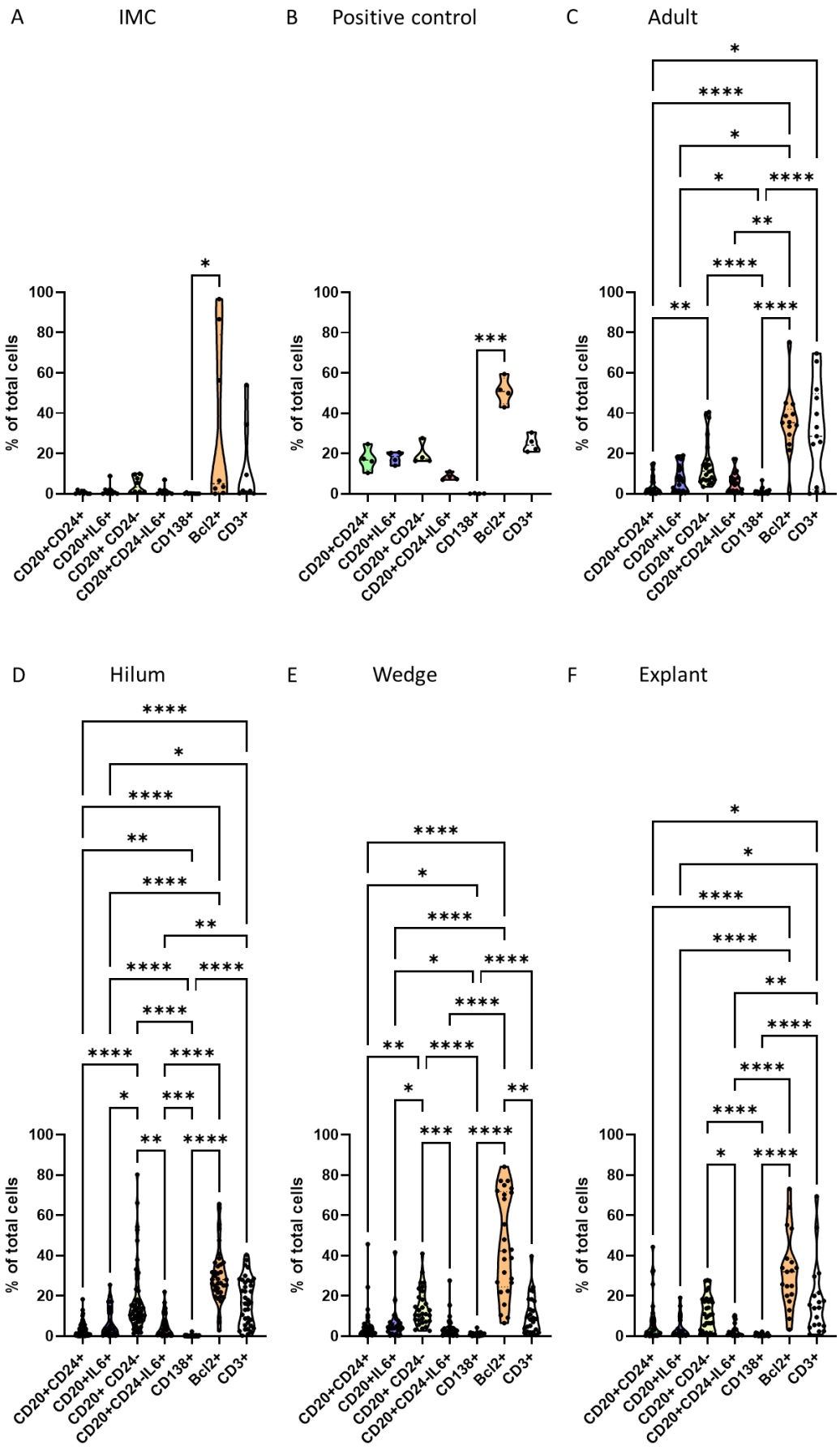

A
IMC
B
Positive control
C
Adult
D
Hilum
E
Wedge
F
Explant
% of total cells
CD20+CD24+
CD20+IL6+
CD20+ CD24-
CD20+CD24-IL6+
CD138+
Bcl2+
CD3+

Figure 3.22 Lymphocyte subsets present at early and late stage in BA. *Subsets analysed in (A) IMC and (B) positive controls, (C) adult PBC and PSC liver explants, (D) BA hilum, (E) wedge and (F) explant samples. Similar expression of subsets were detected across all liver samples analysed. Significant differences were observed between subsets. (A-F) Dunn's multiple comparisons test was used. p-value < 0.0332 (*), p-value < 0.0021 (**), p-value < 0.0002 (***), p-value < 0.0001 (****).*

Table 3.5 The p-values for the comparisons shown in Figure 3.22 are shown in this table. *Adults, BA hilum, wedge and explant samples were analysed, and the frequencies of subsets were compared to each other to test for significance. This table shows the significant p-values amongst the different subsets compared.*

Sample type	**Comparison between subsets**	**p-value**
Adult livers	CD20+CD24+ vs. CD20+ CD24-	0.0087
	CD20+CD24+ vs. Bcl2+	<0.0001
	CD20+CD24+ vs. CD3+	0.0188
	CD20+ CD24- vs. CD138+	<0.0001
	CD20+CD24-IL-6+ vs. Bcl2+	0.0021
	CD138+ vs. Bcl2+	<0.0001
	CD138+ vs. CD3+	<0.0001
	CD138+ vs. CD20+IL-6+	0.0128
	Bcl2+ vs. CD20+IL-6+	0.0207
Hilum	CD20+CD24+ vs. CD20+ CD24-	<0.0001
	CD20+CD24+ vs. CD138+	0.0026
	CD20+CD24+ vs. Bcl2+	<0.0001
	CD20+CD24+ vs. CD3+	<0.0001
	CD20+ CD24- vs. CD20+CD24-IL-6+	0.0011
	CD20+ CD24- vs. CD138+	<0.0001
	CD20+ CD24- vs. CD20+IL-6+	0.0164
	CD20+CD24-IL-6+ vs. CD138+	0.0009
	CD20+CD24-IL-6+ vs. Bcl2+	<0.0001
	CD20+CD24-IL-6+ vs. CD3+	0.0019

	CD138+ vs. Bcl2+	<0.0001
	CD138+ vs. CD3+	<0.0001
	CD138+ vs. CD20+IL-6+	<0.0001
	Bcl2+ vs. CD20+IL-6+	<0.0001
	CD3+ vs. CD20+IL-6+	0.0218
Wedge	CD20+CD24+ vs. CD20+ CD24-	0.0050
	CD20+CD24+ vs. CD138+	0.0167
	CD20+CD24+ vs. Bcl2+	<0.0001
	CD20+ CD24- vs. CD20+CD24-IL-6+	0.0004
	CD20+ CD24- vs. CD138+	<0.0001
	CD20+ CD24- vs. CD20+IL-6+	0.0229
	CD20+CD24-IL-6+ vs. Bcl2+	<0.0001
	CD138+ vs. Bcl2+	<0.0001
	CD138+ vs. CD3+	<0.0001
	CD138+ vs. CD20+IL-6+	0.0160
	Bcl2+ vs. CD3+	0.0036
	Bcl2+ vs. CD20+IL-6+	<0.0001
Explant	CD20+CD24+ vs. Bcl2+	<0.0001
	CD20+CD24+ vs. CD3+	0.0344
	CD20+ CD24- vs. CD20+CD24-IL-6+	0.0261
	CD20+ CD24- vs. CD138+	<0.0001
	CD20+CD24-IL-6+ vs. Bcl2+	<0.0001
	CD20+CD24-IL-6+ vs. CD3+	0.0052
	CD138+ vs. Bcl2+	<0.0001
	CD138+ vs. CD3+	<0.0001
	Bcl2+ vs. CD20+IL-6+	<0.0001
	CD3+ vs. CD20+IL-6+	0.0468

Subsets were analysed for each adult and BA liver samples **(figure 3.23)**. No differences were observed in the distribution of CD20+ CD24+ B cells **(figure 3.23A)**, CD20+ CD24- B cells **(figure 3.23B)**, CD20+ CD24- IL-6+ **(figure 3.23C)**, Bcl2+ CD3- cells **(figure 3.23E)** and CD3+ T cells **(figure 3.23F)** between adult cholestatic liver explants and BA hilum, wedge, and explant samples. CD138+ PCs were significantly different between hilum and wedge (p-value <0.0001), explant (p-value 0.0161) and adult liver samples (p-value 0.0009) **(figure 3.23D)**, however the number of PCs measured in these tissues was very low.

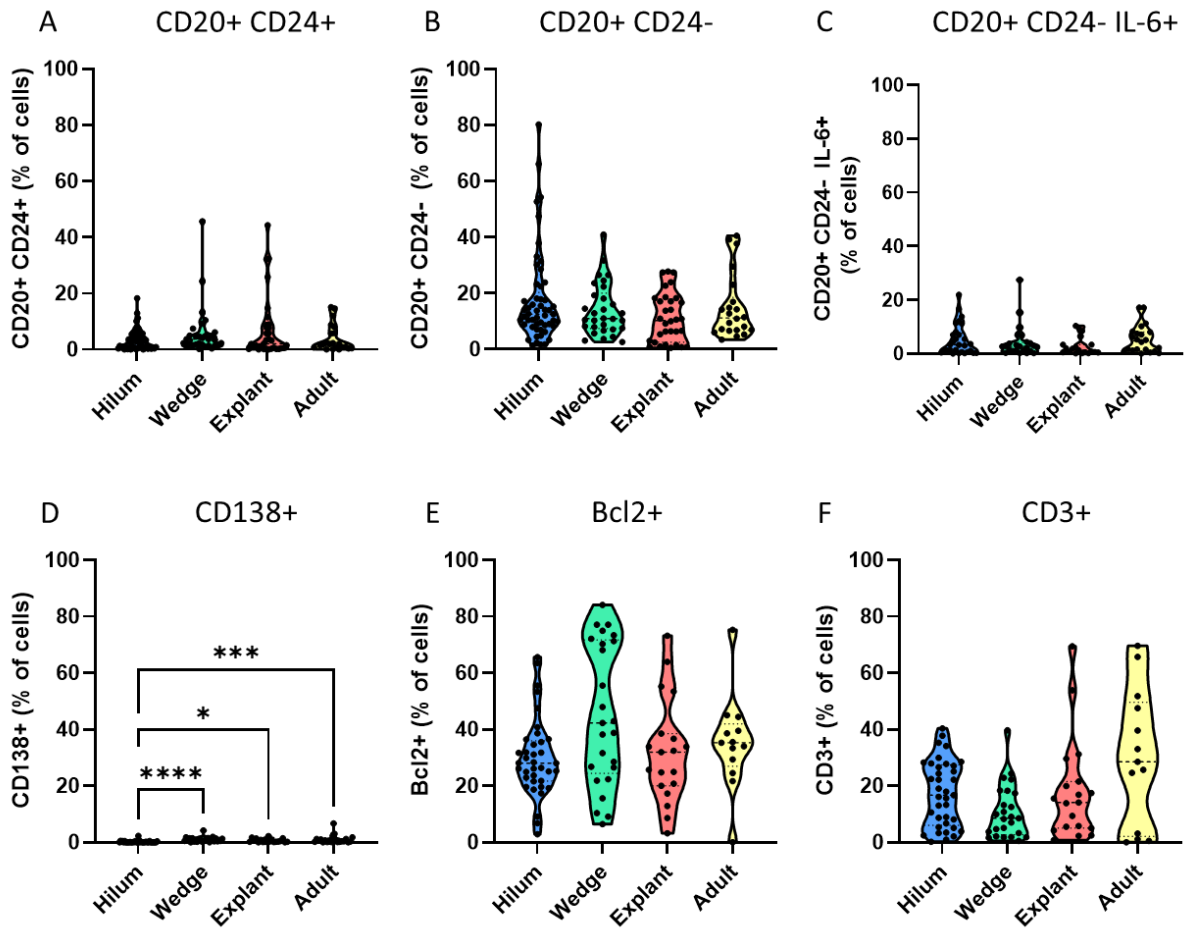


Figure 3.23 No differences were observed in subset expression amongst adult and paediatric livers. *Subset expression analysis was carried out for (A) CD20+ CD24+ B cells, (B) CD20+ CD24- B cells, (C) CD20+ CD24- IL-6+ B cells, hilum (n=53), wedge (n=30), explant (n=32) and adult livers (n=22) (D) CD138+ plasma cells, hilum (n=37), wedge (n=26), explant (n=19) and adult livers (n=22) (E) Bcl2+ CD3- cells and (F) CD3+ T cells hilum (n=37), wedge*

(n=25), explant (n=19) and adult livers (n=13), between BA hilum (blue), wedge (red), explant (purple) and adult cholestatic liver diseases (green). Only CD138+ cells showed significant differences however their percentage expression was low for all samples. (A-F) Dunn's multiple comparisons test was used. p-value < 0.0332 (*), p-value < 0.0002 (***), p-value < 0.0001 (****).

Subsets were compared between non-syndromic and syndromic BA patients for hilum, wedge, and explant liver samples **(appendix 6)**. These data showed no difference between these two groups. A significant difference was detected for CD138 percentage expression between syndromic hilum and syndromic wedge samples (p-value <0.0001) **(appendix 6D)**.

Taken together, these data showed that BA patients had higher lymphocytic infiltration in the hilum compared to wedge and explant. CD20+ CD24- B cells made up majority of the B cell subsets present in BA tissue, within B cell and lymphoid aggregates and around bile ducts. These B cells also expressed IL-6 suggesting that they contribute to inflammation. Furthermore, there was no difference between non-syndromic and syndromic BA patients for the frequencies of subsets present in the liver.

3.4 Discussion

BA is a paediatric disease where samples can be obtained during early disease, at the time of KPE and at end-stage disease, at the time of liver transplantation, giving a unique opportunity to investigate B cell subset incidence in disease progression.

It is not understood if liver damage commences in the biliary tree or the liver periphery for many patients. The hilum region was different from the periphery in early and end-stage disease as the hilum had increased B cells **(figure 3.10A and 3.10B(i))** and immune infiltrates **(figure 3.10B(ii))** which may be due to the close proximity of the hilum to the hepatic artery and portal vein (Rogers and Dintzis, 2012). On the other hand, increased immune infiltrates at the hilar region may indicate ongoing disease.

Furthermore, B cell aggregates were detected in the hilar region in BA samples **(figure 3.9A)** but not in BA wedge samples **(figure 3.9B)** suggesting that the hilum was the site of inflammation in paediatric cholestatic liver diseases. Majority of BA explant samples had no presence of B cell aggregates **(figure 3.9C(ii))** however 5 out of 18 BA patients showed the presence of B cell aggregates during end-stage liver disease **(figure 3.9C(i))** suggesting that B cell aggregates may contribute to disease pathology.

Our BA cohort consisted of 31 females and 24 males between the ages of 22-116 days. Fibrosis status in these patients ranged from no fibrosis to mild/moderate fibrosis. 27 BA patients had the presence of B cells and/or lymphoid aggregates in the hilum. Of these patients, 13 were males and 14 were females showing no difference between sex for the presence of B cell and/or lymphoid aggregates. Patients with B cell and/or lymphoid

aggregates were between 22-77 days old at the time of KPE. The clinical data available does not explain the heterogeneous profiles observed in our cohort of BA patients.

3.4.1 Characterisation of lymphoid aggregates

Characterisation of these aggregates showed that many of the aggregates were lymphoid aggregates. CD20+ CD24- B cells and Bcl2+ cells made up majority of the lymphoid aggregates with few CD3+ T cells dispersed amongst the core and with CD3+ T cells also surrounding the lymphoid aggregates in BA samples **(figure 3.14A, 3.15)** and in adults explanted liver samples **(figure 3.17)**. This composition of lymphoid aggregates was also observed in patients with IBD and colorectal cancer (Nascimbeni et al., 2005), in chronic HCV patients (Dhingra et al., 2016) and in HCV liver biopsies where CD4+ T cells were dispersed amongst the lymphoid aggregates and CD8+ cytotoxic T cells were present surrounding the lymphoid aggregates (Freni et al., 1995). This implies that lymphoid aggregates may contribute to disease pathology through the cytotoxic effects of CD8+ T cells present. In addition, CD4+ T cells may provide T cell help to B cells inducing their differentiation into effector B cells however further characterisation of these aggregates using multiparametric techniques is required to elucidate their roles in disease.

3.4.2 Lymphoid aggregates in disease

The presence of lymphoid aggregates was not disease specific indicating that they may contribute to pathogenesis across many different adult and paediatric diseases. Lymphoid aggregates have also been detected in paediatric patients with gastrointestinal problems (Mansueto et al., 2012, Carpentieri et al., 2000, Jaskiewicz and Kobierska, 2000, Kara et al., 2014) however there was no association between lymphoid aggregates and clinical

symptoms (Mansueto et al., 2012). Liver biopsies from adult acute HCV hepatitis showed that lymphoid aggregates were found near bile ducts and these lymphoid aggregates were associated with biliary epithelium injury (Dhingra et al., 2016). Furthermore, Akyol et al., found that bile duct damage was detected in 45% of HCV biopsies and 27% of HBV biopsies and both groups had the presence of lymphoid aggregates (Akyol et al., 2001). No correlation analyses were done to investigate the association between lymphoid aggregate formation and bile duct damage however, we hypothesise that lymphoid aggregates may contribute to bile duct damage as they expressed IL-6+ B cells. Naemi et al., stated that lymphoid aggregates, from BM biopsies, were made up of B cells surrounded by T cells, which were negative for GC formation and had an increased tendency to be malignant (Naemi et al., 2013). This suggests that lymphoid aggregates observed in the hilum may be pathogenic and contribute to inflammation and fibrosis resulting in the requirement of liver transplant. Furthermore, if these lymphoid aggregates contribute to tissue injury, they could be recruiting more immune cells which would explain why the hilum had increased immune infiltrates in BA patients. The presence of these aggregates shows the potential of these inflammatory lesions to be B cell driven. The microenvironment in the hilum may support B cell proliferation and aggregation through the production of cytokines instead of antigenic stimulation. Hilar aggregates help identify a subset of BA patients which may benefit from anti-inflammatory treatment.

Lymphoid aggregates analysed consisted mainly of CD20+ CD24- B cells and a subset of these B cells produced IL-6 **(figure 3.14A, 3.15 and 3.21C)** implying a role of CD20+ CD24- B cells in BA pathogenesis. CD20+ CD24- B cells and CD20+ CD24- IL-6+ B cells were also present in lymphoid aggregates observed in adult cholestatic liver diseases **(figure 3.17)** suggesting that

they contribute to paediatric and adult liver disease pathology through the production of IL-6, which is a pro-inflammatory cytokine (Widjaja et al., 2020) and these lymphoid aggregates were not disease specific. Inflammatory cytokines also target cholangiocytes in autoimmunity and infections and under chronic inflammation, damage the biliary epithelium which results in the proliferation of bile ducts, 'ductular reaction' (Yamagiwa Y, 2000-2013). Ductular reaction was also observed in BA livers **(figure 3.7D)** indicating that pro-inflammatory cytokines are damaging the biliary epithelia resulting in increased cholangiocyte proliferation. Cholangiocytes themselves may also contribute to liver injury as they secrete IL-6 **(figure 3.16)**. Increased IL-6 secretion was observed from cholangiocytes during inflammation (Yamagiwa Y, 2000-2013, Pinto et al., 2018). Furthermore, IL-6 production by cholangiocytes may contribute to the repair of tissue damage (Pinto et al., 2018) however, during chronic inflammatory disease, altered IL-6 expression resulted in proliferation of cholangiocytes (Yamagiwa Y, 2000-2013) and induced increased IL-6 secretion contributing to liver injury. These lymphoid aggregates observed in BA livers were not GC-like as they expressed Bcl2 **(figure 3.14A, 3.15 and 3.23E)** which was also the case for lymphoid aggregates present in adult liver diseases **(figure 3.17 and 3.23E)**. Furthermore, low CD138+ B cells were present in the hilum **(figure 3.23D)** supporting the data that GC-like structures were not present in paediatric and adult cholestatic livers.

3.4.3 Mixed immune infiltrates observed in livers

Mixed immune infiltrate was observed around bile ducts in BA samples **(figure 3.14D and 3.16)** and in adult livers **(figure 3.18)** suggesting that inflammation in these diseases was not purely driven by B cells. Human BA samples showed increased mRNA expression of Th1 cytokines (IFN-γ, TNF-α, IL-2 and IL-12) in the portal tracts of patients at the time of diagnosis

(Mack et al., 2004). RRV-induced mouse models of BA showed elevated amounts of CD4+ T cells, CD8+ T cells and IFN-γ one week post RRV injection (Mack et al., 2005) corroborating data shown in human BA. Furthermore, RRV-induced mice showed that the loss of *Ifng* resulted in the diminished tropism of lymphocytes to bile ducts, preventing the development of BA (Shivakumar et al., 2004). This all suggests that both cellular and humoral immune responses contribute to the progression of BA.

BA patients had increased immune infiltration in the hilum region compared to the periphery. Furthermore, the hilum was where most of the lymphoid aggregates were found. These lymphoid aggregates consisted of CD20+ CD24- B cells and CD3+ T cells. In majority of these lymphoid aggregates, CD20+ CD24- B cells expressed IL-6 which may contribute to pathogenicity of the aggregates. Furthermore, lymphoid aggregates were surrounded by T cells which could also contribute to disease pathology.

3.5 Conclusions

Due to COVID I was unable to obtain fresh paediatric tissue to characterise the B cell compartment using flow cytometry however I was able to characterise existing FFPE tissue sections. To my knowledge, this was the first time when multi-parametric approached have been used to investigate B cells in the hilum compared to liver periphery in BA. I was also able to investigate B cell subsets in early disease and compare them to explant samples. Adult and children had similar phenotypes in the B cell subsets present during end-stage disease **(figure 3.22 and 3.23)**. Lymphoid aggregates were in their majority Bcl2+ CD3-, and CD20+ CD24- B cells were frequent. CD138+ B cells were rare, indicating a reduced incidence of antigen-specific responses in BA tissues. Often, B cells expressed IL-6. As B cells lacked

centre stage in tissues from our BA patient cohort, it was important to characterise the inflammatory infiltrate more broadly and in more detail. From this chapter, using the CD20 screening of BA sections to identify livers with inflammatory aggregates, I chose BA patients to further characterise using transcriptomics analyses.

CHAPTER 4 – DIFFERENTIAL GENE EXPRESSION IN BILIARY ATRESIA

4.1 Introduction

BA can be split into syndromic and non-syndromic BA (Patel et al., 2021). Syndromic BA is also known as embryonic BA or BA with splenic malformation (BASM) syndrome (Chu et al., 2012). These patients display vascular and cardiac anomalies and appear to have failed development of extrahepatic bile ducts (Lakshminarayanan and Davenport, 2016). Syndromic BA occurs during the first trimester and is thought to have a developmental origin and patients with syndromic BA had a worse prognosis compared to non-syndromic BA patients (Ortiz-Perez et al., 2020). Non-syndromic or isolated BA is the most common BA which does not have any distinguishing features (Lakshminarayanan and Davenport, 2016) and symptoms begin to show after birth (Ortiz-Perez et al., 2020). Identifying differences in genetic profiles between non-syndromic and syndromic BA patients will help to stratify patients and provide targeted therapies to these patients.

4.1.1 Transcriptomic studies in BA

There are limited transcriptomic studies examining BA samples from early disease to end-stage disease. Studies using BALB/c mice infected with rotavirus showed differential gene expression during disease progression (Carvalho et al., 2005). At the onset of injury, *IRF7* and *IRF9* genes were expressed however, at the time of duct obstruction, IFN-γ and IFN-γ related genes such as *STAT1*, *CXCL9*, and *CXCL10* were expressed indicating a pro-inflammatory environment during early BA (Carvalho et al., 2005). Single cell RNA sequencing, carried out in 3 patients with BA identified 11 main lineages including B cells, T cells, natural killer T (NKT) cells, fibroblasts, hepatocytes, and BECs using published gene signatures for each lineage (Ye et al., 2022). The B cell subsets identified in these BA samples included

transitional B cells, immature B cells, naïve B cells and PBs/PCs. Transitional B cells were found in fibrotic niches alongside NKT cells, and these subsets were enriched for fibroblast proliferation suggesting that they contribute to fibrosis and pathogenesis in BA (Ye et al., 2022). Chemokine signalling, TLR signalling, inflammatory response and immune response genes were enriched in six BA explanted liver samples (Min et al., 2020). This study identified 98 differentially regulated genes between BA explants and controls. *CXCL5* and *IL8* were upregulated in BA samples alongside genes associated with hepatic fibrosis: *EPHB2* and *ANXA2* (Min et al., 2020) implying that at end-stage disease, there is increased hepatic fibrosis. The upregulation of *CXCL5* and *IL8* was consistent with the pathogenesis of non-syndromic BA (Bessho and Bezerra, 2011). RNA isolated from the liver tissue of BA patients had upregulated *IL6R* and *C6* and downregulated *MMP7* in BA samples (Xiao et al., 2014). The literature has shown that several inflammatory related genes such as *IFNG* (Bezerra et al., 2002, Vejchapipat et al., 2012, Narayanaswamy et al., 2007), *STAT1* (Carvalho et al., 2005) and *IL18* (Vejchapipat et al., 2012) were differentially expressed in BA samples. The activation of these genes can induce innate immunity and modulate the activation of antigen-specific acquired immunity (Iordanskaia et al., 2013, Saito et al., 2011). It is difficult to work out if the inflammatory response is causal or a consequence of BA-related tissue damage using gene expression analyses, and this is where comparative studies between well-characterised syndromic and non-syndromic cohorts would be useful. Microarray analysis found genes involved in hepatic development, morphogenesis and fibrogenesis to be differentially expressed in BA patients compared to normal and diseased controls (Chen et al., 2003).

4.1.2 Nanostring nCounter panels

Studies investigating hepatocellular carcinoma have used Nanostring technologies to identify prognostic genes in liver samples (Hoshida et al., 2013, Crouchet et al., 2021, Hsu et al., 2021). Studies have also investigated liver diseases such as NAFLD (Kriss et al., 2020) and PBC (Hardie et al., 2016). The Nanostring human immunology v2 code set was used to define transcriptional changes in early NAFLD (Kriss et al., 2020). This transcriptomic study found that osteopontin (OPN) and CXCL10 genes were upregulated in early non-fibrotic NAFLD and that this may be useful as non-invasive biomarkers to detect early NAFLD (Kriss et al., 2020). The Nanostring panCancer panel was used to identify genetic profiles to help stratify PBC patients to improve their care (Hardie et al., 2016).

The Nanostring nCounter human organ transplant (HOT) panel was created in collaboration with Banff Foundation for Allograft Pathology and profiles 770 genes across 37 different pathways (Nanostring, 2020, Mengel et al., 2020). The benefit of this panel is that RNA isolated from FFPE archival tissue can be used. Many studies using the HOT panel have investigated kidney tissue (Smith, 2021, Smith et al., 2023, Rosales et al., 2022, Gambella et al., 2021) however, no studies using this panel have investigated liver tissue. There is no literature on the HOT panel being used to investigate transcriptomics in liver tissue, specifically in paediatric liver tissue. Hardie et al., showed that even at early stage of PBC, high risk patients were biologically different to low-risk patients. Using the HOT panel, we may be able to highlight differences in biology between non-syndromic and syndromic BA which would help tailor their care accordingly. Furthermore, transcriptomics can help identify differences in early disease, compared to end-stage disease.

4.1.3 Aims and objectives

The progression of liver fibrosis in BA occurs rapidly compared to other adult and paediatric liver diseases (Ye et al., 2022) and identifying genetic signatures would be beneficial to elucidate immune signalling pathways that are upregulated in BA compared to other adult and paediatric liver diseases. The literature lacks gene expression studies in the liver during disease progression compared to end-stage disease for BA. Comparative analyses between hilum and liver periphery are also lacking. We had access to a well-characterised patient cohort of syndromic and non-syndromic BA, with FFPE liver biopsy samples from the hilum and liver periphery obtained during KPE, and additional biopsy material from end-stage-disease from the same children, which was obtained from their liver explant tissue.

Objectives

In this chapter, we used the Nanostring Human Organ Transplant v2 panel, and we set out to:

1. Identify distinct inflammatory gene expression profiles between non-syndromic and syndromic BA patients
2. Identify differences in genetic signatures between early-stage BA and end-stage disease
3. Detect differences in gene expression between hilum, wedge and explant BA samples

4.2 Methodology

4.2.1 Paediatric liver samples

Total RNA was isolated from paediatric scrolls from non-syndromic (n=3) and syndromic (n=3) BA patients using the protocol mentioned in 4.2.2.2. These BA patients were the same patients analysed using IHC and IF in chapter 3. Scrolls were taken from the hilum, wedge, and explant regions from patients with end-stage liver disease undergoing transplantation and at the time of KPE, at the Birmingham Children's Hospital, Birmingham. All samples were obtained from the liver unit tissue bank registry (South West – Central Bristol Research ethics committee approval reference 17/SW/0073). Clinical data for these patients is available in **Appendix table 2**.

4.2.2 RNA isolation

4.2.2.1 PureLink FFPE Total RNA Isolation Kit

10 µm scrolls were cut from paraffin blocks by Dr Gary Reynolds and placed into sterile RNase free 1.5 ml Eppendorf tubes. The PureLink FFPE RNA isolation kit was used to determine whether the number of scrolls, the age of the samples and the incubation time would affect RNA quality and yield. Melting buffer was added to each tube and incubated for 10 minutes at 75°C with intermittent mixing every couple of minutes to melt the paraffin. Proteinase K was added to the tubes and incubated at 60°C for 10 – 60 minutes, according to incubation time. Each sample had 2, 4 and 6 scrolls, each incubated for 10, 20, 30, 40 and 60 minutes to determine the most effective incubation time. These samples were obtained from two different years to assess RNA yield based on the age of the samples alongside the number of scrolls required for a high yield of RNA.

At the end of the incubation time the tubes were centrifuged at maximum speed for 1 minute to separate the tissue lysate from the paraffin layer. Using a clean RNase free pipette, the paraffin layer was penetrated, and the tissue lysate was aspirated and transferred to a clean RNase free tube. Binding buffer and 100% ethanol were added to the tubes prior to transferring the solution to a spin cartridge. The tubes were centrifuged at 800 RCF for 1 minute and the flow through was discarded. The tubes were washed with wash buffer three times before the spin cartridge was centrifuged at maximum speed for 1 minute to remove any residual wash buffer. 30 µl RNase free water (pre-heated to 65°C) was added to the centre of the spin cartridge and incubated at room temperature for 1 minute. The cartridge was placed into RNase free 1.5 ml Eppendorf tubes and centrifuged at maximum speed for 1 minute. The isolated total RNA was quantified using the nanophotometer and nanodrop **(table 4.1)** before being store at - 80°C.

Table 4.1 RNA quantity and quality results. *Two samples from different years were analysed using different numbers of scrolls and different incubation times, to get the best quality of isolated RNA with the highest yield. Samples were quantified on the nanophotometer; NP, and the nanodrop; ND to gain a better understanding of RNA quality and quantity.*

Sample year	Sample	RNA yield (ng/ul)		260/280 Ratio		260/230 Ratio	
		ND	NP	ND	NP	ND	NP
2018	2 scrolls 10 min	4.5	-	1.28	-	0.34	-
	2 scrolls 20 min	14.0	20.0	1.55	3.333	0.48	0.370
	2 scrolls 30 min	14.2	10.0	1.53	-	0.31	0.167
	2 scrolls 40 min	8.0	4.0	1.54	-	0.29	-

	2 scrolls 60 min	51.0	40.0	1.53	1.818	0.23	0.137
	4 scrolls 10 min	3.7	2.0	1.88	-	0.05	-
	4 scrolls 20 min	11.1	4.0	1.70	-	0.26	0.77
	4 scrolls 30 min	24.4	26.0	1.55	1.625	0.15	0.115
	4 scrolls 40 min	21.5	18.0	1.70	-	0.11	0.067
	4 scrolls 60 min	68.6	62	1.52	1.722	0.6	0.425
	6 scrolls 10 min	17.9	18.0	1.27	2.250	0.25	0.191
	6 scrolls 20 min	27.6	20.0	1.18	2	0.22	0.12
	6 scrolls 30 min	19.7	16.0	1.54	2	0.41	0.444
	6 scrolls 40 min	8.8	2.0	1.81	-	0.1	0.018
	6 scrolls 60 min	68.7	58.0	1.63	1.812	0.77	0.580
2020	2 scrolls 10 min	5.7	2.0	1.24	-	0.41	-
	2 scrolls 20 min	8.4	2.0	1.71	-	0.06	-
	2 scrolls 30 min	16.1	8.0	1.61	-	0.77	0.4
	2 scrolls 40 min	23.9	26.0	1.67	3.250	0.22	0.167
	2 scrolls 60 min	27.0	16.0	1.64	-	0.59	0.308
	4 scrolls 10 min	6.3	2.0	1.7	1	0.26	0.071

	4 scrolls 20 min	10.2	12.0	1.44	-	0.11	0.097
	4 scrolls 30 min	24.6	18.0	1.54	-	0.41	0.231
	4 scrolls 40 min	16.8	26.0	1.58	1.857	0.25	0.310
	4 scrolls 60 min	43.9	46.0	1.76	1.643	0.32	0.235
	6 scrolls 10 min	11.1	8.0	1.50	-	0.13	0.071
	6 scrolls 20 min	13.1	14.0	1.63	-	0.04	0.022
	6 scrolls 30 min	27.9	22.0	1.67	-	0.44	0.262
	6 scrolls 40 min	16.2	16.0	1.45	2.667	0.31	0.333
	6 scrolls 60 min	74.1	68.0	1.61	1.789	0.68	0.548

The RNA yields were plotted for each number of scrolls **(figure 4.1)** from data obtained from the nanophotometer and nanodrop. The age of the sample did not affect RNA yield as samples obtained from 2018 and 2020 were similar in their quantity of RNA isolated. The number of scrolls required for a good RNA yield was a minimum of 6 scrolls incubated for 60 minutes.

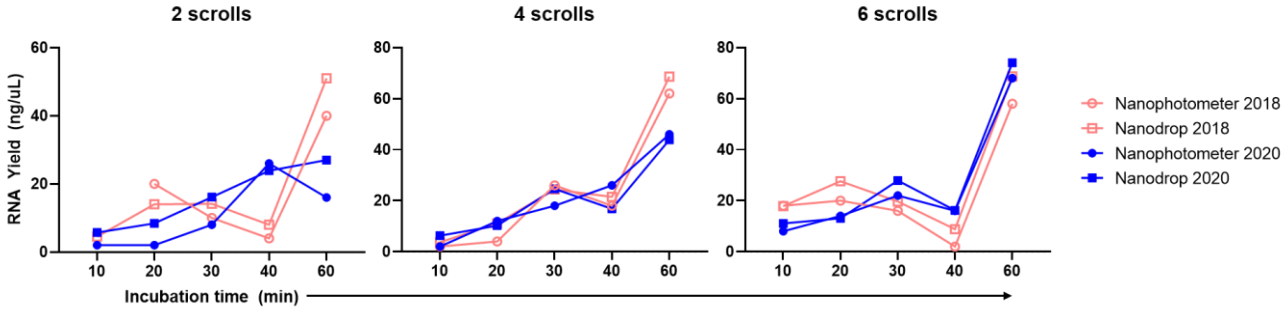


Figure 4.1 RNA optimisation using different numbers of scrolls and different incubation times to get the best RNA yield. *RNA was quantified using the nanophotometer and the nanodrop to assess RNA yield. Samples were used from two different years to assess if age impacted the quality of RNA; it did not. Different number of scrolls were used to determine how many scrolls were needed for the best RNA yield. From this data we needed a minimum of 6 scrolls to get a good RNA yield.*

Quality of RNA is determined by the 260/280 and 260/230 ratios. The 260/280 ratio determines amount of protein contamination with ratios lower than 2.1 indicating protein contamination that can artificially increase RNA quantity measurement. The 260/230 ratio indicates the presence of organic contaminants. Ratios lower than 1.8 have a lot of contamination that can interfere with downstream applications (Nanostring, 2021b). The ideal 260/80 and 260/230 ratios should be as close to 2 as possible. The quality of RNA isolated using the PureLink FFPE RNA isolation kit was not ideal for downstream applications **(table 4.1)** as the samples were contaminated with organic contaminants indicated by the low 260/230 ratios. Nanostring was contacted for advice on how to improve RNA yield and quality and the High Pure RNA isolation kit was suggested.

4.2.2.2 High Pure FFPET RNA Isolation Kit

10 µm scrolls were cut and place into sterile RNase free 1.5 ml Eppendorf tubes. Xylene and absolute ethanol were added to the tubes before being centrifuged at max speed for 2

minutes. 1 ml of absolute ethanol was added to the tubes and centrifuged at max speed for 2 minutes before being blotted onto tissue o remove any ethanol residues. The tubes were heated at 55°C for 10 – 20 minutes with open lids to dry the tissue pellets. RNA tissue lysis buffer, 10% SDS and proteinase K were added to each deparaffinised tissue pellets and incubated at 85°C for 30 minutes. The tubes were then placed on ice to cool them down to 55°C. Proteinase K was added to the tubes and incubated at 55°C for 30 minutes. The tubes were centrifuged at maximum speed for 1 minutes and the supernatant was removed. RNA binding buffer and absolute ethanol were added to the tissue lysates. The lysate solution was transferred to a high pure filter tube and centrifuged at 6000 RCF for 30 seconds. The filter fleece was centrifuged at maximum speed for 2 minutes to dry the fleece prior to the addition of DNase working solution. The tubes were incubated for 15 minutes at room temperature. The tubes were washed with wash buffer 1 and washed twice with wash buffer 2 and the supernatant was removed. The tubes were further centrifuged at 16,000 RCF for 2 minutes to dry the filter fleece. 10-30 µl of elution buffer was added to the centre of the fleece and incubated for 1 minute at room temperature before being centrifuged at 6000 RCF for 1 minute. Total RNA was quantified using the nanodrop **(table 4.2)** before being stored at - 80°C. For this optimisation, different numbers of scrolls were taken from biliary atresia wedge samples as these were the samples with the smallest tissue input size.

Table 4.2 High Pure FFPET RNA isolation kit results. *This kit isolated RNA of a good quality and quantity. The higher the number of scrolls used, the better the RNA yield.*

Number of 10µm scrolls	RNA yield (ng/µl)	260/280 ratio	260/230 ratio
1	21.1	1.81	1.03
2	17.3	2.095	2.065
3	40.8	2.12	1.47
4	38.45	1.92	0.39
6	60.6	1.98	0.48
8	72.0	1.97	0.86

The results showed that the higher the number of scrolls, the higher the yield of RNA **(figure 4.2)**. Furthermore, this new kit had better 260/280 ratios and improved 260/230 ratios.

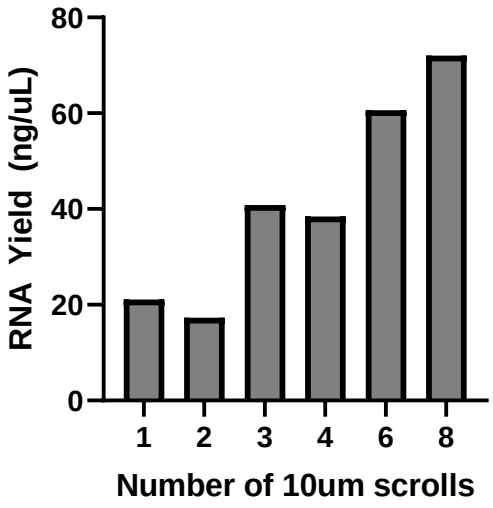


Figure 4.2 RNA yield using the high pure FFPET RNA isolation kit. *RNA yield increased with increasing number of scrolls. The High Pure FFPET RNA isolation kit extracted RNA with improved 260/230 and 260/280 ratios which meant that the RNA was of a good quality with minimal contaminants present.*

RNA was then isolated from selected paediatric liver FFPE scrolls using the high pure RNA isolation kit and quality checked before being sent off to Nanostring.

4.2.2.3 Quality check for isolated total RNA

The RNA samples were quality checked on the Qubit and Tapestation by the Genomics Birmingham Facility **(Appendix table 5)**. Nanostring use the DV200% to determine fragmentation levels in the sample and adjust RNA input accordingly (Nanostring, 2021b). The DV200 is the percentage of fragments that are above 200 nucleotides (Matsubara et al., 2020). The RNA samples were then aliquoted in 10 µl and sent to Nanostring for the nCounter HOT panel assay.

4.2.3 Nanostring nCounter Human Organ Transplant v2 panel

The nCounter HOT panel detects the expression of up to 770 genes and is compatible with RNA isolated from FFPE scrolls. A total RNA input of 300 ng is required for the nCounter run. Specific genes targets of interest were hybridised with reporter code set and capture probe set pipetted into each sample tube. The tubes were mixed by inversion and placed into a pre-heated 65°C thermal cycles and incubated for 16-24 hours for hybridisation reactions to occur. The strip tubes were then loaded onto a nCounter prep station (Nanostring, 2022).

The reagents used for the prep station were equilibrated to room temperature before being processed on the prep station. The prep station prepares the samples for data collection on the digital analyser by performing liquid transfers, magnetic bead separations and immobilisation of molecular labels on the sample cartridge surface. The nCounter digital analyser is a multi-channel epifluorescence scanner that takes images of the immobilised fluorescent reporters in the sample cartridge. The standard data resolution collects 280

fields of views per cartridge lane and the output files contain reporter code counts. These output files were analysed using the nSolver analysis software that also quality checks the data (Nanostring, 2021a).

4.2.4 Statistical analysis

GraphPad Prism 9.4.1 was used to create graphs and perform statistical analysis. The Shapiro-Wilk normality test was used to assess the normal distribution of my samples **(figure 2.4)**. This test calculates the ratio between the standard deviation of our data to the computed standard deviation of the slope from the QQ plot generated for our data. Normality tests were used to determine the statistical tests carried out on our data. Dunnett's T3 multiple comparisons test was used to analyse statistical significance between unpaired, normally distributed samples. Dunn's multiple comparisons test was used to analyse unpaired samples that were not normally distributed.

4.3 Results

Enrichment of B cells was detected in the hilum of BA patients compared to the peripheral samples, alongside lymphoid aggregates containing T cells, and measurable inflammatory infiltrates. We next set out to measure gene expression profiles in children with BA, with a focus on markers of inflammation. We used tissue from the hilum and liver periphery obtained during KPE and compared it to tissue from the same children obtained at end-stage disease during orthotopic liver transplantation. The Nanostring nCounter HOT panel was used to identify gene expression profiles from different cellular pathways of the immune response in BA and to identify any differences between non-syndromic and syndromic disease.

4.3.1 BCR signalling genes were differentially expressed between the hilum and the periphery

We were interested to compare gene expression profiles in patients with non-syndromic vs syndromic BA, to identify signatures of potential immune-driven disease. First, BCR signalling genes were investigated to find any differences between signalling in the hilum, wedge, and explant. Differential gene expression was observed between hilum and peripheral samples in genes related to BCR signalling **(figure 4.3A)**. *CD19* gene expression was higher in the hilum for both non-syndromic and syndromic BA patients **(figure 4.3B)**. Total lymphocytic infiltrate was analysed using CD45 gene *PTPRC*, which was also more abundant in the hilum compared to the periphery **(figure 4.3C)**. *CD79A* which encodes a BCR protein was higher in the hilum **(figure 4.3D)** and *CD22*, which encodes a BCR accessory signalling component (Hatta et al., 1999) was more abundant in the hilum compared to the periphery **(figure 4.3E)**. These data

showed that the hilum had evidence of increased B cell and immune cell infiltration compared to peripheral liver tissue obtained during disease progression, and during end-stage disease. B cell activation signatures were consistently more prominent in the hilum region due to increased expression of BCR signalling genes.

Next, Ig gene expression was compared between the hilum, wedge, and explant samples. *IGHG1-4* gene expression **(appendix 7)** was averaged as these genes were similarly expressed. IgG expression was elevated in explant samples compared to early disease (hilum and wedge) **(figure 4.3F)**. This was also observed for *IGHA1* expression which encodes IgA **(figure 4.3G)**. These data corroborated with previous data showing that the hilum is the site of ongoing disease with increased immune infiltrates and increased BCR signalling however, Ig data shows that class-switched IgG and IgA are found during end-stage disease. Immunofluorescence data showed little to no CD138+ cells present in BA liver tissue samples **(figure 3.23D)** supporting the gene expression profiles for IgG and IgA. Syndecan-1 gene expression was lower in the hilum compared to the periphery **(figure 4.3H)**. A significant difference in *SDC1* was observed between non-syndromic hilum samples compared to non-syndromic wedge (p-value <0.0001) and non-syndromic explant samples (p-value 0.0026) **(figure 4.3H)**.

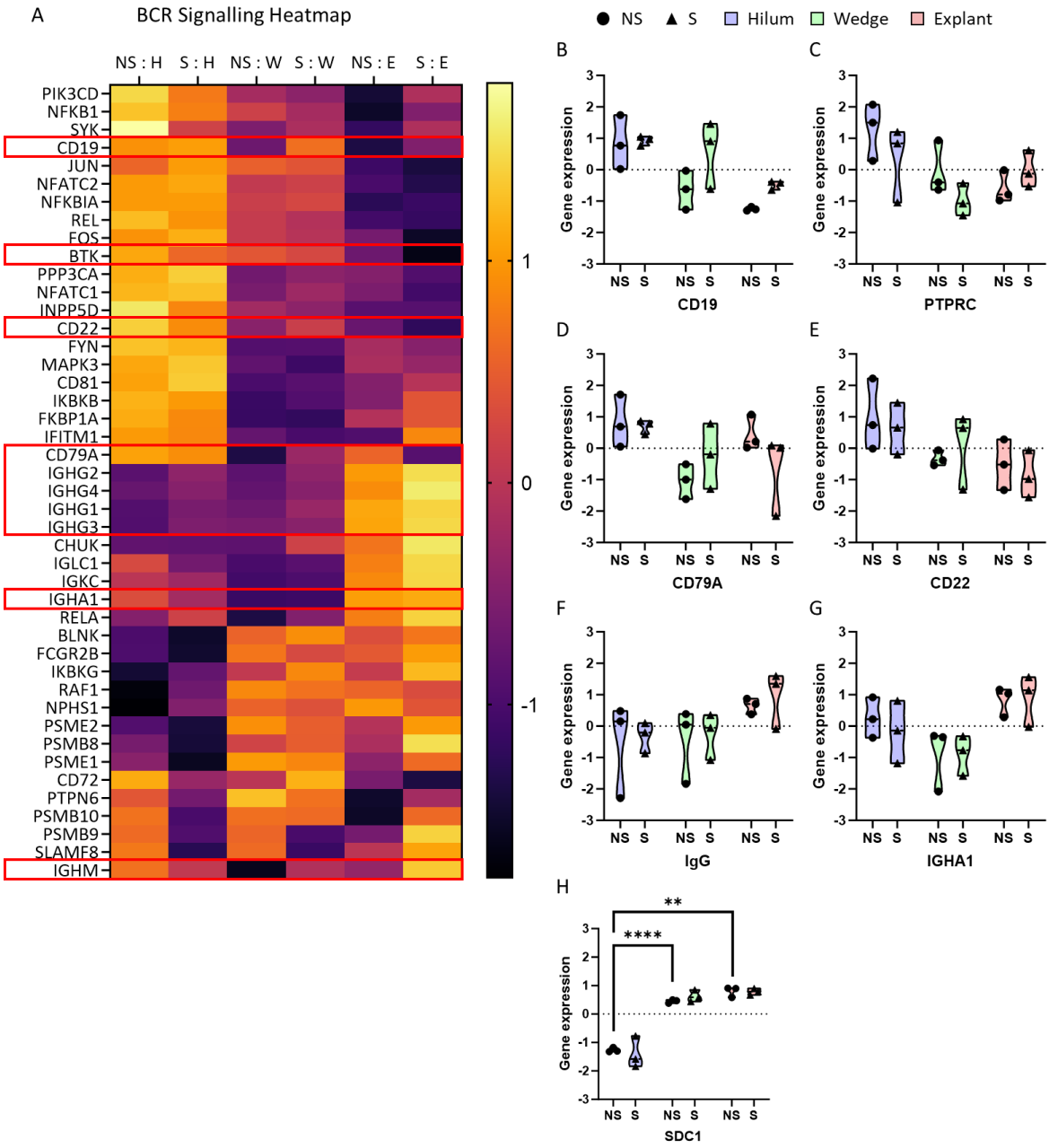


Figure 4.3 Differential gene expression between the hilum and the periphery for BCR signalling genes. *BA livers were used from the hilum, wedge, and explant from non-syndromic (n=3) and syndromic (n=3) patients. (A) Heat map showing BCR signalling gene expression between the hilum, wedge, and explants in syndromic and non-syndromic BA patients. (B) CD19 gene expression data taken from each individual patients from hilum (blue), wedge (green) and explant (red) for non-syndromic; NS (closed circle) and syndromic; S (closed triangle) BA patients. CD19 expression was upregulated in the hilum samples compared to the periphery. (C) CD45 gene PTPRC expression analysis for individual patients showed increased expression in the hilum. (D) CD79A expression for individual patients showed upregulation in the hilum compared to the periphery which was also observed in (E)*

CD22 expression amongst individual BA patients. (F) Combined IgG expression data showed increased expression in explant samples compared to early disease. (G) This was also observed for IgA expression with upregulation of IGHA1 in the explant samples. (H) CD138 gene expression was lower for hilum compared to the periphery. Non-syndromic hilum; NS:H, syndromic hilum; S:H, non-syndromic wedge; NS:W, syndromic wedge; S:W, non-syndromic explant; NS:E and syndromic explant; S:E. (D-H) Dunnett's T3 multiple comparisons test was used. (B and C) Dunn's multiple comparisons test was used. p-value < 0.0332 (*), p-value < 0.0021 (**), p-value < 0.0002 (***), p-value < 0.0001 (****).

We set out to identify any genetic differences between non-syndromic and syndromic BA patients. No significant differences were observed for BCR signalling genes *SYK* **(figure 4.4A)**, *RELA* **(figure 4.4B)**, *CD72* **(figure 4.4C)** and *IGLC1* **(figure 4.4D)**, indicating that BCR signalling genes were comparable between non-syndromic and syndromic patients.

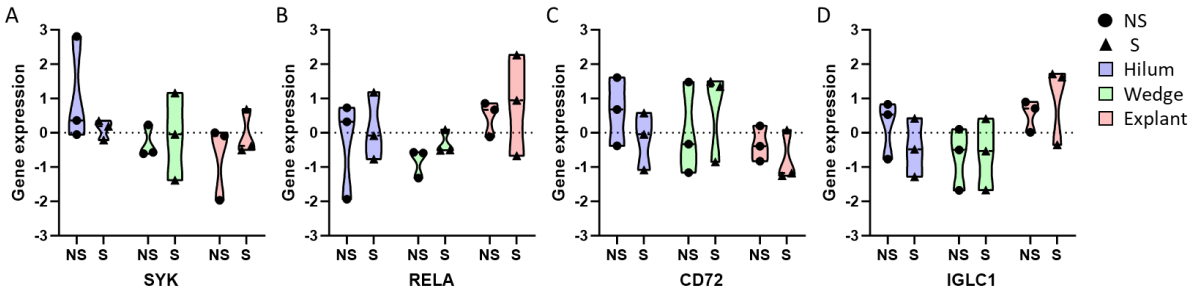


Figure 4.4 Syndromic and non-syndromic were similar in BCR related signalling genes. *BA livers from the hilum, wedge and explant were analysed from non-syndromic (n=3) and syndromic (n=3) patients. No differences were observed between non-syndromic and syndromic BA patients for gene expression of (A) SYK, (B) RELA, (C) CD72 and (D) IGLC1. Non-syndromic; NS (closed circle), syndromic; S (closed triangle), hilum (blue), wedge (green) and explant (red). (A-C) Dunnett's T3 multiple comparisons test was used. (D) Dunn's multiple comparisons test was used.*

4.3.2 Cytokine signalling genes were differentially expressed between the hilum and the periphery

Immunofluorescence data showed that B cells expressed IL-6 in BA liver tissue. IL-6 can also be expressed by other inflammatory cells, including monocytes and macrophages in

response to microbial molecules. We wanted to investigate if cytokine expression would be different between the hilum, wedge, and explants and between non-syndromic and syndromic disease **(figure 4.5A)**. Analysis of gene expression showed that there was no remarkable difference in cytokine gene expression between non-syndromic and syndromic patients **(figure 4.5A)**. The hilum had higher cytokine gene expression compared to the periphery **(figure 4.5A)**. *IL6* gene expression was higher in the hilum compared to the periphery **(figure 4.5B)** suggesting that IL-6 may sustain inflammation. A significant difference in *IL6* gene expression was observed between non-syndromic hilum samples and non-syndromic wedge samples (p-value 0.0324) and between syndromic hilum samples and syndromic wedge samples (p-value 0.0084) **(figure 4.5B).** *IL10* gene expression was lower in the hilum and explant compared to the periphery, however this was of no significance **(figure 4.5C)**. *TNF* expression was higher in the hilum compared to the periphery **(figure 4.5D)**.

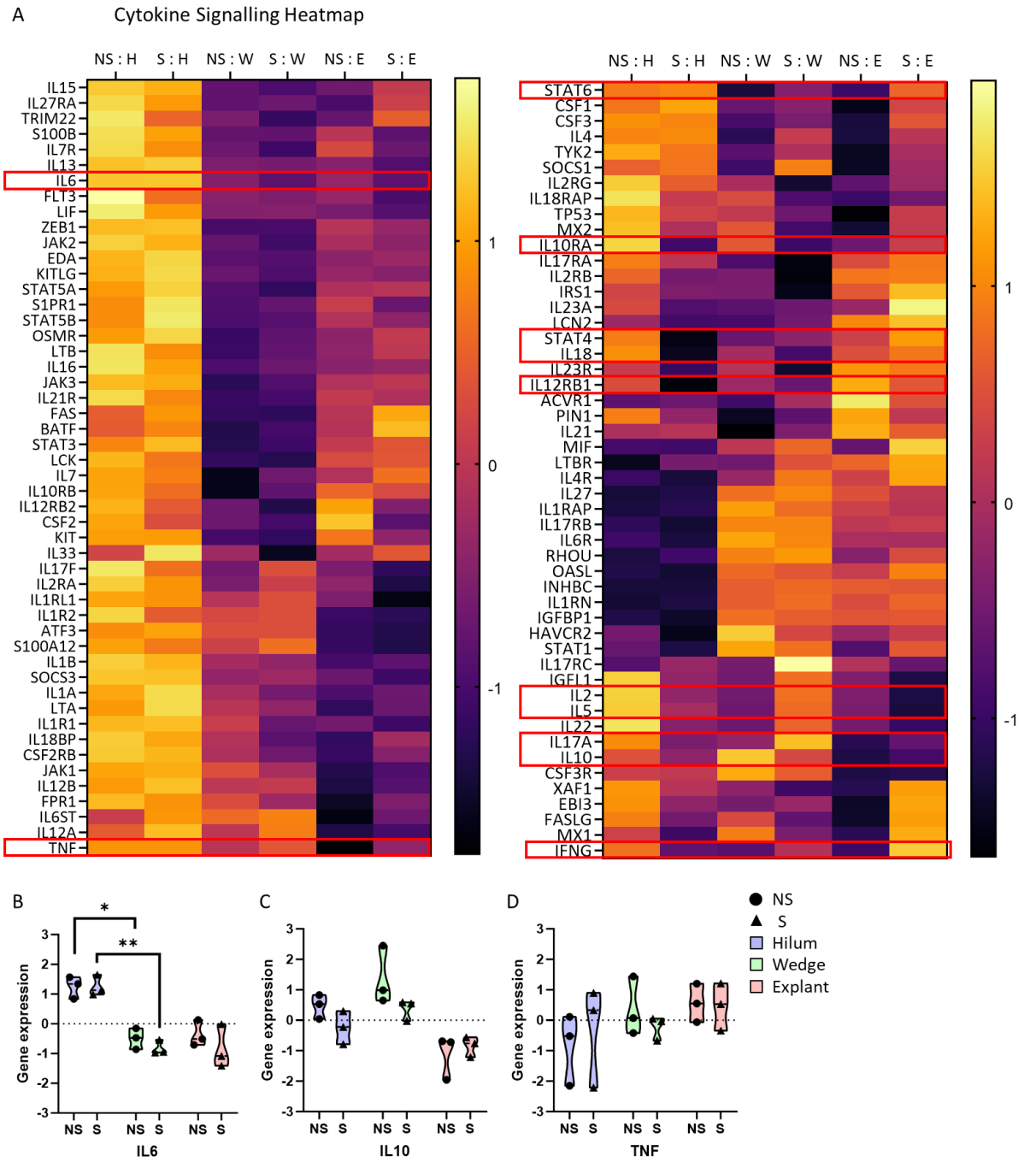


Figure 4.5 Cytokine signalling genes were differentially expressed between hilum and periphery in non-syndromic and syndromic BA patients. *BA livers were used from the hilum, wedge, and explant from non-syndromic (n=3) and syndromic (n=3) patients. (A) Heat map showing gene expression for cytokine related genes in the hilum, wedge, and explants of syndromic and non-syndromic BA patients. (B) IL-6 gene expression in the hilum (blue), wedge (green) and explants (red) for non-syndromic; NS (closed circle) and syndromic; S (closed triangle) BA patients. IL-6 expression was significantly upregulated in the hilum compared to the periphery. (C) IL-10 gene expression in individual BA patients was*

upregulated in wedge samples compared to hilum and explant samples. (D) IFNG gene expression for individual BA patients was upregulated in hilum samples compared to the periphery. Non-syndromic hilum; NS:H, syndromic hilum; S:H, non-syndromic wedge; NS:W, syndromic wedge; S:W, non-syndromic explant; NS:E and syndromic explant; S:E. (B-D) Dunnett's T3 multiple comparisons test was used. p-value < 0.0332 (*), p-value < 0.0021 (**).

Cytokine gene expression was also analysed to identify any differences between non-syndromic and syndromic BA patients. Whist no significant differences were observed between the two groups, some discrepancies were identified. No differences were observed for the gene expression of *IFNG* **(figure 4.6A)** and *IL2* **(figure 4.6B)**. *IL10RA* gene expression was higher in non-syndromic hilum and wedge samples compared to syndromic hilum and wedge samples **(figure 4.6C)**. No differences were observed for *IL17A* **(figure 4.6D)** and *IL18* expression between the two groups **(figure 4.6E)**. *IL21RB1* gene expression was higher in non-syndromic hilum compared to syndromic hilum **(figure 4.6F)**. Significant differences in *IL21RB1* gene expression were observed between syndromic hilum samples and syndromic explant samples (p-value 0.0325) **(figure 4.6F)**. No differences were observed for *STAT6* gene expression between non-syndromic and syndromic BA patients **(figure 4.6G)**. These data showed that there could be some inflammatory differences in cytokine expression profiles between non-syndromic and syndromic BA patients that need to be further investigated with a larger cohort of patients. In addition, these data indicated that the hilum was the site of increased expression of inflammatory cytokine signalling genes.

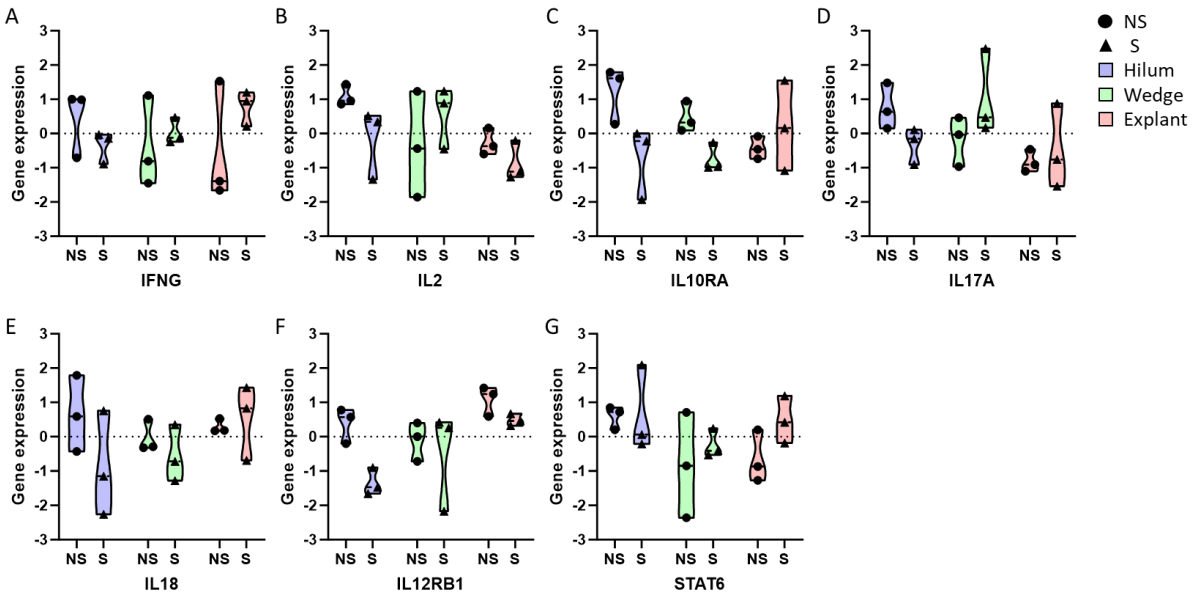


Figure 4.6 Minimal differences between syndromic and non-syndromic patients were observed in cytokine signalling genes. *(A) IFNG expression and (B) IL2 gene expression was similar between non-syndromic and syndromic BA patients. (C) IL10RA gene expression was different between syndromic patients and non-syndromic patients in hilum and wedge samples. No differences were observed for (D) IL17A gene expression and (E) IL18 expression between non-syndromic and syndromic patients. (F) IL12RB1 gene expression was higher in the hilum of non-syndromic patients compared to syndromic patients. (G) STAT6 gene expression was not different between non-syndromic and syndromic patients. Non-syndromic; NS (closed circle), syndromic; S (closed triangle), hilum (blue), wedge (green) and explant (red). (A-G) Dunnett's T3 multiple comparisons test was used.*

Overall, hilum tissue had higher gene expression for the following cytokines: IL-6, IL-4, IL-7, and IL-15. Consistently, in the hilum there was higher gene expression of downstream cytokine signalling components: STAT3, STAT5A, STAT5B, STAT6, JAK1, JAK2 and JAK3. Conversely, there was less IL-4R and IL-6R in the hilum compared to the periphery in both non-syndromic and syndromic patients, and less IL-27.

4.3.3 The hilum had higher expression of oxidative stress-related genes compared to the periphery

Inflammatory damage results in the generation of ROS so genes related to oxidative stress were analysed in BA patients **(figure 4.7)** which showed that the hilum was different to the periphery of BA livers **(figure 4.7A)**. NOX4 generates hydrogen peroxide contributing to inflammation (Guo and Chen, 2015). *NOX4* was upregulated in the hilum and explant samples compared to wedge samples **(figure 4.7B)**. Significant differences were observed between non-syndromic hilum samples and non-syndromic wedge samples (p-value 0.0484) **(figure 4.7B)**. *SOD2*, another oxidative stress gene was highly expressed in explant samples compared to early BA **(figure 4.7C)**. *HIF1A* gene expression was more abundant in the hilum compared to the periphery **(figure 4.7D)**. Oxidative stress results in increased inflammation. *NFKB1* gene expression was higher in the hilum **(figure 4.7E)** where we also saw increased BCR signalling genes and cytokine signalling genes. This suggested that ongoing inflammation occurred at the hilum where there was an increase in oxidative stress and ROS production, that resulted in tissue damage.

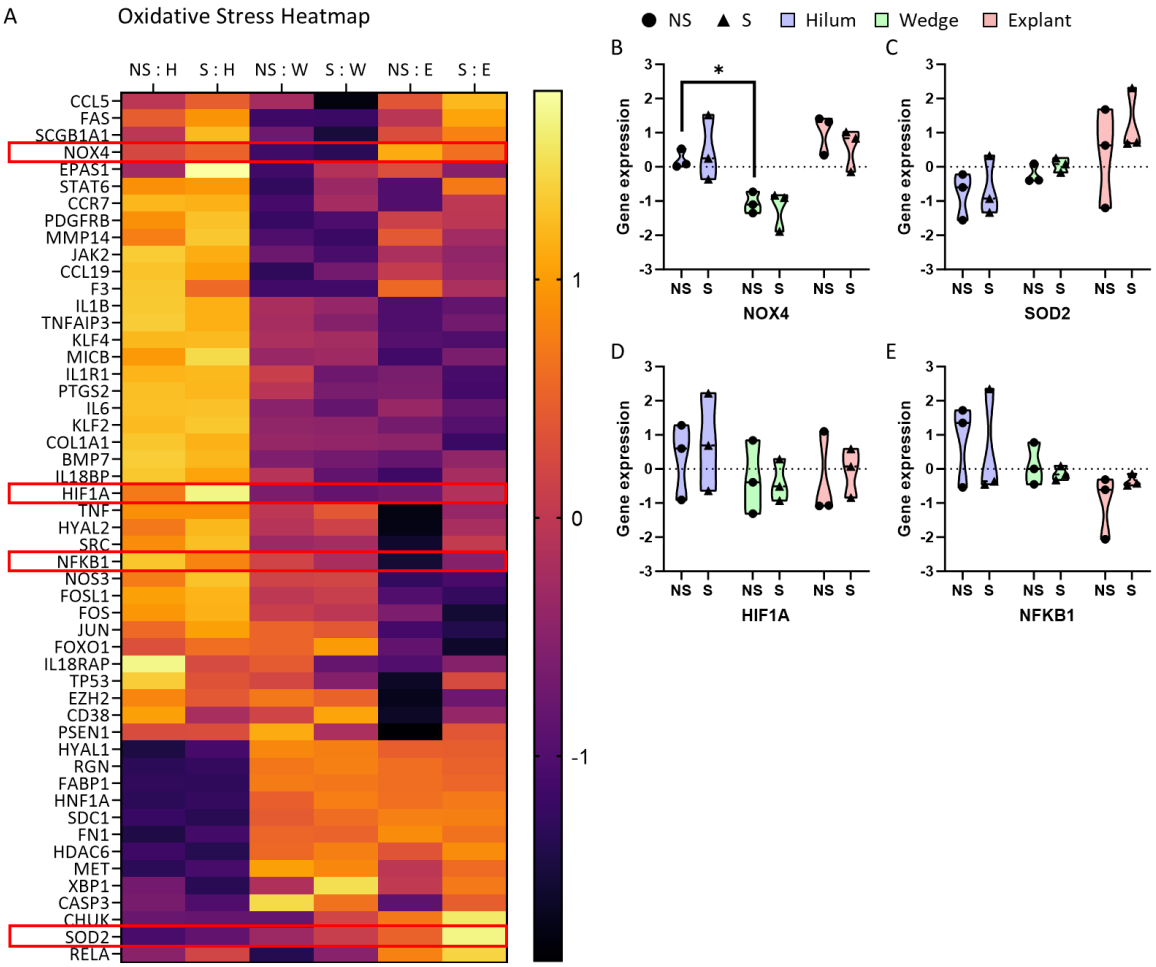


Figure 4.7 Differential oxidative stress-related genes were detected between the hilum and the peripheral BA samples. *BA livers were used from the hilum, wedge, and explant from non-syndromic (n=3) and syndromic (n=3) patients. (A) Heat map showing gene expression for oxidative stress-related genes in the hilum, wedge, and explants of syndromic and non-syndromic BA patients. (B) NOX4 gene expression in the hilum (blue), wedge (green) and explants (red) for non-syndromic; NS (closed circle) and syndromic; S (closed triangle) BA patients. NOX4 expression was upregulated in explant samples compared to early disease. (C) SOD2 gene expression in individual BA patients was upregulated in end-stage disease compared to early disease. (D) HIF1A gene expression for individual BA patients showed no difference in expression between hilum, wedge, and explant. (E) NFKB1 gene expression was upregulated in hilum samples compared to the periphery. Non-syndromic hilum; NS:H, syndromic hilum; S:H, non-syndromic wedge; NS:W, syndromic wedge; S:W, non-syndromic explant; NS:E and syndromic explant; S:E. (B-E) Dunnett's T3 multiple comparisons test was used. p-value < 0.0332 (*).*

We set out to identify any genetic differences in oxidative stress-related genes, between

non-syndromic and syndromic BA patients. No significant differences were observed for

oxidative stress genes *EPAS1* **(figure 4.8A)**, *MX1* **(figure 4.8B)**, *EBI3* **(figure 4.8C)** and *FASLG* **(figure 4.8D)**, indicating that oxidative stress-related genes were comparable between non-syndromic and syndromic patients.

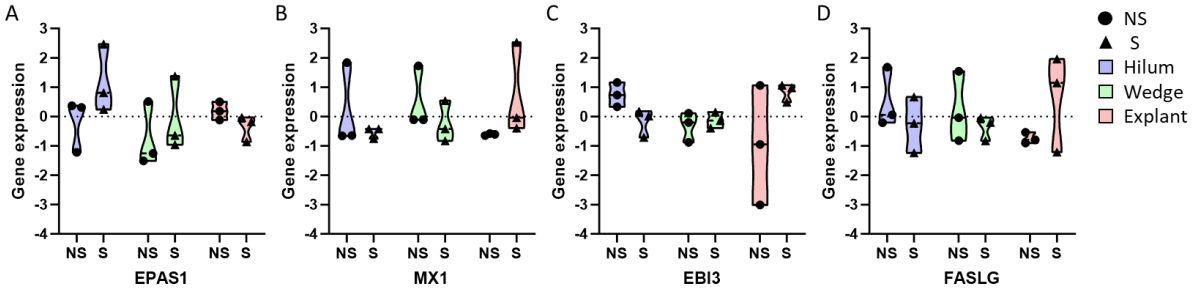
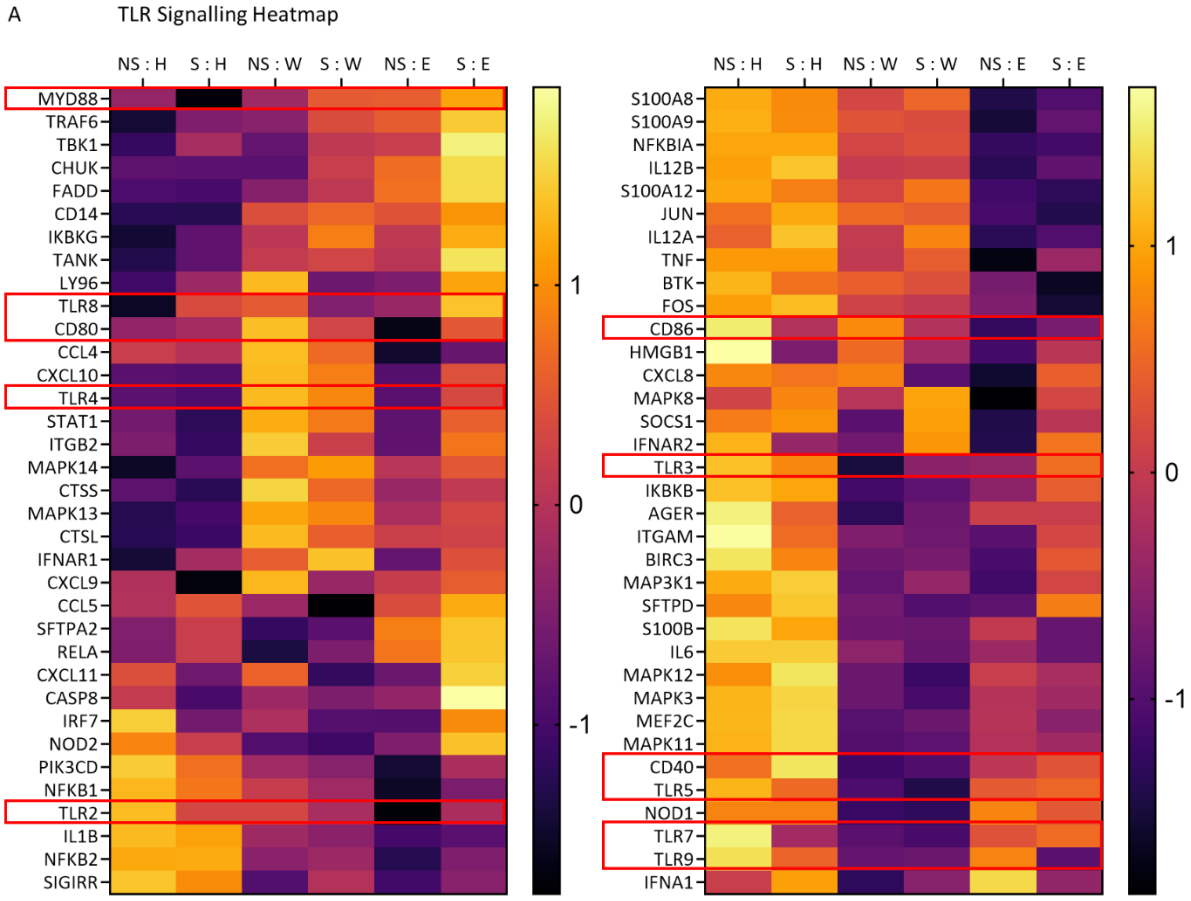


Figure 4.8 Non-syndromic and syndromic BA patients had similar expression of oxidative stress genes. *BA livers were used from the hilum, wedge, and explant from non-syndromic (n=3) and syndromic (n=3) patients. No differences were observed between non-syndromic and syndromic patients for oxidative stress-related genes (A) EPAS1, (B) MX1, (C) EBI3 and (D) FASLG. Non-syndromic; NS (closed circle), syndromic; S (closed triangle), hilum (blue), wedge (green) and explant (red). (A, B and D) Dunnett's T3 multiple comparisons test was used. (C) Dunn's multiple comparisons test was used.*

4.3.4 Activation markers were differentially expressed in hilum samples

Increased intestinal permeability was observed in adult livers (De Munck et al., 2020, Plaza-Diaz et al., 2020) and paediatric livers (Giorgio et al., 2014), suggesting that translocation of PAMPs activates TLR signalling. The hilum was different compared to the periphery for TLR signalling related genes **(figure 4.9A)**. *TLR7* gene expression was more abundant in explant samples **(figure 4.9B)** whereas *TLR9* expression was higher in the hilum **(figure 4.9C)** compared to the periphery. Co-stimulatory marker expression was also analysed. *CD80* expression was higher in wedge samples compared to the hilum and explants **(figure 4.9D)** and *CD86* expression was increased in early disease compared to end-stage disease **(figure 4.9E)**. CD40 is expressed on APCs including B cells (Elgueta et al., 2009). The hilum and

explant samples had increased *CD40* expression compared to wedge samples **(figure 4.9F)**. Significant differences were observed between non-syndromic hilum and non-syndromic wedge samples (p-value 0.0066) and between non-syndromic wedge and non-syndromic explant samples (p-value 0.0342) **(figure 4.9F)**. These results showed that the hilum had increased TLR9 responses and CD86 expression which was suggestive of active disease. Furthermore, *CD40* expression was also elevated indicating that these cells may be poised to become activated upon ligation to CD40L.



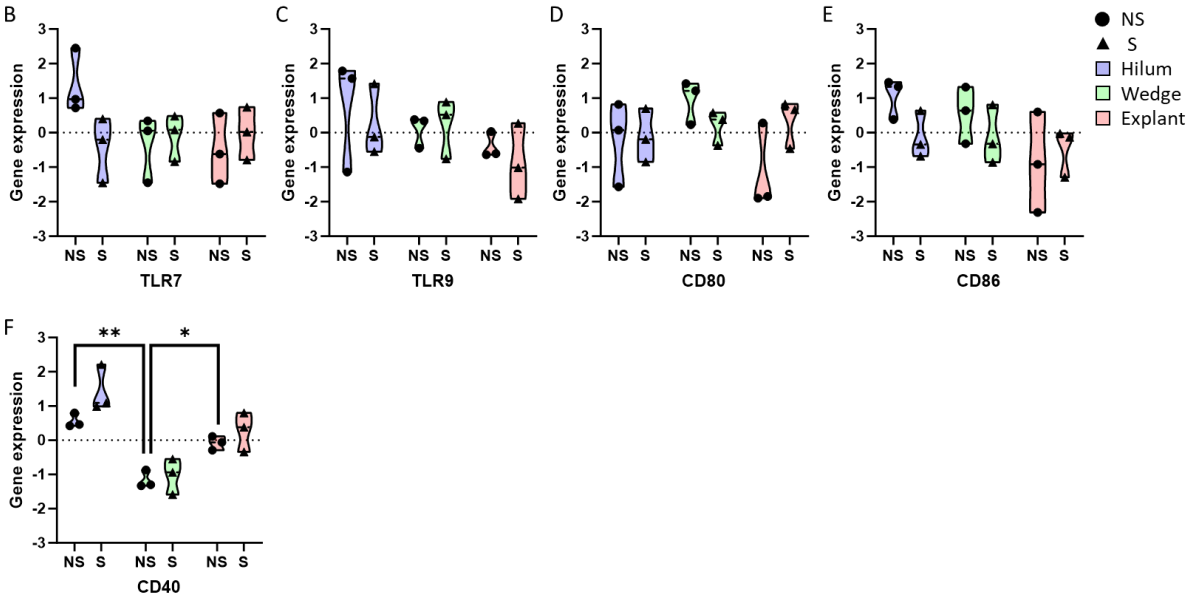


Figure 4.9 Differential TLR related gene signalling was detected between hilum samples and the periphery. *BA livers were used from the hilum, wedge, and explant from non-syndromic (n=3) and syndromic (n=3) patients. (A) Heat map showing gene expression for TLR signalling related genes in the hilum, wedge, and explants of syndromic and non-syndromic BA patients. (B) TLR7 gene expression in the hilum (blue), wedge (green) and explants (red) for non-syndromic; NS (closed circle) and syndromic; S (closed triangle) BA patients. TLR7 expression was upregulated in non-syndromic hilum samples and explants compared to wedge samples. (C) TLR9 gene expression in individual BA patients was upregulated in the hilum and non-syndromic BA explants. (D) CD80 gene expression for individual BA patients was upregulated in wedge samples compared to the hilum and explants. (E) CD86 gene expression was upregulated in non-syndromic BA hilum and wedge samples. (F) CD40 gene expression was downregulated in wedge samples compared to the hilum and explants. Non-syndromic hilum; NS:H, syndromic hilum; S:H, non-syndromic wedge; NS:W, syndromic wedge; S:W, non-syndromic explant; NS:E and syndromic explant; S:E. (C and E) Dunnett's T3 multiple comparisons test was used. (B and D) Dunn's multiple comparisons test was used. p-value < 0.0332 (*), p-value < 0.0021 (**).*

Genetic profiles between non-syndromic and syndromic BA patients for TLR signalling genes were analysed. No significant differences were observed for TLR signalling genes *TLR2* **(figure 4.10A)**. *TLR3* gene expression was higher in non-syndromic hilum samples compared to syndromic hilum samples **(figure 4.10B)**. No difference in gene expression of *TLR5* **(figure 4.10C)** was observed between non-syndromic and syndromic BA patients. Differences

between non-syndromic and syndromic patients were observed for *TLR8* expression in the hilum **(figure 4.10D)** and in wedge samples for *SOCS1* gene expression **(figure 4.10E)**. These markers identified differences between non-syndromic and syndromic patients in TLR signalling genes.

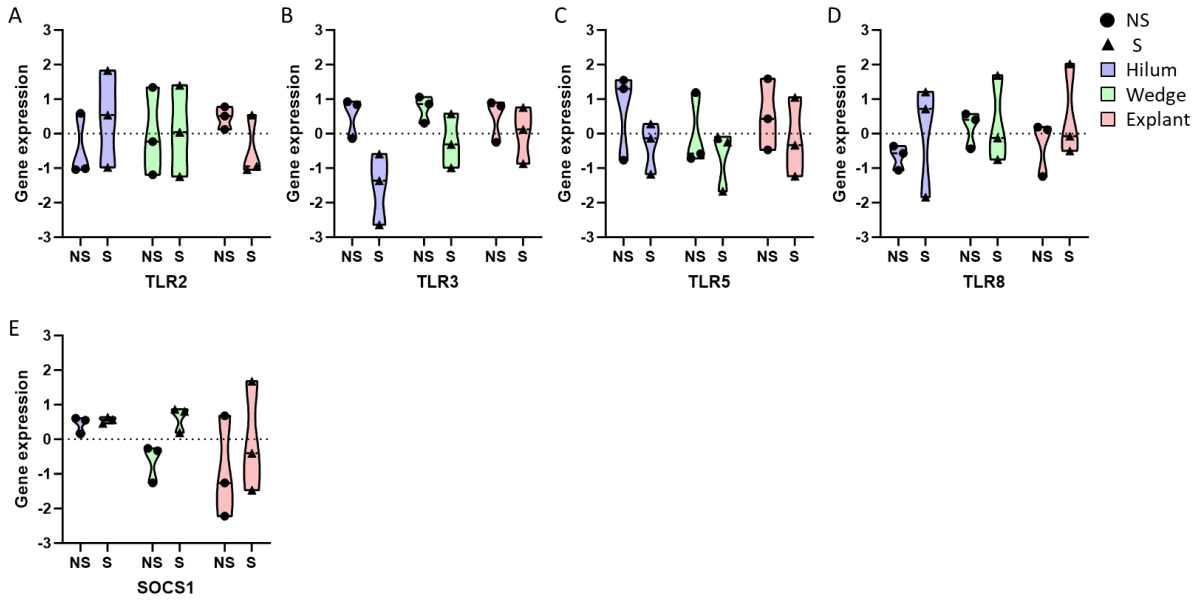


Figure 4.10 Differences were observed for TLR signalling genes between syndromic and non-syndromic BA patients. *(A) TLR2 expression was comparable between non-syndromic and syndromic patients. (B) TLR3 expression was higher in the hilum of non-syndromic patients compared to syndromic patients. (C) TLR5 expression was not different between syndromic and non-syndromic patients. (D) TLR8 gene expression was different between syndromic and non-syndromic patients. (E) SOCS1 gene expression was higher in wedge samples of syndromic patients compared to non-syndromic patients. Non-syndromic; NS (closed circle), syndromic; S (closed triangle), hilum (blue), wedge (green) and explant (red). (A, C and D) Dunnett's T3 multiple comparisons test was used. (B and E) Dunn's multiple comparisons test was used.*

4.3.5 Chemokine signalling genes were highly expressed in the hilum of BA patients

Chemokine signalling was investigated in BA patients as cytokine expression was differentially expressed between hilum and peripheral samples. The hilum was different for chemokine signalling gene expression compared to peripheral wedge and explant samples

(figure 4.11A). *CCR6* **(figure 4.11B)**, *CCR10* **(figure 4.11C)**, *CCR7* **(figure 4.11D)**, *CXCR5* **(figure 4.11E)** and *CXCR4* **(figure 4.11F)** genes expression was higher in the hilum compared to the periphery. *CCR6* and *CCR10* genes were also highly expressed in explant samples. Significant differences were observed in *CCR10* gene expression between syndromic hilum and syndromic wedge samples (p-value 0.0253) **(figure 4.11C)**. This data corroborated with data shown for BCR signalling, cytokine signalling, oxidative stress and TLR signalling suggesting that the hilum is the site of active ongoing disease and inflammation.

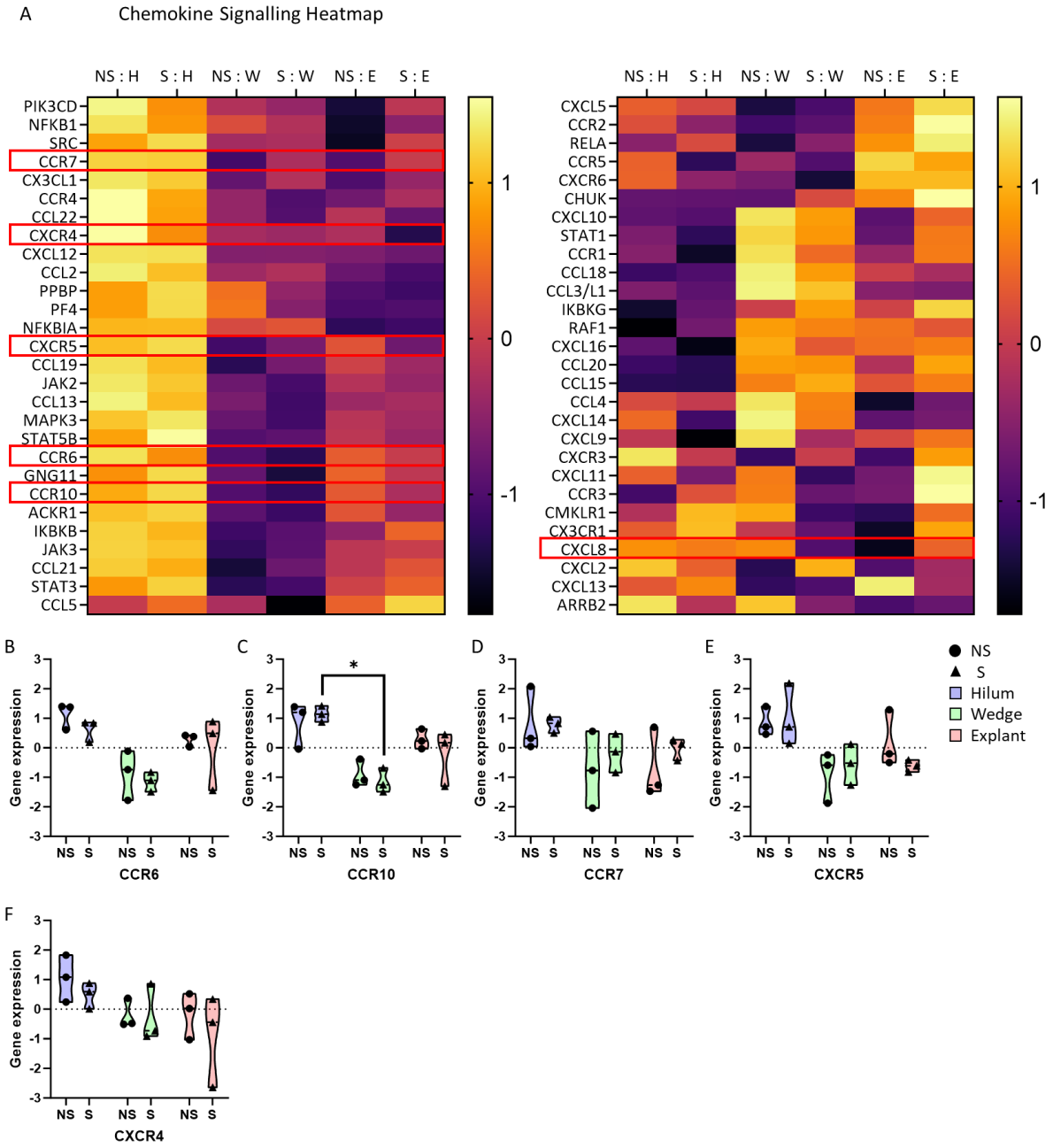


Figure 4.11 Chemokine signalling genes were differentially expressed between the hilum and the periphery. *BA livers were used from the hilum, wedge, and explant from non-syndromic (n=3) and syndromic (n=3) patients. (A) Heat map showing gene expression for chemokine signalling related genes in the hilum, wedge, and explants of syndromic and non-syndromic BA patients. (B) CCR6 gene expression in the hilum (blue), wedge (green) and explants (red) for non-syndromic; NS (closed circle) and syndromic; S (closed triangle) BA patients. CCR6 expression was upregulated in the hilum samples and explants compared to wedge samples. (C) CCR10 gene expression in individual BA patients was upregulated in the hilum and explants compared to wedge samples. (D) CCR7 gene expression for individual BA patients was upregulated in hilum samples compared to the periphery. (E) CXCR5 gene*

expression was upregulated in hilum samples. (F) CXCR4 gene expression was upregulated in the hilum compared to the periphery. Non-syndromic hilum; NS:H, syndromic hilum; S:H, non-syndromic wedge; NS:W, syndromic wedge; S:W, non-syndromic explant; NS:E and syndromic explant; S:E. (C-F) Dunnett's T3 multiple comparisons test was used. (B) Dunn's multiple comparisons test was used. p-value < 0.0332 (*).

We set out to identify any genetic differences between non-syndromic and syndromic BA patients. Significant differences were observed for *CCL5* gene expression between syndromic hilum samples and syndromic wedge samples (p-value 0.0295) **(figure 4.12A)**. No significant difference was observed for *CXCL8* gene expression **(figure 4.12B)**. Syndromic wedge samples showed higher *CXCL2* gene expression compared to non-syndromic wedge samples **(figure 4.12C)**. Significant differences were observed for *CCL5* gene expression between syndromic wedge samples and syndromic explant samples (p-value 0.0303) **(figure 4.12D)**. *CXCL13* gene expression was different between non-syndromic explants compared to syndromic explant samples **(figure 4.12E)**. Significant differences were observed for *CCL5* gene expression between non-syndromic wedge samples and non-syndromic explant samples (p-value 0.0205) **(figure 4.12E)**. Taken together, the hilum had a proportion of chemokine signalling genes which were highly expressed compared to the periphery. These included *CCR6*, *CCR7*, and *CCR10* including genes further downstream such as *STAT3*, *JAK2* and *STAT5B* **(figure 4.11A)**.

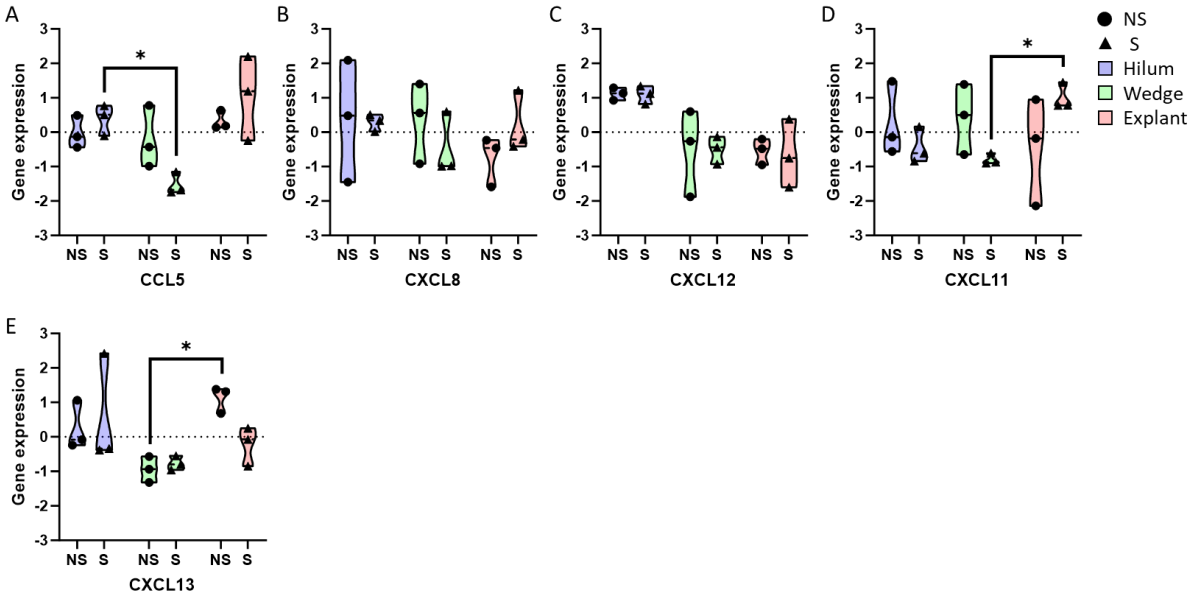


Figure 4.12 Chemokine signalling genes were differentially expressed between non-syndromic and syndromic BA patients. *No difference in gene expression of (A) CCL5 and (B) CXCL8 was observed between non-syndromic and syndromic patients. (C) CXCL2 expression was higher in syndromic wedge samples compared to non-syndromic patients. No difference in (D) CXCL11 expression was observed between non-syndromic and syndromic patients. (E) CXCL13 gene expression was more abundant in non-syndromic BA patients compared to syndromic patients. Non-syndromic; NS (closed circle), syndromic; S (closed triangle), hilum (blue), wedge (green) and explant (red). (A-E) Dunnett's T3 multiple comparisons test was used. p-value < 0.0332 (*).*

Analysis of gene profiles in hilum, wedge and explant samples showed that specific gene expression profiles were higher in the hilum (44 genes), the wedge (66 genes) and the explant (54 genes) samples **(figure 4.13)**. Genes that were highly expressed in the hilum included *TLR7*, *CD86* and *IL17A*. Genes expressed highly in wedge samples included *CD80* and CD45 (*PTPRC*). Genes highly expressed in explant samples included *NOS2* and *IL17F*. 14 genes were upregulated in both the hilum and wedge samples including *IL10*. 14 genes were highly expressed in the hilum and explant samples including *TLR9* and *IL2*. Four genes were found in both wedge and explant samples including *CD244* however, no genes were highly

expressed in all three locations suggesting that the disease course may be different in the different locations.

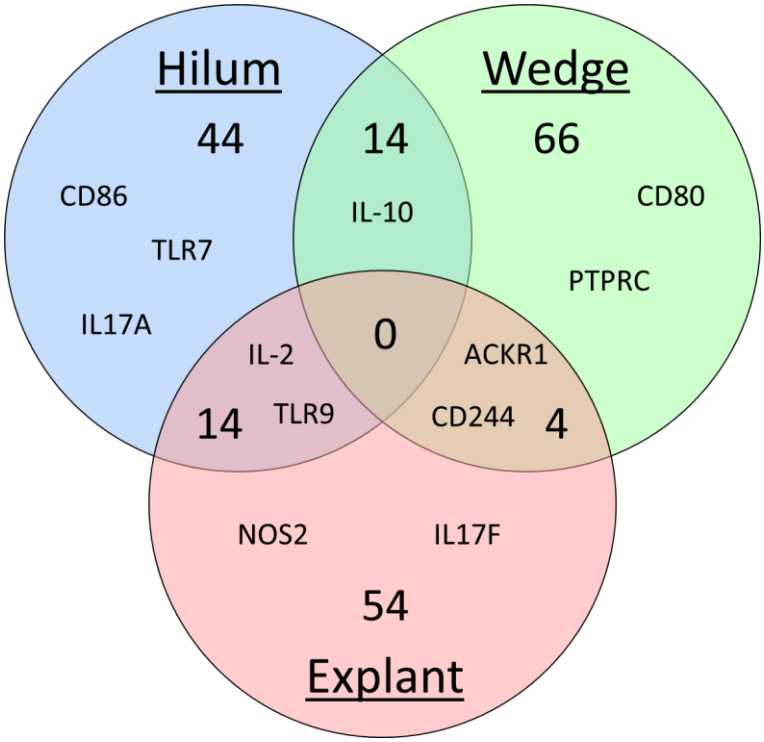


Figure 4.13 Venn diagram showing the number of genes upregulated in the hilum, wedge, and explant BA samples. *BA livers were used from the hilum, wedge, and explant from non-syndromic (n=3) and syndromic (n=3) patients. A few genes have been highlighted for each region based on involvement in cytokine signalling, co-stimulation and TLR signalling. Hilum only (blue) had 44 genes upregulated, wedge only (green) had 66 genes upregulated and explant only (red) had 54 genes upregulated and overlap in gene expression between the three regions was analysed. Hilum and wedge samples had 14 genes upregulated which was also observed for hilum and explant samples. Wedge and explant samples had 4 genes upregulated between the samples in BA livers.*

4.4 Discussion

Hepatic samples from early disease can be compared to end-stage disease in BA giving us an idea of how this disease progresses. HOT panel gene analysis studies the immune response in tissue samples identifying differences in immune signalling pathways. This panel was used to gain an overview of the immune response in BA and to identify any differences between non-syndromic and syndromic patients. nCounter HOT panel also identified any differences between hilum, wedge and explant samples and helped to understand how disease progresses from early stage to end-stage disease.

4.4.1 The hilum was different compared to the periphery

Differential gene expression was detected between the hilum and peripheral samples (wedge and explant) in genes related to the adaptive **(appendix 8)** and innate **(appendix 9)** immune system. *CD4* expression was lower in the hilum and higher in wedge and explant samples **(appendix 8B)** however CD8 related genes were highly expressed in the hilum region compared to the periphery **(appendix 8C)**. These data indicated that CD8+ cytotoxic T cells were present in the hilum and may contribute to pathology. CD8+ T cells have been shown to infiltrate bile ducts in BA patients (Ahmed et al., 2001). Genes related to cytotoxic markers *PRF1* (perforin), *GZMB* (granzyme B) and *FASLG* (Fas ligand) were differentially expressed amongst sample locations and between non-syndromic and syndromic patients **(appendix 10)**. No difference was observed between the hilum and the periphery for granzyme B gene expression **(appendix 10B)**. Hilum and explant samples showed higher perforin expression compared to wedge samples **(appendix 10C)**. Significant differences were observed in perforin expression between non-syndromic wedge samples and non-

syndromic explant samples (p-value 0.0117) **(appendix 10C)** suggesting that CD8+ T cells may contribute to inflammatory damage through expression of granzyme B and perforin. Ahmed et al., clinically followed up BA patients post KPE and showed that bile ducts with CD8+ T cell infiltration were associated with better liver function (Ahmed et al., 2001) implying that CD8+ cytotoxic T cells were beneficial and play a protective role in BA.

The hilum had a different microenvironment compared to the periphery. Active inflammation, indicated by higher expression of genes related to cytokine and chemokine signalling, occurs at the hilum and to some extent, during end-stage disease. Infiltration of immune cells including B cells, was also enhanced in the hilar samples which corroborated our IHC findings showing that the hilum had increased expression of CD20+ B cells and total lymphocytes compared to the periphery **(figure 3.10)**. BCR signalling genes were also more abundant in the hilum compared to the periphery indicating that B cells were becoming activated in the hilum and responding to cognate antigens. The hilum may have increased immune infiltrates as it is near the hepatic artery and portal vein (Rogers and Dintzis, 2012).

Increased B cells were detected in the hilum in IHC CD20 data **(figure 3.10)** and *CD19* gene expression was also increased in the hilum of BA samples indicating that B cells contribute to disease **(figure 4.3)**. No differences were observed between non-syndromic and syndromic patients for *CD19* expression suggesting that B cells contribute to disease pathogenesis in the same capacity. B cells contribute to BA pathology through the production of antibodies (Lu et al., 2010, Hadchouel et al., 1981, Luo et al., 2021, Wang et al., 2020), activation of immune cells such as T cells (Brindley et al., 2012) and through the secretion of cytokines which contribute to inflammation and bile duct damage (Lu et al., 2010, Patel et al., 2021, Bednarek et al., 2018). CD138 gene expression was lower in the hilum **(figure 4.3H)** which

corroborated our data shown in **Figure 2.23** showing low CD138+ B cells BA livers. In adult explanted livers, low frequencies of IgG **(figure 2.13C)** and IgA **(figure 2.13D)** expression were observed, supporting the flow cytometry data showing low percentages of CD138+ cells were present in adult chronic livers **(figure 2.15A)**. These data suggested that there were not many GC reactions occurring and B cells may be becoming activated through other pathways. TCR signalling genes were also upregulated in the hilum compared to the periphery **(appendix 11)**. T cell infiltration has been observed in BA (Lakshminarayanan and Davenport, 2016) and these T cells were oligoclonal in nature indicating that T cell proliferation was a result of specific antigenic stimulation (Mack et al., 2007) such as viral proteins of self-proteins (Feldman and Mack, 2012). At diagnosis of BA, activated CD4+ and CD8+ T cells were found in portal tract areas and these T cells secreted cytokines IL-2 and IFN-γ (Feldman and Mack, 2012) which contribute to inflammatory damage observed in BA. CD8+ cytotoxic T cells have been upregulated in BA indicating a toxic role for these cells in BA (Guo et al., 2012). RRV-primed dendritic cells can stimulate CD8+ T cells to secrete IFN-γ in animal models of BA which could be the mechanism behind cholangiocyte injury (Lages et al., 2012).

4.4.2 Inflammatory gene expression was higher in the hilum compared to the periphery

Increased immune infiltration indicates active disease which is accompanied by inflammation. Cytokine and chemokine signalling genes were differentially expressed in the hilum. Majority of these genes were highly expressed in the hilum suggesting ongoing inflammation. *IL6*, *TNF* and *IFNG* genes expression was higher in the hilum. These proinflammatory genes contribute to ongoing inflammation and are implicated in many

chronic inflammatory diseases (Falasca et al., 2006, Singh et al., 2011, Chae et al., 2018, Tilg et al., 1992, Cao et al., 1998). Narayanaswamy et al., analysed cytokines present in BA plasma at the time of KPE, for six months. They found that IL-2, IFN-γ, IL-4, IL-18 and TNF-α levels increased during this period however IL-10 levels did not (Narayanaswamy et al., 2007). This indicated that whilst KPE restores bile flow, it does not ameliorate the inflammatory response (Narayanaswamy et al., 2007). Our data showed that *IL10* expression was lower in the hilum suggesting that IL-10 anti-inflammatory effects were impaired as inflammatory gene signatures were highly expressed in the hilum **(figure 4.5)**. IL-10 cytokine levels in the blood of BA patients were elevated compared to healthy controls (Udomsinprasert et al., 2022) which is the opposite of what we have shown in the liver of BA patients **(figure 4.5)**. IL-18 and IFN-γ levels were elevated in the serum of older BA patients and correlated with severity of jaundice (Vejchapipat et al., 2012) corroborating data shown in non-syndromic BA patients **(figure 4.5)**. Bezerra et al., showed that IFN-γ and OPN, a Th1 cytokine, were upregulated in BA liver biopsies (Bezerra et al., 2002). OPN has also been shown to be elevated in BA (Feldman and Mack, 2012). Systemic blood cytokine analyses showed no difference in IFN-γ and TNF-α levels between BA patients and healthy controls (Udomsinprasert et al., 2022) suggesting that gene expression may be different between peripheral blood and the liver. No difference was observed in BA patients with and without fibrosis (Udomsinprasert et al., 2022) however, our data showed that *TNF* gene expression was higher in the hilum of BA liver samples and *IFNG* was only highly expressed in the hilum of non-syndromic patients **(figure 4.5 and 4.6)**. IFN-γ may be a useful biomarker to distinguish between non-syndromic and syndromic BA patients in the hilum during early

disease however more studies need to be conducted to establish IFN-γ as a biomarker to distinguish BA disease type.

Chemokines contribute to immunity by mediating the trafficking of immune cells to sites of infection, inflammation, and tissue damage (Yam and Chtanova, 2019). Yang et al., analysed two BA databases and found that BA patients had upregulated *CXCL10*, *CXCR4*, *CCL20*, *CCL2* and *STAT1* (Yang et al., 2022). These databases used liver biopsy samples but did not specify if these were hilum or wedge. Our data showed that *CXCL10* and *STAT1* expression was higher in wedge samples but not in the hilum **(figure 4.11)**. Furthermore, hilum samples showed increased expression of *CXCR4* and *CCL2* but had lower *CCL20* compared to the periphery. This indicated that similar genes were being expressed during early disease however, whilst Yang et al., analysed BA liver biopsies from BA patients (Yang et al., 2022), our data showed gene expression profiles in specific regions of the liver during early liver disease through to end-stage liver disease. IL-8 is crucial for inflammation and progression of BA (Dong and Zheng, 2015). Continual secretion of IL-8 can also result in tissue damage (Atta-ur-Rahman et al., 1999) and increased *CXCL8* levels in the liver contribute to hepatic inflammation and fibrosis (Dong and Zheng, 2015). This may be the case in early BA as *CXCL8*, which encodes IL-8, was highly expressed in early BA **(figure 4.11)**. Furthermore, *CXCL8* may be used as a biomarker for BA diagnosis and outcome (Arafa et al., 2016) as it can be identified in early BA.

CCR7 and *CXCR5* were highly expressed in the hilum of BA patients **(figure 4.11)**, where B cell and lymphoid aggregates were also observed. CCR7 is expressed by B cells and other immune cells and this chemokine guides these cells to lymphoid organs and works in conjunction with CXCR5 to guide T cells to T cell zones and B cell to follicles (Forster et al.,

2008). CCR7 is crucial for T cell homing to lymph nodes and was upregulated on activated B cells to encourage T cell help (Forster et al., 2008). TFH cells downregulate CCR7 and upregulate CXCR5 enabling them to enter B cell follicles and aid in antibody production and class-switching (Forster et al., 2008, Moser, 2015). In our cohort of BA patients, B cell and lymphoid aggregates were observed in the hilum region **(figure 3.9A)** and in some cases, the explanted liver **(figure 3.9C(i)))** however none of these aggregates were GCs. It would be interesting to investigate whether these B cell and lymphoid aggregates eventually become GCs and aid in antibody production which may explain why CCR7 and CXCR5 gene expression was higher in the hilum. On the other hand, there may be an issue in the CCR7-CXCR5 axis that may be preventing GC formation. Further work studying cytokine expression in BA livers needs to be undertaken to investigate the effects of cytokines in disease progression and tissue damage. Identifying which cells produce harmful proinflammatory cytokines may aid in targeting these subsets in a more specific manner.

4.4.3 Oxidative stress-related genes were highly expressed in the hilum

Chronic inflammation also results in oxidative stress and tissue damage through the production of ROS. Oxidative stress-related genes were highly expressed in the hilum **(figure 4.7)** which supported the findings that the hilum was the site of inflammation and tissue damage. ROS arises as a byproduct of mitochondrial metabolism and under normal conditions it is removed by antioxidant enzymes (Candas and Li, 2014) however, an imbalance between antioxidant enzymes and increased ROS production is responsible for DNA damage which results in apoptosis (Li and Zhou, 2011, Guo and Chen, 2015). NOX4 is responsible for the generation of hydrogen peroxide and contributes to cell proliferation and cell migration including hepatocytes (Guo and Chen, 2015). NOX4 is the primary producer of

TNF-α-induced oxidative stress which results in apoptosis of cells including hepatocytes (Guo and Chen, 2015). During homeostasis this pathway may be beneficial in removing dead or dying cells however, under inflammatory conditions, increased *NOX4* expression may enhance cellular death which may be the case for hilar samples in BA patients **(figure 4.7)**. During oxidative stress, SOD2 expression determines the amount of superoxide radical anion that is converted into hydrogen peroxide and oxygen, protecting cells from oxidative damage (Palma et al., 2020). In our cohort of BA patients, *SOD2* gene expression was lower in the hilum region **(figure 4.7)** indicating that the inflammatory environment at hilar regions may lower *SOD2* gene expression enabling ROS and the inflammatory response to further damage the liver. SOD2 levels were high in the liver tissue and significantly correlated with serum bilirubin in 15 BA patients (Hashizume et al., 2020). A strong inflammatory response was detected during early BA along with high oxidative DNA damage (Hashizume et al., 2020) which supported our gene expression data showing that the hilum had increased gene expression of inflammatory and oxidative genes. This suggests that an imbalance between antioxidants and free radicals may also exacerbate the inflammatory response and augment tissue damage.

4.4.4 TLR signalling gene expression was higher in the hilum compared to the periphery

Tissue damage also results in the release of DAMPs which can be recognised by TLRs on immune cells mounting a response. TLRs recognise PAMPs and host-derived endogenous antigens; DAMPs, allowing them to respond to microbial infections and sense danger signals (Goulopoulou et al., 2016). Studies have shown that increased intestinal permeability resulted in the translocation of gut-derived microbes resulting in TLR activation and

inflammation in adult livers (Zwolak et al., 2016, Schwenger et al., 2018, Chung et al., 2018). The liver maintains a tolerogenic environment due to the high exposure to gut-derived antigens that activate PRRs (Kiziltas, 2016). Endogenous nucleic acid and viral or bacterial RNA and DNA is recognised by TLR3,7,8 and 9 whereas TLR1, 2, 3, 5 and 6 bind to molecules expressed on bacterial membranes (Kiziltas, 2016). Half of the TLR signalling genes analysed were highly expressed in the hilum including nucleic acid sensing TLRs; TLR3, TLR5, TLR7 and TLR9. However, half of the genes related to TLR signalling were lower in the hilum including TLR4 and MyD88, a signalling adaptor component in TLR signalling **(figure 4.9)**. TLR3, 7 and 9 signal through TRIF, another adaptor protein in TLR signalling (Ullah et al., 2016). This may explain the low expression of *MYD88* as TLR3, 7 and 9 detect bacterial and viral nucleic acid (Ortiz-Perez et al., 2020) which may be abundant in BA livers due to infection or translocation from the gut. In murine BA, progression of disease is independent of MyD88 signalling (Ortiz-Perez et al., 2020) suggesting that TRIF signalling through ligation of TLR3, 7, 8 and 9 results in the production of inflammatory mediators that damage biliary tissue. TLR7 expression was higher in the hilum and has been shown to be associated with IL-8 gene expression in BA (Dong and Zheng, 2015). TLR9 gene expression was more abundant in the hilum and activation of TLR9 resulted in the activation of IgM-producing B cells (Kiziltas, 2016) indicating a potential mechanism through which TLR activation contributes to pathogenesis in liver disease. TLR3 recognises viral RNA along with TLR7, both of these TLRs have been implicated in BA (Feldman and Mack, 2012). Significantly high TLR3 and TLR7 expression was detected at diagnosis in BA patients who required liver transplants later in life (Feldman and Mack 2012). This suggests that viral antigens, which may have translocated

due to increased intestinal permeability, were recognised by TLRs in BA and induced an immune response.

A study investigated the contribution of bacterial translocation to liver injury post KPE in 45 BA patients (Godbole et al., 2023). They found an increase in serum levels of LBP and CD14 however, mRNA expression of *TLR4* was low suggesting liver injury post KPE was not due to bacterial translocation of LPS (Godbole et al., 2023). Whilst this study showed no evidence of bacterial translocation of LPS, they did observe an increase in *TLR7* mRNA expression which correlated with hepatic fibrogenesis post KPE (Godbole et al., 2023) suggesting that viral RNA or DAMPs from dying cells may activate TLRs inducing an inflammatory response resulting in liver injury. Sensitisation of TLRs to other bile duct ligands may result in excessive inflammation and immune responses targeting BECs, resulting in bile duct damage and leading to the progression of BA (Wu et al., 2022). Acute and chronic inflammation causes a breakdown of tolerance and the release of DAMPs from damaged cells may activate autoreactive immune cells resulting in autoimmunity (Kiziltas, 2016).

Hepatocytes can express TLRs and respond to multiple PAMPs and DAMPs, however they respond poorly to TLR2 and TLR4 ligands (Kiziltas, 2016). BECs are also exposed to gut microbes and express TLRs which become upregulated in response to IFN-γ stimulation resulting in biliary pathogenic responses (Kiziltas, 2016). Cholangiocytes express TLRs and can respond to microbial infections and mediate immune responses (Syal et al., 2012). Cholangiocytes upregulated TLR3 expression in PBC, AIH and in chronic viral hepatitis patients and LPS stimulation of TLR4 induced the release of pro-inflammatory mediators including IL-6, TNF-α and IFN-γ (Syal et al., 2012) highlighting a role for cholangiocytes in inflammation. In the context of disease, cholangiocytes themselves may be contributing to

cellular damage through the release of inflammatory mediators and by modulating immune responses. Our IHC data showed that cholangiocytes expressed IL-6 **(figure 3.6A(ii))** implying that cholangiocytes may contribute to inflammation in BA. Accumulation of LPS in biliary epithelia has been reported in PBC and PSC patient and these BECs upregulated TLR4 expression (Kiziltas, 2016). 64% of PBC patient sera had IgM antibodies targeting components of LPS (Shimoda et al., 2011). In viral hepatitis, TLR2 and TLR4 were the main instigators of inflammation and TLR4 activated hepatic stellate cells were responsible for hepatic fibrogenesis (Kiziltas, 2016). HBV replication can be inhibited by the activation of TLRs however persistent HBV and HCV infection downregulate TLR expression (Kiziltas, 2016) indicating the importance of TLR signalling in protection against viral pathogens.

CD86 expression was highly expressed in hilum samples **(figure 4.9)**. Macrophages also express CD86 and may contribute to inflammatory responses observed in BA patients. Macrophages in BA secreted TNF-α (Feldman and Mack, 2012) contributing to inflammation and liver injury. CCL2 recruits macrophages to sites of liver injury (Yang et al., 2023) where they augment bile duct damage in concert with dendritic cells and Th17 cells (Lages et al., 2017). ROS production through macrophages can damage bile duct cells (Nomden et al., 2020) however polarising M1 classically activated macrophages to resolutive M2, may aid in alleviating cholangiocyte and liver injury in BA (Yang et al., 2022).

4.4.5 Non-syndromic and syndromic BA had similar genetic profiles

Minimal differences were observed in gene expression between non-syndromic and syndromic patients between hilum, wedge and explant samples indicating that the genetic profiles were similar between the two disease groups. Majority of the genes had similar

expression in both non-syndromic and syndromic patients indicating that disease progression is mostly comparable between the two groups. however, there were discrepancies in some genes including IFNG, CXCL2, *CXCL3*, *SOCS1*, *IL12RB1*, *IL10RA*, *TLR8*, and *TLR3* between non-syndromic and syndromic BA patients, these were not significant and further transcriptomic work on a larger cohort needs to be undertaken to identify significant transcriptomic differences between the two groups. In addition, multiparametric flow cytometry could also help to identify differences in immune cell subsets between the two groups to help with correct diagnosis of BA patients.

This genetic profiling data is useful to identify genetic phenotype in BA patients. Further transcriptomic studies need to be undertaken on a larger cohort of BA patients to corroborate our observed findings. Multiparametric flow cytometry experiments investigating B cell phenotype and cytokine expression may help to identify a specific B cell subset that is pathogenic in BA and worth targeting. As mentioned before, BA was composed of mixed immune infiltrates indicating that future investigations should focus on the contribution of T cells and other immune cells in BA pathology. Future therapies need to consider the interactions between different immune cells and identify immune subsets that contribute to tissue damage and pathogenesis.

4.5 Conclusions

In conclusion, the hilum of BA patients had remarkably differential gene expression compared to the peripheral wedge and explant samples. Minor discrepancies were detected in gene expression between non-syndromic and syndromic diseases (IFNG, CXCL2, *CXCL3*, *SOCS1*, *IL12RB1*, *IL10RA*, *TLR8*, and *TLR3*) which could be useful to identify distinctive genetic

profiles to refine therapies and warrant further investigation. These transcriptomic data showed that the hilum was the major site of inflammation with many cytokine genes being highly expressed. Increased TLR signalling and oxidative stress also indicated tissue damage. Furthermore, B cell and T cell signalling genes were also increased in the hilum suggesting that an interplay between lymphocytes and other immune cells may contribute to BA progression. Further investigations need to focus on the interaction between immune cells and how they contribute to disease progression and tissue damage.

CHAPTER 5 – GENERAL DISCUSSION

BA encompasses an umbrella of devastating paediatric diseases from varying aetiologies that lead to catastrophic liver failure in babies and very young children. There have been remarkable advances in characterising BA tissues in the past few years (Carvalho et al., 2005, Ye et al., 2022, Min et al., 2020), however there are no studies that compare the immune compartment of the biliary tree to the liver periphery in syndromic and non-syndromic cases. Furthermore, detailed characterisation of the inflammatory response at end-stage disease in liver explants is also lacking in these children. When I commenced my studies, I aimed to use multi-parametric spectral flow cytometry (Cytek Aurora) in collaboration with the University of Oxford to investigate the B cell compartment in children with BA at unprecedented depth and compare them to adult tissue explants from diseases of known aetiologies. These analyses could provide new clues as to whether some BA cases were similar to known autoimmune cholestatic conditions (PBC/PSC) or to tissue damage (alcohol-related or metabolic liver diseases). Due to the COVID-19 pandemic, I was unable to access fresh paediatric tissue and travel to Oxford for these studies. Thus, I built panels for use in conventional multi-parametric flow cytometry and validated these for use in adult human liver tissue. The studies presented in chapter 2 show the most detailed investigation of human B cell subsets in the liver to-date.

B cells play a vital role in humoral protection against infection and contribute to pathogenesis in autoimmunity. Hepatic B cells have been shown to contribute to the production of autoantibodies, cytokines and contribute to fibrogenesis (Novobrantseva et al., 2005, Xue et al., 2000, Taylor et al., 2019a). Hepatic B cells have not been extensively studied in paediatric and adult livers. Our work has shown that age-associated B cells (ABCs) were present across all adult chronic liver diseases and ABCs may have a protective or

pathogenic role in disease that warrants further phenotypic experiments. In BA and adult cholestatic diseases, we have shown the presence of B cell and lymphoid aggregates which contained CD20+ CD24- B cells. CD20+ CD24- B cells also expressed IL-6 highlighting a pathway for this B cell subset to contribute to tissue damage. Mixed immune infiltrates were observed in the liver around bile ducts, indicating that pathogenesis in BA and adult livers consists of a complex interplay between cells of the immune system. CD3+ T cells were found mixed within the core of lymphoid aggregates and were found to surround the periphery of B cell aggregates potentially highlighting a role for T cells in disease progression. Transcriptomic analyses showed that the hilum had higher expression of inflammatory genes compared to the periphery, indicating that the hilum was the site of active disease.

5.1 Age-associated B cells in adult chronic liver diseases

CD24- CD38- B cells have been shown to be present in higher frequencies in the peripheral blood of the elderly (Buffa et al., 2013). Rubtsov et al., showed that a novel population of B cells accumulated with age in mice which they termed ABCs. ABCs are characterised as CD19+ CD21lo (Rubtsov et al., 2011, Rubtsova et al., 2015) and a proportion of these cells express CD11b, CD11c and T-bet (Duggal et al., 2013, Rubtsov et al., 2011, Trivedi et al., 2019).

Our data showed that the frequencies of ABCs were not disease specific and were present across all liver diseases investigated and this subset was shown to be present in autoimmune diseases like RA, SLE and in infectious diseases like HIV, HCV, Malaria and COVID19 (Sachinidis et al., 2020). CD24- B cells may form a component of the ABC pool as these subsets expressed similar markers to CD21-/lo ABCs. ABCs act as efficient antigen presenters

(Rubtsova et al., 2015) and can play a protective role during infection as this subset produced antigen-specific IgM and IgG antibodies during viral infection in mice (Mouat and Horwitz, 2022) and had upregulated PC marker, CD138, expression (Rubtsov et al., 2011, Rubtsova et al., 2015) suggesting that they contribute to the effector arm of the immune system. Our data showed that CD11c+ T-bet+ ABCs had higher CD138 expression compared to other B cell subsets in adult chronic livers **(figure 2.15B)**.

ABCs have been found to be elevated in autoimmunity and contribute to disease progression through the generation of autoantibodies (Rubtsov et al., 2011). ABCs produce anti-dsDNA antibodies (Naradikian et al., 2016a) which have also been identified in 17% (3/17) of PBC patients and 48% (10/21) of AIH patients (Tsuchiya et al., 1994) suggesting that this autoantibody production was not disease specific. In addition, ABCs produce ANAs (Naradikian et al., 2016a) and these autoantibodies were detected in liver diseases including AIH patients (Moritoki et al., 2006, Than et al., 2016, Zwolak et al., 2016), PBC patients (Moritoki et al., 2006, Ma and Chen, 2019) and in the sera of PSC, viral hepatitis, NAFLD and ArLD patients (Himoto and Nishioka, 2013) indicating the pathogenic properties of ABCs. BA patient samples were not available for flow cytometry assays so the ABC compartment could not be determined for these patients however 11.3% of BA patients had the presence of ANA in the sera compared to 3.3% that was detected in age-matched disease controls (Pang et al., 2018). The presence of ANA did not show any correlation to hepatic fibrosis or outcomes of KPE (Pang et al., 2018).

ABCs from uninfected mice produce IFN-γ (Mouat and Horwitz, 2022), IL-6 and TNF-α (Frasca et al., 2021). During gamma herpesvirus 68 infection, ABCs increased IFN-γ and TNF-α expression (Mouat and Horwitz, 2022, Mouat et al., 2021) suggesting that ABCs contribute

to immune protection against infection by producing pro-inflammatory cytokines. In the context of disease, ABCs may also contribute to chronic inflammation alongside their production of antibodies.

It would be interesting to investigate the presence of ABCs in paediatric liver tissue as this would provide an insight into the protective or pathogenic role of ABCs and highlight a potential mechanism of inflammatory damage that could be targeted for future therapies. ABCs have been implicated in a host of autoimmune (Mouat et al., 2022) and infectious diseases (Mouat and Horwitz, 2022) and investigations of ABCs in BA may highlight why BA is a rapidly progressing liver disease.

5.2 The role of B cell and lymphoid aggregates in chronic liver diseases

Our flow cytometry data showed that CD19+ CD24- B cells expressed similar levels of makers associated with ABCs. Immunofluorescence assays showed that CD20+ CD24- B cells made up majority of the B cells in BA, especially in B cell and lymphoid aggregates found in the hilum and in some BA explant samples. This population of B cells could represent ABCs however there is no literature on ABCs in BA or if they contribute to BA pathology. Further experiments will need to be conducted to see if ABCs are present in BA, if they are protective in BA or if they damage BECs and contribute to pathology.

Three types of lymphocyte aggregates were observed in liver tissue: lymphoid aggregates consisting of B and T cells, B cell aggregates and TLS which resemble GCs (Purswani, 2016). Aggregates identified in BA tissue were a mixture of B cell and lymphoid aggregates which were detected in the hilum region. Interestingly, these were rarely TLS and there was little evidence of PBs/PCs in these tissues. These data were consistent with a proinflammatory

role for B cells, distinct from antigen-driven responses, at least during the disease progression (KPE biopsies).

Lymphoid aggregates were associated with cortical demyelination in MS (Ransohoff, 2023) indicating that these aggregates contribute to progression of disease. Lymphoid aggregates were only detected in hilum samples and not in wedge samples during early disease which suggests that the hilum may be the site of inflammation and these lymphoid aggregates may contribute to pathogenesis of BA. Furthermore, CD20+ CD24- B cells in these B cell and lymphoid aggregates also expressed IL-6 highlighting a role for aggregates in the progression of inflammatory-mediated tissue injury in BA.

Lymphoid aggregates were enriched in the hilum samples and likely contribute to inflammation based on their expression of IL-6 by immunofluorescence. Nanostring HOT panel data showed the hilum to have high expression of many genes related to inflammation, oxidative stress, B and T cell signalling compared to liver peripheral tissue, implying that the hilum is the site of active disease. Increased B and T cell infiltration has been observed in the portal tracts of BA patients (Lakshminarayanan and Davenport, 2016) which may result in increased expression of BCR and TCR signalling genes.

The composition of these lymphoid aggregates in paediatric tissues consisted of a B cell core with a few CD3+ T cells dispersed amongst the core and CD3+ T cells surrounded the B cell core. This aggregate composition was also observed in chronic HCV patients (Dhingra et al., 2016) where they showed that CD4+ T cells were dispersed amongst the B cell core, surrounded by CD8+ cytotoxic T cells (Freni et al., 1995). In our data, gene expression for

CD8+ T cells was higher in the hilum and CD4 expression was lower compared to liver periphery.

These data implied that CD8+ cytotoxic T cells may also contribute to BA pathogenesis through the secretion of granzyme B (Shi et al., 2022) and perforin (Meiraz et al., 2009), both of which were highly expressed in the hilum samples. CD8+ T cells can also secrete pro-inflammatory cytokines contributing the inflammatory milieu observed in BA. Cytotoxic T cells destroy virally-infected cells (Caminero et al., 2023), the presence of CD8+ T cells in the hilum and surrounding aggregates in BA may indicate the presence of a viral infection. Evidence of viral infection in BA is inconclusive however, it may be feasible to imply that a viral infection occurs during early disease at the hilum, due to the proximity to blood vessels. This viral infection induces inflammation and initiates an autoimmune response, potentially due to molecular mimicry or the release of DAMPs, which results in increased inflammation and despite viral clearance, this inflammatory response damages BECs and culminates in the need for a liver transplant (Mack, 2007).

5.3 Differences in TLR signalling in liver B cells between diseases

DAMPs are released upon tissue damage and can activate TLRs alongside PAMPs. The hilum had high expression of many genes related to TLR signalling indicating the presence of PAMPs and/or DAMPs in BA patients. In adult liver diseases, increased intestinal permeability allows the translocation of gut-derived microbial antigens which activates the immune response through TLR signalling (Ma et al., 2015, Schwenger et al., 2018, O'Hara and LaRusso, 2019, Nowak and Relja, 2020), which may be the case for BA patients. Abu Faddan et al., used infant serum samples to perform ELISAs to identify intestinal fatty acid

binding protein and ileal bile acid binding protein, as markers of cellular damage to the intestinal epithelium and they found significantly high levels of these markers in infants with cholestasis, including BA patients (Abu Faddan et al., 2017). This indicated that damage to intestinal epithelia may contribute to increased intestinal permeability allowing the translocation of microbial products and initiating an immune response. However, limited literature is available describing intestinal permeability in BA patients and this avenue needs to be further investigated. It is highly probable that cellular injury releases DAMPs activating TLRs, especially nucleic acid sensing TLRs such as TLR3, TLR7 and TLR9 as expression of these TLRs were increased in BA. Altered intestinal permeability, cellular damage and increased TLR signalling contribute to the inflammatory environment observed in the hilum, further implying that the hilum is the site of active disease.

5.4 Germinal centres; are they found in the liver?

Evidence of GCs have been found in BA patients in their hilar lymph nodes (Bednarek et al., 2018) and in proximal biliary remnants (Luo et al., 2021) however, there is no literature on the presence of B cell and lymphoid aggregates or ectopic GCs in BA. The lymphoid aggregates present in the hilum region were not GCs as they expressed Bcl2, indicating that the hilum does not have an abundance of PCs during early BA in our cohort. Whilst this may be the case, there are many studies that show the presence of IgG antibodies in both mouse models of BA (Lu et al., 2010) and in patients with BA (Lu et al., 2010, Hadchouel et al., 1981). IgG antibodies against α-enolase (Lu et al., 2010) and IgM antibodies against cholangiocyte proteins; CHI3L1, DLL-4 and SFTPD were observed in BA (Luo et al., 2021). The presence of IgG antibodies indicates the presence of GCs and PCs however these studies did not investigate the presence of antibodies during KPE, indicating that these antibodies

observed were present during end-stage disease. This is supported by our HOT panel data which showed that class-switched Igs were not expressed in the hilum but were highly expressed in explant samples at end-stage disease in BA patients. Furthermore, these data support the theory that BA progresses to an autoimmune disease as autoantibodies were present in both the mouse models and in infants with BA.

5.5 Pathogenesis and treatment of biliary atresia

A proposed theory is that infection occurs during pregnancy or after birth initiating the immune response, however despite the clearance of the virus, inflammation continues (Mack, 2007). This may be due to the release of DAMPs from necrotic cells during infection which activate TLRs on APCs and contribute to inflammation. Activated APCs may include B cells which produce pro-inflammatory cytokines and activate T cells which further secrete cytokines such as IFN-γ and TNF-α contributing to inflammatory damage. This inflammatory environment may result in the breakdown of tolerance allowing autoreactive cells to recognise and bind to self-ligands and produce autoantibodies targeting the tissue and resulting in liver injury. This may be the point when the disease becomes autoimmune. Autoantibodies targeting cholangiocyte proteins - CHI3L1, DLL-4 and SFTPD have been detected in BA indicating that autoreactive B cells contribute to BA pathology (Luo et al., 2021). BA pathogenesis consists of a complex interplay between humoral and cellular immunity.

There are no medical treatments for BA, only the surgical intervention of KPE and the eventual requirement of a liver transplant. Identifying the subsets that contribute to inflammation and tissue damage may be useful in creating specific therapies targeting these

cells, to prevent disease progression. In addition, identifying the correct time to administer therapies would be beneficial as anti-inflammatory therapies during the infectious phase of disease would be detrimental but anti-inflammatory therapies administered during early disease, at the hilum, could be beneficial in controlling inflammation. However, this only treats the symptoms and does not target the underlying cells contributing the inflammatory insult observed in BA.

The immune system is very complex, and many cells contribute to inflammation and pathogenesis of BA. Further transcriptomic work needs to be conducted to identify specific gene expression profiles or specific subsets of cells that may be suitable therapeutic targets. This work showed minimal differences between non-syndromic and syndromic BA patients indicating that the immune response associated to tissue damage may be similar in both types of BA and further transcriptomic work needs to be undertaken with a larger cohort of patients, to identify the discrepancies between these two groups.

5.6 General conclusions

Our work showed that ABCs, which can be protective or pathogenic depending upon the context of infection or autoimmunity, were abundant in the liver tissues of patients with liver diseases of multiple aetiologies. ABCs may be present in BA aggregates however this needs to be further investigated and confirmed using multi-parametric approaches. We showed that CD20+ CD24- B cells made up majority of the cells in aggregates in paediatric and adult cholestatic livers and these cells also secreted IL-6 contributing to tissue damage. CD20+ CD24- IL-6+ cells were also detected around bile ducts highlighting a potential role for this subset in tissue damage. CD20+ CD24- B cells may also produce other cytokines, but this needs to be investigated further. T cells surround these B cell and lymphoid aggregates and

may provide T cell help to activate these B cells or B cells could act as APCs to activate T cells. CD8+ T cells have been shown to surround lymphoid aggregates in the literature and these cytotoxic T cells may contribute to BA pathogenesis through the secretion of cytokines, granzyme B and perforin which result in cell damage and the release of DAMPs. These DAMPs can activate TLRs which further release pro-inflammatory mediators exacerbating disease and contributing to tissue injury and creating a vicious cycle of damage and inflammation. Lymphoid aggregate formation may indicate worsening of disease however this needs to be further investigated. In addition, could these lymphoid aggregates develop into TLS in early disease to produce immunoglobulins that target cholangiocytes? In our investigations, CD138+ ASCs were rarely observed. This work has highlighted that the liver hilum was distinct in inflammatory gene expression compared to the periphery and targeting inflammation at the hilar level may prevent the spread of tissue damage to the periphery.

B cell characterisation panels using flow cytometry have been set up and used in adult liver diseases in this work. The next step would be to investigate the B cell compartment in paediatric livers and to assess the cytokines produced by B cells through intracellular staining techniques and cell culture assays. Furthermore, comparison of BA tissues to other age-matched cholestatic and non-cholestatic liver diseases may provide a potential mechanism of disease pathogenesis in BA. The nanostring nCounter HOT panel work was performed using bulk RNA so conclusions about which cell types were producing the pro-inflammatory cytokines cannot be made. Spatial transcriptomics performed on liver tissue sections would be useful in the future, as this would allow localisation of cell types within

the tissue and determine the genes expressed within that cell type. This technology would enable us to gain a better understanding of BA biology with a focus on B cells.

BIBLIOGRAPHY

ABEYSEKERA, K. W. M., FERNANDES, G. S., HAMMERTON, G., PORTAL, A. J., GORDON, F. H., HERON, J. & HICKMAN, M. 2020. Prevalence of steatosis and fibrosis in young adults in the UK: a population-based study. *Lancet Gastroenterol Hepatol,* 5**,** 295-305.

ABOUGHALIA, H., KIM, H. H., DICK, A. A. S., PACHECO, M. C., CILLEY, R. E. & IYER, R. S. 2021. Pediatric biliary disorders: Multimodality imaging evaluation with clinicopathologic correlation. *Clin Imaging,* 75**,** 34-45.

ABU FADDAN, N. H., SHERIF, T. M., MOHAMMED, O. A., NASIF, K. A. & EL GEZAWY, E. M. 2017. Intestinal barrier integrity and function in infants with cholestasis. *Intest Res,* 15**,** 118-123.

AGEMATSU, K., HOKIBARA, S., NAGUMO, H. & KOMIYAMA, A. 2000. CD27: a memory B-cell marker. *Immunol Today,* 21**,** 204-6.

AGNELLO, V., CHUNG, R. T. & KAPLAN, L. M. 1992. A role for hepatitis C virus infection in type II cryoglobulinemia. *N Engl J Med,* 327**,** 1490-5.

AHMED, A. F., OHTANI, H., NIO, M., FUNAKI, N., SHIMAOKA, S., NAGURA, H. & OHI, R. 2001. CD8+ T cells infiltrating into bile ducts in biliary atresia do not appear to function as cytotoxic T cells: a clinicopathological analysis. *J Pathol,* 193**,** 383-9.

AKYOL, G., SÜER, Ö. & SEZER, C. 2001. Comparative Histological Analysis of Hepatitis C Virus with Hepatitis B. *Turkish Journal of Medical Sciences,* 31**,** 405-410.

AL-KHALILI, O. M. & ERICKSON, A. R. 2018. IgG-4 Related Disease: An Introduction. *Mo Med,* 115**,** 253-256.

ALFRAJI, N., UPADHYAYA, V. D., BEKAMPIS, C. & KUZYSHYN, H. 2020. Mixed Cryoglobulinemia Syndrome (MCS) due to untreated hepatitis B with uncommon presentation: case report and literature review. *BMC Rheumatol,* 4**,** 58.

ALMEIDA, J., POLVOROSA, M. A., GONZALEZ-QUINTELA, A., MADRUGA, I., MARCOS, M., PEREZ-NIETO, M. A., HERNANDEZ-CERCENO, M. L., ORFAO, A. & LASO, F. J. 2015. Altered Distribution of Peripheral Blood Maturation-Associated B-Cell Subsets in Chronic Alcoholism. *Alcohol Clin Exp Res,* 39**,** 1476-84.

ALONSO, E. M., HORSLEN, S. P., BEHRENS, E. M. & DOO, E. 2017. Pediatric acute liver failure of undetermined cause: A research workshop. *Hepatology,* 65**,** 1026-1037.

ARAFA, R. S., ABDEL HAIE, O. M., EL-AZAB, D. S., ABDEL-RAHMAN, A. M. & SIRA, M. M. 2016. Significant hepatic expression of IL-2 and IL-8 in biliary atresia compared with other neonatal cholestatic disorders. *Cytokine,* 79**,** 59-65.

ARAI, J., ITO, T., SHIMOZUMA, Y., UCHIKOSHI, M., NAKAJIMA, Y., SAKAKI, M., UOZUMI, S., KAJIWARA, A., SUGIURA, I., OTOYAMA, Y., NOZAWA, H., KURIHARA, T., EGUCHI, J., NOMURA, N., SAKUMA, D., SATO, M., DEGUCHI, Y. & YOSHIDA, H. 2020. Decreased expression of interferon-stimulated genes in B cells of patients with chronic hepatitis C during interferon-free therapy potentially suggests the eradication of hepatitis C virus in the B cells: A cohort study. *Health Sci Rep,* 3**,** e176.

ARICO, M. & CASELLI, D. 2022. Acute, Severe Hepatitis of Unknown Origin: Should We Really Be Afraid of Another Obscure Enemy of Our Children? *Pediatr Rep,* 14**,** 217-219.

ARPIN, C., DECHANET, J., VAN KOOTEN, C., MERVILLE, P., GROUARD, G., BRIERE, F., BANCHEREAU, J. & LIU, Y. J. 1995. Generation of memory B cells and plasma cells in vitro. *Science,* 268**,** 720-2.

ASLAM, M. A., ALEMDEHY, M. F., HAO, B., KRIJGER, P. H. L., PRITCHARD, C. E. J., DE RINK, I., MUHAIMIN, F. I., NURZIJAH, I., VAN BAALEN, M., KERKHOVEN, R. M., VAN DEN BERK, P. C. M., SKOK, J. A. & JACOBS, H. 2020. The Ig heavy chain protein but not its message controls early B cell development. *Proc Natl Acad Sci U S A,* 117**,** 31343-31352.

ASRANI, S. K., DEVARBHAVI, H., EATON, J. & KAMATH, P. S. 2019. Burden of liver diseases in the world. *J Hepatol,* 70**,** 151-171.

ATTA-UR-RAHMAN, HARVEY, K. & SIDDIQUI, R. A. 1999. Interleukin-8: An autocrine inflammatory mediator. *Curr Pharm Des,* 5**,** 241-53.

AYRE, D. C., PALLEGAR, N. K., FAIRBRIDGE, N. A., CANUTI, M., LANG, A. S. & CHRISTIAN, S. L. 2016. Analysis of the structure, evolution, and expression of CD24, an important regulator of cell fate. *Gene,* 590**,** 324-37.

BACH, N., THUNG, S. N. & SCHAFFNER, F. 1992. The histological features of chronic hepatitis C and autoimmune chronic hepatitis: a comparative analysis. *Hepatology,* 15**,** 572-7.

BADIZADEGAN, K., JONAS, M. M., OTT, M. J., NELSON, S. P. & PEREZ-ATAYDE, A. R. 1998. Histopathology of the liver in children with chronic hepatitis C viral infection. *Hepatology,* 28**,** 1416-23.

BAKER, J. M., BUCHFELLNER, M., BRITT, W., SANCHEZ, V., POTTER, J. L., INGRAM, L. A., SHIAU, H., SANCHEZ, L. H. G., SAAYBI, S., KELLY, D., LU, X., VEGA, E. M., AYERS-MILLSAP, S., WILLEFORD, W. G., RASSAEI, N., BULLOCK, H., REAGAN-STEINER, S., MARTIN, A., MOULTON, E. A., LAMSON, D. M., ST GEORGE, K., PARASHAR, U. D., HALL, A. J., MACNEIL, A., TATE, J. E. & KIRKING, H. L. 2022. Acute hepatitis and adenovirus infection among children-Alabama, October 2021-February 2022. *Am J Transplant,* 22**,** 1919-1921.

BASSO, K. & DALLA-FAVERA, R. 2015. Germinal centres and B cell lymphomagenesis. *Nat Rev Immunol,* 15**,** 172-84.

BATISTA, F. D., IBER, D. & NEUBERGER, M. S. 2001. B cells acquire antigen from target cells after synapse formation. *Nature,* 411**,** 489-94.

BEDNAREK, J., TRAXINGER, B., BRIGHAM, D., ROACH, J., ORLICKY, D., WANG, D., PELANDA, R. & MACK, C. L. 2018. Cytokine-Producing B Cells Promote Immune-Mediated Bile Duct Injury in Murine Biliary Atresia. *Hepatology,* 68**,** 1890-1904.

BEHAIRY, B. E., EL-ARABY, H. A., ABD EL KADER, H. H., EHSAN, N. A., SALEM, M. E., ZAKARIA, H. M. & KHEDR, M. A. 2016. Assessment of intrahepatic regulatory T cells in children with autoimmune hepatitis. *Ann Hepatol,* 15**,** 682-90.

BERKOWSKA, M. A., DRIESSEN, G. J., BIKOS, V., GROSSERICHTER-WAGENER, C., STAMATOPOULOS, K., CERUTTI, A., HE, B., BIERMANN, K., LANGE, J. F., VAN DER BURG, M., VAN DONGEN, J. J. & VAN ZELM, M. C. 2011. Human memory B cells originate from three distinct germinal center-dependent and -independent maturation pathways. *Blood,* 118**,** 2150-8.

BERNARD, N. J. 2018. Double-negative B cells. *Nat Rev Rheumatol,* 14**,** 684.

BERNASCONI, N. L., ONAI, N. & LANZAVECCHIA, A. 2003. A role for Toll-like receptors in acquired immunity: up-regulation of TLR9 by BCR triggering in naive B cells and constitutive expression in memory B cells. *Blood,* 101**,** 4500-4.

BERY, A. I., SHEPHERD, H. M., LI, W., KRUPNICK, A. S., GELMAN, A. E. & KREISEL, D. 2022. Role of tertiary lymphoid organs in the regulation of immune responses in the periphery. *Cell Mol Life Sci,* 79**,** 359.

BESSHO, K. & BEZERRA, J. A. 2011. Biliary atresia: will blocking inflammation tame the disease? *Annu Rev Med,* 62**,** 171-85.

BEYER, T. & MEYER-HERMANN, M. 2008. Mechanisms of organogenesis of primary lymphoid follicles. *Int Immunol,* 20**,** 615-23.

BEZERRA, J. A., TIAO, G., RYCKMAN, F. C., ALONSO, M., SABLA, G. E., SHNEIDER, B., SOKOL, R. J. & ARONOW, B. J. 2002. Genetic induction of proinflammatory immunity in children with biliary atresia. *Lancet,* 360**,** 1653-9.

BIOLEGEND. 2023. *Flow Cytometry Controls* [Online]. Available: https://www.biolegend.com/en-us/flow-controls [Accessed April 2020].

BOBO, L., OJEH, C., CHIU, D., MACHADO, A., COLOMBANI, P. & SCHWARZ, K. 1997. Lack of evidence for rotavirus by polymerase chain reaction/enzyme immunoassay of hepatobiliary samples from children with biliary atresia. *Pediatr Res,* 41**,** 229-34.

BOGDANOS, D. P., GAO, B. & GERSHWIN, M. E. 2013. Liver immunology. *Compr Physiol,* 3**,** 567-98.

BOLETO, G., VIEIRA, M., SAADOUN, D. & CACOUB, P. 2021. Hepatitis C virus-related vasculitis. *Clin Res Hepatol Gastroenterol,* 45**,** 101575.

BOOK, R., BEN-EZRA, J., GLAIT SANTAR, C., KAY, S., STEMER, G., OSTER, H. S. & MITTELMAN, M. 2022. Lymphoid aggregates in the bone marrow biopsies of patients with myelodysplastic syndromes - A potential prognostic marker? *Front Oncol,* 12**,** 988998.

BORTOLOTTI, F., VERUCCHI, G., CAMMA, C., CABIBBO, G., ZANCAN, L., INDOLFI, G., GIACCHINO, R., MARCELLINI, M., MARAZZI, M. G., BARBERA, C., MAGGIORE, G., VAJRO, P., BARTOLACCI, S., BALLI, F., MACCABRUNI, A., GUIDO, M., ITALIAN OBSERVATORY FOR, H. C. V. I. & HEPATITIS, C. I. C. 2008. Long-term course of chronic hepatitis C in children: from viral clearance to end-stage liver disease. *Gastroenterology,* 134**,** 1900-7.

BRINDLEY, S. M., LANHAM, A. M., KARRER, F. M., TUCKER, R. M., FONTENOT, A. P. & MACK, C. L. 2012. Cytomegalovirus-specific T-cell reactivity in biliary atresia at the time of diagnosis is associated with deficits in regulatory T cells. *Hepatology,* 55**,** 1130-8.

BRODIN, P. 2022. SARS-CoV-2 infections in children: Understanding diverse outcomes. *Immunity,* 55**,** 201-209.

BRODIN, P. & ARDITI, M. 2022. Severe acute hepatitis in children: investigate SARS-CoV-2 superantigens. *Lancet Gastroenterol Hepatol,* 7**,** 594-595.

BRUZZI, S., SUTTI, S., GIUDICI, G., BURLONE, M. E., RAMAVATH, N. N., TOSCANI, A., BOZZOLA, C., SCHNEIDER, P., MORELLO, E., PAROLA, M., PIRISI, M. & ALBANO, E. 2018. B2-Lymphocyte responses to oxidative stress-derived antigens contribute to the evolution of nonalcoholic fatty liver disease (NAFLD). *Free Radic Biol Med,* 124**,** 249-259.

BUFFA, S., PELLICANO, M., BULATI, M., MARTORANA, A., GOLDECK, D., CARUSO, C., PAWELEC, G. & COLONNA-ROMANO, G. 2013. A novel B cell population revealed by a CD38/CD24 gating strategy: CD38(-)CD24 (-) B cells in centenarian offspring and elderly people. *Age (Dordr),* 35**,** 2009-24.

BURTON, A. R., PALLETT, L. J., MCCOY, L. E., SUVEIZDYTE, K., AMIN, O. E., SWADLING, L., ALBERTS, E., DAVIDSON, B. R., KENNEDY, P. T., GILL, U. S., MAURI, C., BLAIR, P. A., PELLETIER, N. & MAINI, M. K. 2018. Circulating and intrahepatic antiviral B cells are defective in hepatitis B. *J Clin Invest,* 128**,** 4588-4603.

BYUN, J. S. & YI, H. S. 2017. Hepatic Immune Microenvironment in Alcoholic and Nonalcoholic Liver Disease. *Biomed Res Int,* 2017**,** 6862439.

CAMARERO, C., RAMOS, N., MORENO, A., ASENSIO, A., MATEOS, M. L. & ROLDAN, B. 2008. Hepatitis C virus infection acquired in childhood. *Eur J Pediatr,* 167**,** 219-24.

CAMINERO, F., IQBAL, Z. & TADI, P. 2023. Histology, Cytotoxic T Cells. *StatPearls.* Treasure Island (FL) ineligible companies. Disclosure: Zahid Iqbal declares no relevant financial relationships with ineligible companies. Disclosure: Prasanna Tadi declares no relevant financial relationships with ineligible companies.

CANDAS, D. & LI, J. J. 2014. MnSOD in oxidative stress response-potential regulation via mitochondrial protein influx. *Antioxid Redox Signal,* 20**,** 1599-617.

CAO, Q., BATEY, R., PANG, G., RUSSELL, A. & CLANCY, R. 1998. IL-6, IFN-gamma and TNF-alpha production by liver-associated T cells and acute liver injury in rats administered concanavalin A. *Immunol Cell Biol,* 76**,** 542-9.

CARAUX, A., KLEIN, B., PAIVA, B., BRET, C., SCHMITZ, A., FUHLER, G. M., BOS, N. A., JOHNSEN, H. E., ORFAO, A., PEREZ-ANDRES, M. & MYELOMA STEM CELL, N. 2010. Circulating human B and plasma cells. Age-associated changes in counts and detailed characterization of circulating normal CD138- and CD138+ plasma cells. *Haematologica,* 95**,** 1016-20.

CARDOSO, C. R., PROVINCIATTO, P. R., GODOI, D. F., VIEIRA, T. S., FERREIRA, B. R., TEIXEIRA, G., ROSSI, M. A., CUNHA, F. Q. & SILVA, J. S. 2008. B cells are involved in the modulation of pathogenic gut immune response in food-allergic enteropathy. *Clin Exp Immunol,* 154**,** 153-61.

CARPENTIERI, D. F., WENNER, W., LIQUORNIK, K. & RUCHELLI, E. 2000. Significance of lymphoid follicles and aggregates in gastric mucosa of children. *Pediatr Dev Pathol,* 3**,** 177-9.

CARVALHO, E., LIU, C., SHIVAKUMAR, P., SABLA, G., ARONOW, B. & BEZERRA, J. A. 2005. Analysis of the biliary transcriptome in experimental biliary atresia. *Gastroenterology,* 129**,** 713-7.

CASHMAN, S. B., MARSDEN, B. D. & DUSTIN, L. B. 2014. The Humoral Immune Response to HCV: Understanding is Key to Vaccine Development. *Front Immunol,* 5**,** 550.

CHAE, M. S., MOON, K. U., CHUNG, H. S., PARK, C. S., LEE, J., CHOI, J. H. & HONG, S. H. 2018. Serum interleukin-6 and tumor necrosis factor-alpha are associated with early graft regeneration after living donor liver transplantation. *PLoS One,* 13**,** e0195262.

CHAKHACHIRO, Z., SAROUFIM, M., SAFADI, B., ATTIEH, M., ASSAF, N., SHAMSEDDINE, G., TAMIM, H. & BOULOS, F. 2020. Plasma cells and lymphoid aggregates in sleeve gastrectomy specimens: Normal or gastritis? *Medicine (Baltimore),* 99**,** e18926.

CHAPMAN, M. H., THORBURN, D., HIRSCHFIELD, G. M., WEBSTER, G. G. J., RUSHBROOK, S. M., ALEXANDER, G., COLLIER, J., DYSON, J. K., JONES, D. E., PATANWALA, I., THAIN, C., WALMSLEY, M. & PEREIRA, S. P. 2019. British Society of Gastroenterology and UK-PSC guidelines for the diagnosis and management of primary sclerosing cholangitis. *Gut,* 68**,** 1356-1378.

CHARLES, E. D., BRUNETTI, C., MARUKIAN, S., RITOLA, K. D., TALAL, A. H., MARKS, K., JACOBSON, I. M., RICE, C. M. & DUSTIN, L. B. 2011. Clonal B cells in patients with hepatitis C virus-associated mixed cryoglobulinemia contain an expanded anergic CD21low B-cell subset. *Blood,* 117**,** 5425-37.

CHARLES, E. D., ORLOFF, M. I., NISHIUCHI, E., MARUKIAN, S., RICE, C. M. & DUSTIN, L. B. 2013. Somatic hypermutations confer rheumatoid factor activity in hepatitis C virus-associated mixed cryoglobulinemia. *Arthritis Rheum,* 65**,** 2430-40.

CHAUDHRY, M. S. & KARADIMITRIS, A. 2014. Role and regulation of CD1d in normal and pathological B cells. *J Immunol,* 193**,** 4761-8.

CHEN, J., SHU, Q. & ZHAO, Z. Y. 2022a. Response to the outbreak of severe acute hepatitis of unknown origin in children. *World J Pediatr,* 18**,** 525-528.
CHEN, K. & CERUTTI, A. 2011. The function and regulation of immunoglobulin D. *Curr Opin Immunol,* 23**,** 345-52.
CHEN, L., GORYACHEV, A., SUN, J., KIM, P., ZHANG, H., PHILLIPS, M. J., MACGREGOR, P., LEBEL, S., EDWARDS, A. M., CAO, Q. & FURUYA, K. N. 2003. Altered expression of genes involved in hepatic morphogenesis and fibrogenesis are identified by cDNA microarray analysis in biliary atresia. *Hepatology,* 38**,** 567-76.
CHEN, Q., LAI, L., CHI, X., LU, X., WU, H., SUN, J., WU, W., CAI, L., ZENG, X., WANG, C., CHEN, W. & PENG, A. 2020. CD19(+)CD24(hi)CD38(hi) B Cell Dysfunction in Primary Biliary Cholangitis. *Mediators Inflamm,* 2020**,** 3019378.
CHEN, Y. H., LOU, J. G., YANG, Z. H., CHEN, Q. J., HUA, C. Z., YE, S., ZHANG, C. M., CHEN, J., HUANG, Z. W., YU, J. D., GAO, Z. G. & SHU, Q. 2022b. Diagnosis, treatment, and prevention of severe acute hepatitis of unknown etiology in children. *World J Pediatr*.
CHENG, M. L., NAKIB, D., PERCIANI, C. T. & MACPARLAND, S. A. 2021. The immune niche of the liver. *Clin Sci (Lond),* 135**,** 2445-2466.
CHERUKURI, A., CHENG, P. C. & PIERCE, S. K. 2001. The role of the CD19/CD21 complex in B cell processing and presentation of complement-tagged antigens. *J Immunol,* 167**,** 163-72.
CHU, A. S., RUSSO, P. A. & WELLS, R. G. 2012. Cholangiocyte cilia are abnormal in syndromic and non-syndromic biliary atresia. *Mod Pathol,* 25**,** 751-7.
CHUNG, B. K., GUEVEL, B. T., REYNOLDS, G. M., GUPTA UDATHA, D. B., HENRIKSEN, E. K., STAMATAKI, Z., HIRSCHFIELD, G. M., KARLSEN, T. H. & LIASKOU, E. 2017. Phenotyping and auto-antibody production by liver-infiltrating B cells in primary sclerosing cholangitis and primary biliary cholangitis. *J Autoimmun,* 77**,** 45-54.
CHUNG, B. K., HENRIKSEN, E. K. K., JORGENSEN, K. K., KARLSEN, T. H., HIRSCHFIELD, G. M. & LIASKOU, E. 2018. Gut and Liver B Cells of Common Clonal Origin in Primary Sclerosing Cholangitis-Inflammatory Bowel Disease. *Hepatol Commun,* 2**,** 956-967.
CICHOZ-LACH, H., GRYWALSKA, E., MICHALAK, A., KOWALIK, A., MIELNIK, M. & ROLINSKI, J. 2018. Deviations in Peripheral Blood Cell Populations are Associated with the Stage of Primary Biliary Cholangitis and Presence of Itching. *Arch Immunol Ther Exp (Warsz),* 66**,** 443-452.
COSTA, F., DALLA PALMA, B. & GIULIANI, N. 2019. CD38 Expression by Myeloma Cells and Its Role in the Context of Bone Marrow Microenvironment: Modulation by Therapeutic Agents. *Cells,* 8.
CROOTE, D., DARMANIS, S., NADEAU, K. C. & QUAKE, S. R. 2018. High-affinity allergen-specific human antibodies cloned from single IgE B cell transcriptomes. *Science,* 362**,** 1306-1309.
CROUCHET, E., BANDIERA, S., FUJIWARA, N., LI, S., EL SAGHIRE, H., FERNANDEZ-VAQUERO, M., RIEDL, T., SUN, X., HIRSCHFIELD, H., JUHLING, F., ZHU, S., ROEHLEN, N., PONSOLLES, C., HEYDMANN, L., SAVIANO, A., QIAN, T., VENKATESH, A., LUPBERGER, J., VERRIER, E. R., SOJOODI, M., OUDOT, M. A., DUONG, F. H. T., MASIA, R., WEI, L., THUMANN, C., DURAND, S. C., GONZALEZ-MOTOS, V., HEIDE, D., HETZER, J., NAKAGAWA, S., ONO, A., SONG, W. M., HIGASHI, T., SANCHEZ, R., KIM, R. S., BIAN, C. B., KIANI, K., CROONENBORGHS, T., SUBRAMANIAN, A., CHUNG, R. T., STRAUB, B. K., SCHUPPAN, D., ANKAVAY, M., COCQUEREL, L., SCHAEFFER, E., GOOSSENS, N., KOH, A. P., MAHAJAN, M., NAIR, V. D., GUNASEKARAN, G., SCHWARTZ, M. E., BARDEESY, N., SHALEK, A. K., ROZENBLATT-ROSEN, O., REGEV, A., FELLI, E., PESSAUX, P., TANABE, K. K., HEIKENWALDER, M., SCHUSTER, C., POCHET, N., ZEISEL, M. B., FUCHS, B. C., HOSHIDA, Y. & BAUMERT, T. F. 2021. A human liver cell-based system modeling a clinical prognostic liver signature for therapeutic discovery. *Nat Commun,* 12**,** 5525.
CYTEK_BIOSCIENCES. Cytek Biosciences. Available: https://cdn.shopify.com/s/files/1/1654/6801/files/cytek_aurora_brochure.pdf?v=839461969602095242 [Accessed 26 May 2020].
DAMMACCO, F., SANSONNO, D., PICCOLI, C., RACANELLI, V., D'AMORE, F. P. & LAULETTA, G. 2000. The lymphoid system in hepatitis C virus infection: autoimmunity, mixed cryoglobulinemia, and Overt B-cell malignancy. *Semin Liver Dis,* 20**,** 143-57.
DE MUNCK, T. J. I., XU, P., VERWIJS, H. J. A., MASCLEE, A. A. M., JONKERS, D., VERBEEK, J. & KOEK, G. H. 2020. Intestinal permeability in human nonalcoholic fatty liver disease: A systematic review and meta-analysis. *Liver Int,* 40**,** 2906-2916.

DEEP, A., GRAMMATIKOPOULOS, T., HEATON, N., VERMA, A. & DHAWAN, A. 2022. Outbreak of hepatitis in children: clinical course of children with acute liver failure admitted to the intensive care unit. *Intensive Care Med,* 48**,** 958-962.

DESHPANDE, V., ZEN, Y., CHAN, J. K., YI, E. E., SATO, Y., YOSHINO, T., KLOPPEL, G., HEATHCOTE, J. G., KHOSROSHAHI, A., FERRY, J. A., AALBERSE, R. C., BLOCH, D. B., BRUGGE, W. R., BATEMAN, A. C., CARRUTHERS, M. N., CHARI, S. T., CHEUK, W., CORNELL, L. D., FERNANDEZ-DEL CASTILLO, C., FORCIONE, D. G., HAMILOS, D. L., KAMISAWA, T., KASASHIMA, S., KAWA, S., KAWANO, M., LAUWERS, G. Y., MASAKI, Y., NAKANUMA, Y., NOTOHARA, K., OKAZAKI, K., RYU, J. K., SAEKI, T., SAHANI, D. V., SMYRK, T. C., STONE, J. R., TAKAHIRA, M., WEBSTER, G. J., YAMAMOTO, M., ZAMBONI, G., UMEHARA, H. & STONE, J. H. 2012. Consensus statement on the pathology of IgG4-related disease. *Mod Pathol,* 25**,** 1181-92.

DHAWAN, A. & VIMALESVARAN, S. 2022. Hunting down the cause of acute hepatitis in children. *Lancet,* 399**,** 2264.

DHINGRA, S., WARD, S. C. & THUNG, S. N. 2016. Liver pathology of hepatitis C, beyond grading and staging of the disease. *World J Gastroenterol,* 22**,** 1357-66.

DOMINIS, M., PESUT, A., BOROVECKI, A., MARUSIC-VRSALOVIC, M. & KUSEC, R. 2005. Bone marrow lymphoid aggregates in malignant lymphomas. *Croat Med J,* 46**,** 410-6.

DONG, R. & ZHENG, S. 2015. Interleukin-8: A critical chemokine in biliary atresia. *J Gastroenterol Hepatol,* 30**,** 970-6.

DUGGAL, N. A., UPTON, J., PHILLIPS, A. C., SAPEY, E. & LORD, J. M. 2013. An age-related numerical and functional deficit in CD19(+) CD24(hi) CD38(hi) B cells is associated with an increase in systemic autoimmunity. *Aging Cell,* 12**,** 873-81.

DUSTIN, L. B. 2017. Innate and Adaptive Immune Responses in Chronic HCV Infection. *Curr Drug Targets,* 18**,** 826-843.

DYWICKI, J., BUITRAGO-MOLINA, L. E., PIETREK, J., LIEBER, M., BROERING, R., KHERA, T., SCHLUE, J., MANNS, M. P., WEDEMEYER, H., JAECKEL, E. & HARDTKE-WOLENSKI, M. 2020. Autoimmune hepatitis induction can occur in the liver. *Liver Int,* 40**,** 377-381.

EHRHARDT, G. R., HSU, J. T., GARTLAND, L., LEU, C. M., ZHANG, S., DAVIS, R. S. & COOPER, M. D. 2005. Expression of the immunoregulatory molecule FcRH4 defines a distinctive tissue-based population of memory B cells. *J Exp Med,* 202**,** 783-91.

EIBEL, H., KRAUS, H., SIC, H., KIENZLER, A. K. & RIZZI, M. 2014. B cell biology: an overview. *Curr Allergy Asthma Rep,* 14**,** 434.

EINBERG, A. P. & FISCHLER, B. 2022. Acute hepatitis of unknown origin - What we know so far. *Acta Paediatr*.

EIZA, N., ZUCKERMAN, E., CARLEBACH, M., RAINIS, T., GOLDBERG, Y. & VADASZ, Z. 2018. Increased killer B cells in chronic HCV infection may lead to autoimmunity and increased viral load. *Clin Exp Immunol,* 193**,** 183-193.

ELGUETA, R., BENSON, M. J., DE VRIES, V. C., WASIUK, A., GUO, Y. & NOELLE, R. J. 2009. Molecular mechanism and function of CD40/CD40L engagement in the immune system. *Immunol Rev,* 229**,** 152-72.

ELSNER, R. A. & SHLOMCHIK, M. J. 2020. Germinal Center and Extrafollicular B Cell Responses in Vaccination, Immunity, and Autoimmunity. *Immunity,* 53**,** 1136-1150.

FALASCA, K., UCCIFERRI, C., DALESSANDRO, M., ZINGARIELLO, P., MANCINO, P., PETRARCA, C., PIZZIGALLO, E., CONTI, P. & VECCHIET, J. 2006. Cytokine patterns correlate with liver damage in patients with chronic hepatitis B and C. *Ann Clin Lab Sci,* 36**,** 144-50.

FANG, Q., DENG, Y., LIANG, R., MEI, Y., HU, Z., WANG, J., SUN, J., ZHANG, X., BELLANTI, J. A. & ZHENG, S. G. 2020. CD19(+)CD24(hi)CD38(hi) regulatory B cells: a potential immune predictive marker of severity and therapeutic responsiveness of hepatitis C. *Am J Transl Res,* 12**,** 889-900.

FANG, X., ZHENG, P., TANG, J. & LIU, Y. 2010. CD24: from A to Z. *Cell Mol Immunol,* 7**,** 100-3.

FECTEAU, J. F., COTE, G. & NERON, S. 2006. A new memory CD27-IgG+ B cell population in peripheral blood expressing VH genes with low frequency of somatic mutation. *J Immunol,* 177**,** 3728-36.

FELDMAN, A. G. & MACK, C. L. 2012. Biliary atresia: cellular dynamics and immune dysregulation. *Semin Pediatr Surg,* 21**,** 192-200.

FISCHER, S., TRIVEDI, P. J., WARD, S., GREIG, P. D., THERAPONDOS, G. & HIRSCHFIELD, G. M. 2014. Frequency and significance of IgG4 immunohistochemical staining in liver explants from patients with primary sclerosing cholangitis. *Int J Exp Pathol,* 95**,** 209-15.

FISCHER, U., YANG, J. J., IKAWA, T., HEIN, D., VICENTE-DUENAS, C., BORKHARDT, A. & SANCHEZ-GARCIA, I. 2020. Cell Fate Decisions: The Role of Transcription Factors in Early B-cell Development and Leukemia. *Blood Cancer Discov,* 1**,** 224-233.

FORSTER, R., DAVALOS-MISSLITZ, A. C. & ROT, A. 2008. CCR7 and its ligands: balancing immunity and tolerance. *Nat Rev Immunol,* 8**,** 362-71.

FRANCO, A., KRAUS, Z., LI, H., SEIBERT, N., DEMENT-BROWN, J. & TOLNAY, M. 2018. CD21 and FCRL5 form a receptor complex with robust B-cell activating capacity. *Int Immunol,* 30**,** 569-578.

FRASCA, D., ROMERO, M., GARCIA, D., DIAZ, A. & BLOMBERG, B. B. 2021. Hyper-metabolic B cells in the spleens of old mice make antibodies with autoimmune specificities. *Immun Ageing,* 18**,** 9.

FRENI, M. A., ARTUSO, D., GERKEN, G., SPANTI, C., MARAFIOTI, T., ALESSI, N., SPADARO, A., AJELLO, A. & FERRAU, O. 1995. Focal lymphocytic aggregates in chronic hepatitis C: occurrence, immunohistochemical characterization, and relation to markers of autoimmunity. *Hepatology,* 22**,** 389-94.

GAMBELLA, A., BARRECA, A., OSELLA-ABATE, S., BOTTASSO, E., GIARIN, M. M., PAPOTTI, M., BIANCONE, L., METOVIC, J., COLLEMI, G., CASSONI, P. & BERTERO, L. 2021. Caveolin-1 in Kidney Chronic Antibody-Mediated Rejection: An Integrated Immunohistochemical and Transcriptomic Analysis Based on the Banff Human Organ Transplant (B-HOT) Gene Panel. *Biomedicines,* 9.

GAO, B. 2016. Basic liver immunology. *Cell Mol Immunol,* 13**,** 265-6.

GAO, S. H., GONG, M. C. & SONG, H. M. 2022. Acute severe hepatitis of unknown origin in children: considerations from the perspective of immunology. *World J Pediatr*.

GAO, X. & COCKBURN, I. A. 2022. The development and function of CD11c(+) atypical B cells - insights from single cell analysis. *Front Immunol,* 13**,** 979060.

GARAUD, S., TAHER, T. E., DEBANT, M., BURGOS, M., MELAYAH, S., BERTHOU, C., PARIKH, K., PERS, J. O., LUQUE-PAZ, D., CHIOCCHIA, G., PEPPELENBOSCH, M., ISENBERG, D. A., YOUINOU, P., MIGNEN, O., RENAUDINEAU, Y. & MAGEED, R. A. 2018. CD5 expression promotes IL-10 production through activation of the MAPK/Erk pathway and upregulation of TRPC1 channels in B lymphocytes. *Cell Mol Immunol,* 15**,** 158-170.

GARAZZINO, S., CALITRI, C., VERSACE, A., ALFARANO, A., SCOLFARO, C., BERTAINA, C., VATRANO, S., MIGNONE, F., LICCIARDI, F., GABIANO, C. & TOVO, P. A. 2014. Natural history of vertically acquired HCV infection and associated autoimmune phenomena. *Eur J Pediatr,* 173**,** 1025-31.

GARY-GOUY, H., HARRIAGUE, J., BISMUTH, G., PLATZER, C., SCHMITT, C. & DALLOUL, A. H. 2002. Human CD5 promotes B-cell survival through stimulation of autocrine IL-10 production. *Blood,* 100**,** 4537-43.

GAULD, S. B., DAL PORTO, J. M. & CAMBIER, J. C. 2002. B cell antigen receptor signaling: roles in cell development and disease. *Science,* 296**,** 1641-2.

GHAEDI, M., STEER, C. A., MARTINEZ-GONZALEZ, I., HALIM, T. Y. F., ABRAHAM, N. & TAKEI, F. 2016. Common-Lymphoid-Progenitor-Independent Pathways of Innate and T Lymphocyte Development. *Cell Rep,* 15**,** 471-480.

GINES, P., KRAG, A., ABRALDES, J. G., SOLA, E., FABRELLAS, N. & KAMATH, P. S. 2021. Liver cirrhosis. *Lancet,* 398**,** 1359-1376.

GIORGIO, V., MIELE, L., PRINCIPESSA, L., FERRETTI, F., VILLA, M. P., NEGRO, V., GRIECO, A., ALISI, A. & NOBILI, V. 2014. Intestinal permeability is increased in children with non-alcoholic fatty liver disease, and correlates with liver disease severity. *Dig Liver Dis,* 46**,** 556-60.

GIOVANNONE, N., ANTONOPOULOS, A., LIANG, J., GEDDES SWEENEY, J., KUDELKA, M. R., KING, S. L., LEE, G. S., CUMMINGS, R. D., DELL, A., BARTHEL, S. R., WIDLUND, H. R., HASLAM, S. M. & DIMITROFF, C. J. 2018. Human B Cell Differentiation Is Characterized by Progressive Remodeling of O-Linked Glycans. *Front Immunol,* 9**,** 2857.

GLARIA, E. & VALLEDOR, A. F. 2020. Roles of CD38 in the Immune Response to Infection. *Cells,* 9.

GLASER, J. H., BALISTRERI, W. F. & MORECKI, R. 1984. Role of reovirus type 3 in persistent infantile cholestasis. *J Pediatr,* 105**,** 912-5.

GODBOLE, N., KYRONLAHTI, A., HUKKINEN, M., PIHLAJOKI, M., HEIKINHEIMO, M. & PAKARINEN, M. P. 2023. Bacterial translocation markers and toll-like receptors in biliary atresia following successful portoenterostomy. *Acta Paediatr*.

GOODMAN, Z. D., MAKHLOUF, H. R., LIU, L., BALISTRERI, W., GONZALEZ-PERALTA, R. P., HABER, B., JONAS, M. M., MOHAN, P., MOLLESTON, J. P., MURRAY, K. F., NARKEWICZ, M. R., ROSENTHAL, P., SMITH, L. J.,

ROBUCK, P. R. & SCHWARZ, K. B. 2008. Pathology of chronic hepatitis C in children: liver biopsy findings in the Peds-C Trial. *Hepatology,* 47**,** 836-43.
GOULOPOULOU, S., MCCARTHY, C. G. & WEBB, R. C. 2016. Toll-like Receptors in the Vascular System: Sensing the Dangers Within. *Pharmacol Rev,* 68**,** 142-67.
GRONBAEK, L., OTETE, H., BAN, L., CROOKS, C., CARD, T., JEPSEN, P. & WEST, J. 2020. Incidence, prevalence and mortality of autoimmune hepatitis in England 1997-2015. A population-based cohort study. *Liver Int,* 40**,** 1634-1644.
GUO, C., ZHU, J., PU, C. L., DENG, Y. H. & ZHANG, M. M. 2012. Combinatory effects of hepatic CD8+ and NK lymphocytes in bile duct injury from biliary atresia. *Pediatr Res,* 71**,** 638-44.
GUO, S. & CHEN, X. 2015. The human Nox4: gene, structure, physiological function and pathological significance. *J Drug Target,* 23**,** 888-96.
HADCHOUEL, M., HUGON, R. N. & ODIEVRE, M. 1981. Immunoglobulin deposits in the biliary remnants of extrahepatic biliary atresia: a study by immunoperoxidase staining in 128 infants. *Histopathology,* 5**,** 217-21.
HAGA, C. L., EHRHARDT, G. R., BOOHAKER, R. J., DAVIS, R. S. & COOPER, M. D. 2007. Fc receptor-like 5 inhibits B cell activation via SHP-1 tyrosine phosphatase recruitment. *Proc Natl Acad Sci U S A,* 104**,** 9770-5.
HAMPE, C. S. 2012. B Cell in Autoimmune Diseases. *Scientifica (Cairo),* 2012.
HANSEN, I. S., BAETEN, D. L. P. & DEN DUNNEN, J. 2019. The inflammatory function of human IgA. *Cell Mol Life Sci,* 76**,** 1041-1055.
HAO, Y., O'NEILL, P., NARADIKIAN, M. S., SCHOLZ, J. L. & CANCRO, M. P. 2011. A B-cell subset uniquely responsive to innate stimuli accumulates in aged mice. *Blood,* 118**,** 1294-304.
HARDIE, C., GREEN, K., JOPSON, L., MILLAR, B., INNES, B., PAGAN, S., TINIAKOS, D., DYSON, J., HANIFFA, M., BIGLEY, V., JONES, D. E., BRAIN, J. & WALKER, L. J. 2016. Early Molecular Stratification of High-risk Primary Biliary Cholangitis. *EBioMedicine,* 14**,** 65-73.
HARTL, J., MIQUEL, R., ZACHOU, K., WONG, G. W., ASGHAR, A., PAPE, S., SEBODE, M., PEISELER, M., ZENOUZI, R., EHLKEN, H., KRECH, T., WEILER-NORMANN, C., DRENTH, J. P. H., OO, Y. H., DALEKOS, G. N., HENEGHAN, M., SCHRAMM, C. & LOHSE, A. W. 2020. Features and outcome of AIH patients without elevation of IgG. *JHEP Rep,* 2**,** 100094.
HASHIZUME, N., TANAKA, Y., ASAGIRI, K., FUKAHORI, S., ISHII, S., SAIKUSA, N., YOSHIDA, M., TANIKAWA, K., ASAKAWA, T. & YAGI, M. 2020. Perioperative reactive oxygen species in infants with biliary atresia: A retrospective observational study. *Medicine (Baltimore),* 99**,** e21332.
HATTA, Y., TSUCHIYA, N., MATSUSHITA, M., SHIOTA, M., HAGIWARA, K. & TOKUNAGA, K. 1999. Identification of the gene variations in human CD22. *Immunogenetics,* 49**,** 280-6.
HEHLE, V., BERETTA, M., BOURGINE, M., AIT-GOUGHOULTE, M., PLANCHAIS, C., MORISSE, S., VESIN, B., LORIN, V., HIEU, T., STAUFFER, A., FIQUET, O., DIMITROV, J. D., MICHEL, M. L., UNGEHEUER, M. N., SUREAU, C., POL, S., DI SANTO, J. P., STRICK-MARCHAND, H., PELLETIER, N. & MOUQUET, H. 2020. Potent human broadly neutralizing antibodies to hepatitis B virus from natural controllers. *J Exp Med,* 217.
HIMOTO, T. & NISHIOKA, M. 2013. Autoantibodies in liver disease: important clues for the diagnosis, disease activity and prognosis. *Auto Immun Highlights,* 4**,** 39-53.
HIRSCHFIELD, G. M., DYSON, J. K., ALEXANDER, G. J. M., CHAPMAN, M. H., COLLIER, J., HUBSCHER, S., PATANWALA, I., PEREIRA, S. P., THAIN, C., THORBURN, D., TINIAKOS, D., WALMSLEY, M., WEBSTER, G. & JONES, D. E. J. 2018. The British Society of Gastroenterology/UK-PBC primary biliary cholangitis treatment and management guidelines. *Gut,* 67**,** 1568-1594.
HIRSCHFIELD, G. M. & GERSHWIN, M. E. 2013. The immunobiology and pathophysiology of primary biliary cirrhosis. *Annu Rev Pathol,* 8**,** 303-30.
HOGERKORP, C. M. & BORREBAECK, C. A. 2006. The human CD77- B cell population represents a heterogeneous subset of cells comprising centroblasts, centrocytes, and plasmablasts, prompting phenotypical revision. *J Immunol,* 177**,** 4341-9.
HOLLISTER, K., KUSUMANCHI, P., ROSS, R. A., CHANDLER, K., OSHODI, A., HEATHERS, L., TEAGARDEN, S., WANG, L., DENT, A. L. & LIANGPUNSAKUL, S. 2018. Levels of circulating follicular helper T cells, T helper 1 cells, and the prognostic significance of soluble form of CD40 ligand on survival in patients with alcoholic cirrhosis. *Liver Res,* 2**,** 52-59.
HOLT, A. P., STAMATAKI, Z. & ADAMS, D. H. 2006. Attenuated liver fibrosis in the absence of B cells. *Hepatology,* 43**,** 868-71.

HONG, M., SANDALOVA, E., LOW, D., GEHRING, A. J., FIENI, S., AMADEI, B., URBANI, S., CHONG, Y. S., GUCCIONE, E. & BERTOLETTI, A. 2015. Trained immunity in newborn infants of HBV-infected mothers. *Nat Commun,* 6**,** 6588.

HOSHIDA, Y., VILLANUEVA, A., SANGIOVANNI, A., SOLE, M., HUR, C., ANDERSSON, K. L., CHUNG, R. T., GOULD, J., KOJIMA, K., GUPTA, S., TAYLOR, B., CRENSHAW, A., GABRIEL, S., MINGUEZ, B., IAVARONE, M., FRIEDMAN, S. L., COLOMBO, M., LLOVET, J. M. & GOLUB, T. R. 2013. Prognostic gene expression signature for patients with hepatitis C-related early-stage cirrhosis. *Gastroenterology,* 144**,** 1024-30.

HSU, C. L., OU, D. L., BAI, L. Y., CHEN, C. W., LIN, L., HUANG, S. F., CHENG, A. L., JENG, Y. M. & HSU, C. 2021. Exploring Markers of Exhausted CD8 T Cells to Predict Response to Immune Checkpoint Inhibitor Therapy for Hepatocellular Carcinoma. *Liver Cancer,* 10**,** 346-359.

INDOLFI, G., BARTOLINI, E., OLIVITO, B., AZZARI, C. & RESTI, M. 2012. Autoimmunity and extrahepatic manifestations in treatment-naive children with chronic hepatitis C virus infection. *Clin Dev Immunol,* 2012**,** 785627.

INOKUCHI, M., ITO, T., UCHIKOSHI, M., SHIMOZUMA, Y., MORIKAWA, K., NOZAWA, H., SHIMAZAKI, T., HIROISHI, K., MIYAKAWA, Y. & IMAWARI, M. 2009. Infection of B cells with hepatitis C virus for the development of lymphoproliferative disorders in patients with chronic hepatitis C. *J Med Virol,* 81**,** 619-27.

IORDANSKAIA, T., HUBAL, M. J., KOECK, E., ROSSI, C., SCHWARZ, K. & NADLER, E. P. 2013. Dysregulation of upstream and downstream transforming growth factor-beta transcripts in livers of children with biliary atresia and fibrogenic gene signatures. *J Pediatr Surg,* 48**,** 2047-53.

JACOBI, A. M., REITER, K., MACKAY, M., ARANOW, C., HIEPE, F., RADBRUCH, A., HANSEN, A., BURMESTER, G. R., DIAMOND, B., LIPSKY, P. E. & DORNER, T. 2008. Activated memory B cell subsets correlate with disease activity in systemic lupus erythematosus: delineation by expression of CD27, IgD, and CD95. *Arthritis Rheum,* 58**,** 1762-73.

JARA, P., RESTI, M., HIERRO, L., GIACCHINO, R., BARBERA, C., ZANCAN, L., CRIVELLARO, C., SOKAL, E., AZZARI, C., GUIDO, M. & BORTOLOTTI, F. 2003. Chronic hepatitis C virus infection in childhood: clinical patterns and evolution in 224 white children. *Clin Infect Dis,* 36**,** 275-80.

JASKIEWICZ, K. & KOBIERSKA, G. 2000. Lymphoid aggregates in gastric biopsies: relationship to other mucosal lesions. *Arch Immunol Ther Exp (Warsz),* 48**,** 201-4.

JEFFERIES, M., RAUFF, B., RASHID, H., LAM, T. & RAFIQ, S. 2018. Update on global epidemiology of viral hepatitis and preventive strategies. *World J Clin Cases,* 6**,** 589-599.

JEFFERY, H. C., BRAITCH, M. K., BAGNALL, C., HODSON, J., JEFFERY, L. E., WAWMAN, R. E., WONG, L. L., BIRTWISTLE, J., BARTLETT, H., LOHSE, A. W., HIRSCHFIELD, G. M., DYSON, J., JONES, D., HUBSCHER, S. G., KLENERMAN, P., ADAMS, D. H. & OO, Y. H. 2018. Changes in natural killer cells and exhausted memory regulatory T Cells with corticosteroid therapy in acute autoimmune hepatitis. *Hepatol Commun,* 2**,** 421-436.

JEFFERY, H. C., VAN WILGENBURG, B., KURIOKA, A., PAREKH, K., STIRLING, K., ROBERTS, S., DUTTON, E. E., HUNTER, S., GEH, D., BRAITCH, M. K., RAJANAYAGAM, J., IQBAL, T., PINKNEY, T., BROWN, R., WITHERS, D. R., ADAMS, D. H., KLENERMAN, P. & OO, Y. H. 2016. Biliary epithelium and liver B cells exposed to bacteria activate intrahepatic MAIT cells through MR1. *J Hepatol,* 64**,** 1118-1127.

JEVON, G. P. & DIMMICK, J. E. 1999. Biliary atresia and cytomegalovirus infection: a DNA study. *Pediatr Dev Pathol,* 2**,** 11-4.

KAGE, M., FUJISAWA, T., SHIRAKI, K., TANAKA, T., FUJISAWA, T., KIMURA, A., SHIMAMATSU, K., NAKASHIMA, E., KOJIRO, M., KOIKE, M., TAZAWA, Y., ABUKAWA, D., OKANIWA, M., TAKITA, H., MATSUI, A., HAYASHI, T., ETOU, T., TERASAWA, S., SUGIYAMA, K., TAJIRI, H., YODEN, A., KAJIWARA, Y., SATA, M. & UCHIMURA, Y. 1997. Pathology of chronic hepatitis C in children. Child Liver Study Group of Japan. *Hepatology,* 26**,** 771-5.

KAJON, A. E. & ST GEORGE, K. 2022. Mysterious cases of acute hepatitis in children: is adenovirus still a lead suspect? *Emerg Microbes Infect,* 11**,** 1787-1789.

KALRA, A., YETISKUL, E., WEHRLE, C. J. & TUMA, F. 2024. Physiology, Liver. *StatPearls.* Treasure Island (FL) ineligible companies. Disclosure: Ekrem Yetiskul declares no relevant financial relationships with ineligible companies. Disclosure: Chase Wehrle declares no relevant financial relationships with ineligible companies. Disclosure: Faiz Tuma declares no relevant financial relationships with ineligible companies.

KARA, N., URGANCI, N., KALYONCU, D. & YILMAZ, B. 2014. The association between Helicobacter pylori gastritis and lymphoid aggregates, lymphoid follicles and intestinal metaplasia in gastric mucosa of children. *J Paediatr Child Health,* 50**,** 605-9.

KARNELL, J. L., KUMAR, V., WANG, J., WANG, S., VOYNOVA, E. & ETTINGER, R. 2017. Role of CD11c(+) T-bet(+) B cells in human health and disease. *Cell Immunol,* 321**,** 40-45.

KELLY, D. A. & DAVENPORT, M. 2007. Current management of biliary atresia. *Arch Dis Child,* 92**,** 1132-5.

KELLY, D. A. & STAMATAKI, Z. 2022. Sudden onset hepatitis in children. *Nat Rev Gastroenterol Hepatol,* 19**,** 553-554.

KIKUCHI, K., LIAN, Z. X., YANG, G. X., ANSARI, A. A., IKEHARA, S., KAPLAN, M., MIYAKAWA, H., COPPEL, R. L. & GERSHWIN, M. E. 2005. Bacterial CpG induces hyper-IgM production in CD27(+) memory B cells in primary biliary cirrhosis. *Gastroenterology,* 128**,** 304-12.

KIKUCHI, K., TSUNEYAMA, K., YAMADA, H., KAJIYAMA, Y., MATSUMOTO, K., TSUNASHIMA, H., YAMASHITA, R., TAKAI, A., NEGISHI, M., HARA, M., MORITOKI, Y. & MIYAKAWA, H. 2014. Splenic lymph follicles generate immunoglobulin M-producing B cells in primary biliary cirrhosis. *Hepatol Res,* 44**,** E253-E256.

KIM, C. C., BACCARELLA, A. M., BAYAT, A., PEPPER, M. & FONTANA, M. F. 2019. FCRL5(+) Memory B Cells Exhibit Robust Recall Responses. *Cell Rep,* 27**,** 1446-1460 e4.

KIZILTAS, S. 2016. Toll-like receptors in pathophysiology of liver diseases. *World J Hepatol,* 8**,** 1354-1369.

KREMMIDIOTIS, G. & ZOLA, H. 1995. Changes in CD44 expression during B cell differentiation in the human tonsil. *Cell Immunol,* 161**,** 147-57.

KRISS, M., GOLDEN-MASON, L., KAPLAN, J., MIRSHAHI, F., SETIAWAN, V. W., SANYAL, A. J. & ROSEN, H. R. 2020. Increased hepatic and circulating chemokine and osteopontin expression occurs early in human NAFLD development. *PLoS One,* 15**,** e0236353.

KUBES, P. & JENNE, C. 2018. Immune Responses in the Liver. *Annu Rev Immunol,* 36**,** 247-277.

KUPPERS, R. 2019. CD81 as target for B cell lymphomas. *J Exp Med,* 216**,** 1469-1470.

KUPPERS, R. 2021. The life of B cells according to JEM. *J Exp Med,* 218.

LAGES, C. S., SIMMONS, J., CHOUGNET, C. A. & MIETHKE, A. G. 2012. Regulatory T cells control the CD8 adaptive immune response at the time of ductal obstruction in experimental biliary atresia. *Hepatology,* 56**,** 219-27.

LAGES, C. S., SIMMONS, J., MADDOX, A., JONES, K., KARNS, R., SHERIDAN, R., SHANMUKHAPPA, S. K., MOHANTY, S., KOFRON, M., RUSSO, P., WANG, Y. H., CHOUGNET, C. & MIETHKE, A. G. 2017. The dendritic cell-T helper 17-macrophage axis controls cholangiocyte injury and disease progression in murine and human biliary atresia. *Hepatology,* 65**,** 174-188.

LAIDLAW, S. M. & DUSTIN, L. B. 2020. An HCV Vaccine on the Fly. *J Infect Dis,* 221**,** 1216-1218.

LAKSHMINARAYANAN, B. & DAVENPORT, M. 2016. Biliary atresia: A comprehensive review. *J Autoimmun,* 73**,** 1-9.

LANDING, B. H. 1974. Considerations of the pathogenesis of neonatal hepatitis, biliary atresia and choledochal cyst--the concept of infantile obstructive cholangiopathy. *Prog Pediatr Surg,* 6**,** 113-39.

LAPIERRE, P., BELAND, K., YANG, R. & ALVAREZ, F. 2013. Adoptive transfer of ex vivo expanded regulatory T cells in an autoimmune hepatitis murine model restores peripheral tolerance. *Hepatology,* 57**,** 217-27.

LAULETTA, G., RUSSI, S., CONTEDUCA, V. & SANSONNO, L. 2012. Hepatitis C virus infection and mixed cryoglobulinemia. *Clin Dev Immunol,* 2012**,** 502156.

LAW, M., MARUYAMA, T., LEWIS, J., GIANG, E., TARR, A. W., STAMATAKI, Z., GASTAMINZA, P., CHISARI, F. V., JONES, I. M., FOX, R. I., BALL, J. K., MCKEATING, J. A., KNETEMAN, N. M. & BURTON, D. R. 2008. Broadly neutralizing antibodies protect against hepatitis C virus quasispecies challenge. *Nat Med,* 14**,** 25-7.

LEBIEN, T. W. & TEDDER, T. F. 2008. B lymphocytes: how they develop and function. *Blood,* 112**,** 1570-80.

LEE, K. Y., JEON, S. Y., HONG, J. W., KIM, Y. H., SONG, K. H. & KIM, K. H. 2011. CD20 Positive T Cell Lymphoma Involvement of Skin. *Ann Dermatol,* 23**,** 529-35.

LEROUX, A., FERRERE, G., GODIE, V., CAILLEUX, F., RENOUD, M. L., GAUDIN, F., NAVEAU, S., PREVOT, S., MAKHZAMI, S., PERLEMUTER, G. & CASSARD-DOULCIER, A. M. 2012. Toxic lipids stored by Kupffer cells correlates with their pro-inflammatory phenotype at an early stage of steatohepatitis. *J Hepatol,* 57**,** 141-9.

LEUNG, D. H., SQUIRES, J. E., JHAVERI, R., KERKAR, N., LIN, C. H., MOHAN, P., MURRAY, K. F., GONZALEZ-PERALTA, R. P., ROBERTS, E. A. & SUNDARAM, S. S. 2020. Hepatitis C in 2020: A North American

Society for Pediatric Gastroenterology, Hepatology, and Nutrition Position Paper. *J Pediatr Gastroenterol Nutr,* 71**,** 407-417.
LI, C. & ZHOU, H. M. 2011. The role of manganese superoxide dismutase in inflammation defense. *Enzyme Res,* 2011**,** 387176.
LI, H., DEMENT-BROWN, J., LIAO, P. J., MAZO, I., MILLS, F., KRAUS, Z., FITZSIMMONS, S. & TOLNAY, M. 2020. Fc receptor-like 4 and 5 define human atypical memory B cells. *Int Immunol,* 32**,** 755-770.
LI, J., HU, W., ZHANG, J. Y. & WANG, F. S. 2022. Pediatric Acute Severe Hepatitis of Unknown Origin: What is New? *J Clin Transl Hepatol,* 10**,** 509-514.
LIU, N., OHNISHI, N., NI, L., AKIRA, S. & BACON, K. B. 2003. CpG directly induces T-bet expression and inhibits IgG1 and IgE switching in B cells. *Nat Immunol,* 4**,** 687-93.
LIU, Y., CHENG, L. S., WU, S. D., WANG, S. Q., LI, L., SHE, W. M., LI, J., WANG, J. Y. & JIANG, W. 2016. IL-10-producing regulatory B-cells suppressed effector T-cells but enhanced regulatory T-cells in chronic HBV infection. *Clin Sci (Lond),* 130**,** 907-19.
LIU, Y., FAN, L., CHENG, Z., YU, L., CONG, S., HU, Y., ZHU, L., ZHANG, B., CHENG, Y., ZHAO, P., ZHAO, X. & CHENG, M. 2021. Fecal transplantation alleviates acute liver injury in mice through regulating Treg/Th17 cytokines balance. *Sci Rep,* 11**,** 1611.
LOGGI, E., GAMAL, N., BIHL, F., BERNARDI, M. & ANDREONE, P. 2014. Adaptive response in hepatitis B virus infection. *J Viral Hepat,* 21**,** 305-13.
LU, B. R., BRINDLEY, S. M., TUCKER, R. M., LAMBERT, C. L. & MACK, C. L. 2010. alpha-enolase autoantibodies cross-reactive to viral proteins in a mouse model of biliary atresia. *Gastroenterology,* 139**,** 1753-61.
LUO, Y., BRIGHAM, D., BEDNAREK, J., TORRES, R., WANG, D., AHMAD, S. & MACK, C. L. 2021. Unique Cholangiocyte-Targeted IgM Autoantibodies Correlate With Poor Outcome in Biliary Atresia. *Hepatology,* 73**,** 1855-1867.
LUTCKII, A., STRUNZ, B., ZHIRKOV, A., FILIPOVICH, O., RUKOIATKINA, E., GUSEV, D., LOBZIN, Y., FISCHLER, B., ALEMAN, S., SALLBERG, M. & BJORKSTROM, N. K. 2020. Evidence for B cell maturation but not trained immunity in uninfected infants exposed to hepatitis C virus. *Gut,* 69**,** 2203-2213.
MA, H. D., WANG, Y. H., CHANG, C., GERSHWIN, M. E. & LIAN, Z. X. 2015. The intestinal microbiota and microenvironment in liver. *Autoimmun Rev,* 14**,** 183-91.
MA, L., QIN, J., JI, H., ZHAO, P. & JIANG, Y. 2014. Tfh and plasma cells are correlated with hypergammaglobulinaemia in patients with autoimmune hepatitis. *Liver Int,* 34**,** 405-15.
MA, W. T. & CHEN, D. K. 2019. Immunological abnormalities in patients with primary biliary cholangitis. *Clin Sci (Lond),* 133**,** 741-760.
MA, Z., ZHANG, E., GAO, S., XIONG, Y. & LU, M. 2019. Toward a Functional Cure for Hepatitis B: The Rationale and Challenges for Therapeutic Targeting of the B Cell Immune Response. *Front Immunol,* 10**,** 2308.
MACK, C. L. 2007. The pathogenesis of biliary atresia: evidence for a virus-induced autoimmune disease. *Semin Liver Dis,* 27**,** 233-42.
MACK, C. L., FALTA, M. T., SULLIVAN, A. K., KARRER, F., SOKOL, R. J., FREED, B. M. & FONTENOT, A. P. 2007. Oligoclonal expansions of CD4+ and CD8+ T-cells in the target organ of patients with biliary atresia. *Gastroenterology,* 133**,** 278-87.
MACK, C. L., FELDMAN, A. G. & SOKOL, R. J. 2012. Clues to the etiology of bile duct injury in biliary atresia. *Semin Liver Dis,* 32**,** 307-16.
MACK, C. L., TUCKER, R. M., SOKOL, R. J., KARRER, F. M., KOTZIN, B. L., WHITINGTON, P. F. & MILLER, S. D. 2004. Biliary atresia is associated with CD4+ Th1 cell-mediated portal tract inflammation. *Pediatr Res,* 56**,** 79-87.
MACK, C. L., TUCKER, R. M., SOKOL, R. J. & KOTZIN, B. L. 2005. Armed CD4+ Th1 effector cells and activated macrophages participate in bile duct injury in murine biliary atresia. *Clin Immunol,* 115**,** 200-9.
MAEDA, K., MEHTA, H., DREVETS, D. A. & COGGESHALL, K. M. 2010. IL-6 increases B-cell IgG production in a feed-forward proinflammatory mechanism to skew hematopoiesis and elevate myeloid production. *Blood,* 115**,** 4699-706.
MANGENEY, M., RICHARD, Y., COULAUD, D., TURSZ, T. & WIELS, J. 1991. CD77: an antigen of germinal center B cells entering apoptosis. *Eur J Immunol,* 21**,** 1131-40.
MANGENEY, M., ROUSSELET, G., TAGA, S., TURSZ, T. & WIELS, J. 1995. The fate of human CD77+ germinal center B lymphocytes after rescue from apoptosis. *Mol Immunol,* 32**,** 333-9.
MANN, J. P., LENZ, D., STAMATAKI, Z. & KELLY, D. 2022. Common mechanisms in pediatric acute liver failure. *Trends Mol Med*.

MANSUETO, P., IACONO, G., SEIDITA, A., D'ALCAMO, A., SPRINI, D. & CARROCCIO, A. 2012. Review article: intestinal lymphoid nodular hyperplasia in children--the relationship to food hypersensitivity. *Aliment Pharmacol Ther,* 35**,** 1000-9.

MASSONNET, B., DELWAIL, A., AYRAULT, J. M., CHAGNEAU-DERRODE, C., LECRON, J. C. & SILVAIN, C. 2009. Increased immunoglobulin A in alcoholic liver cirrhosis: exploring the response of B cells to Toll-like receptor 9 activation. *Clin Exp Immunol,* 158**,** 115-24.

MATOS, L. C., BATISTA, P., MONTEIRO, N., RIBEIRO, J., CIPRIANO, M. A., HENRIQUES, P., GIRAO, F. & CARVALHO, A. 2013. Lymphocyte subsets in alcoholic liver disease. *World J Hepatol,* 5**,** 46-55.

MATSUBARA, T., SOH, J., MORITA, M., UWABO, T., TOMIDA, S., FUJIWARA, T., KANAZAWA, S., TOYOOKA, S. & HIRASAWA, A. 2020. DV200 Index for Assessing RNA Integrity in Next-Generation Sequencing. *Biomed Res Int,* 2020**,** 9349132.

MCCARRON, M. J., PARK, P. W. & FOOKSMAN, D. R. 2017. CD138 mediates selection of mature plasma cells by regulating their survival. *Blood,* 129**,** 2749-2759.

MCHEYZER-WILLIAMS, L. J. & MCHEYZER-WILLIAMS, M. G. 2005. Antigen-specific memory B cell development. *Annu Rev Immunol,* 23**,** 487-513.

MEIRAZ, A., GARBER, O. G., HARARI, S., HASSIN, D. & BERKE, G. 2009. Switch from perforin-expressing to perforin-deficient CD8(+) T cells accounts for two distinct types of effector cytotoxic T lymphocytes in vivo. *Immunology,* 128**,** 69-82.

MENDEZ-SANCHEZ, N. & PAL, S. C. 2022. Editorial: Acute Hepatitis of Unknown Origin in Children. Is Autoimmunity at Play? *Med Sci Monit,* 28**,** e937371.

MENGEL, M., LOUPY, A., HAAS, M., ROUFOSSE, C., NAESENS, M., AKALIN, E., CLAHSEN-VAN GRONINGEN, M. C., DAGOBERT, J., DEMETRIS, A. J., DUONG VAN HUYEN, J. P., GUEGUEN, J., ISSA, F., ROBIN, B., ROSALES, I., VON DER THUSEN, J. H., SANCHEZ-FUEYO, A., SMITH, R. N., WOOD, K., ADAM, B. & COLVIN, R. B. 2020. Banff 2019 Meeting Report: Molecular diagnostics in solid organ transplantation-Consensus for the Banff Human Organ Transplant (B-HOT) gene panel and open source multicenter validation. *Am J Transplant,* 20**,** 2305-2317.

MEOLA, A., SBARDELLATI, A., BRUNI ERCOLE, B., CERRETANI, M., PEZZANERA, M., CECCACCI, A., VITELLI, A., LEVY, S., NICOSIA, A., TRABONI, C., MCKEATING, J. & SCARSELLI, E. 2000. Binding of hepatitis C virus E2 glycoprotein to CD81 does not correlate with species permissiveness to infection. *J Virol,* 74**,** 5933-8.

MIN, J., NINGAPPA, M., SO, J., SHIN, D., SINDHI, R. & SUBRAMANIAM, S. 2020. Systems Analysis of Biliary Atresia Through Integration of High-Throughput Biological Data. *Front Physiol,* 11**,** 966.

MINAGA, K., WATANABE, T., CHUNG, H. & KUDO, M. 2019. Autoimmune hepatitis and IgG4-related disease. *World J Gastroenterol,* 25**,** 2308-2314.

MISHRA, D., SINGH, S. & NARAYAN, G. 2016. Role of B Cell Development Marker CD10 in Cancer Progression and Prognosis. *Mol Biol Int,* 2016**,** 4328697.

MODIN, L., ARSHAD, A., WILKES, B., BENSELIN, J., LLOYD, C., IRVING, W. L. & KELLY, D. A. 2019. Epidemiology and natural history of hepatitis C virus infection among children and young people. *J Hepatol,* 70**,** 371-378.

MONTECINO-RODRIGUEZ, E. & DORSHKIND, K. 2012. B-1 B cell development in the fetus and adult. *Immunity,* 36**,** 13-21.

MORBACH, H., EICHHORN, E. M., LIESE, J. G. & GIRSCHICK, H. J. 2010. Reference values for B cell subpopulations from infancy to adulthood. *Clin Exp Immunol,* 162**,** 271-9.

MORECKI, R., GLASER, J. H., CHO, S., BALISTRERI, W. F. & HORWITZ, M. S. 1982. Biliary atresia and reovirus type 3 infection. *N Engl J Med,* 307**,** 481-4.

MORITOKI, Y., LIAN, Z. X., OHSUGI, Y., UENO, Y. & GERSHWIN, M. E. 2006. B cells and autoimmune liver diseases. *Autoimmun Rev,* 5**,** 449-57.

MORO-SIBILOT, L., BLANC, P., TAILLARDET, M., BARDEL, E., COUILLAULT, C., BOSCHETTI, G., TRAVERSE-GLEHEN, A., DEFRANCE, T., KAISERLIAN, D. & DUBOIS, B. 2016. Mouse and Human Liver Contain Immunoglobulin A-Secreting Cells Originating From Peyer's Patches and Directed Against Intestinal Antigens. *Gastroenterology,* 151**,** 311-23.

MOSER, B. 2015. CXCR5, the Defining Marker for Follicular B Helper T (TFH) Cells. *Front Immunol,* 6**,** 296.

MOUAT, I. C., GOLDBERG, E. & HORWITZ, M. S. 2022. Age-associated B cells in autoimmune diseases. *Cell Mol Life Sci,* 79**,** 402.

MOUAT, I. C. & HORWITZ, M. S. 2022. Age-associated B cells in viral infection. *PLoS Pathog,* 18**,** e1010297.

MOUAT, I. C., MORSE, Z. J., SHANINA, I., BROWN, K. L. & HORWITZ, M. S. 2021. Latent gammaherpesvirus exacerbates arthritis through modification of age-associated B cells. *Elife,* 10.
MURATORI, P., MURATORI, L., VERUCCHI, G., ATTARD, L., BIANCHI, F. B. & LENZI, M. 2003. Non-organ-specific autoantibodies in children with chronic hepatitis C: clinical significance and impact on interferon treatment. *Clin Infect Dis,* 37**,** 1320-6.
MYLES, A., GEARHART, P. J. & CANCRO, M. P. 2017. Signals that drive T-bet expression in B cells. *Cell Immunol,* 321**,** 3-7.
NAEMI, K., BRYNES, R. K., REISIAN, N., JOHNSTON, A., DHILLON, R., WALAVALKAR, V., ZHAO, X. & REZK, S. A. 2013. Benign lymphoid aggregates in the bone marrow: distribution patterns of B and T lymphocytes. *Hum Pathol,* 44**,** 512-20.
NAKASHIMA, M., KINOSHITA, M., NAKASHIMA, H., HABU, Y., MIYAZAKI, H., SHONO, S., HIROI, S., SHINOMIYA, N., NAKANISHI, K. & SEKI, S. 2012. Pivotal advance: characterization of mouse liver phagocytic B cells in innate immunity. *J Leukoc Biol,* 91**,** 537-46.
NANOSTRING. 2020. *nCounter® Human Organ Transplant Panel* [Online]. Available: https://www.nanostring.com/wp-content/uploads/2020/12/PB_MK1803_Organ_Transplant_Panel_FINAL_R7.pdf [Accessed].
NANOSTRING. 2021a. *nCounter analysis system user manual* [Online]. Available: https://university.nanostring.com/ncounter-max-analysis-system-user-manual/873557 [Accessed 30/11/2022].
NANOSTRING. 2021b. *nCounter Preparing RNA from FFPE Samples User Manual* [Online]. Available: https://nanostring.com/wp-content/uploads/MAN-10050-05-Preparing-RNA-from-FFPE-Samples.pdf [Accessed 21/03/2021].
NANOSTRING. 2022. *nCounter gene expression panels and custom codeset user manual* [Online]. Available: https://nanostring.com/wp-content/uploads/MAN-10056-06-Gene-Expression-Panels-and-Custom-CodeSet-User-Manual.pdf [Accessed 30/11/2022].
NARADIKIAN, M. S., HAO, Y. & CANCRO, M. P. 2016a. Age-associated B cells: key mediators of both protective and autoreactive humoral responses. *Immunol Rev,* 269**,** 118-29.
NARADIKIAN, M. S., MYLES, A., BEITING, D. P., ROBERTS, K. J., DAWSON, L., HERATI, R. S., BENGSCH, B., LINDERMAN, S. L., STELEKATI, E., SPOLSKI, R., WHERRY, E. J., HUNTER, C., HENSLEY, S. E., LEONARD, W. J. & CANCRO, M. P. 2016b. Cutting Edge: IL-4, IL-21, and IFN-gamma Interact To Govern T-bet and CD11c Expression in TLR-Activated B Cells. *J Immunol,* 197**,** 1023-8.
NARAYANASWAMY, B., GONDE, C., TREDGER, J. M., HUSSAIN, M., VERGANI, D. & DAVENPORT, M. 2007. Serial circulating markers of inflammation in biliary atresia--evolution of the post-operative inflammatory process. *Hepatology,* 46**,** 180-7.
NASCIMBENI, R., DI FABIO, F., DI BETTA, E., MARIANI, P., FISOGNI, S. & VILLANACCI, V. 2005. Morphology of colorectal lymphoid aggregates in cancer, diverticular and inflammatory bowel diseases. *Mod Pathol,* 18**,** 681-5.
NHS_ENGLAND. 2019. *NHS Long Term Plan will help problem drinkers and smokers* [Online]. NHS England. Available: https://www.england.nhs.uk/2019/01/nhs-long-term-plan-will-help-problem-drinkers-and-smokers/ [Accessed 19/03/2023].
NI, J., HEMBRADOR, E., DI BISCEGLIE, A. M., JACOBSON, I. M., TALAL, A. H., BUTERA, D., RICE, C. M., CHAMBERS, T. J. & DUSTIN, L. B. 2003. Accumulation of B lymphocytes with a naive, resting phenotype in a subset of hepatitis C patients. *J Immunol,* 170**,** 3429-39.
NOMDEN, M., BELJAARS, L., VERKADE, H. J., HULSCHER, J. B. F. & OLINGA, P. 2020. Current Concepts of Biliary Atresia and Matrix Metalloproteinase-7: A Review of Literature. *Front Med (Lausanne),* 7**,** 617261.
NOVOBRANTSEVA, T. I., MAJEAU, G. R., AMATUCCI, A., KOGAN, S., BRENNER, I., CASOLA, S., SHLOMCHIK, M. J., KOTELIANSKY, V., HOCHMAN, P. S. & IBRAGHIMOV, A. 2005. Attenuated liver fibrosis in the absence of B cells. *J Clin Invest,* 115**,** 3072-82.
NOWAK, A. J. & RELJA, B. 2020. The Impact of Acute or Chronic Alcohol Intake on the NF-kappaB Signaling Pathway in Alcohol-Related Liver Disease. *Int J Mol Sci,* 21.
O'HARA, S. P. & LARUSSO, N. F. 2019. The Gut-Liver Axis in Primary Sclerosing Cholangitis: Are Pathobionts the Missing Link? *Hepatology,* 70**,** 1058-1060.
OFFICE_FOR_NATIONAL_STATISTICS_(ONS). 2021. *Alcohol-specific deaths in the UK: registered in 2020* [Online]. Available:

https://www.ons.gov.uk/peoplepopulationandcommunity/healthandsocialcare/causesofdeath/bulletins/alcoholrelateddeathsintheunitedkingdom/registeredin2020 [Accessed 19/03/2023].
OFFICIAL_STATISTICS. 2022. *Liver disease profiles, January 2022 update* [Online]. Office for Health Improvement & Disparities. Available: https://www.gov.uk/government/statistics/liver-disease-profiles-january-2022-update/liver-disease-profiles-january-2022-update#:~:text=year%20ending%202021.-,Prior%20data%20has%20been%20refreshed%20to%20present%20data%20for%20the,%2D3.8)%20per%20100%2C000%20population. [Accessed 20/03/2023].
OGAWA, S., SAKAGUCHI, K., TAKAKI, A., SHIRAGA, K., SAWAYAMA, T., MOURI, H., MIYASHITA, M., KOIDE, N. & TSUJI, T. 2000. Increase in CD95 (Fas/APO-1)-positive CD4+ and CD8+ T cells in peripheral blood derived from patients with autoimmune hepatitis or chronic hepatitis C with autoimmune phenomena. *J Gastroenterol Hepatol,* 15**,** 69-75.
OKADA, T., MILLER, M. J., PARKER, I., KRUMMEL, M. F., NEIGHBORS, M., HARTLEY, S. B., O'GARRA, A., CAHALAN, M. D. & CYSTER, J. G. 2005. Antigen-engaged B cells undergo chemotaxis toward the T zone and form motile conjugates with helper T cells. *PLoS Biol,* 3**,** e150.
ORTIZ-PEREZ, A., DONNELLY, B., TEMPLE, H., TIAO, G., BANSAL, R. & MOHANTY, S. K. 2020. Innate Immunity and Pathogenesis of Biliary Atresia. *Front Immunol,* 11**,** 329.
OTERO, D. C., ANZELON, A. N. & RICKERT, R. C. 2003. CD19 function in early and late B cell development: I. Maintenance of follicular and marginal zone B cells requires CD19-dependent survival signals. *J Immunol,* 170**,** 73-83.
OWEN, J. J., COOPER, M. D. & RAFF, M. C. 1974. In vitro generation of B lymphocytes in mouse foetal liver, a mammalian 'bursa equivalent'. *Nature,* 249**,** 361-3.
OWEN, J. J., RAFF, M. C. & COOPER, M. D. 1976. Studies on the generation of B lymphocytes in the mouse embryo. *Eur J Immunol,* 5**,** 468-73.
PALMA, F. R., HE, C., DANES, J. M., PAVIANI, V., COELHO, D. R., GANTNER, B. N. & BONINI, M. G. 2020. Mitochondrial Superoxide Dismutase: What the Established, the Intriguing, and the Novel Reveal About a Key Cellular Redox Switch. *Antioxid Redox Signal,* 32**,** 701-714.
PANG, S. Y., DAI, Y. M., ZHANG, R. Z., CHEN, Y. H., PENG, X. F., FU, J., CHEN, Z. R., LIU, Y. F., YANG, L. Y., WEN, Z., YU, J. K. & LIU, H. Y. 2018. Autoimmune liver disease-related autoantibodies in patients with biliary atresia. *World J Gastroenterol,* 24**,** 387-396.
PARKER, R., AITHAL, G. P., BECKER, U., GLEESON, D., MASSON, S., WYATT, J. I., ROWE, I. A. & GROUP, W. S. 2019. Natural history of histologically proven alcohol-related liver disease: A systematic review. *J Hepatol,* 71**,** 586-593.
PATEL, A. M., LIU, Y. S., DAVIES, S. P., BROWN, R. M., KELLY, D. A., SCHEEL-TOELLNER, D., REYNOLDS, G. M. & STAMATAKI, Z. 2021. The Role of B Cells in Adult and Paediatric Liver Injury. *Frontiers in Immunology,* 12.
PATTEN, D. A. & SHETTY, S. 2018. Chronic liver disease: scavenger hunt for novel therapies. *Lancet,* 391**,** 104-105.
PAVLASOVA, G. & MRAZ, M. 2020. The regulation and function of CD20: an "enigma" of B-cell biology and targeted therapy. *Haematologica,* 105**,** 1494-1506.
PEREZ-ANDRES, M., PAIVA, B., NIETO, W. G., CARAUX, A., SCHMITZ, A., ALMEIDA, J., VOGT, R. F., JR., MARTI, G. E., RAWSTRON, A. C., VAN ZELM, M. C., VAN DONGEN, J. J., JOHNSEN, H. E., KLEIN, B., ORFAO, A. & PRIMARY HEALTH CARE GROUP OF SALAMANCA FOR THE STUDY OF, M. B. L. 2010. Human peripheral blood B-cell compartments: a crossroad in B-cell traffic. *Cytometry B Clin Cytom,* 78 Suppl 1**,** S47-60.
PERZ, J. F., ARMSTRONG, G. L., FARRINGTON, L. A., HUTIN, Y. J. & BELL, B. P. 2006. The contributions of hepatitis B virus and hepatitis C virus infections to cirrhosis and primary liver cancer worldwide. *J Hepatol,* 45**,** 529-38.
PIEPER, K., GRIMBACHER, B. & EIBEL, H. 2013. B-cell biology and development. *J Allergy Clin Immunol,* 131**,** 959-71.
PINTO, C., GIORDANO, D. M., MARONI, L. & MARZIONI, M. 2018. Role of inflammation and proinflammatory cytokines in cholangiocyte pathophysiology. *Biochim Biophys Acta Mol Basis Dis,* 1864**,** 1270-1278.
PIPI, E., NAYAR, S., GARDNER, D. H., COLAFRANCESCO, S., SMITH, C. & BARONE, F. 2018. Tertiary Lymphoid Structures: Autoimmunity Goes Local. *Front Immunol,* 9**,** 1952.

PLAZA-DIAZ, J., SOLIS-URRA, P., RODRIGUEZ-RODRIGUEZ, F., OLIVARES-ARANCIBIA, J., NAVARRO-OLIVEROS, M., ABADIA-MOLINA, F. & ALVAREZ-MERCADO, A. I. 2020. The Gut Barrier, Intestinal Microbiota, and Liver Disease: Molecular Mechanisms and Strategies to Manage. *Int J Mol Sci,* 21.

POISSON, J., LEMOINNE, S., BOULANGER, C., DURAND, F., MOREAU, R., VALLA, D. & RAUTOU, P. E. 2017. Liver sinusoidal endothelial cells: Physiology and role in liver diseases. *J Hepatol,* 66**,** 212-227.

POONIA, B., AYITHAN, N., NANDI, M., MASUR, H. & KOTTILIL, S. 2018. HBV induces inhibitory FcRL receptor on B cells and dysregulates B cell-T follicular helper cell axis. *Sci Rep,* 8**,** 15296.

PORTUGAL, S., OBENG-ADJEI, N., MOIR, S., CROMPTON, P. D. & PIERCE, S. K. 2017. Atypical memory B cells in human chronic infectious diseases: An interim report. *Cell Immunol,* 321**,** 18-25.

PORTUGAL, S., TIPTON, C. M., SOHN, H., KONE, Y., WANG, J., LI, S., SKINNER, J., VIRTANEVA, K., STURDEVANT, D. E., PORCELLA, S. F., DOUMBO, O. K., DOUMBO, S., KAYENTAO, K., ONGOIBA, A., TRAORE, B., SANZ, I., PIERCE, S. K. & CROMPTON, P. D. 2015. Malaria-associated atypical memory B cells exhibit markedly reduced B cell receptor signaling and effector function. *Elife,* 4.

PUBLIC_HEALTH_ENGLAND. 2021. *Protecting your baby against hepatitis B guide* [Online]. Available: https://www.gov.uk/government/publications/protecting-your-baby-against-hepatitis-b-leaflet/protecting-your-baby-against-hepatitis-b-with-the-hepatitis-b-vaccine [Accessed 21/03/2023].

PUBLICOVER, J., GAGGAR, A., NISHIMURA, S., VAN HORN, C. M., GOODSELL, A., MUENCH, M. O., REINHARDT, R. L., VAN ROOIJEN, N., WAKIL, A. E., PETERS, M., CYSTER, J. G., ERLE, D. J., ROSENTHAL, P., COOPER, S. & BARON, J. L. 2013. Age-dependent hepatic lymphoid organization directs successful immunity to hepatitis B. *J Clin Invest,* 123**,** 3728-39.

PURSWANI, S. 2016. *Characterising hepatic B cell subsets in human chronic liver disease.* Doctor of Philosophy, University of Birmingham.

RANSOHOFF, R. M. 2023. Multiple sclerosis: role of meningeal lymphoid aggregates in progression independent of relapse activity. *Trends Immunol,* 44**,** 266-275.

REVY, P., MUTO, T., LEVY, Y., GEISSMANN, F., PLEBANI, A., SANAL, O., CATALAN, N., FORVEILLE, M., DUFOURCQ-LABELOUSE, R., GENNERY, A., TEZCAN, I., ERSOY, F., KAYSERILI, H., UGAZIO, A. G., BROUSSE, N., MURAMATSU, M., NOTARANGELO, L. D., KINOSHITA, K., HONJO, T., FISCHER, A. & DURANDY, A. 2000. Activation-induced cytidine deaminase (AID) deficiency causes the autosomal recessive form of the Hyper-IgM syndrome (HIGM2). *Cell,* 102**,** 565-75.

RIEPENHOFF-TALTY, M., GOUVEA, V., EVANS, M. J., SVENSSON, L., HOFFENBERG, E., SOKOL, R. J., UHNOO, I., GREENBERG, S. J., SCHAKEL, K., ZHAORI, G., FITZGERALD, J., CHONG, S., EL-YOUSEF, M., NEMETH, A., BROWN, M., PICCOLI, D., HYAMS, J., RUFFIN, D. & ROSSI, T. 1996. Detection of group C rotavirus in infants with extrahepatic biliary atresia. *J Infect Dis,* 174**,** 8-15.

RIEPENHOFF-TALTY, M., SCHAEKEL, K., CLARK, H. F., MUELLER, W., UHNOO, I., ROSSI, T., FISHER, J. & OGRA, P. L. 1993. Group A rotaviruses produce extrahepatic biliary obstruction in orally inoculated newborn mice. *Pediatr Res,* 33**,** 394-9.

ROBINSON, M. W., HARMON, C. & O'FARRELLY, C. 2016. Liver immunology and its role in inflammation and homeostasis. *Cell Mol Immunol,* 13**,** 267-76.

ROGERS, A. B. & DINTZIS, R. Z. 2012. 13 - Liver and Gallbladder. *Comparative Anatomy and Histology.* Academic Press.

ROSALES, I. A., MAHOWALD, G. K., TOMASZEWSKI, K., HOTTA, K., IWAHARA, N., OTSUKA, T., TSUJI, T., TAKADA, Y., ACHEAMPONG, E., ARAUJO-MEDINA, M., BRUCE, A., RIOS, A., COSIMI, A. B., ELIAS, N., KAWAI, T., GILLIGAN, H., SAFA, K., RIELLA, L. V., TOLKOFF-RUBIN, N. E., WILLIAMS, W. W., JR., SMITH, R. N. & COLVIN, R. B. 2022. Banff Human Organ Transplant Transcripts Correlate with Renal Allograft Pathology and Outcome: Importance of Capillaritis and Subpathologic Rejection. *J Am Soc Nephrol,* 33**,** 2306-2319.

ROSSER, E. C. & MAURI, C. 2015. Regulatory B cells: origin, phenotype, and function. *Immunity,* 42**,** 607-12.

RUBTSOV, A. V., RUBTSOVA, K., FISCHER, A., MEEHAN, R. T., GILLIS, J. Z., KAPPLER, J. W. & MARRACK, P. 2011. Toll-like receptor 7 (TLR7)-driven accumulation of a novel CD11c(+) B-cell population is important for the development of autoimmunity. *Blood,* 118**,** 1305-15.

RUBTSOV, A. V., RUBTSOVA, K., KAPPLER, J. W. & MARRACK, P. 2013. TLR7 drives accumulation of ABCs and autoantibody production in autoimmune-prone mice. *Immunol Res,* 55**,** 210-6.

RUBTSOVA, K., RUBTSOV, A. V., CANCRO, M. P. & MARRACK, P. 2015. Age-Associated B Cells: A T-bet-Dependent Effector with Roles in Protective and Pathogenic Immunity. *J Immunol,* 195**,** 1933-7.

RUBTSOVA, K., RUBTSOV, A. V., THURMAN, J. M., MENNONA, J. M., KAPPLER, J. W. & MARRACK, P. 2017. B cells expressing the transcription factor T-bet drive lupus-like autoimmunity. *J Clin Invest,* 127**,** 1392-1404.

RUMBO, C., FAWAZ, R. L., EMRE, S. H., SUCHY, F. J., KERKAR, N., MOROTTI, R. A. & SHNEIDER, B. L. 2006. Hepatitis C in children: a quaternary referral center perspective. *J Pediatr Gastroenterol Nutr,* 43**,** 209-16.

RYDELL, G. E., PRAKASH, K., NORDER, H. & LINDH, M. 2017. Hepatitis B surface antigen on subviral particles reduces the neutralizing effect of anti-HBs antibodies on hepatitis B viral particles in vitro. *Virology,* 509**,** 67-70.

SAADOUN, D., LANDAU, D. A., CALABRESE, L. H. & CACOUB, P. P. 2007. Hepatitis C-associated mixed cryoglobulinaemia: a crossroad between autoimmunity and lymphoproliferation. *Rheumatology (Oxford),* 46**,** 1234-42.

SACHINIDIS, A., XANTHOPOULOS, K. & GARYFALLOS, A. 2020. Age-Associated B Cells (ABCs) in the Prognosis, Diagnosis and Therapy of Systemic Lupus Erythematosus (SLE). *Mediterr J Rheumatol,* 31**,** 311-318.

SAITO, T., HISHIKI, T., TERUI, K., MITSUNAGA, T., TERUI, E., NAKATA, M. & YOSHIDA, H. 2011. Toll-like receptor mRNA expression in liver tissue from patients with biliary atresia. *J Pediatr Gastroenterol Nutr,* 53**,** 620-6.

SAITO, T., SHINOZAKI, K., MATSUNAGA, T., OGAWA, T., ETOH, T., MURAMATSU, T., KAWAMURA, K., YOSHIDA, H., OHNUMA, N. & SHIRASAWA, H. 2004. Lack of evidence for reovirus infection in tissues from patients with biliary atresia and congenital dilatation of the bile duct. *J Hepatol,* 40**,** 203-11.

SANZ, I., WEI, C., JENKS, S. A., CASHMAN, K. S., TIPTON, C., WOODRUFF, M. C., HOM, J. & LEE, F. E. 2019. Challenges and Opportunities for Consistent Classification of Human B Cell and Plasma Cell Populations. *Front Immunol,* 10**,** 2458.

SATHE, A. & CUSICK, J. K. 2023. Biochemistry, Immunoglobulin M. *StatPearls.* Treasure Island (FL) ineligible companies. Disclosure: John Cusick declares no relevant financial relationships with ineligible companies.

SATO, Y., SILINA, K., VAN DEN BROEK, M., HIRAHARA, K. & YANAGITA, M. 2023. The roles of tertiary lymphoid structures in chronic diseases. *Nat Rev Nephrol***,** 1-13.

SCHLAAK, J. F., LOHR, H., GALLATI, H., MEYER ZUM BUSCHENFELDE, K. H. & FLEISCHER, B. 1993. Analysis of the in vitro cytokine production by liver-infiltrating T cells of patients with autoimmune hepatitis. *Clin Exp Immunol,* 94**,** 168-73.

SCHMELZER, J., DUGAN, E., BLACH, S., COLEMAN, S., CAI, Z., DEPAOLA, M., ESTES, C., GAMKRELIDZE, I., JERABEK, K., MA, S., MONTOYA, S., RAZAVI-SHEARER, D., RAZAVI-SHEARER, K., ROBBINS-SCOTT, S., RAZAVI, H. & EL SAYED, M. H. 2020. Global prevalence of hepatitis C virus in children in 2018: a modelling study. *Lancet Gastroenterol Hepatol,* 5**,** 374-392.

SCHREIBER, R. A., BARKER, C. C., ROBERTS, E. A., MARTIN, S. R., ALVAREZ, F., SMITH, L., BUTZNER, J. D., WROBEL, I., MACK, D., MOROZ, S., RASHID, M., PERSAD, R., LEVESQUE, D., BRILL, H., BRUCE, G., CRITCH, J. & CANADIAN PEDIATRIC HEPATOLOGY RESEARCH, G. 2007. Biliary atresia: the Canadian experience. *J Pediatr,* 151**,** 659-65, 665 e1.

SCHROEDER, H. W., JR. & CAVACINI, L. 2010. Structure and function of immunoglobulins. *J Allergy Clin Immunol,* 125**,** S41-52.

SCHWENGER, K. J. P., CHEN, L., CHELLIAH, A., DA SILVA, H. E., TETERINA, A., COMELLI, E. M., TAIBI, A., ARENDT, B. M., FISCHER, S. & ALLARD, J. P. 2018. Markers of activated inflammatory cells are associated with disease severity and intestinal microbiota in adults with nonalcoholic fatty liver disease. *Int J Mol Med,* 42**,** 2229-2237.

SEBODE, M., WEILER-NORMANN, C., LIWINSKI, T. & SCHRAMM, C. 2018. Autoantibodies in Autoimmune Liver Disease-Clinical and Diagnostic Relevance. *Front Immunol,* 9**,** 609.

SEKI, E. & SCHWABE, R. F. 2015. Hepatic inflammation and fibrosis: functional links and key pathways. *Hepatology,* 61**,** 1066-79.

SHAHAF, G., ZISMAN-ROZEN, S., BENHAMOU, D., MELAMED, D. & MEHR, R. 2016. B Cell Development in the Bone Marrow Is Regulated by Homeostatic Feedback Exerted by Mature B Cells. *Front Immunol,* 7**,** 77.

SHI, Z., DU, Q., WANG, X., WANG, J., CHEN, H., LANG, Y., KONG, L., LUO, W., YANG, M. & ZHOU, H. 2022. Granzyme B in circulating CD8+ T cells as a biomarker of immunotherapy effectiveness and disability in neuromyelitis optica spectrum disorders. *Front Immunol,* 13**,** 1027158.

SHIMODA, S., HARADA, K., NIIRO, H., SHIRABE, K., TAKETOMI, A., MAEHARA, Y., TSUNEYAMA, K., NAKANUMA, Y., LEUNG, P., ANSARI, A. A., GERSHWIN, M. E. & AKASHI, K. 2011. Interaction between Toll-like

receptors and natural killer cells in the destruction of bile ducts in primary biliary cirrhosis. *Hepatology,* 53**,** 1270-81.

SHIVAKUMAR, P., CAMPBELL, K. M., SABLA, G. E., MIETHKE, A., TIAO, G., MCNEAL, M. M., WARD, R. L. & BEZERRA, J. A. 2004. Obstruction of extrahepatic bile ducts by lymphocytes is regulated by IFN-gamma in experimental biliary atresia. *J Clin Invest,* 114**,** 322-9.

SINGH, P., GOODE, T., DEAN, A., AWAD, S. S. & DARLINGTON, G. J. 2011. Elevated interferon gamma signaling contributes to impaired regeneration in the aged liver. *J Gerontol A Biol Sci Med Sci,* 66**,** 944-56.

SMITH, R. N. 2021. In-silico performance, validation, and modeling of the Nanostring Banff Human Organ transplant gene panel using archival data from human kidney transplants. *BMC Med Genomics,* 14**,** 86.

SMITH, R. N., ROSALES, I. A., TOMASZEWSKI, K. T., MAHOWALD, G. T., ARAUJO-MEDINA, M., ACHEAMPONG, E., BRUCE, A., RIOS, A., OTSUKA, T., TSUJI, T., HOTTA, K. & COLVIN, R. 2023. Utility of Banff Human Organ Transplant Gene Panel in Human Kidney Transplant Biopsies. *Transplantation,* 107**,** 1188-1199.

SMULSKI, C. R. & EIBEL, H. 2018. BAFF and BAFF-Receptor in B Cell Selection and Survival. *Front Immunol,* 9**,** 2285.

SOHN, H. W., KRUEGER, P. D., DAVIS, R. S. & PIERCE, S. K. 2011. FcRL4 acts as an adaptive to innate molecular switch dampening BCR signaling and enhancing TLR signaling. *Blood,* 118**,** 6332-41.

STAMATAKI, Z., COATES, S., ABRIGNANI, S., HOUGHTON, M. & MCKEATING, J. A. 2011. Immunization of human volunteers with hepatitis C virus envelope glycoproteins elicits antibodies that cross-neutralize heterologous virus strains. *J Infect Dis,* 204**,** 811-3.

STAMATAKI, Z., SHANNON-LOWE, C., SHAW, J., MUTIMER, D., RICKINSON, A. B., GORDON, J., ADAMS, D. H., BALFE, P. & MCKEATING, J. A. 2009. Hepatitis C virus association with peripheral blood B lymphocytes potentiates viral infection of liver-derived hepatoma cells. *Blood,* 113**,** 585-93.

STEELE, M. I., MARSHALL, C. M., LLOYD, R. E. & RANDOLPH, V. E. 1995. Reovirus 3 not detected by reverse transcriptase-mediated polymerase chain reaction analysis of preserved tissue from infants with cholestatic liver disease. *Hepatology,* 21**,** 697-702.

SUBHANI, M., ELLERAY, R., BETHEA, J., MORLING, J. R. & RYDER, S. D. 2022. Alcohol-related liver disease mortality and missed opportunities in secondary care: A United Kingdom retrospective observational study. *Drug Alcohol Rev,* 41**,** 1331-1340.

SUGDEN, P. B., CAMERON, B., BULL, R., WHITE, P. A. & LLOYD, A. R. 2012. Occult infection with hepatitis C virus: friend or foe? *Immunol Cell Biol,* 90**,** 763-73.

SUTTI, S. & ALBANO, E. 2020. Adaptive immunity: an emerging player in the progression of NAFLD. *Nat Rev Gastroenterol Hepatol,* 17**,** 81-92.

SUTTON, B. J., DAVIES, A. M., BAX, H. J. & KARAGIANNIS, S. N. 2019. IgE Antibodies: From Structure to Function and Clinical Translation. *Antibodies (Basel),* 8.

SWAIN, S. L., KUGLER-UMANA, O., KUANG, Y. & ZHANG, W. 2017. The properties of the unique age-associated B cell subset reveal a shift in strategy of immune response with age. *Cell Immunol,* 321**,** 52-60.

SYAL, G., FAUSTHER, M. & DRANOFF, J. A. 2012. Advances in cholangiocyte immunobiology. *Am J Physiol Gastrointest Liver Physiol,* 303**,** G1077-86.

TAN, A., KOH, S. & BERTOLETTI, A. 2015. Immune Response in Hepatitis B Virus Infection. *Cold Spring Harb Perspect Med,* 5**,** a021428.

TAN, Y. G., WANG, Y. Q., ZHANG, M., HAN, Y. X., HUANG, C. Y., ZHANG, H. P., LI, Z. M., WU, X. L., WANG, X. F., DONG, Y., ZHU, H. M., ZHU, S. D., LI, H. M., LI, N., YAN, H. P. & GAO, Z. H. 2016. Clonal Characteristics of Circulating B Lymphocyte Repertoire in Primary Biliary Cholangitis. *J Immunol,* 197**,** 1609-20.

TANAKA, A. 2019. IgG4-Related Sclerosing Cholangitis and Primary Sclerosing Cholangitis. *Gut Liver,* 13**,** 300-307.

TAUBERT, R., HARDTKE-WOLENSKI, M., NOYAN, F., WILMS, A., BAUMANN, A. K., SCHLUE, J., OLEK, S., FALK, C. S., MANNS, M. P. & JAECKEL, E. 2014. Intrahepatic regulatory T cells in autoimmune hepatitis are associated with treatment response and depleted with current therapies. *J Hepatol,* 61**,** 1106-14.

TAYLOR, S. A., ASSIS, D. N. & MACK, C. L. 2019a. The Contribution of B Cells in Autoimmune Liver Diseases. *Semin Liver Dis,* 39**,** 422-431.

TAYLOR, S. A., MALLADI, P., PAN, X., WECHSLER, J. B., HULSE, K. E., PERLMAN, H. & WHITINGTON, P. F. 2019b. Oligoclonal immunoglobulin repertoire in biliary remnants of biliary atresia. *Sci Rep,* 9**,** 4508.

TEMMING, A. R., DE TAEYE, S. W., DE GRAAF, E. L., DE NEEF, L. A., DEKKERS, G., BRUGGEMAN, C. W., KOERS, J., LIGTHART, P., NAGELKERKE, S. Q., ZIMRING, J. C., KUIJPERS, T. W., WUHRER, M., RISPENS, T. &

VIDARSSON, G. 2019. Functional Attributes of Antibodies, Effector Cells, and Target Cells Affecting NK Cell-Mediated Antibody-Dependent Cellular Cytotoxicity. *J Immunol,* 203**,** 3126-3135.

THAN, N. N., JEFFERY, H. C. & OO, Y. H. 2016. Autoimmune Hepatitis: Progress from Global Immunosuppression to Personalised Regulatory T Cell Therapy. *Can J Gastroenterol Hepatol,* 2016**,** 7181685.

THERMOFISHER_SCIENTIFIC. *Fluorescence SpectraViewer* [Online]. Available: https://www.thermofisher.com/order/fluorescence-spectraviewer?gclid=Cj0KCQjw2cWgBhDYARIsALggUhpT7bF1fRnNlBSI32XQd4fNnSbZxlfYNmxNr-P2kT6Dn9ZCkz9-mGwaAvclEALw_wcB&ef_id=Cj0KCQjw2cWgBhDYARIsALggUhpT7bF1fRnNlBSI32XQd4fNnSbZxlfYNmxNr-P2kT6Dn9ZCkz9-mGwaAvclEALw_wcB:G:s&s_kwcid=AL!3652!3!607635415877!e!!g!!thermo%20spectra%20viewer!20817606 89!127753028375&cid=bid_pca_aup_r01_co_cp1359_pjt0000_bid00000_0se_gaw_bt_pur_con#!/?gclid=Cj0KCQjw2cWgBhDYARIsALggUhpT7bF1fRnNlBSI32XQd4fNnSbZxlfYNmxNr-P2kT6Dn9ZCkz9-mGwaAvclEALw_wcB&ef_id=Cj0KCQjw2cWgBhDYARIsALggUhpT7bF1fRnNlBSI32XQd4fNnSbZxlfYNmxNr-P2kT6Dn9ZCkz9-mGwaAvclEALw_wcB:G:s&s_kwcid=AL!3652!3!607635415877!e!!g!!thermo%20spectra%20viewer!20817606 89!127753028375&cid=bid_pca_aup_r01_co_cp1359_pjt0000_bid00000_0se_gaw_bt_pur_con [Accessed 09/12/2020].

THORARINSDOTTIR, K., CAMPONESCHI, A., CAVALLINI, N., GRIMSHOLM, O., JACOBSSON, L., GJERTSSON, I. & MARTENSSON, I. L. 2016. CD21(-/low) B cells in human blood are memory cells. *Clin Exp Immunol,* 185**,** 252-62.

TILG, H., WILMER, A., VOGEL, W., HEROLD, M., NOLCHEN, B., JUDMAIER, G. & HUBER, C. 1992. Serum levels of cytokines in chronic liver diseases. *Gastroenterology,* 103**,** 264-74.

TREFTS, E., GANNON, M. & WASSERMAN, D. H. 2017. The liver. *Curr Biol,* 27**,** R1147-R1151.

TRIVEDI, N., WEISEL, F., SMITA, S., JOACHIM, S., KADER, M., RADHAKRISHNAN, A., CLOUSER, C., ROSENFELD, A. M., CHIKINA, M., VIGNEAULT, F., HERSHBERG, U., ISMAIL, N. & SHLOMCHIK, M. J. 2019. Liver Is a Generative Site for the B Cell Response to Ehrlichia muris. *Immunity,* 51**,** 1088-1101 e5.

TSUCHIYA, K., KIYOSAWA, K., IMAI, H., SODEYAMA, T. & FURUTA, S. 1994. Detection of anti-double and anti-single stranded DNA antibodies in chronic liver disease: significance of anti-double stranded DNA antibody in autoimmune hepatitis. *J Gastroenterol,* 29**,** 152-8.

TUCCI, F. & KUPPERS, R. 2014. Role of hepatitis C virus in B cell lymphoproliferations. *Virol Sin,* 29**,** 3-6.

TYLER, K. L., SOKOL, R. J., OBERHAUS, S. M., LE, M., KARRER, F. M., NARKEWICZ, M. R., TYSON, R. W., MURPHY, J. R., LOW, R. & BROWN, W. R. 1998. Detection of reovirus RNA in hepatobiliary tissues from patients with extrahepatic biliary atresia and choledochal cysts. *Hepatology,* 27**,** 1475-82.

UBELHART, R., HUG, E., BACH, M. P., WOSSNING, T., DUHREN-VON MINDEN, M., HORN, A. H., TSIANTOULAS, D., KOMETANI, K., KUROSAKI, T., BINDER, C. J., STICHT, H., NITSCHKE, L., RETH, M. & JUMAA, H. 2015. Responsiveness of B cells is regulated by the hinge region of IgD. *Nat Immunol,* 16**,** 534-43.

UDOMSINPRASERT, W., UNGSUDECHACHAI, T., VEJCHAPIPAT, P., POOVORAWAN, Y. & HONSAWEK, S. 2022. Systemic cytokine profiles in biliary atresia. *PLoS One,* 17**,** e0267363.

UHL, P., FRICKER, G., HABERKORN, U. & MIER, W. 2014. Current status in the therapy of liver diseases. *Int J Mol Sci,* 15**,** 7500-12.

ULLAH, M. O., SWEET, M. J., MANSELL, A., KELLIE, S. & KOBE, B. 2016. TRIF-dependent TLR signaling, its functions in host defense and inflammation, and its potential as a therapeutic target. *J Leukoc Biol,* 100**,** 27-45.

VAN ZELM, M. C., SZCZEPANSKI, T., VAN DER BURG, M. & VAN DONGEN, J. J. 2007. Replication history of B lymphocytes reveals homeostatic proliferation and extensive antigen-induced B cell expansion. *J Exp Med,* 204**,** 645-55.

VANWOLLEGHEM, T., GROOTHUISMINK, Z. M. A., KREEFFT, K., HUNG, M., NOVIKOV, N. & BOONSTRA, A. 2020. Hepatitis B core-specific memory B cell responses associate with clinical parameters in patients with chronic HBV. *J Hepatol,* 73**,** 52-61.

VEJCHAPIPAT, P., POOMSAWAT, S., CHONGSRISAWAT, V., HONSAWEK, S. & POOVORAWAN, Y. 2012. Elevated serum IL-18 and interferon-gamma in medium-term survivors of biliary atresia. *Eur J Pediatr Surg,* 22**,** 29-33.

VENKATESH, V., SEETHARAMAN, K. & ANUSHREE, N. 2022. Treatment of hepatitis C in children and adolescents: how far have we reached? *World J Pediatr*.

VIDARSSON, G., DEKKERS, G. & RISPENS, T. 2014. IgG subclasses and allotypes: from structure to effector functions. *Front Immunol,* 5**,** 520.

VON HAHN, T., YOON, J. C., ALTER, H., RICE, C. M., REHERMANN, B., BALFE, P. & MCKEATING, J. A. 2007. Hepatitis C virus continuously escapes from neutralizing antibody and T-cell responses during chronic infection in vivo. *Gastroenterology,* 132**,** 667-78.

VORUP-JENSEN, T. & JENSEN, R. K. 2018. Structural Immunology of Complement Receptors 3 and 4. *Front Immunol,* 9**,** 2716.

WANG, J., XU, Y., CHEN, Z., LIANG, J., LIN, Z., LIANG, H., XU, Y., WU, Q., GUO, X., NIE, J., LU, B., HUANG, B., XIAN, H., WANG, X., WU, Q., ZENG, J., CHAI, C., ZHANG, M., LIN, Y., ZHANG, L., ZHAO, S., TONG, Y., ZENG, L., GU, X., CHEN, Z. G., YI, S., ZHANG, T., DELFOUNESO, D., ZHANG, Y., NUTT, S. L., LEW, A. M., LU, L., BAI, F., XIA, H., WEN, Z. & ZHANG, Y. 2020. Liver Immune Profiling Reveals Pathogenesis and Therapeutics for Biliary Atresia. *Cell,* 183**,** 1867-1883 e26.

WANG, K., WEI, G. & LIU, D. 2012. CD19: a biomarker for B cell development, lymphoma diagnosis and therapy. *Exp Hematol Oncol,* 1**,** 36.

WANG, L., SUN, X., QIU, J., CAI, Y., MA, L., ZHAO, P. & JIANG, Y. 2015a. Increased numbers of circulating ICOS(+) follicular helper T and CD38(+) plasma cells in patients with newly diagnosed primary biliary cirrhosis. *Dig Dis Sci,* 60**,** 405-13.

WANG, L., SUN, Y., ZHANG, Z., JIA, Y., ZOU, Z., DING, J., LI, Y., XU, X., JIN, L., YANG, T., LI, Z., SUN, Y., ZHANG, J. Y., LV, S., CHEN, L., LI, B., GERSHWIN, M. E. & WANG, F. S. 2015b. CXCR5+ CD4+ T follicular helper cells participate in the pathogenesis of primary biliary cirrhosis. *Hepatology,* 61**,** 627-38.

WANG, L. D. & CLARK, M. R. 2003. B-cell antigen-receptor signalling in lymphocyte development. *Immunology,* 110**,** 411-20.

WANG, P., WANG, Y., XIE, L., XIAO, M., WU, J., XU, L., BAI, Q., HAO, Y., HUANG, Q., CHEN, X., HE, R., LI, B., YANG, S., CHEN, Y., WU, Y. & YE, L. 2019. The Transcription Factor T-Bet Is Required for Optimal Type I Follicular Helper T Cell Maintenance During Acute Viral Infection. *Front Immunol,* 10**,** 606.

WANG, R., XIE, R. & SONG, Z. 2018. Circulating regulatory Tfh cells are enriched in patients with chronic hepatitis B infection and induce the differentiation of regulatory B cells. *Exp Cell Res,* 365**,** 171-176.

WARNATZ, K., SALZER, U., RIZZI, M., FISCHER, B., GUTENBERGER, S., BOHM, J., KIENZLER, A. K., PAN-HAMMARSTROM, Q., HAMMARSTROM, L., RAKHMANOV, M., SCHLESIER, M., GRIMBACHER, B., PETER, H. H. & EIBEL, H. 2009. B-cell activating factor receptor deficiency is associated with an adult-onset antibody deficiency syndrome in humans. *Proc Natl Acad Sci U S A,* 106**,** 13945-50.

WEI, C., ANOLIK, J., CAPPIONE, A., ZHENG, B., PUGH-BERNARD, A., BROOKS, J., LEE, E. H., MILNER, E. C. & SANZ, I. 2007. A new population of cells lacking expression of CD27 represents a notable component of the B cell memory compartment in systemic lupus erythematosus. *J Immunol,* 178**,** 6624-33.

WEILL, J. C. & REYNAUD, C. A. 2020. IgM memory B cells: specific effectors of innate-like and adaptive responses. *Curr Opin Immunol,* 63**,** 1-6.

WHO 2012. Prevention & Control of Viral HEpatitis Infection: Framework for Global Action.

WIDJAJA, A. A., CHOTHANI, S. P. & COOK, S. A. 2020. Different roles of interleukin 6 and interleukin 11 in the liver: implications for therapy. *Hum Vaccin Immunother,* 16**,** 2357-2362.

WIGGINS, B. G., PALLETT, L. J., LI, X., DAVIES, S. P., AMIN, O. E., GILL, U. S., KUCYKOWICZ, S., PATEL, A. M., ALIAZIS, K., LIU, Y. S., REYNOLDS, G. M., DAVIDSON, B. R., GANDER, A., LUONG, T. V., HIRSCHFIELD, G. M., KENNEDY, P. T. F., HUANG, Y., MAINI, M. K. & STAMATAKI, Z. 2021. The human liver microenvironment shapes the homing and function of CD4(+) T-cell populations. *Gut*.

WONG, V. S., WIGHT, D. G., PALMER, C. R. & ALEXANDER, G. J. 1996. Fibrosis and other histological features in chronic hepatitis C virus infection: a statistical model. *J Clin Pathol,* 49**,** 465-9.

WU, W., WU, W., YE, Y., LI, T. & WANG, B. 2022. mRNA and lncRNA expression profiles of liver tissues in children with biliary atresia. *Exp Ther Med,* 24**,** 634.

WU, Y. C., KIPLING, D. & DUNN-WALTERS, D. K. 2011. The relationship between CD27 negative and positive B cell populations in human peripheral blood. *Front Immunol,* 2**,** 81.

WU, Z., XU, J., TAN, J., SONG, Y., LIU, L., ZHANG, F., ZHANG, Y., LI, X., CHI, Y. & LIU, Y. 2019. Mesenteric adipose tissue B lymphocytes promote local and hepatic inflammation in non-alcoholic fatty liver disease mice. *J Cell Mol Med,* 23**,** 3375-3385.

XIAO, J., XIA, S. Y., XIA, Y., XIA, Q. & WANG, X. R. 2014. Transcriptome profiling of biliary atresia from new born infants by deep sequencing. *Mol Biol Rep,* 41**,** 8063-9.
XU, Y., YU, J., ZHANG, R., YIN, Y., YE, J., TAN, L. & XIA, H. 2012. The perinatal infection of cytomegalovirus is an important etiology for biliary atresia in China. *Clin Pediatr (Phila),* 51**,** 109-13.
XUE, H., MCCAULEY, R. L. & ZHANG, W. 2000. Elevated interleukin-6 expression in keloid fibroblasts. *J Surg Res,* 89**,** 74-7.
YAGHOBI, R., DIDARI, M., GRAMIZADEH, B., RAHSAZ, M., HEIDARI, T., BANIHASHEMI, M. & KARGAR, M. 2011. Study of viral infections in infants with biliary atresia. *Indian J Pediatr,* 78**,** 478-81.
YAM, A. O. & CHTANOVA, T. 2019. The Ins and Outs of Chemokine-Mediated Immune Cell Trafficking in Skin Cancer. *Front Immunol,* 10**,** 386.
YAMAGIWA Y, P. T. 2000-2013. Cytokine Regulation of Cholangiocyte Growth. *Madame Curie Bioscience Database.* Austin (TX): Landes Bioscience.
YANG, C., XING, H., TAN, B. & ZHANG, M. 2022. Immune Characteristics in Biliary Atresia Based on Immune Genes and Immune Cell Infiltration. *Front Pediatr,* 10**,** 902571.
YANG, S., CHANG, N., LI, W., YANG, T., XUE, R., LIU, J., ZHANG, L., YAO, X., CHEN, Y., WANG, H., YANG, L., HUANG, J. & LI, L. 2023. Necroptosis of macrophage is a key pathological feature in biliary atresia via GDCA/S1PR2/ZBP1/p-MLKL axis. *Cell Death Dis,* 14**,** 175.
YANG, Y., WANG, J., ZHAN, Y., CHEN, G., SHEN, Z., ZHENG, S. & DONG, R. 2020. The synthetic toxin biliatresone causes biliary atresia in mice. *Lab Invest,* 100**,** 1425-1435.
YAO, K. H., MENG, Q. H. & YU, D. 2022. [The investigation on the acute, severe hepatitis of unknown origin in children]. *Zhongguo Dang Dai Er Ke Za Zhi,* 24**,** 604-613.
YAROVINSKY, T. O., MOHNING, M. P., BRADFORD, M. A., MONICK, M. M. & HUNNINGHAKE, G. W. 2005. Increased sensitivity to staphylococcal enterotoxin B following adenoviral infection. *Infect Immun,* 73**,** 3375-84.
YE, C., ZHU, J., WANG, J., CHEN, D., MENG, L., ZHAN, Y., YANG, R., HE, S., LI, Z., DAI, S., LI, Y., SUN, S., SHEN, Z., HUANG, Y., DONG, R., CHEN, G. & ZHENG, S. 2022. Single-cell and spatial transcriptomics reveal the fibrosis-related immune landscape of biliary atresia. *Clin Transl Med,* 12**,** e1070.
ZANI, A., QUAGLIA, A., HADZIC, N., ZUCKERMAN, M. & DAVENPORT, M. 2015. Cytomegalovirus-associated biliary atresia: An aetiological and prognostic subgroup. *J Pediatr Surg,* 50**,** 1739-45.
ZEN, Y., BRITTON, D., MITRA, V., PIKE, I., HEATON, N. & QUAGLIA, A. 2016. A global proteomic study identifies distinct pathological features of IgG4-related and primary sclerosing cholangitis. *Histopathology,* 68**,** 796-809.
ZEN, Y., QUAGLIA, A. & PORTMANN, B. 2011. Immunoglobulin G4-positive plasma cell infiltration in explanted livers for primary sclerosing cholangitis. *Histopathology,* 58**,** 414-22.
ZENG, F., ZHANG, Y., HAN, X., ZENG, M., GAO, Y. & WENG, J. 2020. Predicting Non-Alcoholic Fatty Liver Disease Progression and Immune Deregulations by Specific Gene Expression Patterns. *Front Immunol,* 11**,** 609900.
ZHANG, B., HU, M., ZHANG, P., CAO, H., WANG, Y., WANG, Z. & SU, T. 2013. BAFF promotes regulatory T-cell apoptosis and blocks cytokine production by activating B cells in primary biliary cirrhosis. *Braz J Med Biol Res,* 46**,** 433-9.
ZHANG, J., ZHANG, W., LEUNG, P. S., BOWLUS, C. L., DHALIWAL, S., COPPEL, R. L., ANSARI, A. A., YANG, G. X., WANG, J., KENNY, T. P., HE, X. S., MACKAY, I. R. & GERSHWIN, M. E. 2014. Ongoing activation of autoantigen-specific B cells in primary biliary cirrhosis. *Hepatology,* 60**,** 1708-16.
ZHANG, L. Y., HUANG, L. S., YUE, Y. H., FAWAZ, R., LIM, J. K. & FAN, J. G. 2022. Acute Hepatitis of Unknown Origin in Children: Early Observations from the 2022 Outbreak. *J Clin Transl Hepatol,* 10**,** 522-530.
ZHANG, P. & LU, Q. 2018. Genetic and epigenetic influences on the loss of tolerance in autoimmunity. *Cell Mol Immunol,* 15**,** 575-585.
ZHANG, T., SUN, J., CHENG, J., YIN, W., LI, J., MILLER, H., HERRADA, A. A., GU, H., SONG, H., CHEN, Y., GONG, Q. & LIU, C. 2021. The role of ubiquitinase in B cell development and function. *J Leukoc Biol,* 109**,** 395-405.
ZHOU, Z. & ZHONG, W. 2017. Targeting the gut barrier for the treatment of alcoholic liver disease. *Liver Res,* 1**,** 197-207.
ZHOU, Z. Q., TONG, D. N., GUAN, J., LI, M. F., FENG, Q. M., ZHOU, M. J. & ZHANG, Z. Y. 2017. Circulating follicular helper T cells presented distinctively different responses toward bacterial antigens in primary biliary cholangitis. *Int Immunopharmacol,* 51**,** 76-81.

ZWOLAK, A., SURDACKA, A. & DANILUK, J. 2016. Bcl-2 and Fas expression in peripheral blood leukocytes of patients with alcoholic and autoimmune liver disorders. *Hum Exp Toxicol,* 35**,** 799-807.

APPENDICES

Appendix table 1 Clinical data for adult liver and blood patients. *These samples were processed following patient consent and in approval with local research ethics committee guidelines (LREC; reference number 06/Q2702/61 and 18-WA-0214).*

CLR number	Disease	Sex	Age at transplant	CMV	EBV	VZV	Virus	Medication
CLR6494	AAT1	M	71	Neg	not done	VZV + past infection	Hep B, C, HIV Neg	Rifaimin 500mg bd, Lactulose 20ml bd, Spironolactone 100mg od, Frusomide 40mg od, Adcal-D3 daily, Tiotropium 2puffs daily, Salbutamol PRN
CLR6079	AIH	F	56	Neg	not done	VZV + past infection	Hep B, C, HIV Neg	Carvedilol 6.25ng BD, Mycophenolate 500 BD, Prednisolone 2mg every other day, Spironolatone 50mg,
CLR7538	AIH	M	59	Neg	not done	VZV + past infection	Hep B, C, HIV Neg Covid-19 + prior to Tx	Rifaxmin 550mg bd, prednisolone 10mg od,
CLR6273	ALD	M	53	Pos	pos	VZV + past infection	Hep B, C, HIV Neg	Carvedilo 12.5mg od, Chlorpenamine 4mg, Ciproflaxacin 500mg od, folic acid 1mg od, furoseminde 40mg od, Rivaximin 550mg bd, thiamine hydrochloride 100mg tds
CLR6935	ALD	M	65	Pos	not done	VZV + past infection	Hep B, C, HIV Neg	Lantus 30 od, humalog 30 tds, thiamine, folic acid, ferrous sulphate, rifaximin, renapro 120g od, ciprofloacin,

CLR6948	ALD	M	67	Neg	770 iu	VZV + past infection	Hep B, C, HIV Neg, Cryptococcal neg, C-Dif Pos,	Adcal, Baclofen, Propranlol, Omeprazole, Zinc Supplements
CLR7092	ALD	M	45	Pos	not done	VZV + past infection	Hep B, C HIV Neg	Ventolin, Steroid inhalers, Rifaximin 550mg BD, Citalopram 40mg od, Omeprazole 40mg od, Mirtazaine 45mg ON, Thiamine Bd, Metoclopromide, Creon, Melatonin 4mg, Ciproflaxacin
CLR7240	ALD	M	53	Pos	286iu	VZV + past infection	Hep B Core Pos, Hep B Surface Ag, Hep C, HIV Neg, Hep D Neg, Hep E Neg	Spironolactone 100mg BD, Asprin 75mg OD, Atorvastatin 20, Omeprazole 20, Carvedilol 12.5mg
CLR6502	ALD/HCC	M	59	Neg	not done	VZV + past infection	All Virology Hep B, C HIV Neg	Tace Treatment, Spironolactone, Furosemide, Adcal-D3, Ferrous Sulphate, Testosterone replacement
CLR7084	ALD	M	63	Pos	-	VZV + past infection	No immunity to Hep A & Hep B, needed vaccination, Hep B, C, HIV Neg	omeprazole, thiamine, Carvedilol, Rifaximin,
CLR7342	ALD	M	42	Pos	not done	not done	Hep B, C HIV Neg	Creon 25000, Enoxparin, Esomeprazole, Furosemide, Hydrocortisone 100mg BD, Sandoz, Piperacillin/Tazobactam, Potassium

								Chloride, Reapro Shot, Rifaximin, Terlipressin, Thiamine Hydrocloride
CLR6094	Donor	M	52	Neg	Pos	-	Hep B, C, HIV Neg	Noradrenaline, Metaraminol, Frusemide/Laside, Propofol/Diprivan, Magnesium, Potassium, Dantoprazole, Pabrinex, Paracetamol
CLR6414	Donor	M	34	Pos	Pos	-	Hep B, C, HIV Neg	Noradrenaline, Vasopressin, Labetalol, Propofol/Diprivan, Fondoparinux, Levofloxacin, Metronidazole, Pabrinex, Omeprazole
CLR6469	Donor	M	60	Pos	Pos	-	Hep B, C, HIV Neg	Noradrenaline, Propofol/Diprivan, Alfentanil, Tirofiban, Tazocin, Co-trimoxazole, Co-amoxiclav
CLR6451	Donor	F	56	Pos	Pos	-	Hep B, C, HIV Neg	Noradrenaline, Cefuroxime, Metronidazole, Pantoprazole
CLR6793	Donor	M	61	Pos	-	-	Hep B, C, HIV Neg	Insulin, Levetiracetam, Aciclovir, Fluconazole, Labetalol
CLR6968	Donor	M	51	Pos	Pos	Hep B Pos	Hep C, HIV Neg	Methyl prednisolone, Noradrenaline, Vasopressin, Piperacillin, Tazobactam
CLR7386	HFE	F	63	not done	not done	not done	Neg	no meds
CLR7392	HFE	M	63	not done	not done	not done	not done	no meds

CLR7431	HFE	M	64	not done	not done	not done	Neg	Semaglutide 14mg, Losartan 25mg, Lansoprazole 30mg, Pregablin 150mg BD
CLR7436	HFE	M	63	not done	not done	not done	not done	no meds
CLR7429	HFE liver	M	50	Neg	not done	VZV + past infection	Hep B, C HIV Neg	Carvedilol 6.25 bd, venesection Programme, Folate, Rifaximin, Melatonin
CLR6797	NAFLD	M	68	Pos	not done	VZV + past infection	Hep B, C HIV Neg	Adcal D3, Carvedilol, Ferrous Fumerate, Insulin, Omeprazole, Rifaximin
CLR6595	NASH	M	57	Pos		VZV + past infection	Hep B, C HIV Neg	Chlorphenamine, Topical Clobetasol, Neomycin, Creon, Furosomide, Propranolol, Renapro shots, Spironolactone, Thiamine
CLR6952	NASH	F	66	Pos	not done	VZV + past infection	Hep B, C HIV Neg	Mycophenolate 250mg od, Prednisolone 5mg OD, Lansoprazole 30mg OD, Spironolactone 50mg OD, Forusomide 20mg od, Carvedilol 6.25 Bd, Rifaximin 550mg BD, Ferrous Fumarate 210mg daily
CLR7366	NASH	M	60	Pos	not done	VZV + past infection	Hep B, C HIV Neg	Atorvastatin 40mg, Dapagliflozin 10mg, Lercanidipine, Spironalactone, Carvedilol, Levothyroxine, Metformin, Gliclazide, Omeprazole, Ramipril, Zultophy inj 50 Dose units

CLR7453	NASH	M	62	Pos	not done	VZV + past infection	Hep B, C HIV Neg	Simvastatin, Thiamine, Spiro, Rifaximin, Carvedilol, Lansoprazole
CLR6706	NASH/ Cirrhosis	F	69	Pos	not done	VZV + past infection	Hep B, C HIV Neg	Bisoprolol, Co-beneldopa, Colestyramine, Dermol 500, Furosemide, Gliclazide, Lactulose, Lansoprazole, Levothyroxine Sodium, Magnesium Citrate, Primidone, Renapro Shot, Rifaximin, Spironolactone
CLR6088	PBC	F	60	Neg	not done	VZV + past infection	Hep B, C HIV Neg	Ursodeoxycholic Acid
CLR6871	PBC	F	66	Pos	10473 iu	VZV + past infection	Hep B, C HIV Neg, Hep E<500, Hep A IGM Neg, Hep A Total Pos	Adcal d3, Tacrolimus 3.5mg BD, Amlodipine, Asprin, Azathioprine 75mg od, Co-trimoxazole, Creon 25000, Doxazosin, Gliclazide, Enoxaparin, Lansoprazole, Prednisolone 20mg OD, Ursodeoxycholic acid, Valganciclovir
CLR6821	PBC	M	55	Pos	not done	not done	Hep A pos, Hep B (surface and cured antibody), Hep C, HIV neg	Adcal D3 1 tab BD, Carvedilol 6.25mg BD, Colecalciferol (Vitamin D) 800 units BD, Enoxaparin 40mg OD, Fortisip Compact Protein 125ml TDS, Lactulose 5ml BD, Omeprazole 40mg OD, Renapro Shot 60ml TDS, Spironolactone 50mg BD, Ursodeoxycholic Acid 1250mg/d 2SPLT

CLR6886	PBC	F	49	Pos	not done	VZV + past infection	Hep B, C & HIV Neg	Ursodeoxycholic acid, Naltrexone, Bezafibrate, Obeticholic
CLR7232	PBC	F	53	Neg	<150iu/ml	VZV + past infection	Hep E <500 iu, Hep B, C, HIV neg	Ursodeoxycholic, Sertraline, Bezafibrate, Rifampicin, Gabapentin, Quetiapine, Melatonin, Fexofenadine, Renapro Shots
CLR7515	PBC	F	71	Neg	not done	VZV + past infection	Hep B, C & HIV Neg	Spironolactone, Rifaximin, Ramipril, UDCA, Adcal D
CLR5509	Polycystic	F	54	Neg	not done	VZV + past infection	no recent virology results	Folic Acid, Omeprazole, Chlorphenamine, Sodium Bicarbonate, Frusomide, Asprin
CLR6497	PSC	M	39	Neg	<150iu/ml	VZV + past infection	Hep B, C & HIV Neg	Salbutamol inhaler
CLR6525	PSC	M	55	Neg	NA IgG Pos, VCA IgM Neg, VCA IgG Pos, <150iu	VZV + past infection	Hep B, C & HIV Neg. Hep E <500	Rifampicin, Ursodeoxycholic Acid, Pentasa, Lansoprazole
CLR6596	PSC	F	27	Pos	not done	not done	Hep B, C & HIV Neg	Rifampicin, Vitamins A, D & K, Melatonin,

CLR6795	PSC	M	69	Neg	not done	not done	Hep B, C & HIV Neg	Carvedilol, Enoxaparin, Lansoprazole, Mesalazine, Renapro Shot, Rifaximin, Salbutamol, Sertraline, Ursodeoxycholic Acid
CLR7556	PSC	M	53	Pos	<150 iu	VZV + past infection	Hep B, C & HIV Neg	Chlorphenamine, Ciprofloxacin, Colestysramine, Creon 25000, Enoxaparin, Humalog Insulin, Morphine Sulfate oral solution, Renapro Shot, Sertraline, Tresiba, Vitamins A&D, Zinc Sulphate
CLR6416	PSC/AMR/PSC	F	46	Pos	<150iu/ml	VZV + past infection	Hep E <500 iu, Hep B, C, HIV neg	Adcal-D3, Chlorphenamine, Creon 25000, Gliclazide, Lansoprazole, Mesalazine, Prednisolone 15mg OD, Prograf 0.5mg BD, Sodium bicarbonate, Terlipressin

Appendix table 2 Clinical data for biliary atresia patients. ** Patients used for Nanostring HOT panel RNA analysis in Chapter 4.*

Patient	**Sex**	**Date of birth**	**Date of KPE**	**Date of Transplant**	**Other anomalies**

1	F	09/05/2013	12/06/2013	04/04/2014	none
2	M	29/03/2013	16/05/2013	11/10/2014	Jejunal atresia: 02/04/2013 laparotomy with resection
3	F	15/12/2013	20/01/2014	23/07/2014	none
5	F	05/12/2014	15/01/2015	02/09/2015	none
6*	M	10/01/2015	10/02/2015	06/08/2015	none
7	F	10/02/2015	15/04/2015	29/07/2015	none
8	M	30/08/2014	23/10/2014	30/03/2016	Perforation of bowel at birth - required surgery; Two episodes of necrotising enterocolitis - cause unknown
9*	M	13/10/2015	19/11/2015	06/07/2016	None
10	M	01/09/2015	09/10/2015	22/06/2016	none
11	M	26/08/2015	30/09/2015	13/07/2016	none
12	F	28/11/2015	31/12/2015	30/09/2016	none
13	F	04/05/2016	03/06/2016	14/04/2017	Left multicystic dysplastic kidney
14	F	15/10/2015	02/12/2015	24/10/2017	Malrotation
15*	F	28/11/2011	24/01/2012	30/07/2017	none
16*	M	14/09/2016	27/10/2016	11/03/2017	Complex cardiac anatomy
20	F	08/01/2014	23/02/2014	03/01/2016	None

21*	F	27/08/2012	24/10/2012	30/07/2013	Malrotation; Pre-duodenal portal vein, interrupted IVC and azygous continuation
22	F	05/01/1999	25/02/1999	11/06/2014	Spleno renal shunt
23*	F	11/04/2013	29/04/2013	23/02/2014	Cystic Biliary Atresia, type III
24	F	19/06/2020	16/07/2020		
25	F	30/04/2020	01/06/2020		
26	F	01/02/2020	27/04/2020		
27	F	15/01/2020	17/03/2020		
28	M	25/11/2019	22/01/2020		
29	M	16/12/2019	22/01/2020		
30	M	02/12/2019	14/01/2020		
31	F	20/08/2019	10/10/2019		
32	F	22/08/2019	25/09/2019		
33	F	13/07/2019	11/09/2019		
34	M	02/07/2019	29/08/2019		
35	M	26/04/2019	10/07/2019		
36	M	05/02/2019	24/04/2019		
37	F	11/02/2019	12/04/2019		
38	F	02/02/2019	15/03/2019		Cystic BA

39	M	25/01/2019	07/03/2019		
40	F	28/09/2018	23/11/2018		
41	M	06/07/2018	05/09/2018		
42	F	31/05/2018	12/07/2018		
43	M	12/03/2018	13/06/2018		
44	F	24/01/2018	28/02/2018		
45	M	23/12/2017	06/02/2018		
46	F	04/10/2017	20/12/2017		
47	F	19/10/2017	27/11/2017		
48	M	22/08/2017	20/09/2017		
49	M	07/08/2017	12/09/2017		
50	F	04/07/2017	26/07/2017		
51	F	29/06/2017	21/07/2017		
52	F	09/06/2017	24/07/2017		
53	M	01/05/2017	19/06/2017		
54	F	24/04/2017	08/06/2017		
55	M	05/05/2017	07/06/2017		
56	F	04/04/2017	26/05/2017		

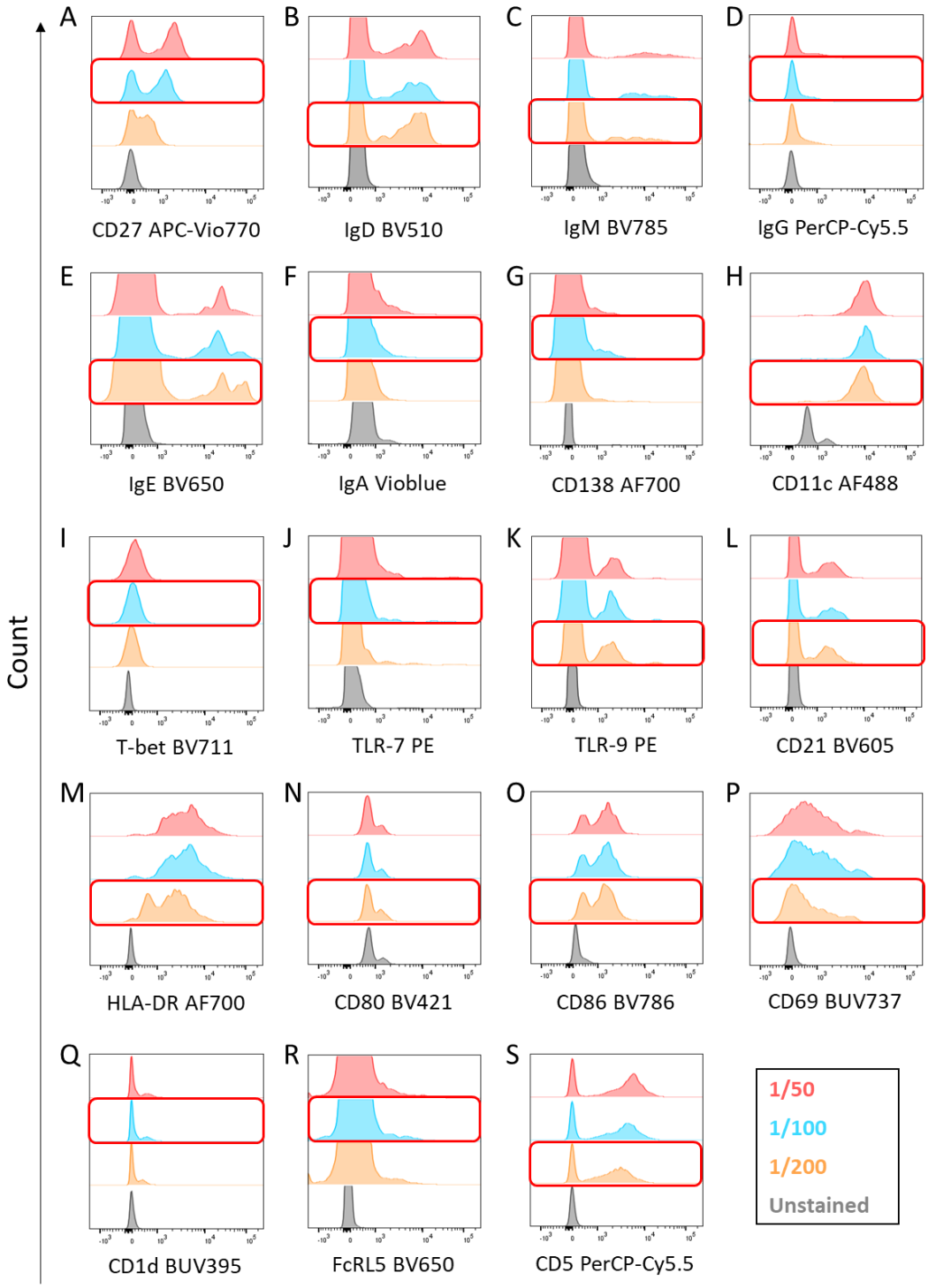
57	M	07/04/2017	12/05/2017		
58	M	16/01/2017	12/05/2017		
59	M	08/03/2017	05/04/2017		

Appendix table 3 Clinical data for sudden onset acute liver failure patients.

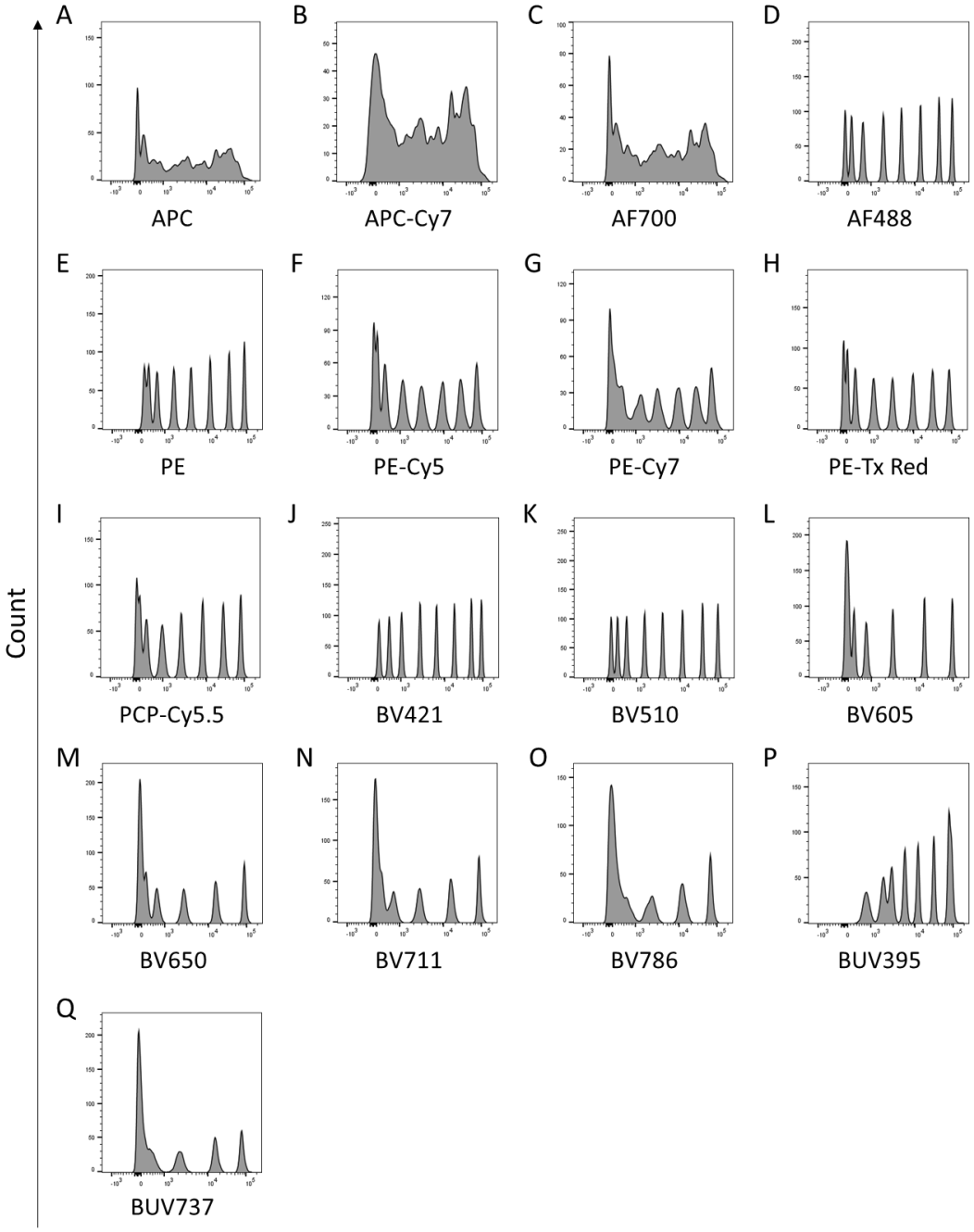
Patient	Sex	Date of birth	Date of Transplant	Virus
ALF 1	F	19/11/2020	21/01/2022	Adenovirus neg
ALF 2	F	22/12/2019	02/02/2022	Adenovirus neg
ALF 3	M	27/06/2018	19/04/2022	Adenovirus neg
ALF 4	M	05/03/2018	14/04/2022	Adenovirus neg
ALF 5	M	22/09/2020	15/04/2022	Adenovirus neg
ALF 6	F	11/11/2019	19/04/2022	Adenovirus neg
ALF 7	F	04/12/2018	25/05/2022	Adenovirus neg

Appendix table 4 Clinical data for HHV6 patients.

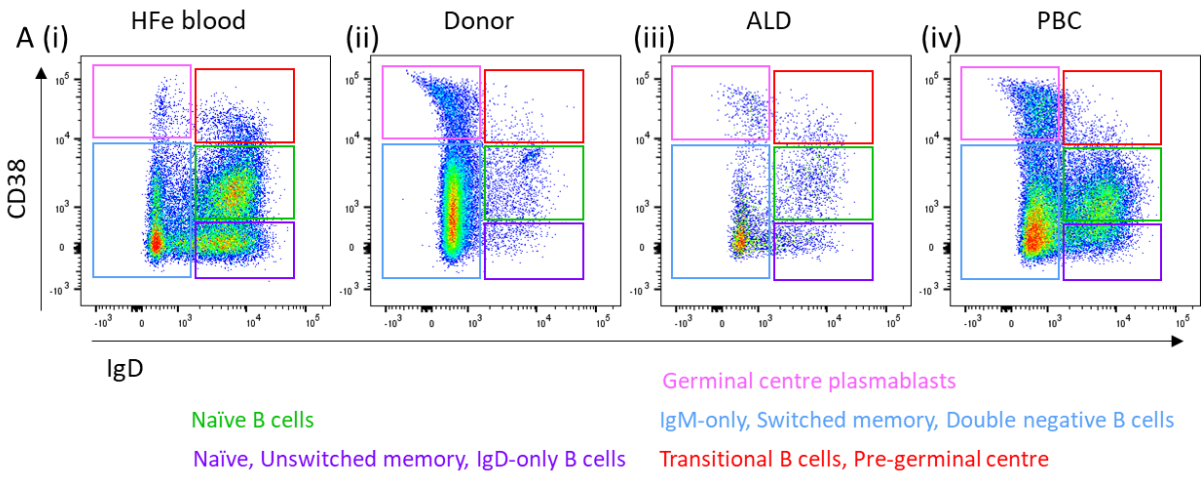
Patient	Sex	Date of birth	Date of Transplant
HHV6 1	F	04/03/2005	20/04/2006
HHV6 2	F	11/04/2013	03/12/2013
HHV6 3	F	05/07/2014	12/01/2015



Appendix 1 Antibody titrations used to find the optimal working dilution for each antibody. *Total PBMCs from one experiment were used to identify the optimal working dilution for each antibody. This was determined by identifying positive and negative peaks that had clear separation. These dilutions were used for all flow cytometry experiments.*

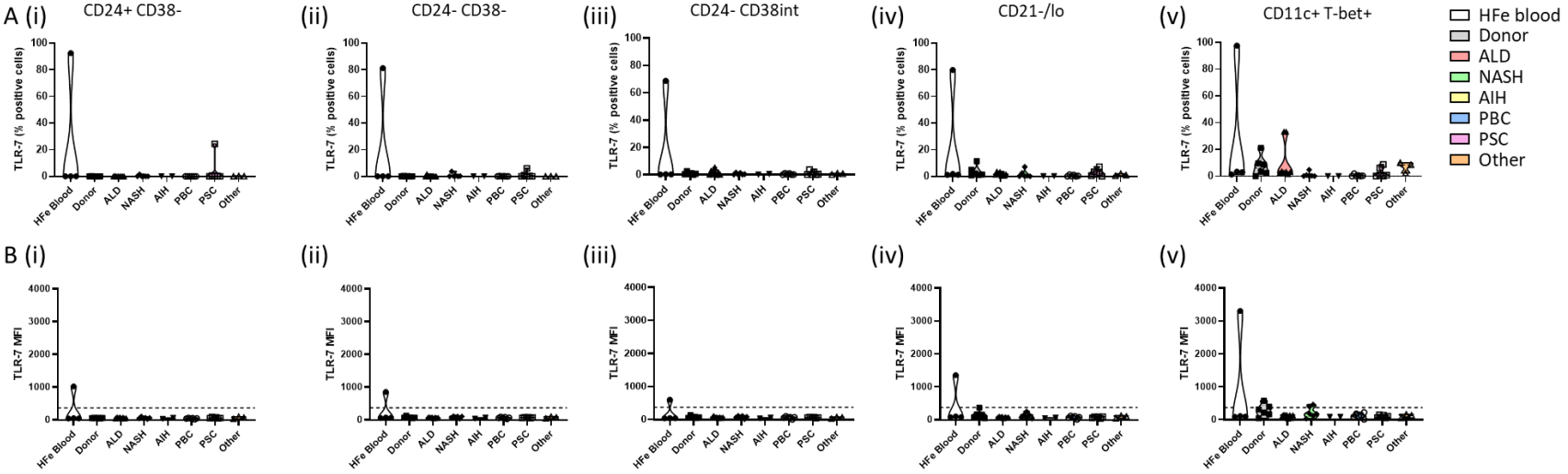


Appendix 2 Rainbow beads were used to calibrate the machine before each flow cytometry experiment. *Each fluorophore was designated a peak out of the 8 peaks and these peaks were positioned at the same place before samples were run through the flow cytometer. This ensured consistency across different experiments.*

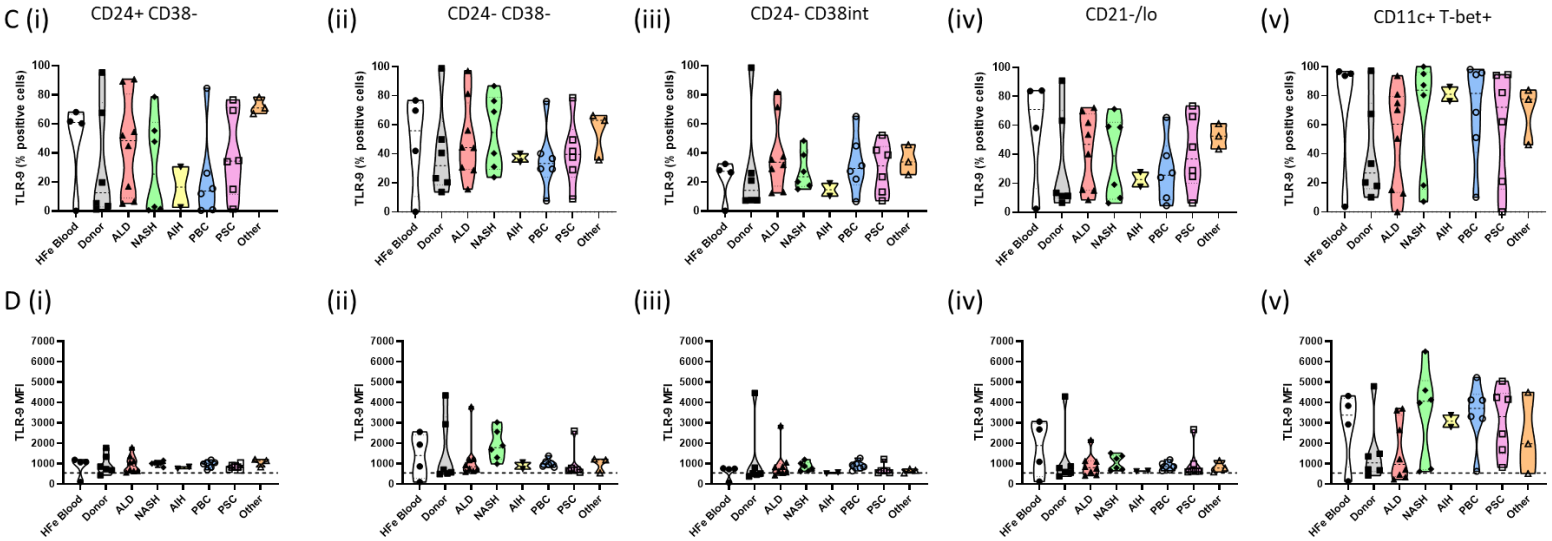


Appendix 3 Classical gating strategy for B cells using CD38 and IgD. *(A) CD38 and IgD were used to identify 5 groups of B cells between HFe blood and adult livers. These groups included germinal centre plasmablasts (pink), IgM-only, switched memory and double negative B cells (blue), transitional B cells and pre-germinal centre B cells (red), naïve B cells (green), naïve, unswitched memory and IgD-only B cells (purple). These B cell subsets were identified in (i) HFe blood, (ii) donor livers, (iii) ALD livers and (iv) PBC livers.*

TLR7

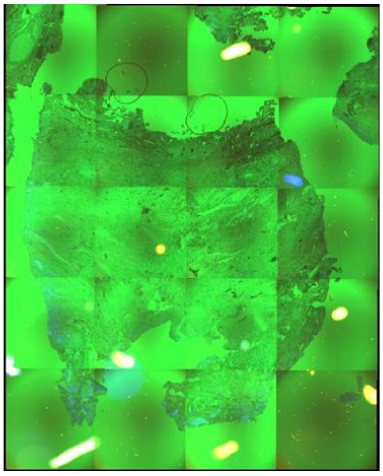

A (i)
CD24+ CD38-
(ii)
CD24- CD38-
(iii)
CD24- CD38int
(iv)
CD21-/lo
(v)
CD11c+ T-bet+
TLR-7 (% positive cells)
B (i)
(ii)
(iii)
(iv)
(v)
TLR-7 MFI
HFe Blood
Donor
ALD
NASH
AIH
PBC
PSC
Other
HFe blood
Donor
ALD
NASH
AIH
PBC
PSC
Other

TLR9

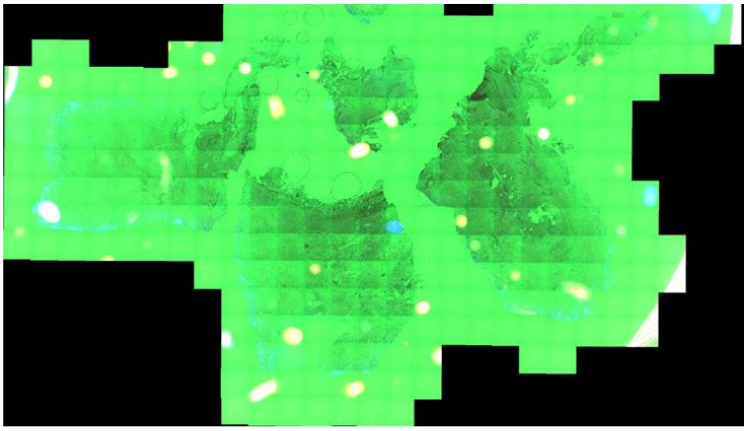

C (i)
CD24+ CD38-
(ii)
CD24- CD38-
(iii)
CD24- CD38int
(iv)
CD21-/lo
(v)
CD11c+ T-bet+
TLR-9 (% positive cells)
D (i)
(ii)
(iii)
(iv)
(v)
TLR-9 MFI
HFe Blood
Donor
ALD
NASH
AIH
PBC
PSC
Other

Appendix 4 TLR9 expression was detected across CD24+ CD38- B cells, CD24- B cells and ABC populations. *(A) TLR7 percentage expression and (B) TLR7 MFI was not detected in any of the liver subsets analysed. (C) TLR9 percentage positive cells were present in all subsets across all livers whereas (D) TLR9 MFI was detected in high numbers in CD11c+ T-bet+ ABCs. HFe blood (n=4), donor livers (n=6), ALD (n=8), NASH (n=6), AIH (n=2), PBC (n=6), PSC (n=6) and other livers (n=3). The dashed line for MFI data represents the IMC, anything above this line is positive. (C(i, ii and iv) and D(v)) Dunnett's T3 multiple comparisons test was used. (A, B, C(iii, v) and D(i-iv)) Dunn's multiple comparisons test was used.*

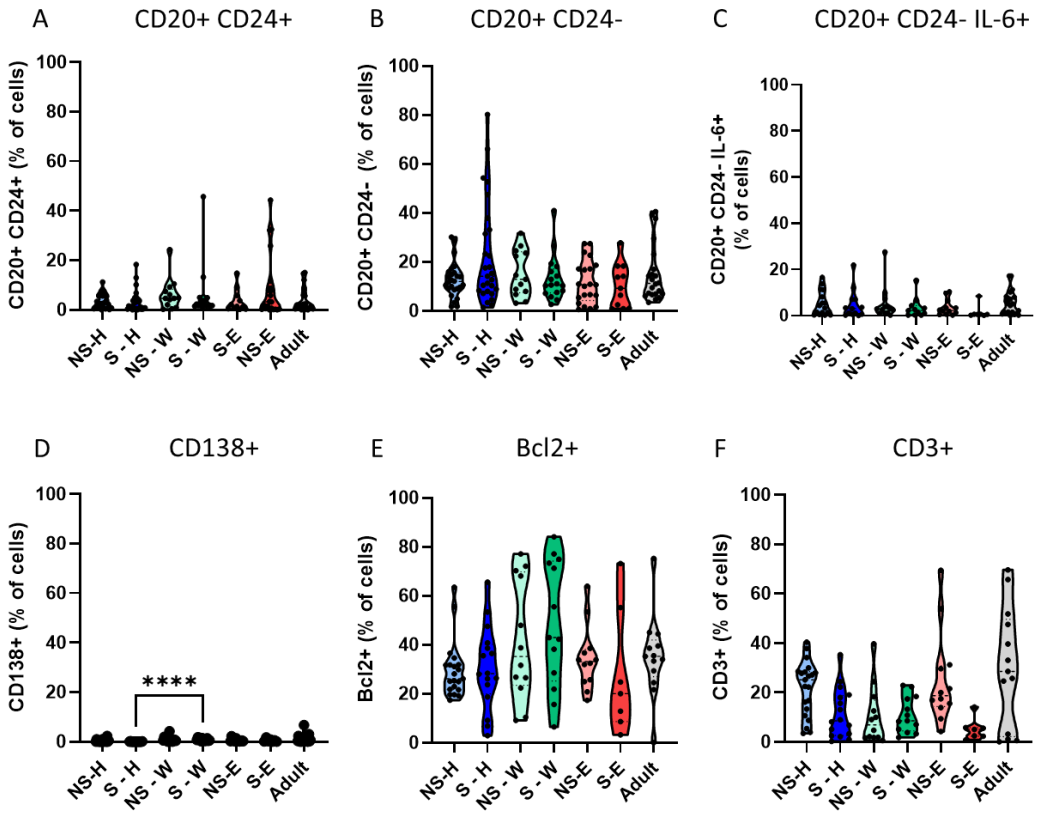
A (i)



(ii)



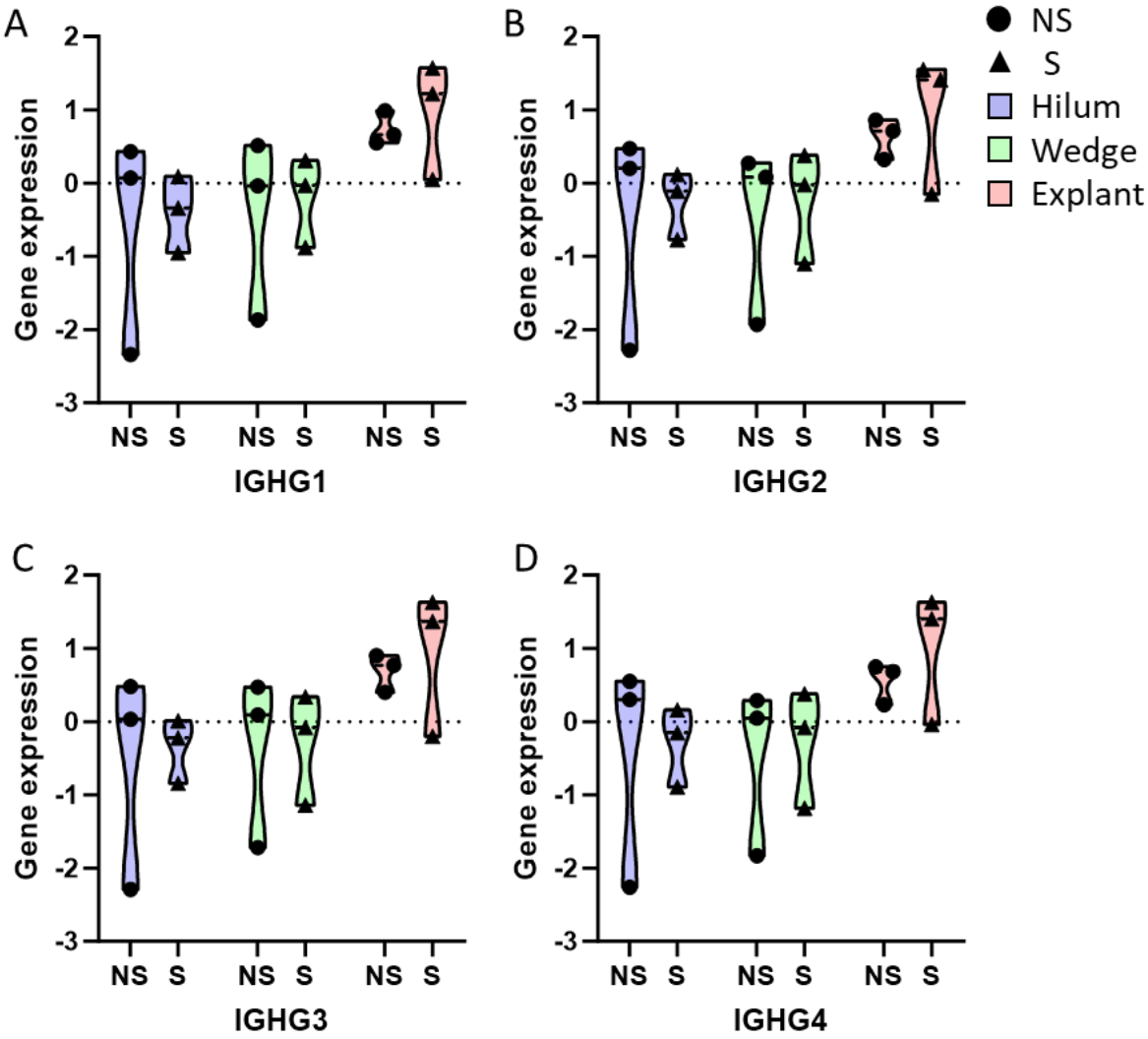
Appendix 5 Whole image immunofluorescence imaging was not possible. *We decided to attempt to image the whole section using the slide scanner however this was not possible.*



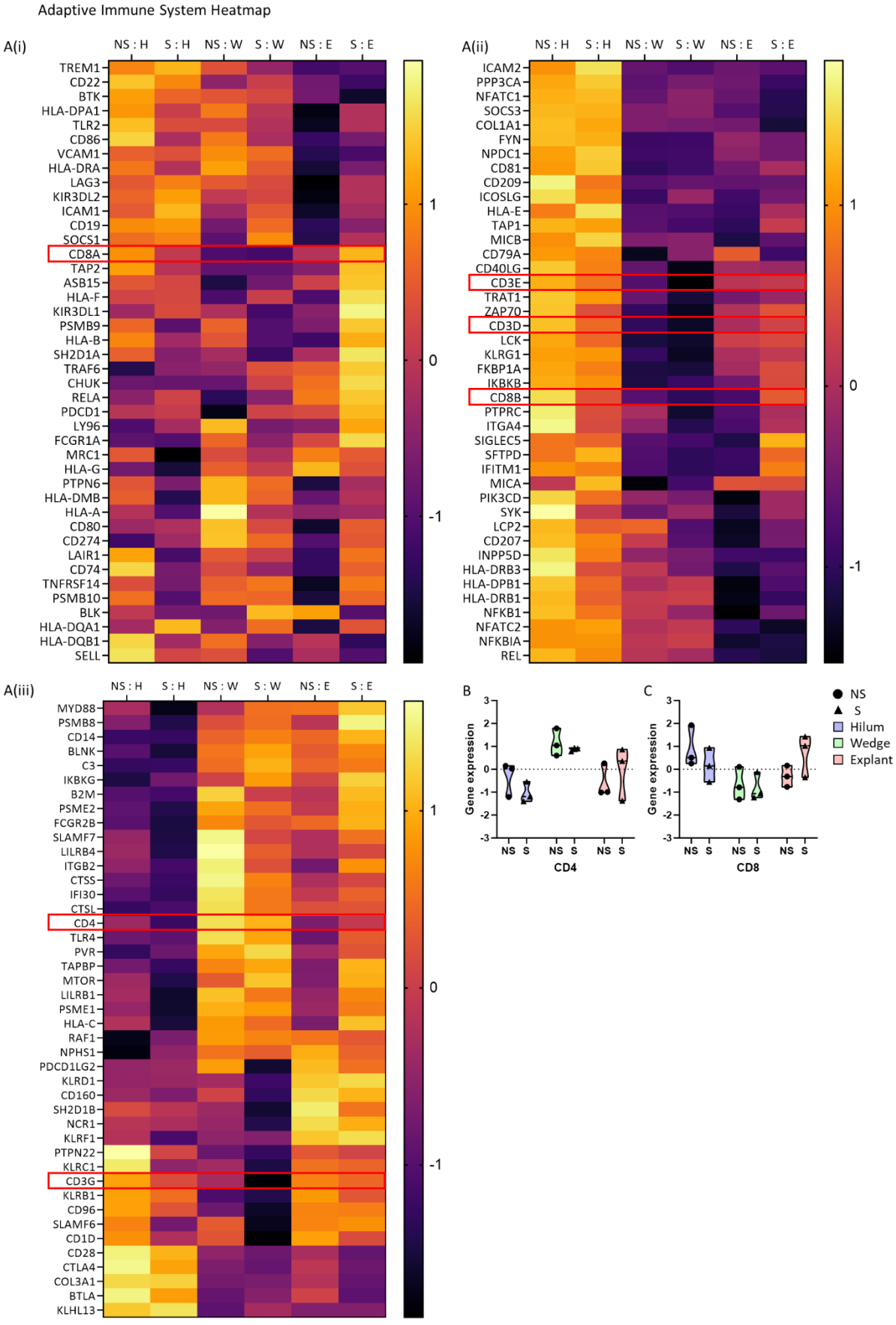
Appendix 6 No difference was observed between non-syndromic and syndromic BA patients for B cell subsets. *CellProfiler was used to quantify fluorophore for each marker and normalised to total cells present. These subsets were plotted for BA samples and compared to adult explants. Expression of (A) CD20+ CD24+ B cells, (B) CD20+ CD24- B cells, (C) CD20+ CD24- IL-6+ B cells, (D) CD138+ B cells, (E) Bcl2+ CD3- cells and (F) CD3+ T cells was analysed across BA patients. Non-syndromic hilum; NS:H, syndromic hilum; S:H, non-syndromic wedge; NS:W, syndromic wedge; S:W, non-syndromic explant; NS:E and syndromic explant; S:E. (A-F) Dunn's multiple comparisons test was used. p-value < 0.0001 (****).*

Appendix table 5 RNA Quality check results for paediatric samples used in the Nanostring HOT panel experiment.

BA Sample	**ng/ul**	**RIN**	**DV200 %**
16	83.8	1.3	22.31
17	96.1	2.3	78.5
18	110.6	3.1	71.3
25	52.6	1.4	13.98
26	68.2	1	31.88
27	67.4	2.8	71.4
43	70.4	1.1	22.37
44	58.2	1	29.99
45	214.3	2.1	67.9
46	86.4	1.2	17.23
47	41.5	1.8	50.8
48	48.9	2.7	74.1
52	56	1	26.77
53	40.2	1.6	45.8
54	43.6	2.9	61.2
58	47.8	1	23.56
59	35.7	2	51.4
60	101.9	1.8	46.1

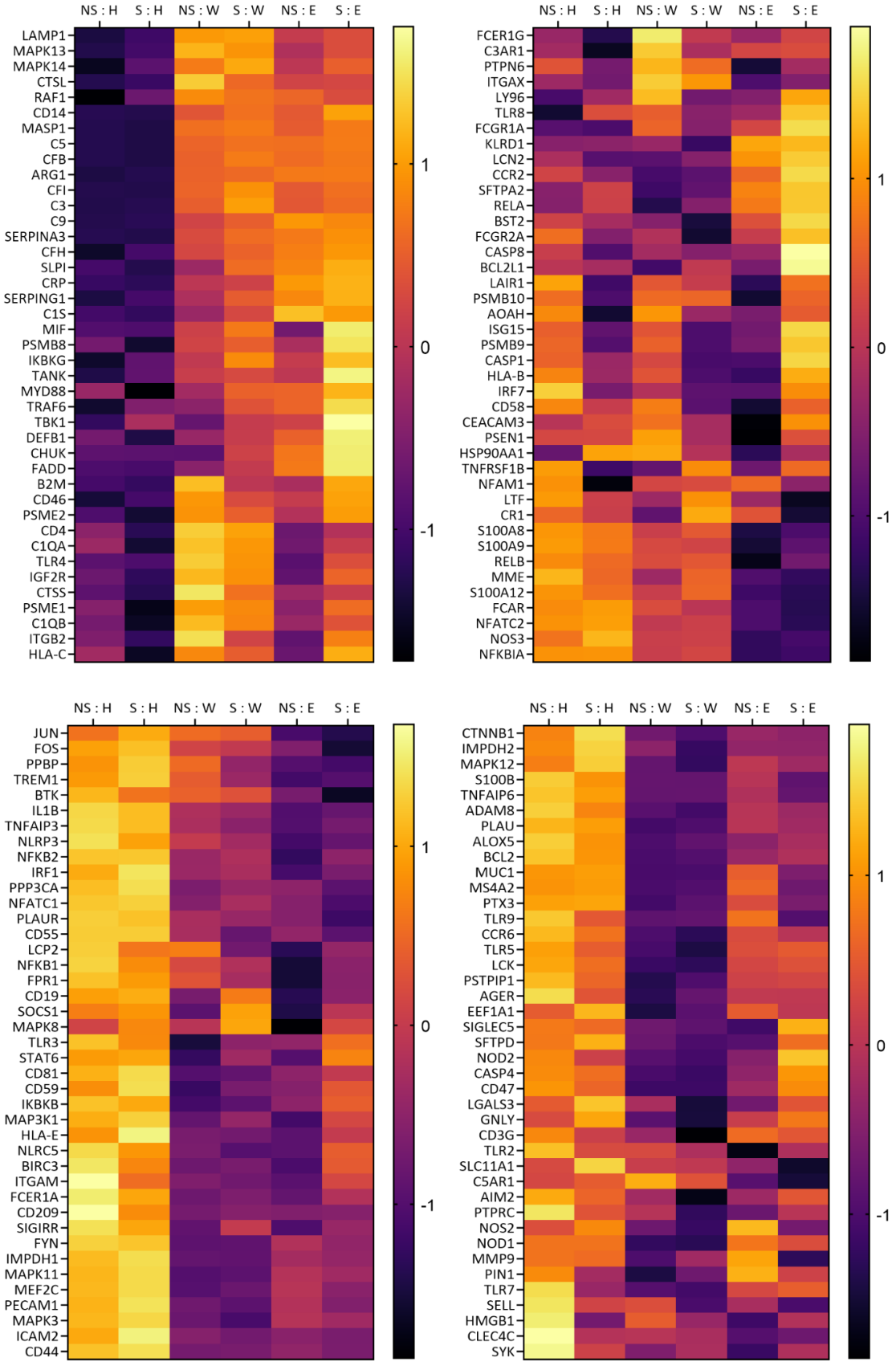


Appendix 7 IgG gene expression in BA livers. *Four IgG genes were analysed (A) IGHG1, (B) IGHG2, (C) IGHG3 and (D) IGHG4 in hilum (blue), wedge (green) and explant (red) for NS (closed circle) and syndromic; S (closed triangle) BA patients. (A-D) Dunn's multiple comparisons test was used.*

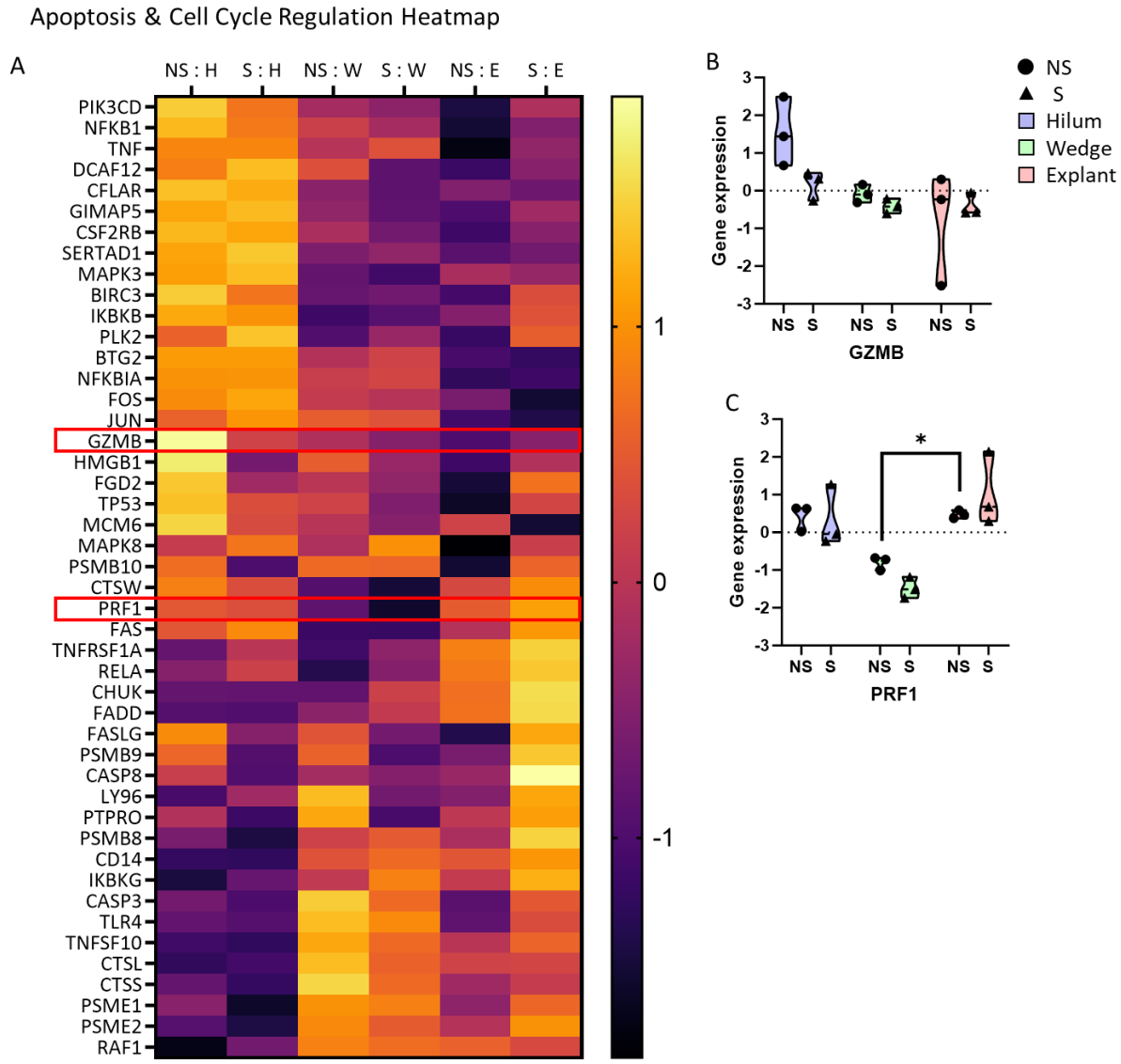

Adaptive Immune System Heatmap
A(i)
NS : H
S : H
NS : W
S : W
NS : E
S : E
TREM1
CD22
BTK
HLA-DPA1
TLR2
CD86
VCAM1
HLA-DRA
LAG3
KIR3DL2
ICAM1
CD19
SOCS1
CD8A
TAP2
ASB15
HLA-F
KIR3DL1
PSMB9
HLA-B
SH2D1A
TRAF6
CHUK
RELA
PDCD1
LY96
FCGR1A
MRC1
HLA-G
PTPN6
HLA-DMB
HLA-A
CD80
CD274
LAIR1
CD74
TNFRSF14
PSMB10
BLK
HLA-DQA1
HLA-DQB1
SELL
1
0
-1
A(ii)
ICAM2
PPP3CA
NFATC1
SOCS3
COL1A1
FYN
NPDC1
CD81
CD209
ICOSLG
HLA-E
TAP1
MICB
CD79A
CD40LG
CD3E
TRAT1
ZAP70
CD3D
LCK
KLRG1
FKBP1A
IKBKB
CD8B
PTPRC
ITGA4
SIGLEC5
SFTPD
IFITM1
MICA
PIK3CD
SYK
LCP2
CD207
INPP5D
HLA-DRB3
HLA-DPB1
HLA-DRB1
NFKB1
NFATC2
NFKBIA
REL
A(iii)
MYD88
PSMB8
CD14
BLNK
C3
IKBKG
B2M
PSME2
FCGR2B
SLAMF7
LILRB4
ITGB2
CTSS
IFI30
CTSL
CD4
TLR4
PVR
TAPBP
MTOR
LILRB1
PSME1
HLA-C
RAF1
NPHS1
PDCD1LG2
KLRD1
CD160
SH2D1B
NCR1
KLRF1
PTPN22
KLRC1
CD3G
KLRB1
CD96
SLAMF6
CD1D
CD28
CTLA4
COL3A1
BTLA
KLHL13
B
Gene expression
NS S NS S NS S
CD4
C
Gene expression
NS S NS S NS S
CD8
NS
S
Hilum
Wedge
Explant

Appendix 8 Adaptive immune system genes were differentially expressed between the hilum and the periphery. *BA livers were used from the hilum, wedge, and explant from non-syndromic (n=3) and syndromic (n=3) patients. (A) Heat map showing adaptive immune gene expression between the hilum, wedge, and explants in syndromic and non-syndromic BA patients. (B) CD4 gene expression was higher in wedge samples compared to hilum and explant samples. (C) CD8 expression was lower in wedge samples compared to the hilum and explant samples. Non-syndromic hilum; NS:H, syndromic hilum; S:H, non-syndromic wedge; NS:W, syndromic wedge; S:W, non-syndromic explant; NS:E and syndromic explant; S:E. (B and C) Non-syndromic; NS (closed circle) and syndromic; S (closed triangle) BA patients. Dunnett's T3 multiple comparisons test was used.*

Innate Immune System Heatmap

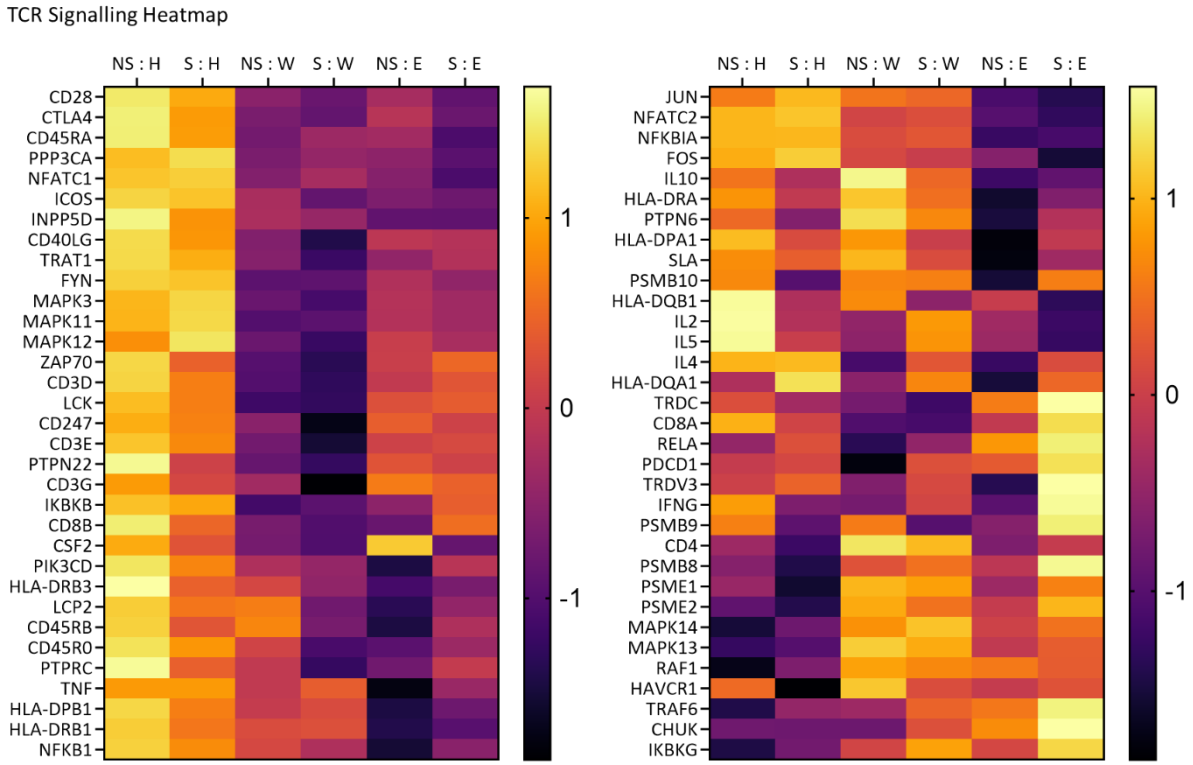


Appendix 9 Innate immune system genes were differentially expressed between the hilum and the periphery. *BA livers were used from the hilum, wedge, and explant from non-syndromic (n=3) and syndromic (n=3) patients. Non-syndromic hilum; NS:H, syndromic hilum; S:H, non-syndromic wedge; NS:W, syndromic wedge; S:W, non-syndromic explant; NS:E and syndromic explant; S:E.*



Appendix 10 Apoptosis and cell cycle regulation genes were differentially expressed between the hilum and the periphery. *BA livers were used from the hilum, wedge, and explant from non-syndromic (n=3) and syndromic (n=3) patients. (A) Heat map showing apoptosis and cell cycle regulation gene expression between the hilum, wedge, and explants in syndromic and non-syndromic BA patients. (B) Granzyme B gene expression was higher in hilum samples compared to the periphery. (C) Perforin expression was lower in wedge*

samples compared to the hilum and explant samples. Non-syndromic hilum; NS:H, syndromic hilum; S:H, non-syndromic wedge; NS:W, syndromic wedge; S:W, non-syndromic explant; NS:E and syndromic explant; S:E. (B and C) Non-syndromic; NS (closed circle) and syndromic; S (closed triangle) BA patients. Dunnett's T3 multiple comparisons test was used. p-value < 0.0001 (*).



Appendix 11 TLR signalling genes were differentially expressed between the hilum and the periphery. *BA livers were used from the hilum, wedge, and explant from non-syndromic (n=3) and syndromic (n=3) patients. Non-syndromic hilum; NS:H, syndromic hilum; S:H, non-syndromic wedge; NS:W, syndromic wedge; S:W, non-syndromic explant; NS:E and syndromic explant; S:E.*